AIRCRAFT STRUCTURAL SAFETY: EFFECTS OF EXPLICIT AND IMPLICIT SAFETY MEASURES AND UNCERTAINTY REDUCTION MECHANISMS

By

ERDEM ACAR

A DISSERTATION PRESENTED TO THE GRADUATE SCHOOL
OF THE UNIVERSITY OF FLORIDA IN PARTIAL FULFILLMENT
OF THE REQUIREMENTS FOR THE DEGREE OF
DOCTOR OF PHILOSOPHY

UNIVERSITY OF FLORIDA

2006

This dissertation is dedicated to my family: my father Zuhuri Acar, my mother Şerife Acar, and my sister Asiye Acar.

ACKNOWLEDGMENTS

I would like to express special thanks and appreciation to Dr. Raphael T. Haftka, chairman of my advisory committee. I am grateful to him for providing me with this excellent opportunity and financial support to complete my doctoral studies under his exceptional guidance. He encouraged me to attend several conferences and assisted in finding an internship during my studies. Through our weekly meetings and his open door policy, which I definitely over-exploited, he greatly contributed to this dissertation. His limitless knowledge and patience are inspiration to me. During the past three years, he was more than my PhD supervisor; he was a friend, and sometimes like a father. I sincerely hope we will remain in contact in the future.

I would also like to thank the members of my advisory committee, Dr. Bhavani V. Sankar, co-chair of the committee, Dr. Nagaraj Arakere, Dr. Nam-Ho Kim and Dr. Stanislav Uryasev. I am grateful for their willingness to review my Ph.D. research and to provide me with the constructive comments which helped me to complete this dissertation. In particular, I would like to extend special thanks to Dr. Bhavani V. Sankar for his guidance on the papers we co-authored, and Dr. Nam-Ho Kim for his comments and suggestions during the meetings of the Structural and Multidisciplinary Group.

I also wish to express my gratitude to my M.Sc. advisor, Dr. Mehmet A. Akgun, who provided a large share of motivation for pursuing a doctorate degree. The experience he supplied me during my master's degree studies contributed to this dissertation.

I also wish to thank to my colleagues at the Structural and Multidisciplinary Group of the Mechanical and Aerospace Engineering Department of the University of Florida for their support, friendship and many technical discussions. In particular, I would like to thank Dr. Melih Papila, Dr. Jaco Schutte, my soul sister Lisa Schutte, Tushar Goel and Ben Smarslok for their friendship (in the order of meeting with them).

Financial support provided by NASA Cooperative Agreement NCC3-994, NASA University Research, Engineering and Technology Institute and NASA Langley Research Center Grant Number NAG1-03070 is gratefully acknowledged.

Finally, my deepest appreciation goes to my family: my father Zuhuri Acar, my mother Şerife Acar and my sister Asiye Acar. The initiation, continuation and final completion of this thesis would not have happened without their continuous support, encouragement and love. I am incredibly lucky to have them in my life.

TABLE OF CONTENTS

LIST OF TABLES

LIST OF FIGURES

NOMENCLATURE

ARS = Analysis response surface

A'_{req} = Minimum required cross sectional area for the component to carry the service loading without failure

A_0 = Load carrying area if there is no variability and no safety measures

α_1, α_2 = Coefficient of thermal expansion along and transverse to fiber direction

b_e = Bound of error

β = Reliability index

C = Capacity of structure, for example, failure stress

CFD = Cumulative distribution function

CFR = Certification failure rate

CLT = Classical lamination theory

c.o.v. = Coefficient of variation

DRS = Design response surface

Δ^* = Relative change in the characteristic stress σ^* corresponding to a relative change of Δ in stress σ

e = Error factor

e_{fc} = Error in failure prediction at the coupon level

e_C = Error in capacity calculation

e_{fe} = Error in failure prediction at the element level

e_{fs} = Error in failure prediction at the structural level

e_{fT} = Total error in failure prediction

e_m = Error in material property prediction

e_P = Error in load calculation

e_R = Error in response calculation

e_σ = Error in stress calculation

e_t = Error in thickness calculation

e_{total} = Total error factor

e_w = Error in width calculation

e^A = Error in facture toughness assessment if traditional (averaging) method is used

e^{MM} = Error in facture toughness assessment if traditional (averaging) method is used

ER = Error reduction

E_1, E_2 = Young's modulus along and transverse to fiber direction

ε_1, ε_2 = Strains in the fiber direction and transverse to the fiber direction

f( ) = Probability density function of the failure stress

F( ) = Cumulative distribution function of the failure stress

FAA = Federal Aviation Administration

G = Strain energy release rate

G_C = Fracture toughness

G_{12} = Shear modulus

γ_{12} = Shear strain

k = Error multiplier

k_A, k_B = Tolerance coefficients for A-basis and B-basis value calculation

k_{dc} = Knock-down factor used to calculate allowable stress

K_I, K_{II} = Model I and II stress intensity factors, respectively

M = Number of simulations in the first stage of MCS

MCS = Monte Carlo simulation

MEF model = Multiple error factor model

N = Number of simulations in the second stage of MCS

N_x, N_y = Mechanical loading in x and y directions, respectively

n_c = Number of coupon tests

n_e = Number of structural element tests

p_{allow} = Allowable flight load

P = Load

PDF = Probability density function

PSF = Probability sufficiency factor

P_d = Design load according to the FAA specifications

P_f = Probability of failure of a component

P_f* = Approximate probability of failure of probabilistic design

P_{fd} = Probability of failure of deterministic design

P_F = Probability of failure of a system

$\overline{P}_c$ = Average probability of failure after certification test

$\overline{P}_{nc}$ = Average probability of failure before certification test

QC = Quality control for manufacturing

r_{et} = Ratio of failure stresses measured in test and its predicted value

R = Response of a structure, for example, stress

RMSE = Root mean square error

RSA = Response surface approximation

R^2_{adj} = Adjusted coefficient of multiple determination

ρ = Coefficient of correlation

s( ) = Probability density function of the stress

SEF model = Single error factor model

S_c = Additional company safety factor

S_{cl} = Additional company safety factor if the failure stress measured in element tests are lower than the predicted failure stress

S_{ch} = Additional company safety factor if the failure stress measured in element tests are higher than the predicted failure stress

S_{fe} = Total safety factor added during structural element tests

S_{FL} = Load safety factor of 1.5 (FAA specification)

S_F = Total safety factor

σ = Stress

σ^* = Characteristic stress

σ_a = Allowable stress

σ_f = Failure stress

t = Thickness

v_t = Variability in built thickness

v_w = Variability in built width

V_R = Coefficient of variation

w = Width

W = Weight

W_d = Weight of the deterministic design

Φ = Cumulative distribution function of the standard normal distribution

ψ = Mode-mixity angle

Subscripts

act = The value of the relevant quantity in actual flight conditions

built = Built value of the relevant quantity, which is different than the design value due to errors in construction

calc = Calculated value of the relevant quantity, which is different from the true value due to errors

cert = The value of the relevant quantity after certification test

d = Deterministic design

design = The design value of the relevant quantity

spec = Specified value of the relevant qunatity

target = Target value of the relevant quantity

true = The true value of the relevant quantity

worst = The worst value of the relevant quantity

W = Wing

T = Tail

Subscripts

ave = Average value of the relevant quantity

ini = Initial value of the relevant quantity

upd = Updated value of the relevant quantity

U = Upper limit of the relevant quantity

L = Lower limit of the relevant quantity

Abstract of Dissertation Presented to the Graduate School
of the University of Florida in Partial Fulfillment of the
Requirements for the Degree of Doctor of Philosophy

AIRCRAFT STRUCTURAL SAFETY: EFFECTS OF EXPLICIT AND IMPLICIT SAFETY MEASURES AND UNCERTAINTY REDUCTION MECHANISMS

By

Erdem Acar

August 2006

Chair: Raphael T. Haftka
Cochair: Bhavani V. Sankar
Major Department: Mechanical and Aerospace Engineering

Aircraft structural safety is achieved by using different safety measures such as safety and knockdown factors, tests and redundancy. Safety factors or knockdown factors can be either explicit (e.g., load safety factor of 1.5) or implicit (e.g., conservative design decisions). Safety measures protect against uncertainties in loading, material and geometry properties along with uncertainties in structural modeling and analysis. The two main objectives of this dissertation are: (i) Analyzing and comparing the effectiveness of structural safety measures and their interaction. (ii) Allocating the resources for reducing uncertainties, instead of living with the uncertainties and allocating the resources for heavier structures for the given uncertainties.

Certification tests are found to be most effective when error is large and variability is small. Certification testing is more effective for improving safety than increased safety factors, but it cannot compete with even a small reduction in errors. Variability reduction is even more effective than error reduction for our examples.

The effects of structural element tests on reducing uncertainty and the optimal choice of additional knockdown factors are explored. We find that instead of using implicit knockdown factors based on worst-case scenarios (current practice), using test-dependent explicit knockdown factors may lead weight savings. Surprisingly, we find that a more conservative knockdown factor should be used if the failure stresses measured in tests exceeds predicted failure stresses in order to reduce the variability in knockdown factors generated by variability in material properties.

Finally, we perform probabilistic optimization of a wing and tail system under limited statistical data for the stress distribution and show that the ratio of the probabilities of failure of the probabilistic design and deterministic design is not sensitive to errors in statistical data. We find that the deviation of the probabilistic design and deterministic design is a small perturbation, which can be achieved by a small redistribution of knockdown factors.

CHAPTER 1
INTRODUCTION

Motivation

Traditionally, the design of aerospace structures relies on a deterministic design (code-based design) philosophy, in which safety factors (both explicit and implicit), conservative material properties, redundancy and certification testing are used to design against uncertainties. An example of explicit safety factor is the load safety factor of 1.5 (FAR 25-303), while the conservative decisions employed while updating the failure stress allowables based on structural element tests are examples for implicit safety factors. In the past few years, however, there has been growing interest in applying probabilistic methods to design of aerospace structures (e.g., Lincoln 1980, Wirsching 1992, Aerospace Information Report of SAE 1997, Long and Narciso 1999) to design against uncertainties by effectively modeling them.

Even though probabilistic design is a more efficient way of improving structural safety than deterministic design, many engineers are skeptical of probability of failure calculations of structural designs for the following reasons. First, data on statistical variability in material properties, geometry and loading distributions are not always available in full (e.g., joint distributions), and it has been shown that insufficient information may lead to large errors in probability calculations (e.g., Ben-Haim and Elishakoff 1990, Neal *et al*. 1992). Second, the magnitude of errors in calculating loads and predicting structural response is not known precisely, and there is no consensus on how to model these errors in a probabilistic setting. As a result of these concerns, it is

possible that transition to probability based design will be gradual. An important step in this transition is to understand the way safety is built into aircraft structures now, via deterministic design practices.

One step taken in the transition to probabilistic design is in the definition of conservative material properties (A-basis or B-basis material property values depending on the failure path in the structure) by the Federal Aviation Administration (FAA) regulation (FAR 25.613). A-basis material property is one in which 99 percent of the material property distribution is better than the design value with a 95 percent level of confidence, and B-basis material property is one in which 90 percent of the material property distribution is better than the design value with a 95 percent level of confidence. The use of conservative material properties is intended to protect against variability in material properties.

In deterministic design the safety of a structure is achieved through safety factors. Even though some safety factors are explicitly specified, others are implicit. Examples of explicit safety factors are the load safety factor and material property knock-down values. The FAA regulations require a load safety factor equal to 1.5 for aircraft structures (FAR 25-303). The load safety factor compensates for uncertainties such as uncertainty in loading and errors in load calculations, structural stress analysis, accumulated damage, variations in material properties due to manufacturing defects and imperfections, and variations in fabrication and inspection standards. Safety factors are generally developed from empirically based design guidelines established from years of structural testing of aluminum structures. Muller and Schmid (1978) review the historical evolution of the load safety factor of 1.5 in the United States. Similarly, the use of A-basis or B-basis

material properties leads to a knock-down factor from the average values of the material properties measured in the tests. Note that these knock-down factors depend on the number of tests, because they compensate for both variability in material properties and uncertainty due to a finite number of tests.

As noted earlier, an important step in transition to probabilistic design is to analyze the probabilistic impact of the safety measures used in deterministic design. This probabilistic analysis requires quantification of uncertainties encountered in design, manufacturing and actual service conditions of the aircraft structures.

A good analysis of different sources of uncertainty in engineering modeling and simulations is provided by Oberkampf *et al*. (2000, 2002). These papers also supply good literature reviews on uncertainty quantification and divide the uncertainty into three types: variability, uncertainty, and error. In this distinction, variability refers to aleatory uncertainty (inherent randomness), uncertainty refers to epistemic uncertainty (due to lack of knowledge), and error is defined as a recognizable deficiency in any phase or activity of modeling and simulation that is not due to lack of knowledge.

To simplify the treatment of uncertainty control, in this dissertation we combine the unrecognized (epistemic) and recognized error in the classification of Oberkampf *et al*. and name it error. That is, we use a simple classification that divides the uncertainty in the failure of a structural member into two types: errors and variability. Errors reflect inaccurate modeling of physical phenomena, errors in structural analysis, errors in load calculations, or deliberate use of materials and tooling in construction that are different from those specified by the designer. Errors affect all the copies of the structural components made and are therefore fleet-level uncertainties. Variability, on the other

hand, reflects the departure of material properties, geometry parameters or loading of an individual component from the fleet-average values and hence are individual uncertainties.

Modeling and quantification of variability are much easier compared to that of error. Improvements in tooling and construction or application of tight quality control techniques can reduce variability. Quantification of variability control can be easily done by statistical analysis of records taken throughout process of quality control. However, quantification of errors is not as easy, because errors are largely not known before a structure is built. So, errors can only be quantified after the structure has been built. Errors can be controlled by improving accuracy of load and stress calculations, by using more sophisticated analysis and failure prediction techniques or by testing of structural components.

Testing of aircraft structural components is performed in a building block type of approach starting with material characterization tests, followed by testing of structural elements and including a final certification test. Testing of structures is discussed in detail in the next chapter.

The comparison of deterministic design and probabilistic design can be performed in many views. First of all, input and output variables of deterministic design are all deterministic values, while input and output variables of probabilistic design are random (along with some deterministic variables, of course). Here, on the other hand, we compare probabilistic design and deterministic design in terms of use of safety factors. In deterministic design uniform safety factors are used; that is, the same safety factor is used for all components of a system. However, probabilistic design allows using variable

safety factors through allowing risk and reliability allocation between different components. That is, instead of using the same safety factor for all components, probabilistic design allows to use higher factors for components or failure modes that can be controlled with low weight expenditure (Yang, 1989). This means the failure modes with small scatter and lightweight components. In addition, probabilistic design allows a designer to trade off uncertainty control for lower safety factors. That is, by reducing uncertainty, the designer can avoid using high safety factors in the design and thereby can reduce the weight of the structural system. This design paradigm allows the designer to allocate risk and reliability between different components in a rational way to achieve a safer design for a fixed weight compared to the deterministic design.

Objectives

There are two main objectives of this dissertation. The first is to analyze and compare the effectiveness of safety measure that improve structural safety such as safety factors (explicit or implicit), structural tests, redundancy and uncertainty reduction mechanisms (e.g., improved structural analysis and failure prediction, manufacturing quality control). The second objective is to explore the advantage of uncertainty reduction mechanisms (e.g., improved structural analysis and failure prediction, tighter manufacturing quality control) versus safety factors. That is, we consider the possibility of allocating the resources for reducing uncertainties, instead of living with the uncertainties and allocating the resources for designing the aircraft structures for the given uncertainties.

We aim to analyze the effectiveness of safety measures taken in deterministic design methodology and investigate the interaction and effectiveness of these safety measures with one another and also with uncertainties. In particular, the effectiveness of

uncertainty reduction mechanisms is analyzed and compared. The uncertainty reduction mechanisms considered in this dissertation are reduction of errors by improving the accuracy of structural analysis and failure prediction (analytically or through tests), and reduction of variability in failure stress as a result of tighter quality control.

We explore the optimal choice of additional company safety factors used on top of the FAA regulation safety factors by using probabilistic design, which provides a rational way in the analysis. Additional company safety factors we consider are the conservative decisions of aircraft companies while updating the allowable stresses based on the results of structural element tests.

We perform probabilistic design optimization for the case of limited statistical data on stress distribution and show that when the probabilistic design is achieved by taking the deterministic design as a starting point, the ratio of probabilities of failure of the probabilistic design and deterministic design is not sensitive to errors due to limited statistical data, which would lead to substantial errors in the probabilistic design if the probabilistic design starts from scratch. In addition, we propose a probabilistic design methodology in which the probability of failure calculation is confined only to stress limits, thereby eliminating the necessity for assessment of stress distribution that usually requires computationally expensive finite element analyses.

Methodology

Probability of failure calculation of structures can be performed by using either analytical techniques or simulation techniques. Analytical methods are more accurate but for complex systems they may not be practical. Simulation techniques include direct Monte Carlo simulation (MCS) as well as many variance-reduction methods including

stratified sampling, importance sampling, and adaptive importance sampling (Ayyub and McCuen 1995).

In probabilistic design of structures, the use of inverse reliability measures helps a designer to have an easy estimate of the change in structural weight from the values of probabilistic performance measure and its target value as well as computational advantages (Ramu *et al*. 2004). Amongst those measures we use probabilistic sufficiency factor (PSF) developed by Qu and Haftka (2003).

Here we consider a simplified design problem for illustration purposes, so that the reliability analysis can be performed by analytical means. The effect of testing then can be analyzed by using Bayesian approach. The Bayesian approach has special importance in engineering design where the available information is limited and it is often necessary to make subjective decisions. Bayesian updating is used to obtain the updated (or posterior) distribution of a random variable upon combining the initial (or prior) distribution with new information about the random variable. The detailed theory and procedures for applying Bayesian methods in reliability and risk analysis can be found in texts by Morgan (1968) and Martz and Waller (1982).

Outline

A literature survey on the historical evolution of probabilistic design, comparison of deterministic design and probabilistic design practices, uncertainty control measures and testing of aircraft structures is given in Chapter 2.

Chapter 3 investigates the effects of error, variability, safety measures and tests on structural safety of aircraft. A simple example of point stress design and a simple error model are used to illustrate the effects of several safety measures taken in aircraft design: safety factors, conservative material properties, and certification tests. This chapter serves

as the opening chapter; therefore the analysis and the number of safety measures are kept at a minimum level. For instance, only certification tests are included in the analysis. The effects of coupon tests and structural element tests are delayed until Chapter 7. The simplifying assumptions in Chapter 3 allow us to perform analytical calculations for probability of failure and Bayesian updating. The interactions of the safety measures with one another and also with errors and variabilities are investigated. For instance, we find that the certification tests are most effective when errors are large and variabilities are small. We also find that as safety measures combine to reduce the probability of failure, our confidence in the probability of failure estimates is reduced.

Chapter 4 extends the analysis presented in Chapter 3 by delivering the following refinements. The effectiveness of safety measures is compared with one another in terms of safety improvement and weight savings. Structural redundancy, a safety measure which is omitted in Chapter 3, is also included in the analysis. The simple error model used in Chapter 3 is replaced with a more detailed error model in which we consider individual error components in load calculation, stress calculation, material properties and geometry parameters including the effect of damage. The analysis in Chapter 4 enables us to discover that while certification testing is more effective than increased safety factors for improving safety, it cannot compete with even a small reduction in errors. We also find that variability reduction is even more effective than error reduction.

Realizing in Chapter 4 how powerful uncertainty reduction mechanisms are, we analyze the tradeoffs of uncertainty reduction mechanisms, structural weight and structural safety in Chapters 5 and 6. The effect of error reduction (due to improved failure prediction model) on increasing the allowable flight loads of existing aircraft

structures is investigated in Chapter 5. The analysis is performed for a sandwich panel because the improved model is developed by Prof. Bhavani Sankar (co-chair of the advisory committee for this dissertation) so that we had good access to the details of experiments and computations. We find that the improved modeling can increase the allowable load of a sandwich panel on average by about 13 percent without changing the safety level of the panel when deterministic design principles is followed. The use of probabilistic design is found to double the load increase.

Similarly to improvements of accuracy in failure predictions, the improvements in the accuracy of structural analysis also lead to error reduction. The improved structural analysis through taking the chemical shrinkage of composite laminates is considered as the error reduction mechanism in Chapter 6. The work by Qu *et al*. (2003), which explored the effect of variability reduction through quality control, is extended in Chapter 6 to investigate the tradeoffs of error and variability reduction mechanisms for reducing the weight of the composite laminates at cryogenic temperatures. Tradeoff plots of uncertainty reduction mechanisms, probability of failure and weight are generated that enable a designer to choose the optimal uncertainty control mechanism combination to reach a target probability of failure with minimum cost.

Chapter 7 finalizes the analysis of effects of explicit and implicit knockdown factors and uncertainty control mechanisms. In particular, Chapter 7 analyzes the optimal choice of the knockdown factors. These knockdown factors refer to conservative decisions of aircraft companies in choice of material properties and while updating the allowable stresses based on the results of structural element tests. We find that instead of using implicit knockdown factors based on worst-case scenarios (current practice), using

test-dependent explicit knockdown factors may lead weight savings. Surprisingly, we find that a more conservative knockdown factor should be used if the failure stresses measured in tests exceeds predicted failure stresses in order to reduce the variability in knockdown factors generated by variability in material properties. In addition, the effects of coupon tests, structural element tests and uncertainty control mechanisms (such as error reduction by improved structural modeling or improved failure prediction, variability reduction by tighter quality control) on the choice of company safety factors are investigated. Using a simple cost function in terms of structural weight, we show that decisions can be made whether to invest resources on coupon tests, structural element tests, uncertainty reduction mechanisms or extra structural weight.

The analyses presented in Chapters 3-7 show how probabilistic design can be exploited to improve aircraft structural safety by allowing a rational analysis of interactions of safety and knockdown factors and uncertainty reduction mechanisms. There are, however, two main reasons for reluctance of engineers for pursuing the probabilistic design: the sensitivity of probabilistic design to limited statistical data and computational expense associated to the probabilistic design. Besides, Chapters 3-7 include analyses of a single aircraft structural component, so in Chapter 8 the probabilistic design of an aircraft structural system is presented. We show in Chapter 8, by use of probabilistic design of a representative wing and tail system, that errors due to limited statistical data affect the probability of failure of both probabilistic and deterministic designs, but the ratio of these probabilities is quite insensitive to even very large errors. In addition, to alleviate the problem of computational expense, a probabilistic design optimization method is proposed in which the probability of failure

calculation is limited to failure stresses to dispense with most of the expensive structural response calculations (typically done via finite element analysis). The proposed optimization methodology is illustrated with the design of the wing and tail system. Chapter 8 reveals that the difference between probabilistic design and deterministic design is a small perturbation, which can be achieved by choosing the additional knockdown factors through probabilistic design, instead of choosing them based on experience. In addition, the proposed approximate method is found to lead to similar re-distribution of material between structural components and similar system probability of failure.

Finally, the dissertation culminates with Chapter 9, where the concluding remarks are listed.

CHAPTER 2
LITERATURE REVIEW

The literature review in this chapter first compares deterministic and probabilistic design methodologies. Then, we review structural safety analysis, followed by probability of failure estimation techniques. Next, reliability-based design optimization is reviewed. Then, uncertainty classifications available in the literature are discussed followed by our simplified classification based on simplifying the analysis of uncertainty reduction measures. Finally, the utilization of structural tests in probabilistic design is reviewed.

Probabilistic vs. Deterministic Design

Aircraft structural design still relies on the Federal Aviation Administration (FAA) deterministic design code. In deterministic design, conservative material properties are used and safety factors are introduced to protect against uncertainties. The FAA regulations (FAR-25.613) state that conservative material properties are characterized as A-basis or B-basis values. Detailed information on these values was provided in Chapter 8 of Volume 1 of Composite Materials Handbook (2002). The safety factor compensates for uncertainties such as uncertainty in loading and errors in load calculations, errors in structural stress analysis and accumulated damage, variations in material properties due to manufacturing defects and imperfections, and variations in fabrication and inspection standards. Safety factors are generally developed from empirically based design guidelines established from years of structural testing and flight experience. In transport aircraft design, the FAA regulations state the use of safety factor of 1.5 (FAR-25.303).

Muller and Schmid (1978) reviewed the historical evolution of the 1.5 factor of safety in the United States.

On the other hand, probabilistic design methodology deals with uncertainties by the use of statistical characterization of uncertainties and attempts to provide a desired reliability in the design. The uncertainties of individual design parameters and loads are modeled by appropriate probability density functions. The credibility of this approach depends on several factors such as the accuracy of the analytical model used to predict the structural response, the accuracy of the data and the probabilistic techniques employed. Examples of the use of probabilistic design in aerospace applications include the following.

Pai *et al*. (1990, 1991 and 1992) performed probabilistic structural analysis of space truss structures for a typical space station. Murthy and Chamis (1995) performed probabilistic analysis of composite aircraft structure based on first ply failure using FORM[*]. The probabilistic methodology has shown some success in the design of composite structures where parameter uncertainties are relatively well known. For example, the IPACS (Integrated Probabilistic Assessment of Composite Structures) computer code was developed at NASA Glenn Research Center (Chamis and Murthy 1991). Fadale and Sues (1999) performed reliability-based design optimization of an integral airframe structure lap joint. A probabilistic stability analysis for predicting the buckling loads of compression loaded composite cylinders was developed at Delft University of Technology (Arbocz *et al*. 2000).

[*] The FORM method is discussed later in this chapter.

Although probabilistic design methodology offers the potential of safer and lighter designs than deterministic design, transition from deterministic design to probabilistic design is difficult to achieve. Zang *et al*. (2002) discussed the reasons for this difficulty, and some of these reasons are given below.

- Industry feels comfortable with traditional design methods.
- Few demonstrations of the benefits of probabilistic design methods are available.
- Current probabilistic design methods are more complex and computationally expensive than deterministic methods.
- Characterization of structural imperfections and uncertainties necessary to facilitate accurate analysis and design of the structure is time-consuming and is highly dependent on structural configuration, material system, and manufacturing processes.
- Effective approaches for characterizing model form error are lacking.
- Researchers and analysts lack training in statistical methods and probabilistic assessment.

Structural Safety Analysis

In probabilistic design, the safety of a structure is evaluated in terms of its probability of failure P_f. The structures are designed such that the probability of failure of the structure is kept below a pre-specified level. The term reliability is defined in terms of probability of failure such that

$$Reliability = 1 - P_f \tag{2.1}$$

A brief history of development of the methods for probability of failure calculation for structures was presented in a report by Wirsching (1992). As Wirsching noted, the development of theories goes back some 50 to 60 years.

The modern era of probabilistic design started with the paper by Fruedenthal (1947). Most of the ingredients of structural reliability such as probability theory,

statistics, structural analysis and design, quality control existed prior to that time; however, Fruedenthal was the first to put them together in a definitive and compressive manner. The development of reliability theory progressed in 1950s and 1960s. There are three cornerstone papers in 1960's. The first one is the paper by Cornell (1967), who suggested the use of a second moment method and demonstrated that Cornell's safety index could be used to derive set of factors on loads and resistance. However, Cornell's safety index had a problem of invariance in that it was not constant when the problem was reformulated in a mechanically equivalent way. Hasofer and Lind (1974) defined a generalized safety index which was invariant to mechanical formulation. The third paper is the one by Turkstra (1970), who presented structural design as a problem of decision making under uncertainty and risk. More recent papers are sophisticated extensions of these papers, and some of them are referenced in the following sections.

Probability of Failure Estimation

This section reviews the literature on probability of failure estimation. First, analytical calculation of probability of failure is discussed, followed by moment-based methods and simulation techniques.

Analytical calculation of probability of failure

In its most general form, the probability of failure can be expressed as

$$P_f = \int_{G(\mathbf{x})\le 0} \cdots \int f_{\mathbf{X}}(\mathbf{x}) d\mathbf{x} \tag{2.2}$$

where $G(\mathbf{x})$ is the limit-state function whose negative values corresponds to failure and $f_{\mathbf{X}}(\mathbf{x})$ is the joint probability density function for the vector $\mathbf{X}$ of random variables. The analytical calculation of this expression is challenging due to the following reasons

(Melchers 1999). First, the joint probability density function $f_{\mathbf{X}}(\mathbf{x})$ is not always readily obtainable. Second, for the cases when $f_{\mathbf{X}}(\mathbf{x})$ is obtainable, the integration over the failure domain is not easy. The calculation of probability of failure can be made more tractable by simplifying (1) the limit-state definition, (2) the integration process, and (3) the integrand $f_{\mathbf{X}}(\mathbf{x})$.

Moment-based techniques

When the calculation of limit-state is expensive, moment-based techniques such as First Order Reliability Method (FORM) or Second Order Reliability Method (SORM) are used (Melchers, 1999). The basic idea behind these techniques is to transform the original random variables into a set of uncorrelated standard normal random variables, and then approximate the limit-state function linearly (FORM) or quadratically (SORM) about the most probable failure point (MPP). The probability of failure of the component is estimated in terms of reliability index β such that

$$P_f = \Phi(-\beta) \tag{2.3}$$

where Φ is the cumulative distribution function of a standard normal variable.

The first paper on the use of FORM is probability of failure calculation appears to be Hasofer and Lind's (1974). There exist enormous amount of papers on the use of FORM. The pioneer papers include Rackwitz and Fiessler (1978), Hohenbichler and Rackwitz (1983), Gollwitzer and Rackwitz (1983).

FORM is usually accurate for limit state functions that are not highly nonlinear. SORM has been proposed to improve the reliability estimation by using a quadratic approximation of the limit state surface. Some papers on the use of SORM include

Fiessler *et al*. (1979), Breitung (1984), Der Kiureghian *et al*. (1987), Hohenbichler *et al*. (1987), Der Kiureghian and De Stefano (1991), Koyluoglu and Nielsen (1994) and Zhao and Ono (1999).

Simulation techniques

For most problems the number of variables in the problem definition is high, so the analytical calculation of the integral in Eq. (2.2) requires challenging multidimensional integration. Also the moment based approximations gives inaccurate results for high number of random variables (Melchers 1999). Under such conditions, simulation techniques such as Monte Carlo simulations (MCS) are used to compute the probability of failure.

In MCS technique, samples of the random variables are generated according to their probabilistic distributions and then failure condition is checked. The probability of failure P_f can be estimated by

$$P_f = \frac{N_f}{N} \tag{2.4}$$

where N_f is the number of simulations leading to failure and N is the total number of simulations. The statistical accuracy of the probability of failure estimation is commonly measured by its coefficient of variation $c.o.v.\left(P_f\right)$ as

$$c.o.v.(P_f) = \frac{\sqrt{\dfrac{P_f\,(1-P_f)}{N}}}{P_f} = \sqrt{\frac{(1-P_f)}{N\,P_f}} \tag{2.5}$$

From Eqs. (2.4) and (2.5) it is seen that a small probability of failure will require a very large number of simulations for acceptable accuracy. This usually results in an increase in computational cost. When limit-state function calculations are obtained

directly from analysis, then computational cost of MCS is not sensitive to the number of variables. When surrogate models are used, on the other hand, the computational cost of MCS is dependent on the number of variables. To overcome the deficiency of MCS, several more efficient alternative sampling methods are introduced. Ayyub and McCuen (1995) supplied basic information and good references for these sampling techniques. Some useful references taken from Ayyub and McCuen (1995) are the followings: Importance sampling (Madsen *et al*., 1986, Melchers, 1989), stratified sampling (Law and Kelton 1982, Schuller *et al*. 1989), Latin hypercube sampling (Iman and Canover 1980, Ayyub and Lai 1989), adaptive importance sampling (Busher 1988, Karamchandani *et al*. 1989, Schuller *et al*. 1989), conditional expectation (Law and Kelton 1982, Ayyub and Haldar 1984), antithetic variates (Law and Kelton 1982, Ayyub and Haldar 1984).

In this study, we mainly deal with problems with simple limit-state functions. For these simple cases the integrand $f_{\mathbf{X}}(\mathbf{x})$ can easily be obtained when the random variables are statistically independent. The beneficial properties of normal and lognormal distributions are utilized for the variables with small coefficients of variations. Approximate analytical calculations of probability of failure are checked with Monte Carlo simulations to validate the acceptability of assumptions. When limit-state functions are complex, Monte Carlo simulations are used to calculate the probability of failure.

Separable Monte Carlo simulations

As noted earlier, when estimating very low probabilities, the number of required samples for MCS can be high, thus MCS becomes a costly process. In most structural problems, the failure condition may be written as response exceeding capacity. When the

response and capacity are independent, it may be possible to analyze them separately with a moderate sample size, and still be able to estimate very low probabilities of failure. This is due to the fact that most failures do not involve extreme values of response or capacity but instead moderately high response along with moderately low capacity. Therefore, to bypass the requirement of sampling the extreme tail of the limit-state function, the variables could be considered independently, by separating the response and the capacity, as discussed by Melchers (1999, Chapter 3). A good analysis of efficiency and accuracy of separable Monte Carlo simulations can be found in Smarslok *et al*. (2006).

The common formulation of the structural failure condition is in the form of a stress exceeding the material limit. This form, however, does not satisfy the separability requirement. For example, the stress depends on variability in material properties as well as design area, which reflects errors in the analysis process. In that case, the limit-state function can still be re-formulated in a separable form. In this dissertation we re-write the limit-state in terms of the required area (depends only on variabilities) and built area (depends only on errors) to bring the limit state to separable form (see Chapter 4).

Response surface approximations

Response surface approximations (RSA) can be used to obtain a closed-form approximation to the limit state function to facilitate reliability analysis. Response surface approximations usually fit low-order polynomials to the structural response in terms of random variables. The probability of failure can then be calculated inexpensively by Monte Carlo simulation or by FORM or SORM using the fitted polynomials.

Response surface approximations can be applied in different ways. One approach is to construct local response surfaces in the MPP region that contributes most to the

probability of failure of the structure. Bucher and Bourgund (1990), Rajashekhar and Ellingwood (1993), Koch and Kodiyalam (1999), Das and Zheng (2000a, 2000b) and Gayton, Bourinet and Lemaire (2003) used local response surfaces.

Another approach is to construct global response surface over the entire range of random variables. The examples include Fox (1994, and 1996), Romero and Bankston (1998), Qu *et al*. (2003), Youn and Choi (2004) and Kale *et al*. (2005).

Reliability-Based Design Optimization

Design optimization under a probability of failure constraint is usually referred as reliability-based design optimization (RBDO). The basic structure of an RBDO problem is stated as

$$\begin{aligned} &\min\ f \\ &s.t.\quad P \le P_{target} \end{aligned} \tag{2.6}$$

where f is the objective function (for most problems it is weight), and P and P_{target} are the probabilistic performance function and the target value for it. The probabilistic performance function can be probability of failure P_f, reliability index β or an inverse reliability measure such as probabilistic sufficiency factor, PSF.

Double loop (Nested) RBDO

Conventional RBDO approach is formulated as a double-loop optimization problem, where an outer loop performs the design optimization, while an inner loop optimization is also used for estimating probability of failure (or another probabilistic performance function). The reliability index approach (RIA) is the most straightforward approach. In RIA, the probability of failure is usually calculated via FORM, which is an iterative process an so computationally expensive and sometimes troubled by

convergence problems (Tu e*t al*. 1999). To reduce the computational cost of double loop approach, various techniques has been proposed, which can be divided into two categories: (i) techniques that improve the efficiency of uncertainty analysis methods, such as the methods of fast probability integration (Wu 1994) and two-point adaptive nonlinear approximations (Grandhi and Wang 1998); (ii) techniques that modify the formulation of probabilistic constraints, for instance, using inverse reliability measures, such as the performance measure approach (Tu *et al*. 1999), probabilistic sufficiency factor (Qu and Haftka 2003).

Inverse reliability measures are based on margin of safety or safety factors, which are safety measures in deterministic design. The safety factor is usually defined as the ratio of structural resistance (e.g., failure stress) to structural response (e.g., stress). Safety factors permit the designer to estimate the change in structural weight to satisfy a target safety factor requirement. In probabilistic design, however, the difference between the probabilistic performance measure and its target value does not provide the designer with an estimate of the required change in structural weight. Inverse safety measures thus help the designer to easily estimate the change in structural weight from the values of probabilistic performance measure and its target value and the inverse safety measures also improve the computational efficiency (Qu and Haftka 2004). A good analysis and survey on safety factor and inverse reliability measures was presented by Ramu *et al*. (2004).

Single loop RBDO

Single loop formulation avoids nested loops of optimization and reliability assessment. Some single loop formulations are based on formulating the probabilistic constraints as deterministic constraints by either approximating the Karush-Kuhn-Tucker

conditions at the MPP or defining a relationship between probabilistic design and safety factors of deterministic design (e.g., Chen *et al*. 1997, Kuschel and Rackwitz 2000, Wu *et al*. 2001, Qu *et al*. 2004, Liang *et al*. 2004). Single loop formulation increases the efficiency by allowing the solution to be infeasible before convergence and satisfying the probability constraints only at the optimum. There exist also singe loop formulations that performs optimization and reliability assessment sequentially (e.g., Royset *et al*. 2001, Du and Chen 2004). Sequential optimization and reliability assessment (SORA) of Du and Chen (2004), for instance, decouples the optimization and reliability assessment by separating each random design variable into a deterministic component, which is used in a deterministic optimization, and a stochastic component, which is used in reliability assessment.

Error and Variability

Uncertainty Classification

Over years researchers proposed many different classifications for uncertainty. For instance, Melchers (1999) divided uncertainty into seven types: phenomenological uncertainty, decision uncertainty, modeling uncertainty, prediction uncertainty, physical uncertainty, statistical uncertainty and human error. Haimes *et al*. (1994) and Hoffman and Hammonds (1994) distinguished uncertainty into two types: uncertainty (epistemic part) and variability (aleatory part). Epistemic uncertainties arise from lack of knowledge about the behavior of a phenomenon. They may be reduced by review of literature, expert consultation, close examination of data and further research. Tools such as scoring system, expert system and fish-bone diagram can also help in reducing epistemic uncertainties. Aleatory uncertainties arise from possible variation and random errors in

the values of the parameters and their estimates. They can be reduced by using reliable manufacturing tools and quality control measures.

Oberkampf *et al*. (2000, 2002) provided a good analysis of different sources of uncertainty in engineering modeling and simulations, supply good literature review on uncertainty quantification and divide the uncertainty into three types: variability, uncertainty and error. The classification provided by Oberkampf *et al*. is discussed in the Motivation section of Chapter 1.

Reliability Improvement by Error and Variability Reduction

Before designing a new structure, material properties and loading conditions are assessed. The data is collected to constitute the probability distributions of material properties and loads. The data on material properties is obtained by performing tests on batches of materials and also from the material manufacturer. To reduce the variability in material properties quality controls may be applied. Qu *et al*. (2003) analyzed the effect of application of quality controls over material allowables in the design of composite laminates for cryogenic environments. They found that employing quality control reduces the probability of failure significantly, allowing substantial weight reduction for the same level of safety.

Similarly, before a newly designed structure is put into service, its performance under predicted operational conditions is evaluated by collecting data. The data is used to validate the initial assumptions being made through the design and manufacturing processes to reduce error in those assumptions. This can be accomplished by the use of Bayesian statistical methods to modify the assumed probability distributions of error. The present author will investigate this issue on following the chapters.

After the structure is put into service inspections are performed to detect the damage developed in the structure. Hence, the inspections are another form of uncertainty reduction. The effect of inspections in the safety of structures was analyzed (among others) by Harkness *et al*. (1994), Provan *et al*. (1994), Fujimoto *et al*. (1998), Kale *et al*. (2003) and Acar *et al*. (2004b).

Testing and Probabilistic Design

In probabilistic design, models for predicting uncertainties and performance of structures are employed. These models involve idealizations and approximations; hence, validation and verification of these models is necessary. The validation is done by testing of structures, and verification is done by using more detailed models.

Historical development of testing of structures was given in the papers by Pugsley (1944) and Whittemore (1954). A literature survey of load testing by Hall and Lind (1979) presented many uses for load testing in design and safety validation of structures. Conventional "design by calculation" relies upon tensile coupon tests to estimate material strength (Hall and Tsai, 1989). Coupon testing is a destructive test to measure loads and displacements at failure. On the other hand, proof load testing is not a destructive test in which the structure is tested at a fixed load to measure resistance level of the structure. Proof load testing in a variety of applications was studied by several authors such as Barnett and Herman (1965), Shinozuka (1969), Yang (1976), Fujino and Lind (1977), Rackwitz and Schurpp (1985) and Herbert and Trilling (2006).

Jiao and Moan (1990) illustrated a methodology for probability density function updating of structural resistance by additional events such as proof loading and non-destructive inspection by utilizing FORM or SORM methods. Ke (1999) proposed an approach that specifically addressed the means to design component tests satisfying

reliability requirements and objectives by assuming that the component life distribution follows Weibull distribution. Zhang and Mahadevan (2001) developed a methodology that utilizes Bayesian updating to integrate testing and analysis for test plan determination of a structural components. They considered two kinds of tests: failure probability estimation and life estimation tests. Soundappan *et al*. (2004) presented a method for designing targeted analytical and physical tests to validated reliability of structures obtained from reliability based designs. They found that the optimum number of tests for a component is nearly proportional to the square root of probability of failure.

Guidelines for testing of composite materials were presented in Volume 1, Chapter 2 of Composite Materials Handbook (2002). The following are quoted from this source (pages 2-1 and 2-2). Analysis alone is generally not considered adequate for substantiation of composite structural designs. Instead, the "building-block approach" to design development testing is used in concert with analysis. This approach is often considered essential to the qualification/certification of composite structures due to the sensitivity of composites to out-of-plane loads, the multiplicity of composite failure modes and the lack of standard analytical methods. The building-block approach is also used to establish environmental compensation values applied to full-scale tests at room-temperature ambient environment, as it is often impractical to conduct these tests under the actual moisture and temperature environment. Lower-level tests justify these environmental compensation factors. Similarly, other building-block tests determine truncation approaches for fatigue spectra and compensation for fatigue scatter at the full-scale level. The building-block approach is shown schematically in Figure 2.1.

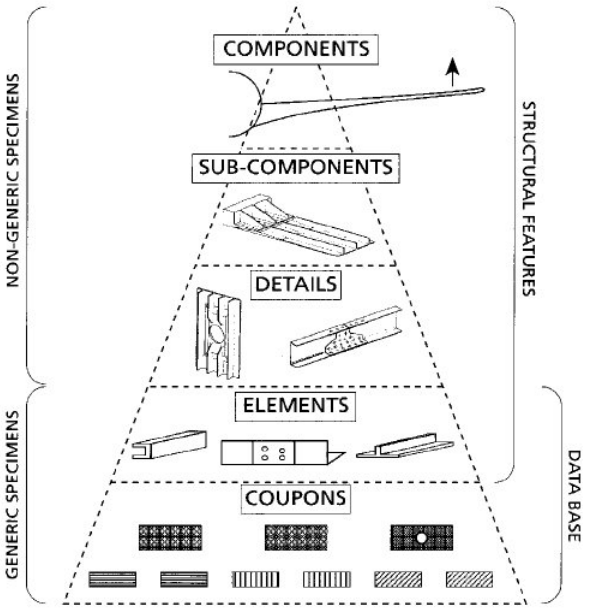

Figure 2-1. Building block approach (Reprinted, with permission, from MIL 17- The Composite Materials Handbook, Vol. 1, Chapter 2, copyright ASTM International, 100 Barr Harbor Drive, West Conshohocken, PA 19428)

The approach can be summarized in the following steps:

1. Generate material basis values and preliminary design allowables.
2. Based on the design/analysis of the structure, select critical areas for subsequent test verification.
3. Determine the most strength-critical failure mode for each design feature.
4. Select the test environment that will produce the strength-critical failure mode. Special attention should be given to matrix-sensitive failure modes (such as compression, out-of-plane shear, and bondlines) and potential "hot-spots" caused by out-of-plane loads or stiffness tailored designs.
5. Design and test a series of test specimens, each one of which simulates a single selected failure mode and loading condition, compare to analytical predictions, and adjust analysis models or design allowables as necessary.
6. Design and conduct increasingly more complicated tests that evaluate more complicated loading situations with the possibility of failure from several potential failure modes. Compare to analytical predictions and adjust analysis models as necessary.
7. Design (including compensation factors) and conduct, as required, full-scale component static and fatigue testing for final validation of internal loads and structural integrity. Compare to analysis.

As noted earlier, validation is done by testing of structures, and verification is done by using more detailed models. Detailed models may reduce the errors in analysis models; however errors in the uncertainty models cannot be reduced by this approach. In

addition, very detailed models can be computationally prohibitive. Similarly, while testing of structures reduces both the errors in response models and uncertainty models, it is expensive. Therefore, the testing of structures needs to be performed simultaneously with the structural design to reduce cost while still keeping a specified reliability level.

CHAPTER 3
WHY ARE AIRPLANES SO SAFE STRUCTURALLY? EFFECT OF VARIOUS SAFETY MEASURES

This chapter investigates the effects of error, variability, safety measures and tests on the structural safety of aircraft. A simple point stress design problem and a simple uncertainty classification are used. Since this chapter serves as the opening chapter, the level of analysis and the number of safety measures are kept at a minimum level. Safety measures considered in this chapter are the load safety factor of 1.5, the use of conservative material properties and certification test. Other safety measures such as structural redundancy, coupon and structural element tests will be included in the following chapters. Interaction of the considered safety measures with one another and their effectiveness with respect to uncertainties are also explored.

The work given in this chapter was also published in Acar *et al*. (2006a). My colleague Dr. Amit Kale's contribution to this work is acknowledged.

Introduction

In the past few years, there has been growing interest in applying probability methods to aircraft structural design (e.g., Lincoln 1980, Wirsching 1992, Aerospace Information Report of Society of Automotive Engineers 1997, Long and Narciso 1999). However, many engineers are skeptical of our ability to calculate the probability of failure of structural designs for the following reasons. First, data on statistical variability in material properties, geometry and loading distributions are not always available in full (e.g., joint distributions), and it has been shown that insufficient information may lead to

large errors in probability calculations (e.g., Ben-Haim and Elishakoff 1990, Neal *et al*. 1992). Second, the magnitude of errors in calculating loads and predicting structural response is not known precisely, and there is no consensus on how to model these errors in a probabilistic setting. As a result of these concerns, it is possible that transition to probability based design will be gradual. In such circumstances it is important to understand the impact of existing design practices on safety. This chapter is a first attempt to explore the effects of various safety measures taken during aircraft structural design using the deterministic design approach based on FAA regulations.

The safety measures that we include in this chapter are (i) the use of safety factors, (ii) the use of conservative material properties (A-basis), and (iii) the use of final certification tests. These safety measures are representative rather than all inclusive. For example, the use of A-basis properties is a representative measure for the use of conservative material properties. The safety measures (e.g., structural redundancy) are discussed in the following chapters. We use A-Basis value rather than B-basis because we did not include redundancy in this chapter. FAA suggests that (FAR 25.613) when there is a single failure path, A-Basis properties should be employed, but in case of multiple failure paths, B-Basis properties are to be used. In next chapter, for instance, we include structural redundancy in our analysis, so we use B-basis values in Chapter 4. The effect of the three individual safety measures and their combined effect on the probability of structural failure of the aircraft are demonstrated. We use Monte Carlo simulations to calculate the effect of these safety measures on the probability of failure of a structural component.

We start with a structural design employing all considered safety measures. The effects of variability in geometry, loads, and material properties are readily incorporated by the appropriate random variables. However, there is also uncertainty due to various errors such as modeling errors in the analysis. These errors are fixed but unknown for a given airplane. To simulate these epistemic uncertainties, we transform the error into a random variable by considering the design of multiple aircraft models. As a consequence, for each model the structure is different. It is as if we pretend that there are hundreds of companies (Airbus, Boeing, Bombardier, Embraer, etc.) each designing essentially the same airplane, but each having different errors in their structural analysis. This assumption is only a device to model lack of knowledge or errors in probabilistic setting. However, pretending that the distribution represents a large number of aircraft companies helps to motivate the probabilistic setting.

For each model we simulate certification testing. If the airplane passes the test, then an entire fleet of airplanes with the same design is assumed to be built with different members of the fleet having different geometry, loads, and material properties based on assumed models for variability in these properties. That is, the uncertainty due to variability is simulated by considering multiple realizations of the same design, and the uncertainty due to errors is simulated by designing different structures to carry the same loads.

Structural Uncertainties

A good analysis of different sources of uncertainty is provided by Oberkampf *et al*. (2000, 2002). Here we simplify the classification, with a view to the question of how to control uncertainty. We propose in Table 3-1 a classification that distinguishes between errors (uncertainties that apply equally to the entire fleet of an aircraft model) and

variabilities (uncertainties that vary for the individual aircraft). The distinction is important because safety measures usually target one or the other. While variabilities are random uncertainties that can be readily modeled probabilistically, errors are fixed for a given aircraft model (e.g., Boeing 737-400) but they are largely unknown.

Errors reflect inaccurate modeling of physical phenomena, errors in structural analysis, errors in load calculations, or use of materials and tooling in construction that are different from those specified by the designer. Systemic errors affect all the copies of the structural components made and are therefore fleet-level uncertainties. They can reflect differences in analysis, manufacturing and operation of the aircraft from an ideal. The ideal aircraft is an aircraft designed assuming that it is possible to perfectly predict structural loads and structural failure for a given structure, that there are no biases in the average material properties and dimensions of the fleet with respect to design specifications, and that there exists an operating environment that on average agrees with the design specifications. The other type of uncertainty reflects variability in material properties, geometry, or loading between different copies of the same structure and is called here individual uncertainty.

Table 3-1. Uncertainty classification

Type of uncertainty	Spread	Cause	Remedies
Systemic error (modeling errors)	Entire fleet of components designed using the model	Errors in predicting structural failure and differences between properties used in design and average fleet properties.	Testing and simulation to improve math model and the solution.
Variability	Individual component level	Variability in tooling, manufacturing process, and flying environments.	Improve tooling and construction. Quality control.

Safety Measures

Aircraft structural design is still done, by and large, using code-based design rather than probabilistic approaches. Safety is improved through conservative design practices that include use of safety factors and conservative material properties. It is also improved by tests of components and certification tests that can reveal inadequacies in analysis or construction. In the following we detail some of these safety measures.

Load Safety Factor: Traditionally all aircraft structures are designed with a load safety factor to withstand 1.5 times the limit-load without failure.

A-Basis Properties: In order to account for uncertainty in material properties, the Federal Aviation Administration (FAA) states the use of conservative material properties. This is determined by testing a specified number of coupons selected at random from a batch of material. The A-basis property is determined by calculating the value of a material property exceeded by 99% of the population with 95% confidence.

Component and Certification Tests: Component tests and certification tests of major structural components reduce stress and material uncertainties for given extreme loads due to inadequate structural models. These tests are conducted in a building block procedure. First, individual coupons are tested, and then a sub assembly is tested followed by a full-scale test of the entire structure. Since these tests cannot apply every load condition to the structure, they leave uncertainties with respect to some loading conditions. It is possible to reduce the probability of failure by performing more tests to reduce uncertainty or by extra structural weight to reduce stresses. If certification tests were designed together with the structure, it is possible that additional tests would become cost effective because they would allow reduced structural weight.

We simulate the effect of these three safety measures by assuming the statistical distribution of the uncertainties and incorporating them in approximate probability calculations and Monte Carlo simulation. For variability the simulation is straightforward. However, while systemic errors are uncertain at the time of the design, they will not vary for a single structural component on a particular aircraft. Therefore, to simulate the uncertainty, we assume that we have a large number of nominally identical aircraft being designed (e.g., by Airbus, Boeing, Bombardier, Embraer, etc.), with the errors being fixed for each aircraft. This creates a two-level Monte Carlo simulation, with different aircraft models being considered at the upper level, and different instances of the same aircraft at the lower level.

To illustrate the procedure we consider point stress design of a small part of an aircraft structure. Aircraft structures have more complex failure modes, such as fatigue and fracture, which require substantially different treatment and the consideration of the effects of inspections (See Kale *et al*., 2003). However, this simple example serves to further our understanding of the interaction between various safety measures. The procedure is summarized in Fig. 3-1, which is described in detail in the next section.

Design of a Generic Component

Design and Certification Testing

We assume that we have N different aircraft models, i.e., we have N different companies producing a model with errors. We consider a generic component to represent the entire aircraft structure. The true stress (σ_{true}) is found from the equation

$$\sigma_{true} = \frac{P}{wt} \tag{3.1}$$

where P is the applied load on the component of width w and thickness t. In a more general situation, Eq. (3.1) may apply to a small element in a more complex component.

When errors are included in the analysis, the true stress in the component is different from the calculated stress. We include the errors by introducing an error factor e while computing the stress as

$$\sigma_{calc} = (1+e)\ \sigma_{true} \tag{3.2}$$

Positive values of e yield conservative estimates of the true stress and negative values yield unconservative stress estimation. The other random variables account for variability. Combining Eqs. (3.1) and (3.2), the stress in the component is calculated as

$$\sigma_{calc} = (1+e)\frac{P}{w\ \ t} \tag{3.3}$$

The design thickness is determined so that the calculated stress in the component is equal to material allowable stress for a design load P_d multiplied by a safety factor S_F, hence the design thickness of the component is calculated from Eq. (3.3) as

$$t_{design} = (1+e)\frac{S_F P_d}{w_{design}\sigma_a} \tag{3.4}$$

where the design component width, w_{design}, is taken here to be 1.0, and σ_a is the material stress allowable obtained from testing a batch of coupons according to procedures that depend on design practices. Here, we assume that A-basis properties are used (see Appendix A). During the design process, the only random quantities are σ_a and e. The thickness obtained from Eq. (3.4), step A in Fig. 3-1, is the nominal thickness for a given aircraft model. The actual thickness will vary due to individual–level manufacturing uncertainties.

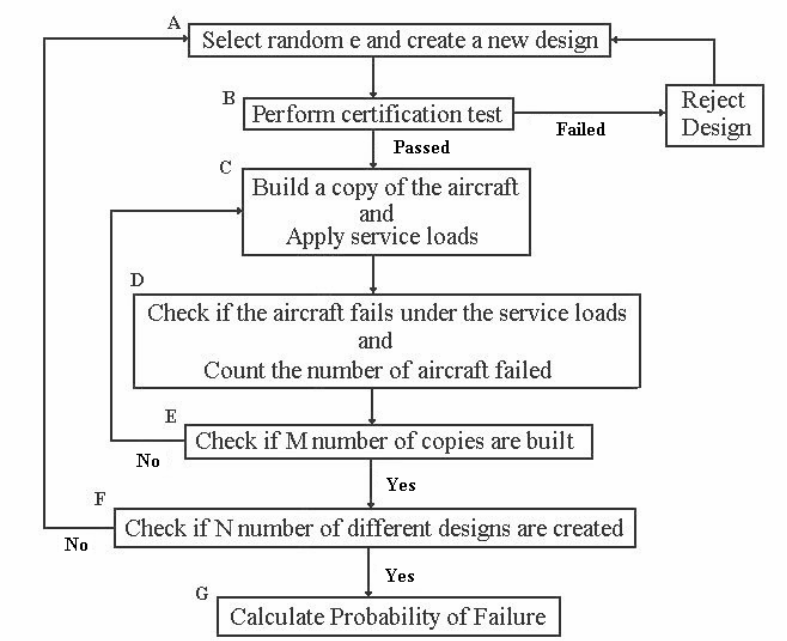

Figure 3-1. Flowchart for Monte Carlo simulation of component design and failure

After the component has been designed (that is, thickness is determined from Eq. (3.4)), we simulate certification testing for the aircraft. Here we assume that the component will not be built with complete fidelity to the design due to variability in geometry (width and thickness). The component is then loaded with the design axial force of S_F times P_d, and the stress in the component is recorded. If this stress exceeds the failure stress (itself a random variable, see Table 3-2) then the design is rejected, otherwise it is certified for use. That is, the airplane is certified (step B in Fig. 3-1) if the following inequality is satisfied

$$\sigma - \sigma_f = \frac{S_F P_d}{wt} - \sigma_f \le 0 \tag{3.5}$$

and we can build multiple copies of the airplane. We subject the component in each airplane to actual random maximum (over a lifetime) service loads (step D in Fig. 3-1) and decide whether it fails using Eq. (3.6).

$$P \geq C = t\, w\, \sigma_f \tag{3.6}$$

Here, P is the applied load, and C is the load carrying capacity of the structure in terms of the width w, thickness t and failure stress σ_f. A summary of the distributions for the random variables used in design and certification is listed in Table 3-2.

Table 3-2. Distribution of random variables used for component design and certification

Variables	Distribution	Mean	Scatter
Plate width (w)	Uniform	1.0	(1%) bounds
Plate thickness (t)	Uniform	t_{design}	(3%) bounds
Failure stress (σ_f)	Lognormal	150.0	8 % coefficient of variation
Service Load (P)	Lognormal	100.0	10 % coefficient of variation
Error factor (e)	Uniform	0.0	10% to 50%

This procedure of design and testing is repeated (steps A-B) for N different aircraft models. For each new model, a different random error factor e is picked for the design, and different allowable properties are generated from coupon testing (Appendix A). Then in the testing, different thicknesses and widths, and different failure stresses are generated at random from their distributions.

Effect of Certification Tests on Distribution of Error Factor e

One can argue that the way certification tests reduce the probability of failure is by changing the distribution of the error factor e. Without certification testing, we assume symmetric distribution of this error factor. However, designs based on unconservative models are more likely to fail certification, and so the distribution of e becomes conservative for structures that pass certification. In order to quantify this effect, we calculated the updated distribution of the error factor e. The updated distribution is calculated analytically by Bayesian updating by making some approximations, and Monte Carlo simulations are conducted to check the validity of those approximations.

Bayesian updating is a commonly used technique to obtain updated (or posterior) distribution of a random variable upon obtaining new information about the random variable. The new information here is that the component has passed the certification test.

Using Bayes' Theorem, the updated (posterior) distribution $f^U(\theta)$ of a random variable θ is obtained from the initial (prior) distribution $f^I(\theta)$ based on new information as

$$f^U(\theta) = \frac{\Pr(\in|\theta)\, f^I(\theta)}{\int_{-\infty}^{\infty} \Pr(\in|\theta)\, f^I(\theta) d\theta} \tag{3.7}$$

where $Pr(\in|\theta)$ is the conditional probability of observing the experimental data $\in$ given that the value of the random variable is θ.

For our case, the posterior distribution $f^U(e)$ of the error factor *e* is given as

$$f^U(e) = \frac{\Pr(CT|e)\, f^I(e)}{\int_{-b}^{b} \Pr(CT|e)\, f^I(e)\, de} \tag{3.8}$$

where *CT* is the event of passing certification, and Pr*(CT|e)* is the probability of passing certification for a given *e*. Initially, *e* is assumed to be uniformly distributed. The procedure of calculation of *Pr(CT|e)* is described in Appendix B, where we approximate the distribution of the geometrical variables, *t* and *w* as lognormal, taking advantage of the fact that their coefficient of variation is small compared to that of the failure stress (see Table 3-2).

We illustrate the effect of certification tests for the components designed with A-Basis material properties. An initial and updated distribution plot of error factor *e* with 50 % bound is shown in Fig. 3-2. Monte Carlo simulation with 50,000 aircraft models is also

shown. Figure 3-2 shows that the certification tests greatly reduce the probability of negative error, hence eliminating most unconservative designs. As seen from the figure, the approximate distribution calculated by the analytical approach matches well the distribution obtained from Monte Carlo simulations.

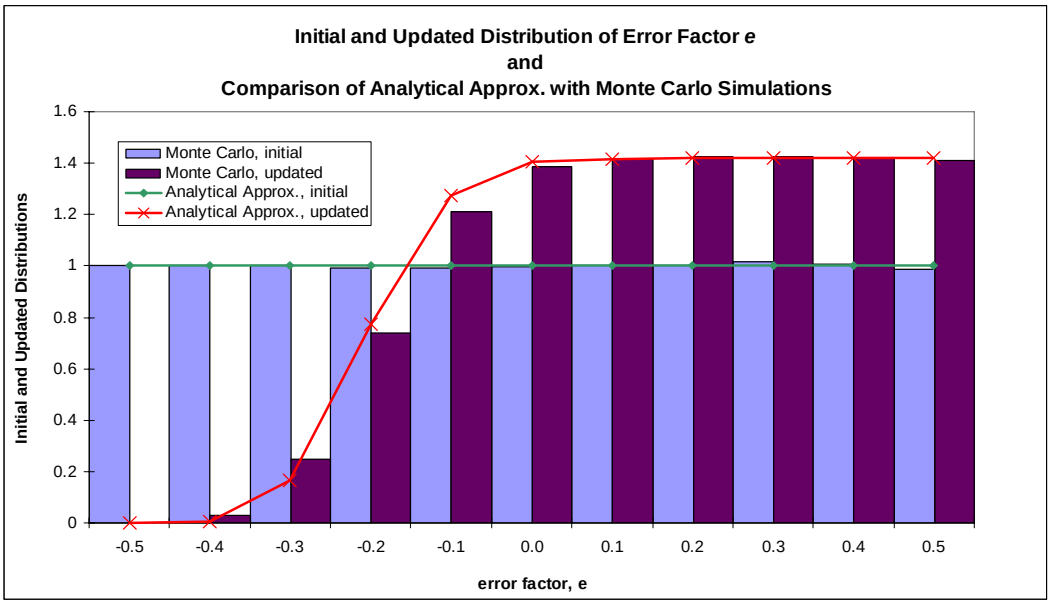

Figure 3-2. Initial and updated probability distribution functions of error factor *e*. Error bound is 50% and Monte Carlo simulation done with sample size of 50,000.

Probability of Failure Calculation by Analytical Approximation

The stress analysis represented by Eq. (3.1) is trivial, so that the computational cost of Monte Carlo simulation of the probability of failure is not high. However, it is desirable to obtain also analytical probabilities that may be used for more complex stress analysis and to check the Monte Carlo simulations.

In order to take advantage of simplifying approximations of the distribution of the geometry parameters, it is convenient to perform the probability calculation in two stages, corresponding to the inner and outer loops of Fig. 3-1. That is, we first obtain expressions

for the probability of failure of a single aircraft model (that is, given *e* and allowable stress). We then calculate the probability of failure over all aircraft models.

The mean value of the probability of failure over all aircraft models is calculated as

$$\bar{P}_f = \int P_f(t_{design})\ f(t_{design})\ dt_{design} \tag{3.9}$$

where t_{design} is the non-deterministic distribution parameter, and $f(t_{design})$ is the probability density function of t_{design}.

It is important to have a measure of variability in this probability from one aircraft model to another. The standard deviation of failure probability gives a measure of this variability. In addition, it provides information on how accurate is the probability of failure obtained from Monte Carlo simulations. The standard deviation can be calculated from

$$\sigma_{Pf} = \left\{ \int \left[P_f(t_{design}) - \bar{P}_f \right]^2\ f(t_{design})\ dt_{design} \right\}^{1/2} \tag{3.10}$$

Probability of Failure Calculation by Monte Carlo Simulations

The inner loop in Fig. 3-1 (steps C-E) represents the simulation of a population of *M* airplanes (hence components) that all have the same design. However, each component is different due to variability in geometry, failure stress, and loading (step D). We subject the component in each airplane to actual random maximum (over a lifetime) service loads (step E) and calculate whether it fails using Eq. (3.6).

For airplane model that pass certification, we count the number of components failed. The failure probability is calculated by dividing the number of failures by the

number of airplane models that passed certification, times the number of copies of each model.

The analytical approximation for the probability of failure suffers due to the approximations used, while the Monte Carlo simulation is subject to sampling errors, especially for low probabilities of failure. Using large samples, though, can reduce the latter. Therefore, we compared the two methods for a relatively large sample of 10,000 aircraft models with 100,000 instances of each model. In addition, the comparison is performed for the case where mean material properties (rather than A-basis properties) are used for the design, so that the probability of failure is high enough for the Monte Carlo simulation to capture it accurately. Table 3-3 shows the results for this case.

Table 3-3. Comparison of probability of failures for components designed using safety factor of 1.5, mean value for allowable stress and error bound of 50%

Value	Analytical Approximation	Monte Carlo Simulation*	% error
Average Value of P_f without certification (P_{nt})	1.715×10^{-1}	1.726×10^{-1}	0.6
Standard Deviation of P_{nt}	3.058×10^{-1}	3.068×10^{-1}	0.3
Average Value of P_f with certification (P_t)	3.166×10^{-4}	3.071×10^{-4}	3.1
Standard Deviation of P_t	2.285×10^{-3}	2.322×10^{-3}	1.6
Average Value of Initial error factor (e^i)	0.0000	-0.00024	---
Standard Deviation of e^I	0.2887	0.2905	0.6
Average Value of Updated error factor (e^{up})	0.2468	0.2491	0.9
Standard Deviation of e^{up}	0.1536	0.1542	0.4

* N = 10,000 and M = 100,000 is used in the Monte Carlo Simulations

The last column of Table 3-3 shows the percent error of the analytical approximation compared to Monte Carlo simulations. It is seen that the analytical approximation is in good agreement with the values obtained through Monte Carlo simulations. It is remarkable that the standard deviation of the probability of failure is almost twice the average value of the probability (the ratio, the coefficient of variation, is about 178%) before certification, and about seven times larger after certification. This

indicates huge variability in the probability of failure for different aircraft models, and this is due to the large error bound, b_e=*50%*. With 10,000 different aircraft models (N), the standard deviation in the Monte Carlo estimates is about 1%, and the differences between the Monte Carlo simulation and the analytical approximation are of that order.

Effect of Three Safety Measures on Probability of Failure

We next investigate the effect of other safety measures on failure probability of the components using Monte Carlo simulations. We performed the simulation for a range of variability in error factor *e* for 5000 airplane models (*N* samples in outer loop) and 20,000 copies of each airplane model (*M* samples in inner loop). Here, we compare the probability of failure of a structure designed with three safety measures (safety factor, conservative material property and certification testing) to that of a structure designed without safety measures.

Table 3-4 presents the results when all safety measures are used for different bounds on the error. The second column shows the mean and standard deviation of design thicknesses generated for components that passed certification. These components correspond to the outer loop of Fig. 3-1. The variability in design thickness is due to the randomness in the error *e* and in the stress allowable. The average thickness before certification was 1.269, so that the column shows the conservative effect of certification testing. When the error bound is 10%, 98.8% of the components pass certification (third column in Table 3-4), and the average thickness is increased by only 0.24% due to the certification process. On the other hand, when the error bound is 50%, 29% of the components do not pass certification, and this raises the average thickness to 1.453. Thus, the increase in error bound has two opposite effects. Without certification testing, increasing the error bound greatly increases the probability of failure. For example, when

the error bound changes from 30% to 50%, the probability of failure without certification changes from *0.00091* to *0.0449*, or by a factor of 49. On the other hand, with the increased average thickness, after certification the probability increases only from $1.343x10^{-4}$ to $1.664x10^{-4}$.

Table 3-4. Probability of failure for different bounds on error *e* for components designed using safety factor of 1.5 and A-basis property for allowable stress. Numbers in parenthesis denote the coefficient of variation of the quantity. Average design thickness without certification is 1.271.

Error Bound b_e	Average design thickness after certification*	Certification failure rate %	Probability of failure after certification $(P_t)\times10^{-4}$	Probability of failure without certification $(P_{nt})\times10^{-4}$	Probability ratio (P_t/P_{nt})	Probability difference $(P_{nt}-P_t)$
50%	1.453 (0.19)	29.3	1.664 (7.86)	449.0 (2.74)	3.706×10^{-3}	4.473×10^{-2}
40%	1.389 (0.17)	24.3	1.586 (6.92)	89.77 (3.22)	1.767×10^{-2}	8.818×10^{-3}
30%	1.329 (0.15)	16.3	1.343 (5.28)	9.086 (3.46)	1.479×10^{-1}	7.742×10^{-4}
20%	1.283 (0.12)	6.2	0.304 (4.81)	0.477 (3.51)	6.377×10^{-1}	1.727×10^{-5}
10%	1.272 (0.07)	1.2	0.027 (4.71)	0.029 (4.59)	9.147×10^{-1}	2.490×10^{-7}

*Average over N=5000 models

The effectiveness of the certification tests can be expressed by two measures of probability improvement. The first measure is the ratio of the probability of failure with the test, P_t, to the probability of failure without tests, P_{nt}. The second measure is the difference of these probabilities. The ratio is a more useful indicator for low probabilities of failure, while the difference is more meaningful for high probabilities of failure. However, when P_t is high, the ratio can mislead. That is, an improvement from a probability of failure of 0.5 to 0.1 is more substantial than an improvement in probability of failure of 0.1 to 0.01, because it “saves” more airplanes. However, the ratio is more useful when the probabilities are small, and the difference is not very informative.

Table 3-4 shows that certification testing is more important for large error bounds *e*. For these higher values the number of components that did not pass certification is higher, thereby reducing the failure probability for those that passed certification. While the effect of component tests (building block tests) is not simulated, their main effect is to reduce the error magnitude *e*. This is primarily due to the usefulness of component tests in improving analytical models and revealing unmodeled failure modes. With that in mind, we note that the failure probability for the 50% error range is 1.7×10^{-4}, and it reduces to 2.7×10^{-6} for the 10% error range-that is, by a factor of 63.

The actual failure probability of aircraft components is expected to be of the order of 10^{-8} per flight, much lower than the best number in the fourth column of Table 3-4. However, the number in Table 3-4 is for a lifetime for a single structural component. Assuming about 10,000 flights in the life of a component and 100 independent structural components, this 10^{-5} failure probability for a component will translate to a per flight probability of failure of 10^{-7} per airplane. This factor of 10 discrepancy is exacerbated by other failure modes like fatigue that have not been considered. However, other safety measures, such as conservative load specifications may account for this discrepancy.

Table 3-5 shows results when average rather than conservative material properties are used. It can be seen from Table 3-5 that the average thickness determined using the mean value of allowable stress is lower than that determined using the A-basis value of allowable stress (Table 3-4). This is equivalent to adding an additional safety factor over an already existing safety factor of 1.5. For the distribution (lognormal with 8% coefficient of variation) and number of batch tests (40 tests) considered here, a typical value of the safety factor due to A-Basis property is around 1.27.

Table 3-5. Probability of failure for different bounds on error e for components designed using safety factor of 1.5 and mean value for allowable stress. Numbers in parenthesis denote the coefficient of variation of the quantity. Average design thickness without certification is 1.000.

Error bound b_e	Average design thickness after certification *	Certification failure rate+ %	Probability of Failure after certification $(P_t)\times10^{-4}$	Probability of failure without certification $(P_{nt})\times10^{-4}$	Probability ratio (P_t/P_{nt})	Probability difference $(P_{nt}-P_t)$
50%	1.243 (0.13)	50.1	3.420 (5.82)	1681 (1.81)	2.035×10^{-3}	1.677×10^{-1}
40%	1.191 (0.11)	50.1	4.086 (6.78)	969.0 (1.99)	4.217×10^{-3}	9.649×10^{-2}
30%	1.139 (0.09)	50.8	5.616 (5.45)	376.6 (2.00)	1.495×10^{-2}	3.700×10^{-2}
20%	1.086 (0.07)	50.7	6.253 (3.19)	92.67 (1.83)	6.748×10^{-2}	8.642×10^{-3}
10%	1.029 (0.05)	51.0	9.209 (1.70)	19.63 (1.25)	4.690×10^{-1}	1.043×10^{-3}

*Average over N=5000 models

+With only 5000 models, the standard deviation in the certification failure rate is about 0.71%. Thus, all the numbers in this column are about 50% as may be expected when mean material properties are used.

Without the A-basis properties, the stress in the certification test is approximately equal to the average ultimate service stress, so that about 50% of the components fail certification. When the errors are large, this raises substantially the average thickness of the components that pass certification, so that for an error bound of 50% the certification test is equivalent to a safety factor of 1.243. Large errors produce some super-strong and some super-weak components (see Fig. 3-3b). The super-weak components are mostly caught by the certification tests, leaving the super-strong components to reduce the probability of failure. Another way of looking at this effect is to note that when there are no errors, there is no point to the tests. Indeed, it can be seen that the probability of failure without certification tests improves with reduced error bound e, but that the reduced effect of the certification tests reverses the trend. Thus for this case we obtain the counter-intuitive results that larger errors produce safer designs.

Comparing the first row of Table 3-5 to that of Table 3-3 we see the effect of the smaller sample for the Monte Carlo simulations. Table 3-3 was obtained with 10,000

models and 100,000 copies per model, while Table 3-5 was obtained with 5000 models, and 20,000 copies per model. The difference in the probability of failure after certification between the two tables is about 11 percent. However, the two values straddle the analytical approximation.

The effects of building block type of tests that are conducted before certification are not included in this study. These tests reduce the errors in analytical models. For instance, if there is 50% error in the analytical model the building block type of tests may reduce this error to lower values. Hence, the difference between the rows of Table 3-4, may be viewed as indicating the benefits of reducing the error by building block tests.

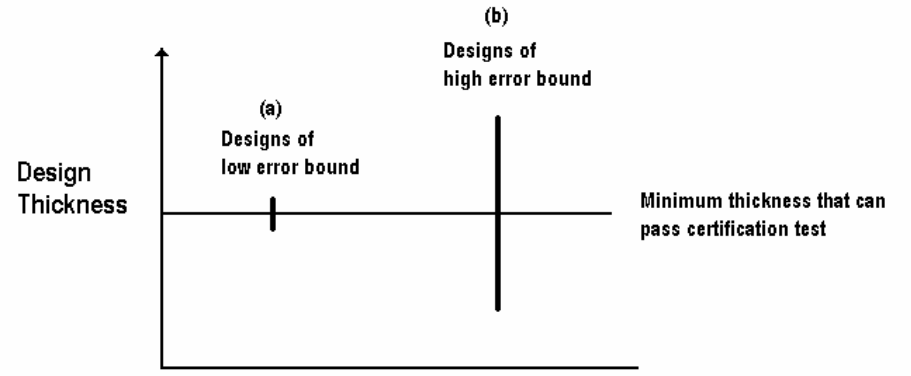

Figure 3-3. Design thickness variation with low and high error bounds. Note that after certification testing only the designs above the minimum thickness are built and flown. Those on the right have a much higher average design thickness than those on the left.

Table 3-6 shows the effect of not using a safety factor. Although certification tests improve the reliability, again in a general trend of high improvement with high error, the lack of safety factor of 1.5 limits the improvement. Comparing Tables 3-4 and 3-6 it can be seen that the safety factor reduces the probability of failure by two to four orders of magnitudes. It is interesting to note that the effect of the error bound on the probability of

failure after certification is not monotonic, and this phenomenon is discussed in Appendix C.

Table 3-6. Probability of failure for different bounds on error *e* for safety factor of 1.0 and A-basis allowable stress. Numbers in parenthesis denote the c.o.v. of the quantity. Average design thickness without certification is 0.847.

Error bound b_e	Average design thickness after certification *	Certification failure rate %	Failure probability after certification $(P_t)\times10^{-2}$	Failure probability with no certification $(P_{nt})\times10^{-2}$	Probability ratio (P_t/P_{nt})	Probability difference $(P_{nt}-P_t)$
50%	0.969 (0.19)	29.4	6.978 (2.12)	29.49 (1.31)	2.366×10^{-1}	2.251×10^{-1}
40%	0.929 (0.17)	25.0	7.543 (1.98)	24.56 (1.38)	3.071×10^{-1}	1.702×10^{-1}
30%	0.886 (0.15)	16.6	8.923 (1.73)	17.11 (1.43)	5.216×10^{-1}	8.184×10^{-2}
20%	0.855 (0.11)	5.7	8.171 (1.40)	9.665 (1.34)	8.454×10^{-1}	1.494×10^{-2}
10%	0.847 (0.06)	1.3	4.879 (0.97)	4.996 (0.97)	9.767×10^{-1}	1.163×10^{-3}

*Average over N=5000 models

Table 3-7, shows results when the only safety measure is certification testing. Certification tests can reduce the probability of failure of components by 38%, the highest improvement corresponds to the highest error. As can be expected, without certification tests and safety measures, the probability of failure is near 50%. Tables 3-4 through 3-7 illustrate the probability of failure for a fixed 8 % coefficient of variation in failure stress. The general conclusion that can be drawn from these results is that the error bound e is one of the main parameters affecting the efficacy of certification tests to improve reliability of components.

Table 3-7. Probability of failure for different error bounds for safety factor of 1.0 and mean value for allowable stress. Average design thickness without certification is 0.667.

Error bound b_e	Average design thickness after certification *	Certification failure rate %	Probability of Failure after certification (P_t)	Probability of failure without certification (P_{nt})	Probability ratio (P_t/P_{nt})	Probability difference $(P_{nt}-P_t)$
50%	0.830 (0.12)	50.1	0.125 (1.39)	0.505 (0.83)	2.463×10^{-1}	3.808×10^{-1}
40%	0.796 (0.11)	50.2	0.158 (1.20)	0.504 (0.79)	3.140×10^{-1}	3.459×10^{-1}
30%	0.761 (0.09)	50.4	0.205 (0.92)	0.503 (0.72)	4.075×10^{-1}	2.981×10^{-1}
20%	0.727 (0.08)	50.9	0.285 (0.64)	0.503 (0.58)	5.653×10^{-1}	2.189×10^{-1}
10%	0.686 (0.05)	50.7	0.412 (0.34)	0.500 (0.34)	8.228×10^{-1}	8.869×10^{-2}

*Average over N=5000 models

Next, we will explore how another parameter, variability, influences the efficacy of tests. This is accomplished by changing the coefficient of variation of failure stress σf between 0–16% and keeping the error bound constant.

Table 3-8. Probability of failure for different uncertainty in failure stress for the components designed with safety factor of 1.5, 50% error bounds *e* and A-basis allowable stress.

Coefficient of variation of σ_f	Average design thickness without certification *	Average design thickness after certification *	Certification failure rate %	Probability of failure after certification (P_t)×10^{-4}	Probability of failure without certification (P_{nt})×10^{-4}	Probability ratio (P_t/P_{nt})	Probability difference (P_{nt}-P_t)
0 %	0.998 (0.29)	1.250 (0.11)	50.2	0.017 (6.85)	1699 (1.87)	1.004×10^{-5}	1.698×10^{-1}
4%	1.127 (0.29)	1.347 (0.15)	38.9	0.087 (7.20)	970.4 (2.35)	8.973×10^{-5}	9.703×10^{-2}
8 %	1.269 (0.29)	1.453 (0.19)	29.3	1.664 (7.86)	449.0 (2.74)	3.706×10^{-3}	4.473×10^{-2}
12 %	1.431 (0.29)	1.574 (0.22)	20.9	13.33 (7.71)	206.1 (3.08)	6.469×10^{-2}	1.927×10^{-2}
16%	1.616 (0.30)	1.723 (0.25)	14.1	22.52 (5.54)	107.3 (3.24)	2.100×10^{-1}	8.476×10^{-3}

*Average over N=5000 models

Table 3-9. Probability of failure for different uncertainty in failure stress for the components designed with safety factor of 1.5, 30% error bound e and A-basis allowable stress.

Coefficient of variation of σ_f	Average design thickness without certification *	Average design thickness after certification *	Certification failure rate %	Probability of failure after certification (P_t)×10^{-4}	Probability of failure without certification (P_{nt})×10^{-4}	Probability ratio (P_t/P_{nt})	Probability difference (P_{nt}-P_t)
0 %	1.001 (0.17)	1.148 (0.08)	50.1	0.026 (4.79)	223.8 (2.50)	1.163×10^{-4}	2.238×10^{-2}
4 %	1.126 (0.17)	1.232 (0.11)	31.6	0.146 (6.03)	35.25 (2.97)	4.149×10^{-3}	3.511×10^{-3}
8 %	1.269 (0.17)	1.329 (0.15)	16.3	1.343 (5.28)	9.086 (3.46)	1.479×10^{-1}	7.742×10^{-4}
12 %	1.431 (0.18)	1.459 (0.17)	7.2	2.404 (3.87)	4.314 (3.45)	5.572×10^{-1}	1.911×10^{-4}
16%	1.617 (0.18)	1.630 (0.18)	3.3	2.513 (3.73)	3.102 (3.54)	8.099×10^{-1}	5.896×10^{-5}

* Average over N=5000 models

Table 3.10. Probability of failure for uncertainty in failure stress for components designed using safety factor of 1.5, 10% error bounds e and A-basis properties

Coefficient of variation of σ_f	Average design thickness without certification *	Average design thickness after certification *	Certification failure rate %	Probability of failure after certification $(P_t)\times10^{-4}$	Probability of failure without certification $(P_{nt})\times10^{-4}$	Probability ratio (P_t/P_{nt})	Probability difference $(P_{nt}-P_t)$
0 %	1.000 (0.06)	1.048 (0.03)	50.3	0.075 (2.91)	1.745 (1.78)	4.304×10^{-2}	1.669×10^{-4}
4 %	1.126 (0.06)	1.131 (0.06)	5.9	0.053 (3.85)	0.070 (3.56)	7.548×10^{-1}	1.716×10^{-6}
8%	1.269 (0.06)	1.272 (0.07)	1.2	0.027 (4.71)	0.029 (4.59)	9.147×10^{-1}	2.490×10^{-7}
12 %	1.431 (0.07)	1.432 (0.07)	0.8	0.049 (4.30)	0.051 (4.23)	9.623×10^{-1}	1.926×10^{-7}
16%	1.623 (0.08)	1.624 (0.08)	0.5	0.085 (3.50)	0.083 (3.55)	9.781×10^{-1}	1.853×10^{-7}

*Average over N=5000 models

The increase in the variability in failure stress has a large effect on the allowable stress because A-basis properties specify an allowable that is below 99% of the sample. Increased variability reduces the allowable stress and therefore increases the design thickness. It is seen from Tables 3-8 through 3-10 that when the variability increases from 0% to 16%, the design thickness increases by more than 60%. This greatly reduces the probability of failure without certification. However, the probability of failure with certification still deteriorates. That is, the use of A-basis properties fails to fully compensate for the variability in material properties. This opposite behavior of the probability of failure before and after certification is discussed in more detail in Appendix C.

The variability in failure stress greatly changes the effect of certification tests. Although the average design thicknesses of the components increase with the increase in variability, we see that when the variability is large, the value of the tests is reduced because the tested aircraft can be greatly different from the airplanes in actual service.

We indeed see from the Tables 3-8, 3-9 and 3-10 that the effect of certification tests is reduced as the variability in the failure stress increases. Recall that the effect of certification tests is also reduced when the error *e* decreases. Indeed, Table 3-8 shows a much smaller effect of the tests than Table 3-10. Comparing the second and third columns of Tables 3-8, 3-9 and 3-10 we see that as the bound of error decreases, the change in the average value of design thicknesses of the components become less which is an indication of loss in the efficacy of certification tests.

Up to now, both the probability difference (P_{nt}-P_t) and the probability ratio (P_t/P_{nt}) seem to be good indicators of efficacy of tests. To allow easy visualization, we combined the errors and the variability in a single ratio (Bound of e) / $V_R(\sigma/\sigma_f)$ ratio (ratio of error bound e to the coefficient of variation of the stress ratio). The denominator accounts for the major contributors to the variability. The value in the denominator is a function of four variables; service load *P*, width *w*, thickness *t*, and failure stress σ_f. Here, *P* and σ_f have lognormal distributions but w and t are uniformly distributed. Since the coefficient of variations of w and t is very small, they can also be treated as lognormally distributed to make calculation of the denominator easy while plotting the graphs. Since the standard deviations of the variables are small, the denominator is now the square root of the sum of the squares of coefficient of variations of the four variables mentioned above, that is

$$V_R(\sigma/\sigma_f) \cong \sqrt{V_R^2(P) + V_R^2(w) + V_R^2(t) + V_R^2(\sigma_f)} \tag{3.11}$$

The effective safety factor is the ratio of the design thickness of the component when safety measures (such as usage of A-basis values for material properties and safety factor) are applied to the thickness of the component when no safety measures are taken.

Figures 3-4 and 3-5, present the P_t/P_{nt} ratio in visual formats. It can be seen that as expected, the ratio decreases as the (Bounds on *e*)/$V_R(\sigma/\sigma_f)$ ratio increases. However, these two figures do not give a clear indication of how certification tests are influenced by the effective safety factor.

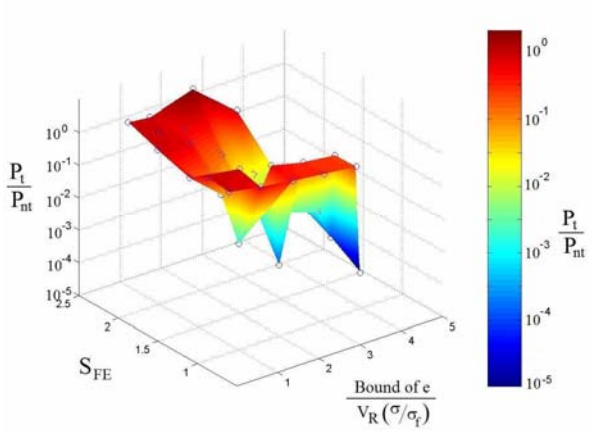

Figure 3-4. Influence of effective safety factor, error, and variability on the probability ratio (3-D view)

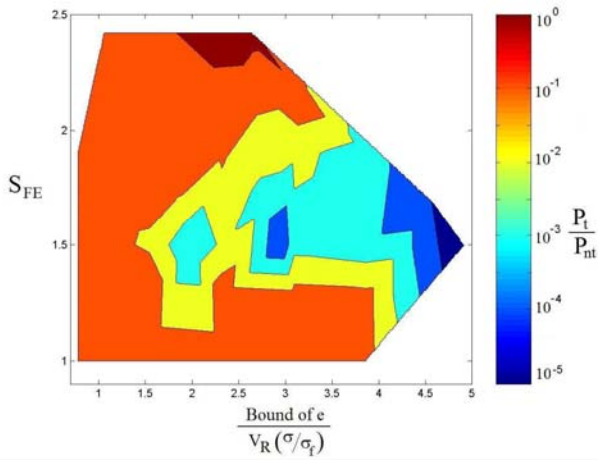

Figure 3-5. Influence of effective safety factor, error and variability on the probability ratio (2-D plot)

Figures 3-6 and 3-7 show the probability difference, P_{nt}-P_t. In these cases, the dependence on the effective safety factor is monotonic. As expected, it is seen that as the effective safety factor increases, the improvement in the safety of component decreases; meaning that the certification tests become less useful. The probability difference is more descriptive as it is proportional to the number of aircraft failures prevented by certification testing. The probability ratio lacks such clear physical interpretation, even though it is a more attractive measure when the probability of failure is very small.

Considering the results presented by Figures 3-4 through 3-7, the probability difference (P_{nt}-P_t) is the more appropriate choice for expressing the effectiveness of tests.

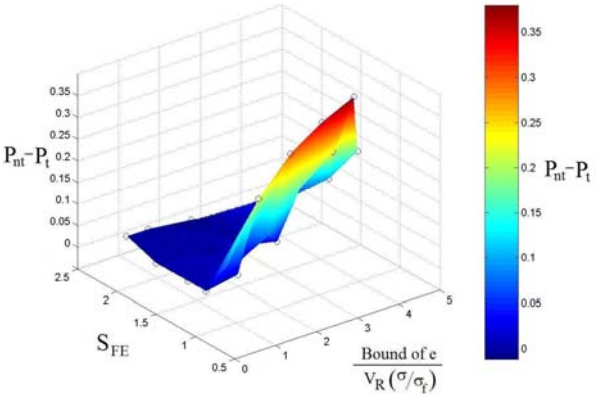

Figure 3-6. Influence of effective safety factor, error and variability on the probability difference (3-D view)

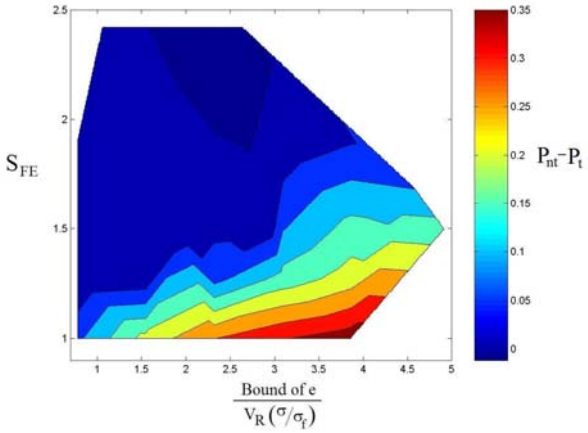

Figure 3-7. Influence of effective safety factor, error and variability on the probability difference (2-D plot)

Summary

We have used a simple example of point stress design for yield to illustrate the effects of several safety measures taken in aircraft design: safety factors, conservative material properties, and certification tests. Analytical calculations and Monte Carlo simulation were performed to account for both fleet-level uncertainties (such as errors in analytical models) and individual uncertainties (such as variability in material properties).

It was seen that an increase of the systemic errors in the analysis causes an increase in the probability of failure. We found that the systemic errors can be reduced by the use of certification tests, thereby reducing the probability of failure. Also we found that design thicknesses of the components increased as the bounds of systemic errors increased.

We found that the effect of certification tests is most important when errors in analytical models are high and when the variability between airplanes is low. This leads to the surprising result that in some situations larger error variability in analytical models reduces the probability of failure if certification tests are conducted. For the simple

example analyzed here, the use of conservative (A-basis) material properties was equivalent to a safety factor of up to 1.6, depending on the scatter in failure stresses.

The effectiveness of the certification tests is expressed by two measures of probability improvement. The ratio of the probability of failure with the test, P_t, to the probability of failure without tests, P_{nt}, is useful when P_t is small. The difference is more meaningful when the probability is high. Using these measures we have shown that the effectiveness of certification tests increases when the ratio of error to variability is large and when the effective safety factor is small.

The effect of building-block type tests that are conducted before certification was not assessed here. However, these tests reduce the errors in the analytical models, and on that basis we determined that they can reduce the probability of failure by one or two orders of magnitude.

The calculated probabilities of failure with all the considered safety margins explain why passenger aircraft are so safe structurally. They were still somewhat high — about 10^{-7}—compared to the probability of failure of actual aircraft structural components—about 10^{-8}. This may be due to additional safety measures, such as conservative design loads or to the effect of design against additional failure modes.

CHAPTER 4
COMPARING EFFECTIVENESS OF MEASURES THAT IMPROVE AIRCRAFT STRUCTURAL SAFETY

Chapter 3 explored how safety measures compensate for errors and variability. The major finding of that chapter was that certification tests are most effective when errors are large, variability is low, and the overall safety factor is low. Chapter 3 mainly focused on the effectiveness of certification testing, but the relative effectiveness of safety measures was not addressed. The present chapter takes a further step and aims to discover how measures that improve aircraft structural safety compare with one another in terms of weight effectiveness. In addition, structural redundancy—another safety measure—is included in the analysis. In addition the simple error model of Chapter 3 is replaced by a more detailed error model. Comparison of the effectiveness of error and variability reduction with other safety measures is also given.

The research presented in this chapter is submitted for publication (Acar *et al*. 2006d). My colleague Dr. Amit Kale's contribution to this work is acknowledged.

Introduction

As noted earlier, aircraft structural design is still carried out by using code-based design, rather than probabilistic design. Safety is improved through conservative design practices that include the use of safety factors and conservative material properties. Safety is also improved by testing of components, redundancy, improved modeling to reduce errors and improved manufacturing to reduce variability. The following gives brief description of these safety measures.

Load Safety Factor

In transport aircraft design, FAA regulations state the use of a load safety factor of 1.5 (FAR 25.303). That is, aircraft structures are designed to withstand 1.5 times the limit load without failure.

Conservative Material Properties

In order to account for uncertainty in material properties, FAA regulations state the use of conservative material properties (FAR 25.613). The conservative material properties are characterized as A-basis and B-basis material property values, and the use of A-basis or B-basis values depends on the redundancy. If there is single failure path in the structure, A-basis values are used, while for the case of multiple failure paths (i.e., redundant structures), B-basis values are used. Detailed information on these values is provided in Chapter 8 of Volume 1 of the Composite Materials Handbook (2000). The basis values are determined by testing a number of coupons selected at random from a material batch. The A-basis value is determined by calculating the value of a material property exceeded by 99% of the population with 95% confidence, while the B-basis value is the value of a material property exceeded by 90% of the population with 95% confidence. Here, we take the redundancy of the structure into account, so we use B-basis values (see Appendix A for the B-basis value calculation). The number of coupon tests is assumed to be 40.

Tests

Tests of major structural components reduce stress and material uncertainties for given extreme loads due to inadequate structural models. These tests are conducted in a building block procedure (Composite Materials Handbook (2000), Volume 1, Chapter 2). First, individual coupons are tested, and then a sub-assembly is tested, followed by a full-

scale test of the entire structure. Here, we only consider the final certification test for an aircraft. Other tests are assumed to be error reduction measures and their effect is analyzed indirectly by considering the effect of error reduction.

Redundancy

Transport airliners are designed with double and triple redundancy features in all major systems to minimize the failure probability. Redundancy is intended to ensure that a single component failure does not lead to catastrophic failure of the system. In the present work, we assume that an aircraft structure will fail if two local failures occur in the structure.

Error Reduction

Improvements in the accuracy of structural analysis and failure prediction of aircraft structures reduce errors and enhance the level of safety of the structures. These improvements may be due to better modeling techniques developed by researchers, more detailed finite element models made possible by faster computers, or more accurate failure predictions due to extensive testing.

Variability Reduction

Examples of mechanisms that reduce variability in material properties include quality control and improved manufacturing processes. Variability in damage and ageing effects is accomplished through inspections and structural health monitoring. Variability in loads may be reduced by better pilot training and information that allows pilots to more effectively avoid regions of high turbulence. Here we investigate only the effect of reduced variability in material properties.

The next section of this chapter discusses the more detailed error model used in this chapter, along with variability and total safety factor. Next, the effect of certification tests

on error distribution is analyzed. Then, details of the calculation of the probability of failure via separable Monte Carlo simulations (MCS) are given. Finally, the chapter finalizes with the results and summary.

Errors, Variability and Total Safety Factor

The simplified uncertainty classification used in Chapter 3 is also used in this chapter, where errors are uncertainties that apply equally to the entire fleet of an aircraft model and variabilities are uncertainties that vary for the individual aircraft (see Table 3-1, Chapter3). This section first discusses the errors in design and construction. Next, total error factor and total safety factor are introduced, finally, simulation of variability is discussed.

Errors in Design

We consider static point stress design for simplicity. Other types of failures such as fatigue, corrosion or crack instability are not taken into account. We assume that an aircraft structure will fail only if two local failure events occur. For example, we assume that the wing will fail structurally if two local failures occur at the wing panels. The correlation coefficient between the probabilities of these two events is assumed to be 0.5.

Before starting the structural design, aerodynamic analysis needs to be performed to determine the loads acting on the aircraft. However, the calculated design load value, P_{calc}, differs from the actual loading P_d under conditions corresponding to FAA design specifications (e.g., gust-strength specifications). Since each company has different design practices, the error in load calculation, e_p, is different from one company to another. The calculated design load P_{calc} is expressed in terms of the true design load P_d as

$$P_{calc} = (1 + e_P) P_d \tag{4.1}$$

Besides the error in load calculation, an aircraft company may also make errors in stress calculation. We consider a small region in a structural part, characterized by a thickness t and width w, that resists the load in that region. The value of the stress in a structural part calculated by the stress analysis team, σ_{calc}, can be expressed in terms of the load values calculated by the load team P_{calc}, the design width w_{design}, and the thickness t of the structural part by introducing the term e_σ representing error in the stress analysis

$$\sigma_{calc} = (1 + e_\sigma) \frac{P_{calc}}{w_{design}\, t} \tag{4.2}$$

Equation (4.3) is used by a structural designer to calculate the design thickness t_{design} required to carry the calculated design load times the safety factor S_{FL}. That is,

$$t_{design} = \left(1 + e_\sigma\right) \frac{S_{FL} P_{calc}}{w_{design} \left(\sigma_a\right)_{calc}} = \left(1 + e_\sigma\right)\left(1 + e_P\right) \frac{S_{FL} P_d}{w_{design} \left(\sigma_a\right)_{calc}} \tag{4.3}$$

where $\left(\sigma_a\right)_{calc}$ is the value of allowable stress for the structure used in the design, which is calculated based on coupon tests using failure models such as Tresca or von Mises. Since these failure theories are not exact, we have

$$\left(\sigma_a\right)_{calc} = \left(1 - e_f\right)\left(\sigma_a\right)_{true} \tag{4.4}$$

where e_f is the error associated with failure prediction. Moreover, the errors due to the limited amount of coupon testing to determine the allowables, and the differences between the material properties used by the designer and the average true properties of the material used in production are included in this error. Note that the formulation of Eq. (4.4) is different to that of Eqs. (4.1) and (4.2) in that the sign in front of the error factor

e_f is negative, because we consistently formulate the expressions such that positive error implies a conservative decision.

Combining Eqs. (4.3) and (4.4), we can express the design value of the load carrying area as

$$A_{design} = t_{design} w_{design} = \frac{(1+e_\sigma)(1+e_P)}{1-e_f} \frac{S_{FL} P_d}{(\sigma_a)_{true}} \tag{4.5}$$

Errors in Construction

In addition to the above errors, there will also be construction errors in the geometric parameters. These construction errors represent the difference between the values of these parameters in an average airplane (fleet-average) built by an aircraft company and the design values of these parameters. The error in width, e_w, represents the deviation of the design width of the structural part, w_{design}, from the average value of the width of the structural part built by the company, w_{built}. Thus,

$$w_{built} = (1+e_w)\, w_{design} \tag{4.6}$$

Similarly, the built thickness value will differ from its design value such that

$$t_{built} = (1+e_t)\, t_{design} \tag{4.7}$$

Then, the built load carrying area A_{built} can be expressed using the first equality of Eq. (4.5) as

$$A_{built} = (1+e_t)(1+e_w) A_{design} \tag{4.8}$$

Table 4-1 presents nominal values for the errors assumed here. In the results section of this chapter we will vary these error bounds and investigate the effects of these changes on the probability of failure. As seen in Table 4-2, the error having the largest

bound in its distribution is the error in failure prediction e_f, because we use it to model also the likelihood of unexpected failure modes.

Table 4-1. Distribution of error factors and their bounds

Error factors	Distribution Type	Mean	Bounds
Error in stress calculation, e_σ	Uniform	0.0	± 5%
Error in load calculation, e_P	Uniform	0.0	± 10%
Error in width, e_w	Uniform	0.0	± 1%
Error in thickness, e_t	Uniform	0.0	± 2%
Error in failure prediction, e_f	Uniform	0.0	± 20%

The errors here are modeled by uniform distributions, following the principle of maximum entropy. For instance, the error in the built thickness of a structural part (e_t) is defined in terms of the error bound $(b_t)_{built}$ via Eq. (4.9).

$$e_t = U\left[0, (b_t)_{built}\right] \tag{4.9}$$

Here 'U' indicates that the distribution is uniform and '0 (zero)' is the average value of e_t. Table 4-1 shows that $(b_t)_{built}$ = 0.02. Hence, the lower bound for the thickness value is the average value minus 2% of the average and the upper bound for the thickness value is the average value plus 2% of the average. Commonly available random number generators provide random numbers uniformly distributed between 0 and 1. Then, the error in the built thickness can be calculated from Eq. (4.10) using such random numbers r as

$$e_t = (2r-1)(b_t)_{built} \tag{4.10}$$

Total Error Factor

The expression for the built load carrying area, A_{built}, of a structural part can be reformulated by combining Eqs. (4.5) and (4.8) as

$$A_{built} = (1+e_{total})\frac{S_{FL}P_d}{(\sigma_a)_{true}} \tag{4.11}$$

where

$$e_{total} = \frac{(1+e_\sigma)(1+e_P)(1+e_t)(1+e_w)}{1-e_f} - 1 \tag{4.12}$$

Here e_{total} represents the cumulative effect of the individual errors (e_σ, e_P, …) on the load carrying capacity of the structural part.

Total Safety Factor

The total safety factor, S_F, of a structural part represents the effects of all safety measures and errors on the built structural part. Without safety measures and errors, we would have a load carrying area, A_0, required to carry the design load

$$A_0 = \frac{P_d}{\bar{\sigma}_f} \tag{4.13}$$

where $\bar{\sigma}_f$ is the average value of the failure stress. Then, the total safety factor of a built structural component can be defined as the ratio of A_{built}/A_0

$$(S_F)_{built} = \frac{A_{built}}{A_0} = (1+e_{total})\, S_{FL} \frac{\bar{\sigma}_f}{(\sigma_a)_{true}} \tag{4.14}$$

Here we take S_{FL} = 1.5 and conservative material properties are based on B-basis values. Certification tests add another layer of safety. Structures with large negative e_{total} (unconservative) fail certification, so the certification process adds safety by biasing the distribution of e_{total}. Denoting the built area after certification (or certified area) by A_{cert}, the total safety factor of a certified structural part is

$$(S_F)_{cert} = \frac{A_{cert}}{A_0} \tag{4.15}$$

Variability

In the previous sections, we analyzed the different types of errors made in the design and construction stages, representing the differences between the fleet average values of geometry, material and loading parameters and their corresponding design values. For a given design, these parameters vary from one aircraft to another in the fleet due to variabilities in tooling, construction, flying environment, etc. For instance, the actual value of the thickness of a structural part, tact, is defined in terms of its fleet average built value, t_{built}, by

$$t_{act} = (1 + v_t) t_{built} \tag{4.16}$$

We assume that v_t has a uniform distribution with 3% bounds (see Table 4-2). Then, the actual load carrying area A_{act} can be defined as

$$A_{act} = t_{act} w_{act} = (1 + v_t) t_{built} (1 + v_w) w_{built} = (1 + v_t)(1 + v_w) A_{built} \tag{4.17}$$

where v_w represents effect of the variability on the built width.

Table 4-2 presents the assumed distributions for variabilities. Note that the thickness error in Table 4-1 is uniformly distributed with bounds of ±2%. Thus the difference between all thicknesses over the fleets of all companies is up to ±5%. However, the combined effect of the uniformly distributed error and variability is not uniformly distributed.

Table 4-2. Distribution of random variables having variability

Variables	Distribution	Mean	Scatter
Actual service load, P_{act}	Lognormal	$P_d = 100$	10% c.o.v.
Actual structural part width, w_{act}	Uniform	w_{built}	1% bounds
Actual structural part thickness, t_{act}	Uniform	t_{built}	3% bounds
Failure stress, σ_f	Lognormal	150	8% c.o.v.
Variability in built width, v_w	Uniform	0	1% bounds
Variability in built thickness, v_t	Uniform	0	3% bounds

c.o.v.= coefficient of variation

Certification Tests

After a structural part has been built with random errors in stress, load, width, allowable stress and thickness, we simulate certification testing for the structural part. Recall that the structural part will not be manufactured with complete fidelity to the design due to variability in the geometric properties. That is, the actual values of these parameters w_{act} and t_{act} will be different from their fleet-average values w_{built} and t_{built} due to variability. The structural part is then loaded with the design axial force of S_{FL} times P_{calc}, and if the stress exceeds the failure stress of the structure σ_f, then the structure fails and the design is rejected; otherwise it is certified for use. That is, the structural part is certified if the following inequality is satisfied

$$\sigma - \sigma_f = \frac{S_{FL} P_{calc}}{w_{act} t_{act}} - \sigma_f \leq 0 \tag{4.18}$$

The total safety factor (see Eq. (4.14)) depends on the load safety factor, the ratio of the failure stress to the B-basis allowable stress and the total error factor. Note that the B-basis properties are affected by the number of coupon tests. As the number of tests increases, the B-basis value is also increases, so a lower total safety factor is used. Amongst the terms in the total safety factor expression, the error term is subject to the largest change due to certification testing. Certification tests reduce the probability of failure by mainly changing the distribution of the error factor e_{total}. Without certification testing, we assume uniform distributions for all the individual errors. However, since designs based on unconservative models are more likely to fail certification, the distribution of e_{total} becomes conservative for structures that pass certification. In order to quantify this effect, we calculated the updated distribution of the error factor e_{total} by Monte Carlo Simulation (MCS) of a sample size of 1,000,000.

In Chapter 3, we represented the overall error with a single error factor e, hereinafter termed the "Single Error Factor model (SEF model)", and we used uniform distribution for the initial (i.e., built) distribution of this error. In the present work, we use a more complex representation of error with individual error factors, hereinafter termed the "Multiple Error Factor model (MEF model)", and we represent the initial distribution of each individual error factor with uniform distribution. In this case, the distribution of the total error is no longer uniform. Figure 4-1 shows how certification tests update the distribution of the total error for the SEF and MEF models. For both models the initial distribution is updated such that the likelihood of conservative values of the total error is increased. This is due to the fact that structures designed with unconservative (negative) errors are likely to be rejected in certification tests. Notice that the SEF model exaggerates the effectiveness of certification testing. The reader is referred to Appendix D for a detailed comparison of the two error models.

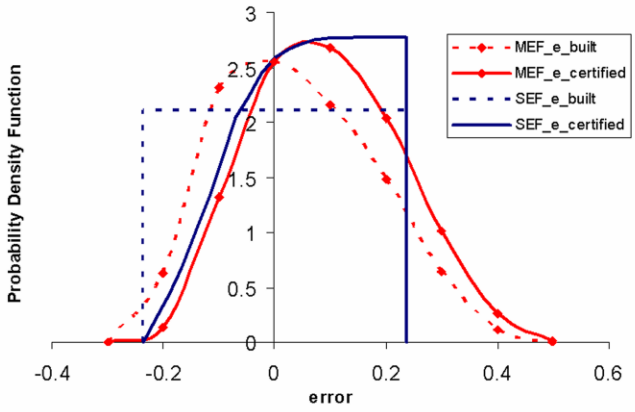

Figure 4-1. Comparing distributions of built and certified total error e_{total} of SEF and MEF models. The distributions are obtained from simulation of 1,000,000 structural parts. The lower and upper bounds for the single error are taken as -22.3% and 25.0%, respectively, to match the mean and standard deviation of the total error factor in the MEF model (see Table D-1 of Appendix D).

Figure 4-2 shows the distributions of the built and certified total safety factors of the MEF model. Notice that the structural parts designed with low total safety factors are likely to be rejected in the certification testing. The mean and standard deviations of built and certified distributions of the error factor and the total safety factor are listed in Table 4-3. Comparing the mean and standard deviation of the built and certified total error (and similarly the total safety factor), we see that the mean is increased and the standard deviation is reduced due to certification testing.

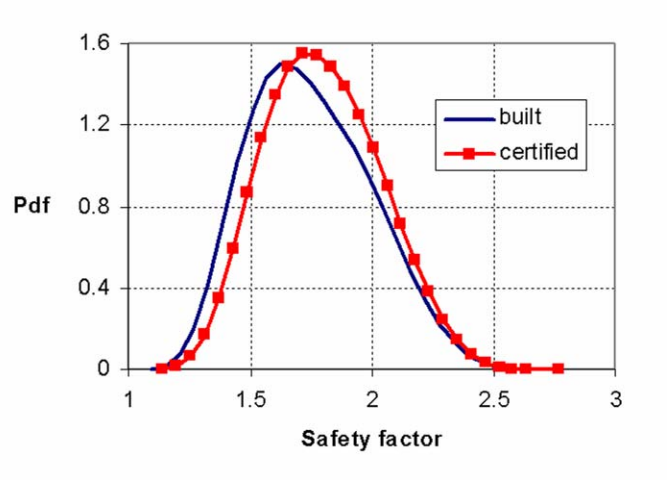

Figure 4-2. Initial and updated distribution of the total safety factor S_F. The distributions are obtained via Monte Carlo Simulations with 1,000,000 structural part models.

Table 4-3. Mean and standard deviations of the built and certified distributions of the error factor e_{total} and the total safety factor S_F shown in Figures 4-1 and 4-2. The calculations are performed with 1,000,000 MCS.

	Mean	Std. dev.
Built total error	0.0137	0.137
Certified total error	0.0429	0.130
Built safety factor	1.747	0.237
Certified safety factor	1.799	0.226

Probability of Failure Calculation

As noted earlier, we assume that structural failure requires the failure of two structural parts. In this section, we first describe the probability of failure calculations of a single structural part by using separable MCS. Then, we discuss the calculation of the system probability of failure.

Probability of Failure Calculation by Separable MCS

To calculate the probability of failure, we first incorporate the statistical distributions of errors and variability in a Monte Carlo simulation. Errors are uncertain at the time of design, but do not change for individual realizations (in actual service) of a particular design. On the other hand, all individual realizations of a particular design are different from each other due to variability. In Chapter 3, we implemented this through a two-level Monte Carlo simulation. At the upper level we simulated different aircraft companies by assigning random errors to each, and at the lower level we simulated variability in dimensions, material properties, and loads related to manufacturing variability and variability in service conditions. This provided not only the overall probability of failure, but also its variation from one company to another (which we measured by the standard deviation of the probability of failure). This variation is important because it is a measure of the confidence in the value of the probability of failure due to the epistemic uncertainty (lack of knowledge) in the errors. However, the process requires trillions of simulations for good accuracy.

In order to address the computational burden, we turned to the separable Monte Carlo procedure (e.g., Smarslok and Haftka (2006)). This procedure applies when the failure condition can be expressed as $g_1(x_1)>g_2(x_2)$, where x_1 and x_2 are two disjoint sets of random variables. To take advantage of this procedure, we need to formulate the

failure condition in a separable form, so that g_1 will depend only on variabilities and g_2 only on errors. The common formulation of the structural failure condition is in the form of a stress exceeding the material limit. This form, however, does not satisfy the separability requirement. For example, the stress depends on variability in material properties as well as design area, which reflects errors in the analysis process. To bring the failure condition to the right form, we instead formulate it as the required cross sectional area A'_{req} being larger than the built area A_{built}, as given in Eq. (4.19)

$$A_{built} < \frac{A_{req}}{(1+v_t)(1+v_w)} \equiv A'_{req} \tag{4.19}$$

where A_{req} is the cross-sectional area required to carry the actual loading conditions for a particular copy of an aircraft model, and A'_{req} is what the built area (fleet-average) needs to be in order for the particular copy to have the required area after allowing for variability in width and thickness.

$$A_{req} = P/\sigma_f \tag{4.20}$$

The required area depends only on variability, while the built area depends only on errors. When certification testing is taken into account, the built area, A_{built}, is replaced by the certified area, A_{cert}, which is the same as the built area for companies that pass certification. However, companies that fail are not included. That is, the failure condition is written as

Failure without certification tests: $A'_{req} - A_{built} > 0$ (4.21-a)

Failure with certification tests: $A'_{req} - A_{cert} > 0$ (4.21-b)

Equation (4.21) can be normalized by dividing the terms with A_0 (load carrying area without errors or safety measures, Eq. (4.13)). Since A_{built}/A_0 or A_{cert}/A_0 are the total safety factors, Eq. (4.21) is equivalent to the requirement that failure occurs when the required safety factor is larger than the built one.

Failure without certification tests: $\left(S_F\right)_{req} - \left(S_F\right)_{built} > 0$ (4.22-a)

Failure with certification tests: $\left(S_F\right)_{req} - \left(S_F\right)_{cert} > 0$ (4.22-b)

where $\left(S_F\right)_{built}$ and $\left(S_F\right)_{cert}$ are the built and certified total safety factors given in Eqs. (4.14) and (4.15), and the required total safety factor $\left(S_F\right)_{req}$ is calculated from

$$\left(S_F\right)_{req} = \frac{A'_{req}}{A_0} \tag{4.23}$$

For a given $\left(S_F\right)_{built}$ we can calculate the probability of failure, Eq. (4.22.a), by simulating all the variabilities with MCS. Figure 4-3 shows the dependence of the probability of failure on the total safety factor using MCS with 1,000,000 variability samples. The zigzagging in Figure 4-3 at high safety factor values is due to the limited MCS sample. Note that the probability of failure for a given total safety factor is one minus the cumulative distribution function (CDF) of the total required safety factor. This required safety factor depends on the four random variables P_{act}, σ_f, v_t and v_w. Among them P_{act} and σ_f have larger variabilities compared to v_t and v_w (see Table 4-2). We found that $\left(S_F\right)_{req}$ is accurately represented with a lognormal distribution, since P_{act} and σ_f follow lognormal distributions. Figure 4-3 also shows the probability of failure from the lognormal distribution with the same mean and standard deviation. Note that the nominal load safety factor of 1.5 is associated with a probability of failure of about 10^{-3}, while the

probabilities of failure observed in practice (about 10^{-7}) correspond to a total safety factor of about two.

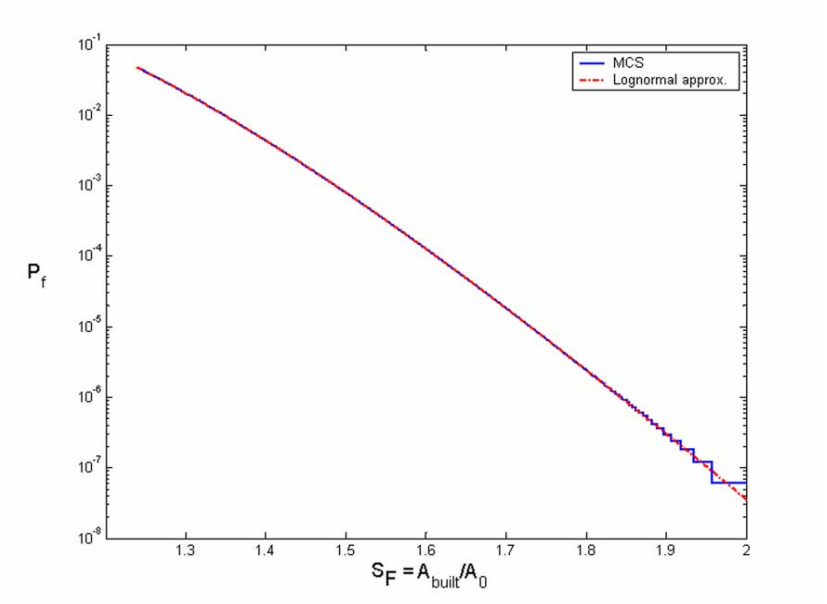

Figure 4-3. The variation of the probability of failure with the built total safety factor. Note that P_f is one minus the cumulative distribution function of $(S_F)_{req}$.

Figure 4-4 represents flowchart of a separable MCS procedure. Stage-1 represents the simulation of variabilities in the actual service conditions to generate the probability of failure as shown in Figure 4-3. This probability of failure is one minus the cumulative distribution function (CDF) of the required safety factor $(S_F)_{req}$. In Stage-1, M=1,000,000 simulations are performed and CDF of $(S_F)_{req}$ is assessed. A detailed discussion on CDF assessment for $(S_F)_{req}$ is given in Appendix E.

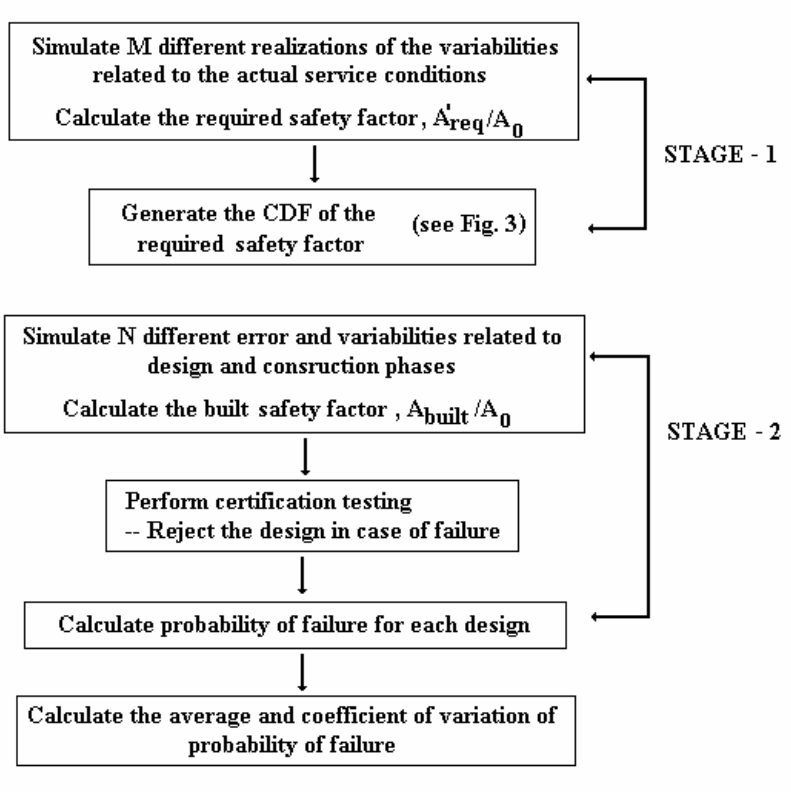

Figure 4-4. Flowchart for MCS of component design and failure

In Stage-2, N=1,000,000 designs are generated for N different aircraft companies. For each new design, different random error factors e_σ, e_P, e_w, e_t and e_f are picked from their corresponding distributions to generate the built safety factor, $(S_F)_{built}$. Then, each design is subjected to certification testing. If it passes, we obtain the probability of failure from the distribution obtained in Stage-1 (Figure 4-3). We calculate the average and coefficient of variation (c.o.v.) of the failure probability over all designs and explore the effects of error, variability, and safety measures on these values in Results section.

The separable Monte Carlo procedure reduces the computational burden greatly. For instance, if the probability of failure is 2.5×10^{-5}, a million simulations varying both errors and variability simultaneously estimate this probability with 20% error. We found for our problem that the use of the separable Monte Carlo procedure requires only 20,000

simulations (10,000 simulations for Stage-1 and 10,000 for Stage-2) for the same level of accuracy.

Including Redundancy

The requirement of two failure events is modeled here as a parallel system. We assume that the limit-states of the both failure events follow normal distribution to take advantage of known properties of the bivariate normal distribution. For a parallel system of two elements with equal failure probabilities, Eq. (4.24) is used to calculate the system probability of failure P_{FS} (see Appendix F for details)

$$P_{FS} = P_f^2 + \frac{1}{2\pi}\int_0^{\rho} \frac{1}{\sqrt{1-z^2}} \exp\left(-\frac{\beta^2}{1+z}\right) dz \tag{4.24}$$

where P_f is the probability of failure of a single structural part, ρ is the correlation coefficient of the two limit-states and β is the reliability index for a single structural part, which is related to P_f through Eq. (4.25)

$$P_f = \Phi(-\beta) \tag{4.25}$$

Results

In this section, the effectiveness of safety measures is investigated and the results are reported. First, we discuss the effects of error reduction. Then, the relative effectiveness of error reduction and certification is compared. Next, the effectiveness of redundancy is explored. Finally, the effectiveness of variability reduction is investigated.

Effect of Errors

We first investigate the effect of errors on the probability of failure of a single *structural part*. For the sake of simplicity, we scale all error components with a single multiplier, *k*, replacing Eq. (4.12) by

$$e_{total} = \frac{(1+k\,e_\sigma)(1+k\,e_P)(1+k\,e_t)(1+k\,e_w)}{1-k\,e_f} - 1 \tag{4.26}$$

and explore the effect of k on the probability of failure.

Table 4-4 presents the average and coefficient of variation of the probability of failure of a single structural part. The coefficient of variation of the failure probability is computed to explore our confidence in the probability of failure estimate, since it reflects the effect of the unknown errors. Columns 5 and 6 of Table 4-4 show a very high coefficient of variation for the failure probabilities (variability in the probability of failure for different aircraft models). We see that as the error grows (i.e., k increases), the coefficient of variation of failure probabilities after certification also grows. Comparing the failure probabilities before certification (column 5) and after certification (column 6), we notice that even though certification tests reduce the mean failure probability, they increase the variability in failure probability.

Table 4-4 shows that for nominal error (i.e., k=1) the total safety factor before certification is 1.747, which is translated into a probability of failure of 8.83×10^{-4}. When the certification testing is included, the safety factor is increased to 1.799, which reduces the probability of failure to 3.79×10^{-4}. Notice also that the coefficient of variation of the safety factor is reduced from 13.6% to 12.5%, which is a first glimpse of an indication that the certification testing is more effective than simply increasing the safety factor with an increased built area. A detailed analysis of the effectiveness of certification testing is given in the next subsection.

Column 2 of Table 4-4 shows a rapid increase in the certification failure rate with increasing error. This is reflected in a rapid increase in the average safety factor of

certified designs in column 4, $(S_F)_{cert}$. This increased safety factor manifests itself in the last column of Table 4-4 that presents the effect of certification tests on failure probabilities. As we can see from that column, when the error increases, the ratio of the two failure probabilities decreases, demonstrating that the certification tests become more effective. This trend of the increase of the design areas and the probability ratios is similar to the one observed in Chapter 3. Note, however, that even the average safety factor before certification ($(S_F)_{built}$ in column 3) increases with the error due to the asymmetry of the initial total error distribution (see Figure 4-1).

Table 4-4. Average and coefficient of variation of the probability of failure for the structural parts designed with B-basis properties and S_{FL}=1.5. The numbers inside the parentheses represent the coefficient of variation of the relevant quantity.

k	CFR[(a)] (%)	$(S_F)_{built}$ [(b)]	$(S_F)_{cert}$ [(b)]	P_{nc} [(c)]/10^{-4}	P_c [(c)]/10^{-4}	$\bar{P}_c / \bar{P}_{nc}$
0.25	6.4	1.725 (4.2%)	1.728 (4.1%)	0.244 (148%)	0.227 (148%)	0.930
0.50	9.3	1.730 (6.9%)	1.741 (6.7%)	0.763 (247%)	0.609 (257%)	0.798
0.75	13.4	1.737 (10.2%)	1.764 (9.7%)	2.70 (324%)	1.66 (357%)	0.616
0.82	14.7	1.740 (11.2%)	1.773 (10.6%)	3.79 (340%)	2.13 (384%)	0.561
1	18.0	1.747 (13.6%)	1.799 (12.5%)	8.83 (371%)	3.79 (450%)	0.430
1.5	26.0	1.779 (20.5%)	1.901 (17.8%)	60.0 (385%)	11.5 (583%)	0.191

[(a)] CFR: Certification failure rate.

[(b)] $(S_F)_{built}$ and $(S_F)_{cert}$ are the total safety factors before and after certification testing, respectively.

[(c)] P_{nc} and P_c are the probabilities of failure before and after certification testing, respectively.

Table 4-4 shows the huge waste of weight due to errors. For instance, for the nominal error (i.e., k=1.0), an average built total safety factor of 1.747 corresponds to a probability of failure of 8.83×10^{-4} according to Table 4-4, but we see from Figure 4-3 that a safety factor of 1.747 approximately corresponds to a probability of failure of 7×10^{-6}, two orders of magnitude lower. This discrepancy is due to the high value of the coefficient of variation of the safety factor. For the nominal error, the coefficient of variation of the total safety factor is 14%. Two standard deviations below the mean safety

factor is 1.272, and two standard deviations above the mean safety factor is 2.222. The probability of failure corresponding to the safety factor of 1.272 (from Figure 4-3) is about 2.98×10^{-2}, while the safety of 1.985 the probability of failure is essentially zero. So even though about 0.8% of the designs a have safety factor below 1.272 (Figure 4-2), these designs have a huge impact on the probability of failure. Reducing the error by half (i.e., k=0.50), reduces the weight by 1%, while at the same time the probability of failure is reduced by a factor of 3.

Weight Saving Due to Certification Testing and Error Reduction

We have seen in Table 4-4 that since structures built with unconservative errors are eliminated by certification testing; the tests increase the average safety factor of the designs and therefore reduce the average probability of failure. Since certification testing is expensive, it is useful to check if the same decrease in the probability of failure can be achieved by simply increasing the load carrying area by the same amount (i.e., by increasing the safety factor) without certification testing. Column 2 of Table 4-5 shows that the required area with no certification testing, $A_{r,nc}$, is greater than the certified area, A_{cert}, (i.e., area after certification testing) shown in column 3. The last column shows that the weight saving by using certification test instead of a mere increase of the safety factor. We notice that weight saving increases rapidly as the error increases. For instance, when k=0.25 the weight saving is very small. Columns 4 and 5 show that even though we match the average probability of failure, there are small differences in the coefficients of variation.

Table 4-5. Reduction of the weight of structural parts by certification testing for a given probability of failure. The numbers inside the parentheses represent the coefficient of variation of the relevant quantity.

k	$A_{r,nc}/A_0$ [(a)]	A_{cert}/A_0	P_{nc} [(b)]$/10^{-4}$	P_c [(b)]$/10^{-4}$	%ΔA [(c)]
0.25	1.7285 (4.2%)	1.7283 (4.1%)	0.227 (148%)	0.227 (148%)	-0.01
0.50	1.743 (6.9%)	1.741 (6.7%)	0.609 (252%)	0.609 (257%)	-0.14
0.75	1.770 (10.3%)	1.764 (9.7%)	1.66 (342%)	1.66 (357%)	-0.36
1	1.815 (13.7%)	1.799 (12.5%)	3.79 (416%)	3.79 (450%)	-0.87
1.5	1.961 (20.7%)	1.901 (17.8%)	11.5 (530%)	11.5 (583%)	-3.09

[(a)] $A_{r,nc}$ is the required area with no certification testing, the area required to achieve the same probability of failure as certification.
[(b)] P_{nc} and P_c are the probabilities of failure before and after certification testing, respectively.
[(c)] $\Delta A = (A_{cert}-A_{r,nc})/A_{r,nc}$ indicates weight saving due to testing while keeping the same level of safety

We notice from Table 4-5 that, for the nominal error (i.e., k=1.0), certification testing reduces the weight by 0.87% for the same probability of failure (3.79×10^{-4}). The same probability of failure could have been attained by reducing the error bounds by 18%, that is by reducing k from 1.0 to 0.82. This reduction would be accompanied by an $\left(S_F\right)_{built}$ =1.740 (see Table 4-4). Compared to the 1.799 reduction $\left(S_F\right)_{built}$, this represents a reduction of 4.13% in average weight, so error reduction is much more effective than certification testing in reducing weight.

Effect of Redundancy

To explore the effect of redundancy, we first compare the failure probability of a single structural part to that of a structural system that fails due to failure of two structural parts. Certification testing is simulated by modeling the testing of one structural part and certifying the structural system based on this test. Table 4-6 shows that while the average failure probability is reduced through structural redundancy, the coefficients of variation of the failure probabilities are increased. That is, even though the safety is improved, our confidence in the failure probability estimation is reduced. This behavior is similar to the

effect of certification (Table 4-4). In addition, we also notice that as the error grows, the benefit of redundancy also diminishes. This result reflects the fact that high errors result in high probabilities of failure, and redundancy is more effective for smaller probabilities of failure. This behavior, however, is opposite to that resulting from certification testing. We notice that even though one safety measure—certification testing—is more effective when errors are high, another safety measure—redundancy—is more effective when errors are low. So the level of uncertainty in the problem may decide on the efficient use of safety measures.

Comparing the reduction probabilities of failure before and after certification listed in the columns 4 and 7 of Table 4-6, we notice that the effect of redundancy is enhanced through certification testing.

Table 4-6. Effect of redundancy on the probabilities of failure. The numbers inside the parentheses represent the coefficient of variation of the relevant quantity. The coefficient correlation between failures of structural parts is taken as 0.5.

	Before certification			After certification		
	Part	System		Part	System	
k	P_{nc} [(a)]/10^{-4}	P_{nc} [(a)]/10^{-4}	reduction	P_c [(a)]/10^{-4}	P_c [(a)]/10^{-4}	reduction
0.25	0.244 (148%)	0.005 (230%)	52.1	0.227 (148%)	0.004 (230%)	53.5
0.50	0.763 (247%)	0.029 (388%)	26.3	0.609 (257%)	0.022 (408%)	28.0
0.75	2.70 (324%)	0.195 (503%)	13.8	1.66 (357%)	0.106 (568%)	15.6
1.0	8.83 (371%)	1.11 (563%)	7.9	3.79 (450%)	0.390 (718%)	9.7
1.5	60.0 (385%)	17.2 (549%)	3.5	11.5 (583%)	2.21 (945%)	5.2

[(a)] P_{nc} and P_c are the probabilities of failure before and after certification testing, respectively.
[(b)] The ratio of probabilities of failure of the structural part and the system of two parts

Next, we investigate the interaction of two safety measures: redundancy and certification testing. Comparing the probability ratios in Table 4-7, we see that including redundancy improves the effectiveness of certification testing. Mathematically, this can be explained with the following example. For a nominal error, k=1.0, the probabilities of failure before and after certification of a structural part are 8.83×10^{-4} and 3.79×10^{-4},

respectively. The system probabilities of failure before and after certification are calculated by using Eq. (4.24) as 1.31×10^{-4} and 0.39×10^{-4}, respectively. Notice that the system failure probability ratio is smaller than the component probability ratio, because redundancy is more effective for small probabilities of failure. Physically, the reason for the increase in the effectiveness certification is that in the certification test, failure of a single part leads to rejection of the design of structural system, while under actual service conditions, two failure events are needed for the failure of the structure. Thus, modeling redundancy is equivalent to modeling a relatively more severe certification testing. This result is similar to the finding of Kale and Haftka (2003), who explored the effect of safety measures on aircraft structures designed for fatigue. They found that certification testing of an aircraft structure with a large machined crack of B-basis initial size was more effective than testing the structure with a random (natural) crack.

Table 4-7. Effect of redundancy on the effectiveness of certification testing. The coefficient correlation between failures of structural parts is taken as 0.5.

k	$\overline{P}_c / \overline{P}_{nc}$ (part)	$\overline{P}_c / \overline{P}_{nc}$ (system)
0.25	0.930	0.905
0.50	0.798	0.749
0.75	0.616	0.543
1	0.430	0.350
1.5	0.191	0.129

$\overline{P}_{nc}$ and $\overline{P}_c$ are the mean values of probabilities of failure before and after certification testing, respectively.

Effect of the correlation coefficient

Recall that the correlation coefficient of the probabilities of failure of the two structural parts was assumed to be 0.5. Table 4-8 shows that as the correlation coefficient decreases, the probability of failure of the system also decreases, but at the same time our confidence in the probability estimation also reduces. The last column of Table 4-8 shows that as the correlation coefficient decreases, certification testing becomes more effective,

which can be explained as follows. As the coefficient of correlation decreases, the structural parts behave more independently. Applying certification testing based on the failure of a single structural part means using more severe certification testing. This reminds us that as with any redundant system it pays to reduce the correlation coefficient of duplicate hardware (e.g., to use a back up part made by a different company). It is intriguing to speculate on the possible application to structural design. Is it feasible, for example, to buy structural materials from different vendors for skin and stiffeners?

Table 4-8. Effect of correlation coefficient ρ on *system* failure probabilities and effectiveness of certification testing. The numbers inside the parentheses represent the coefficient of variation of the relevant quantity. The error multiplier k is taken as 1.0.

ρ	$P_{nc}/10^{-4}$	$P_c/10^{-4}$	$\bar{P}_c / \bar{P}_{nc}$
0.3	0.506 (678%)	0.161 (885%)	0.319
0.4	0.761 (615%)	0.255 (794%)	0.335
0.5	1.11 (563%)	0.390 (718%)	0.350
0.6	1.60 (519%)	0.583 (655%)	0.365
0.7	2.27 (480%)	0.859 (516%)	0.378

Additional Safety Factor Due to Redundancy

Recall that the results given in Table 4-6 show how redundancy reduces the probability of failure. For instance, for k=1.0 the average probability of failure before certification, P_{nc}, is reduced from 8.83×10^{-4} to 1.11×10^{-4}. This reduction in probability of failure leads to an increase in the total safety factor. For each error multiplier k value, we calculate the additional safety factor required to reduce the probability of failure of a structural part to that of the structural system. The second and third columns of Table 4-9 show two opposing effects on the additional safety factor. As the error grows, the probabilities of failure before and after certification increase, so the effect of redundancy decreases because the redundancy is more effective for lower failure probabilities. Hence, the additional safety factor due to redundancy decreases with increased error (see also

Figure 4-5). However, as indicated in the last column of Table 4-9 the ratio of safety factors after and before certification testing increases with increased error because the certification is more effective for high errors.

Table 4-9. Additional safety factor due to redundancy

k	$(S_{F-add})_{nc}$	$(S_{F-add})_{c}$	% increase due certification
0.25	1.120	1.120	0.0
0.50	1.111	1.112	0.1
0.75	1.101	1.103	0.2
1	1.093	1.096	0.3
1.5	1.078	1.085	0.7

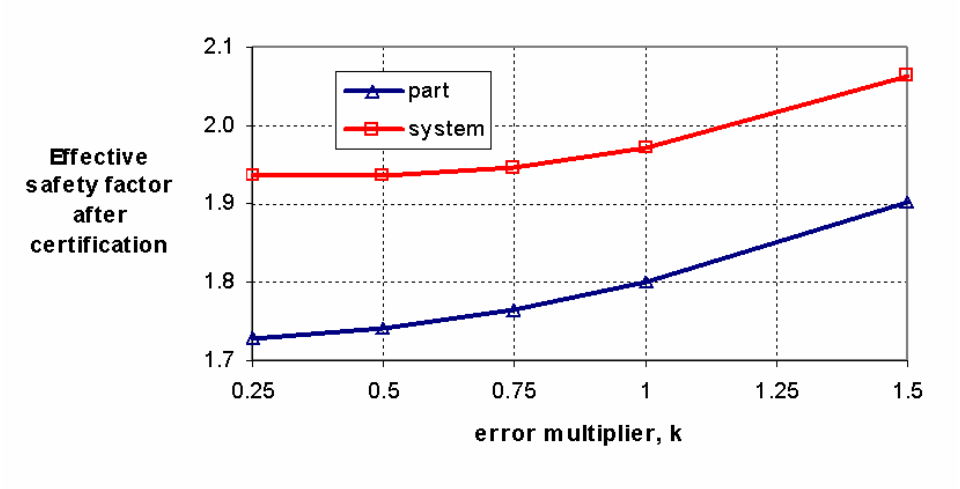

Figure 4-5. Total safety factors for MEF model for the structural part and system after certification

Effect of Variability Reduction

Finally, we investigate the effect of variability reduction on the average safety factor, design area and system probability of failure. We observe from Table 4-10 that the average safety factor and design area increase with the increase of variability in failure stress. In addition, we observe from the P_f ratio given in the last column of Table 4-10 that certification testing becomes less effective as variability increases. Figure 4-6 also shows the reduced efficiency of testing with increased variability. The second column of Table 4-10 shows that the certification testing failure rate (CFR) reduces with increased

variability. As variability is increased, the built load carrying area is also increased (column 5), so CFR is reduced accordingly.

Table 4-10. Comparison of system failure probabilities corresponding to different variability in failure stress σ_f.

c.o.v. (σ_f)	CFR[(a)] (%)	Average A_{built}/A_0 [(b)]	Average A_{cert}/A_0 [(b)]	$\bar{P}_{nc}/10^{-4}$	$\bar{P}_c/10^{-4}$	P_f Ratio
0	50.0	1.521	1.676	9.27	0.001	0.001
4%	32.3	1.629	1.727	2.00	0.008	0.040
8%	18.0	1.747	1.799	1.11	0.390	0.350
12%	11.6	1.878	1.910	1.19	0.737	0.619

[(a)]CFR: Certification failure rate

[(b)] A_{built}/A_0 and A_{cert}/A_0 are the total safety factors before and after certification testing, respectively.

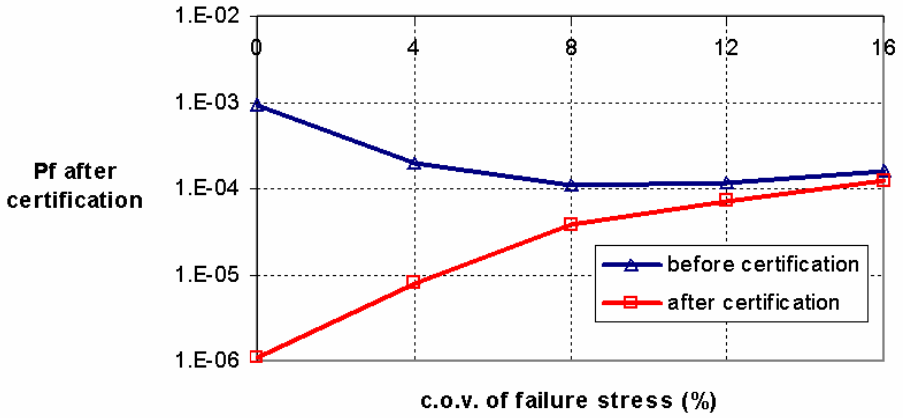

Figure 4-6. Effect of variability on failure probability

Table 4-10 shows two opposing effects of variability on the two failure probabilities (before certification, $\bar{P}_{nc}$, and after certification, $\bar{P}_c$, see columns 7 and 8). When the coefficient of variation in the failure stress is increased from 0% to 8%, the safety factor before certification (column 3) increases from 1.521 to 1.676, because a smaller B-basis value is used for the allowable failure stress. Note that the initial safety factor for no variability would be 1.5 if the error distribution (hence the safety factor distribution) is symmetric, but since the distributions are skewed (see Figures 4-1 and 4-

2) the safety factor is 1.521. The increase in the safety factor with increased error leads to a reduction in the probability of failure before certification (column 5). However, for higher coefficients of variation, the probability of failure before certification increases again, because the increased safety factor is not enough to compensate for the large variation in airplanes. However, once certification is included, the picture is different. For no variability, even though the safety factor is increased by 10% (from 1.521 to 1.676, see columns 3 and 4), the probability of failure reduces four order of magnitudes (columns 5 and 6) due to the high effectiveness of certification testing at low variability. As variability increases, the effectiveness of certification testing reduces (column 7), so the probability of failure after certification is still high.

Table 4-10 also indicates the advantage of reducing variability. Reducing variability from 8% to 4% reduces the weight by 4%, while at the same time reducing the probability of failure by a factor of 50. However, the certification failure rate is unacceptably increased from 18% to 32%. To compensate for this, however, a company may reduce the weight gain back to an additional safety factor of 1.747/1.629=1.072, and have a reduced system probability of failure of 3.64×10^{-6} (compared to 3.90×10^{-5}) and a reduced certification failure rate of 14.7% (compared to 18.0%). However, in reality companies reduce the chance of certification failure by structural element tests and conservative interpretation of the results of these tests. These are not analyzed in this chapter. The effects of structural element tests will be discussed in detail in Chapter 7.

In addition, Table 4-10 reveals that variability reduction is more effective than error reduction. For example, reducing all errors by half (i.e., reducing k from 1 to 0.5) leads to reducing the built safety factor from 1.747 to 1.730 (Table 4-4), along with reducing the

system probability of failure from 3.90×10^{-5} to 2.20×10^{-6} (Table 4-6). On the other hand, reducing variability by half (that is, reducing c.o.v. of the failure stress from 8% to 4%) leads to reducing the built safety factor from 1.747 to 1.629, along with reducing the system probability of failure from 3.90×10^{-5} to 8.0×10^{-7} (Table 4-10). That is, variability reduction leads to more weight saving and probability of failure reduction than error reduction.

Summary

The relative effectiveness of safety measures taken during aircraft structural design is demonstrated in this chapter. The safety factor, conservative material properties, certification testing, redundancy, error and variability reduction were included in this study and the following was observed.

- While certification testing is more effective for improving safety rather than increased safety factors, it cannot compete with even a small reduction in errors.
- Variability reduction is even more effective than error reduction, but it needs to be accompanied by additional knockdown factors to compensate for the increase in the B-basis value.
- Our probabilities of failure are still high compared with the historical record (probability of failure of 10^{-7}). This is probably due to the effect of building block tests, which we will address in Chapter 7.
- One safety measure, certification testing, is more effective when errors are large, while another safety measure, redundancy, is more effective when errors are low. Certification testing is more effective when the variability is low. At a low variability level, redundancy accompanied with certification testing is effective.
- Adding redundancy is equivalent to using an additional safety factor of about 1.1.

CHAPTER 5
INCREASING ALLOWABLE FLIGHT LOADS BY IMPROVED STRUCTURAL MODELING

In this chapter we analyze the tradeoffs of allowable flight loads and safety of aerospace structures via deterministic and probabilistic design methodologies. The design methodologies are illustrated by performing allowable flight load calculation of a sandwich panel used in aerospace structures. We explore the effect of using a more accurate prediction technique for interfacial fracture toughness, which combines interfacial fracture toughness with mode-mixity instead of using the traditional model that disregards mode-mixity, on increasing the allowable design load of existing structures.

The work presented in this chapter was also published in Acar *et al*. (2006b). Mr. Xueshi Qiu is acknowledged for his contribution to this work.

Introduction

Structural design of aerospace structures is still performed with deterministic design philosophy. Researchers are constantly improving the accuracy of structural analysis and failure prediction. This improvement in accuracy reduces uncertainty in aircraft design and can therefore be used to enhance safety. However, since the record of structural safety in civilian transport aircraft is very good, it makes sense to ask how to translate the reduced uncertainty to increased flight loads or weight reduction if safety is to be maintained at a specified level. The term "allowable flight load" here refers to the maximum allowable load that can be carried by the structure for a specific failure mode.

Currently, there is no accepted way to translate the improvements in accuracy to weight savings or increased allowable flight loads. The objective of this chapter is to take the first step in this direction by utilizing probabilistic design methodology. Haftka (2005) describes how works of Starnes and colleagues (e.g., Li *et al.* 1997, Arbocz and Starnes 2002) to model variability in buckling of circular cylinders inspired work in his research group on using variability control on reducing the weight of composite liquid hydrogen tanks. Qu *et al*. (2003) showed that for fixed probability of failure, small reductions in variability can be translated to substantial weight savings. Here we seek to investigate the potential of improved structural modeling.

Some commercial aircraft which entered service in 1970's or 1980's are expected to reach their design service life soon. However, since researchers are constantly improving the accuracy of structural analysis and failure prediction, the maximum allowable flight loads of those aircraft can be recalculated to utilize the full potential of their structures. Motivated by this goal, we consider a given aerospace structure that is already designed and we aim to re-calculate the allowable flight load of the structure due to improved analysis. We expect that for some designs, lower allowable loads will be predicted by the improved analysis, whereas for others higher allowable flight loads will be predicted. However, because improved models reduce uncertainty, we may expect an average increase of the allow-able flight loads over all designs. An important focus of the chapter is to show that modeling error can masquerade as observed variability, which can be reduced (or even eliminated) by better understanding of the physical phenomenon.

Here, we chose a sandwich panel as an example because the improved model was developed by one of the authors and we had good access to the details of experiments and

computations. Sandwich structures are used in aerospace vehicles due to their low areal density and high stiffness. Debonding of core from the face sheet is a common failure mode in sandwich construction, and the interfacial fracture is traditionally characterized by a single fracture toughness parameter. However, in reality the fracture toughness is a function of the relative amount of mode II to mode I (mode-mixity) acting on the interface (e.g., Suo 1999). Stiffness of sandwich structures depends very much on the integrity of the face sheet/core bonding. Even a small disbond can significantly reduce the load carrying capacity, especially when the structure is under compressive loads (Avery and Sankar 2000, Sankar and Narayanan 2001). Grau *et al*. (2005) measured the interfacial fracture toughness as a function of mode-mixity to characterize the propagation of the disbond between the face sheet and the core. They performed asymmetric double cantilever beam fracture tests to determine the interfacial fracture toughness of the sandwich composite, and then demonstrated its application in predicting the performance of a sandwich structure containing a disbond. The use of mode-mixity dependent fracture toughness led to improvement in the accuracy of failure prediction of the debonded structure. We perform probabilistic analysis of the debonded sandwich structure analyzed by deterministic approach by Grau *et al*. (2005) to explore a possible increase in the allowable flight load of the structure.

The following section discusses the design of a sandwich structure used as an illustration. Next, the analysis of structural uncertainties (error and variability), with the main perspective of how to control uncertainty, is presented. Then, discussion on calculation of B-basis properties and allowable flight load calculation for sandwich structures by deterministic design are given. Next, the assessment of probability of failure

of sandwich structures is presented, followed by discussion of the tradeoffs of accuracy and allowable flight load via probabilistic design. The chapter is finalized with concluding remarks given in Summary section.

Structural Analysis of a Sandwich Structure

Sandwich panels are susceptible to debonding of the face sheet from the core. This is similar to the phenomenon of delamination in laminated composites. Disbonds can develop due to poor manufacturing or during service, for example, due to foreign object impact damage. Evaluation of damage and prediction of residual strength and stiffness of debonded sandwich panels is critical because the disbonds can grow in an unstable manner and can lead to catastrophic failure. Stiffness of sandwich structures depends very much on the integrity of the face sheet/core bonding. Even a small disbond can significantly reduce the load carrying capacity, when the structure is under compressive loads (Avery and Sankar 2000, Sankar and Narayanan 2001), because the debonded face sheet can buckle and create conditions at the crack tip that are conducive for unstable propagation of the disbond. This problem has become very significant after the historic failure of X-33 vehicle fuel tank made of sandwich panels of polymer matrix composite face sheets and honeycomb core.

Fracture at the interface between dissimilar materials is a critical phenomenon in many multi-material systems including sandwich construction. Traditionally, in engineering practice, the interfacial fracture was characterized by a single fracture toughness parameter obtained by averaging the interfacial fracture toughness, hereinafter termed as "average G_c" or G_c^A, obtained for some number of K_I and K_{II} combinations, where K_I and K_{II} are the mode I and mode II stress intensity factors, respectively. Later, studies have indicated, e.g. Suo (1999), that for these multi-material systems, the

interfacial fracture is a strong function of the relative amount of mode II to mode I acting on the inter-face, hereinafter termed as "G_c with mode-mixity" or G_c^{MM}. The criterion for initiation of crack advance at the inter-face can be stated as

$$G = G_c(\psi), \quad \psi = \tan^{-1}(K_{II}/K_I) \tag{5.1}$$

where G is the strain energy release rate and G_c is the interfacial fracture toughness, which depends on the mode-mixity angle ψ. In bimaterial fracture, K_I and K_{II} are the real and imaginary parts of the complex stress intensity factor K. The toughness of interface $G_c(\psi)$ can be thought of as an effective surface energy that depends on the mode of loading.

Grau *et al*. (2005) analyzed a debonded sandwich panel, and determined the maximum internal gas pressure in the core before the disbond could propagate. They used interfacial fracture mechanics concepts to analyze this problem. The main premise here is that the crack will propagate when the energy release rate equals the fracture toughness for the core/face-sheet interface. The load and boundary conditions for the model problem are depicted in Figure 5-1.

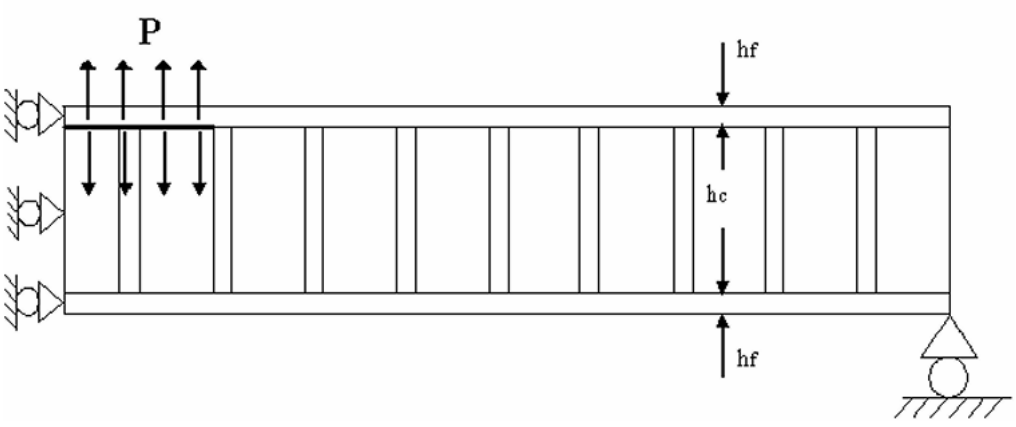

Figure 5-1. The model of face-sheet/core debonding in a one-dimensional sandwich panel with pressure load. Note that due to symmetry only half of the structure is modeled.

The maximum allowable pressure for a given disbond length is calculated from the energy release rate G_0 for a unit applied pressure. The energy release rate G is proportional to the square of the applied load or

$$G = G_0 p^2 \tag{5.2}$$

where p is the applied pressure. This failure assessment is a good approximation within the limits of a linear analysis. We assume that the epistemic uncertainty related to this failure function is negligible compared to the uncertainty in fracture toughness. The critical pressure p_{max} can be obtained using

$$p_{\max} = \sqrt{\frac{G_c}{G_0}} \tag{5.3}$$

where G_c is the interfacial fracture toughness of the sandwich material system obtained from testing.

Grau (2003) conducted asymmetric Double Cantilever Beam (DCB) tests to determine the interfacial fracture toughness of the sandwich composite. The face sheet material was A50TF266 S6 Class E, Fiber designation T800HB-12K-40B, matrix 3631 and the core sheet material was Euro-Composites aramid (ECA) fiber type honeycomb. Grau *et al*. (2005) performed finite element analyses to compute the mode-mixity angle corresponding to designs tested in experiments. The average interfacial fracture toughness prediction and the fracture toughness in terms of mode-mixity angle based on their work are presented in Figure 5-2.

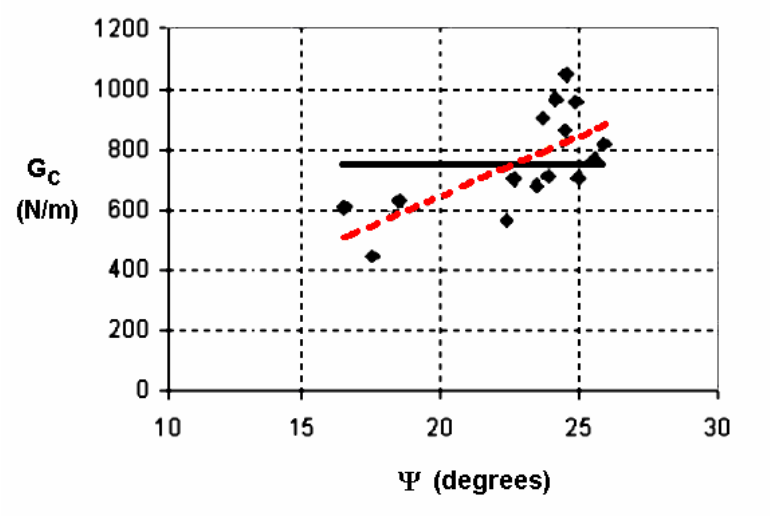

Figure 5-2. Critical energy release rate as a function of mode mixity. The continuous line denotes average G_c (G_c^A) and the dashed line denotes a linear least square to fit to G_c (G_c^{MM}) as a function of mode-mixity angle. The linear fit has R^2_{adj}=0.473, e_{rms}=121.6 N/m.

As shown in Fig.5-2, a simple way of determining the interfacial fracture toughness parameter is to perform fracture toughness tests for different core thickness, face sheet thickness and crack length combinations, which correspond to different mode-mixity values, and to take the average fracture toughness value. However, as seen from Fig. 5-2 that the critical energy release rate is assessed better as a function of mode-mixity. Grau *et al*. (2005) represent the critical energy release rate as a linear function of the mode-mixity (which they calculate from finite element analysis), that improves the accuracy of estimate of G_c.

From Fig. 5-2 we note that without the mode-mixity model, G_c would exhibit huge scatter (443 N/m to 1047 N/m). The mode-mixity model reduces the scatter, because instead of a constant, G_c is now predicted to vary from 513 N/m to 875 N/m. That is, the simplicity of the average G_c model causes error in that model to masquerade as variability. For instance, the model of constant gravity acceleration (constant g) will lead to a scatter when measured in different towns partially due to difference in altitude. A

model that takes altitude into account will show less scatter around the computed value of g. The uncertainty reduction in turn can be used to increase the safety or the effectiveness of the structure.

Analysis of Error and Variability

As in the previous chapters, we classify the uncertainties into two as errors and variability. The uncertainties that affect the entire fleet are called here errors. They reflect inaccurate modeling of physical phenomena, errors in structural analysis, errors in load calculations, or use of materials and tooling in construction that are different from those specified by the designer. The variability (aleatory uncertainty) reflects variability in material properties, geometry, or loading between different copies of the same structure.

For the sake of simplicity, we assume that with mode-mixity there are no remaining errors in the predicted value of G_c for given mode-mixity angle calculated from finite element analysis. Adding an estimate of the remaining error can be easily accommodated by the analysis below. However, we assume that the scatter of G_c around mode-mixity dependent G_c represents variability. The experimental values given in Table 5-1 are the mean values of the fracture toughness measured through five experiments in Grau *et al*. (2005) for each mode-mixity. We assume that the use of these mean values eliminates most of the measurement variability and leaves out only the material variability. On the other hand, the scatter around the average G_c represents combined error and variability.

The deviations of experimentally measured fracture toughness values from the two fits d_A and d^{MM} (the deviations from the constant fit and from the linear fit, see Fig. 5-2) given in Table 5-1 are calculated from

$$d^{\mathrm{A}} = G_c^{\mathrm{EXP}} - G_c^{\mathrm{A}}, \quad d^{\mathrm{MM}} = G_c^{\mathrm{EXP}} - G_c^{\mathrm{MM}} \tag{5.4}$$

where G_c^{EXP} is the experimentally measured fracture toughness, G_c^{A} and G_c^{MM} are the fracture toughness from the constant fit and linear fit, respectively.

Table 5-1. Deviations between measured and fitted values of "average G_c" and "G_c with mode mixity" for different designs. The superscript 'A' denotes the average fracture toughness and 'MM' indicates mode-mixity dependent fracture toughness, and 'd' represents the deviation of experimental values from the constant fit or from the linear fit.

Specimen	ψ (deg)	G_c^{EXP} (N/m)	G_c^{A} (N/m)	G_c^{MM} (N/m)	d^{A} (N/m)	d^{MM} (N/m)
1	16.52	609.4	746.6	513.2	-137.1	96.2
2	17.53	443.1	746.6	552.2	-303.5	-109.1
3	18.05	577.9	746.6	572.3	-168.7	5.6
4	18.50	628.7	746.6	589.7	-117.9	39.0
5	22.39	565.7	746.6	739.5	-180.9	-173.8
6	23.89	711.0	746.6	797.1	-35.6	-86.1
7	24.50	863.4	746.6	820.6	116.8	42.8
8	24.89	956.2	746.6	835.9	209.6	120.3
9	23.48	679.5	746.6	781.4	-67.1	-101.9
10	24.98	707.5	746.6	839.3	-39.1	-131.7
11	25.55	767.1	746.6	861.1	20.5	-94.1
12	25.90	817.8	746.6	874.8	71.3	-56.9
13	22.65	702.3	746.6	749.3	-44.3	-47.1
14	23.69	903.7	746.6	789.5	157.1	114.1
15	24.15	964.9	746.6	807.2	218.4	157.7
16	24.54	1047.3	746.6	822.3	300.7	224.9
Standard deviation		162.2	0	115.6	162.2	113.8

Each row of Table 5-1 corresponds to a different specimen. Each specimen has a different core thickness, face sheet thickness and crack length, thus having a different mode-mixity angle (calculated through finite element analysis). The sixth column of Table 5-1 presents the deviations of G_c values obtained through experiments from their average values. These deviations combine variability and error. Errors are due to neglecting the effect of mode-mixity in G_c. We assume that these are the only errors so that d^{MM} represents only variability.

Approximate cumulative distribution function (CDF) for the variability is obtained by using ARENA software (Kelton *et al*. 1998). The distribution parameters and

goodness-of-fit statistics for the distributions are as follows. For variability, d^{MM}, ARENA found the best distribution as the normal distribution with a mean value of zero and a standard deviation of 113.8 N/m. For obtaining goodness-of-fit statistics, Chi-square and Kolmogorov-Smirnov tests are the commonly used. For our case the number of data points is low; hence, the Chi-square test does not provide reliable statistics, therefore ARENA uses the Kolmogorov-Smirnov test to decide if a sample comes from a population with a specific distribution. The p-value of Kolmogorov-Smirnov test is greater than 0.15. For total uncertainty, d^{A}, ARENA found the best distribution as the normal distribution with a mean value of zero and a standard deviation of 162.2 N/m. The p-value for Kolmogorov-Smirnov test is again greater than 0.15. The corresponding p-value is a measure for goodness of the fit. Larger p-values indicate better fits (Kelton *et al*. 1998), with p-values less than about 0.05 indicating poor fit.

Figures 5-3 and 5-4 show the comparison of the actual and fitted CDFs of the variability (Fig. 5-3) and the total uncertainty (Fig. 5-4) of the average fracture toughness, respectively. In the figures, x-axis represents the fitted CDF while y-axis represents the actual CDF. If the fits were exact, they would follow the linear lines shown in the figures. We see in Figs. 5-3 and 5-4 that the deviations from the linear lines are not high; and hence the fitted distributions are acceptable.

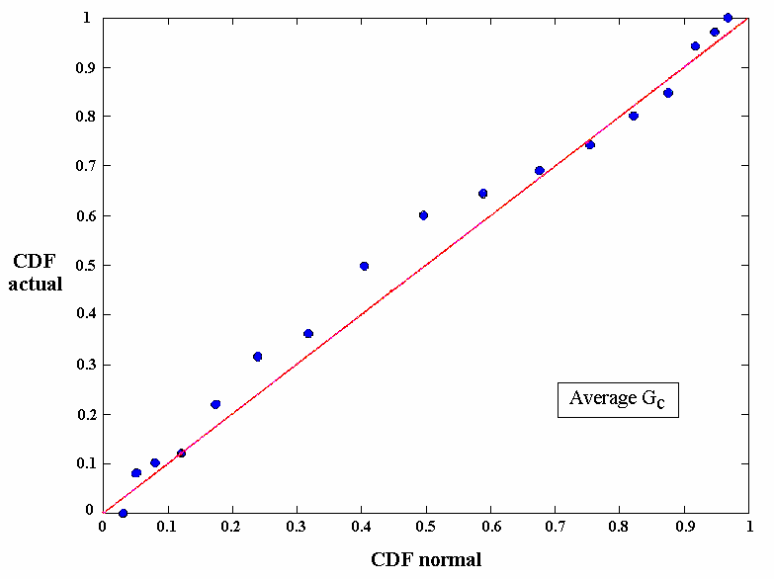

Figure 5-3. Comparison of actual and fitted cumulative distribution functions of variability, d_{MM}, of G_c.

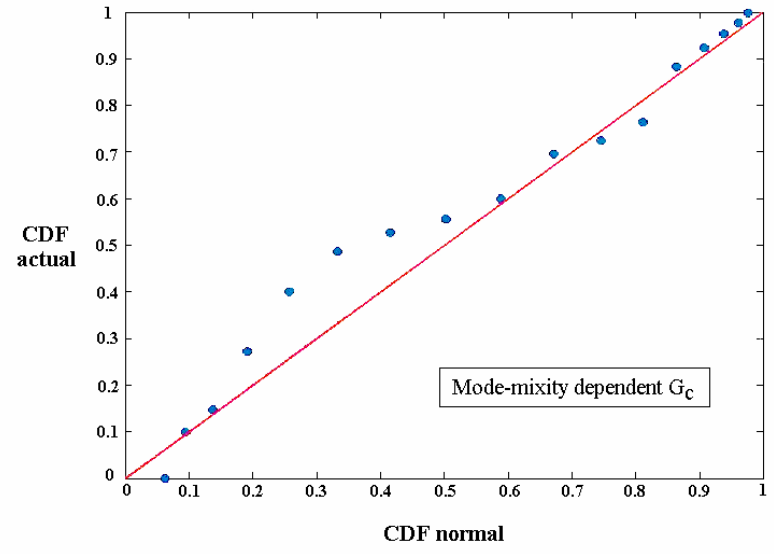

Figure 5-4. Comparison of actual and fitted cumulative distribution functions of total uncertainty (error and variability, d^A) of G_c.

In addition to variability in G_c predictions, there is also variability in the pressure p. We assume that the maxi-mum lifetime loading p follows lognormal distribution with mean value of p_{allow} and coefficient of variation (c.o.v.) of 10%.

Deterministic Design and B-basis Value Calculations

In deterministic design, the only use of probabilistic (or statistical) information is via conservative material properties, which are determined by statistical analysis of material tests. FAA regulations (FAR-25.613) state that the conservative material properties are characterized as A-basis and B-basis material property values. A-basis values are used when there is a single failure path in the structure, while the B-basis values are used when there are multiple failure paths in the structure. Detailed information on these values is provided in Chapter 8 of Volume 1 of Composite Materials Handbook (2002).

Here we use B-basis G_c, which is defined as the value exceeded by 90% of the population (of material batches) with 95% confidence. This is given by

$$B-basis = \bar{X} - k_B\, s \tag{5.5}$$

where $\bar{X}$ is the sample average, s is the sample standard deviation and k_B is the tolerance coefficient needed to achieve the 90% set-off and the 95% confidence. If infinitely many material characterization tests were carried out, there would be no issue of confidence, and for normal distribution 90% of the population will be exceeded by $k_B = z_{0.1} = \Phi(0.1) = 1.282$, where Φ is the CDF of the standard normal distribution. With a finite sample of N tests, this is adjusted as

$$\begin{aligned} k_B &= \frac{z_{0.1} + \sqrt{z_{0.1}^2 - ab}}{a} \\ a &= 1 - \frac{z_{0.05}^2}{2(N-1)}\ ;\ b = z_{0.1}^2 - \frac{z_{0.05}^2}{N} \end{aligned} \tag{5.6}$$

where $z_{0.1} = \Phi(0.1)$ is the critical value of normal distribution that is exceeded with a probability of 10%.

Grau *et al.* (2005) used the fracture toughness values obtained from experiments to calculate the predicted failure load of a debonded sandwich structure shown earlier in Fig. 5-2. They used different core thickness, face sheet thickness and crack length combinations and compared the predicted failure load of the structures designed via the use of average G_c and mode-mixity dependent G_c. In their failure load calculation, Grau *et al*. (2005) used the mean values for the fracture toughness and they did not use a safety factor.

Here, we use B-basis values for fracture toughness and a safety factor of 1.4 for loading to assess the allowable flight load of the same sandwich designs used by Grau *et al*. (2005). To calculate B-basis values, we use the standard deviations for fracture toughness given in Table 5-1. The mean values and the corresponding B-basis values of the fracture toughness for the thirteen designs given in the example in Grau *et al*. (2005) are given in Table 5-2.

Table 5-2. The mean and B-basis values of the fracture toughness of the designs analyzed (total 13 designs). The B-basis values are calculated assuming that the improvements in accuracy affect the B-basis values

Design number	Mode-mixity angle (deg)	$(G_c)^{A}_{mean}$ (N/m)	$(G_c)^{MM}_{mean}$ (N/m)	$(G_c)^{A}_{Bbasis}$ (N/m)	$(G_c)^{MM}_{Bbasis}$ (N/m)
1	16.24	638.8	498.4	308.8	266.9
2	17.15	638.8	529.0	308.8	297.5
3	18.95	638.8	589.6	308.8	358.1
4	21.08	638.8	661.3	308.8	429.8
5	22.27	638.8	701.3	308.8	469.8
6	18.32	638.8	568.4	308.8	336.9
7	20.18	638.8	630.9	308.8	399.4
8	22.27	638.8	701.4	308.8	469.9
9	23.41	638.8	739.7	308.8	508.2
10	18.28	638.8	567.1	308.8	335.6
11	19.86	638.8	620.2	308.8	388.7
12	21.57	638.8	708.6	308.8	477.1
13	16.24	638.8	498.4	308.8	266.9

Even though the scatter around the average G_c is combination of error and variability, for deterministic design following FAA regulations it is treated as variability. The reduced standard deviation of the mode-mixity dependent G_c allows then increasing the B-basis allowable. Figure 5-5 shows the fitted and B-basis values of the two approaches.

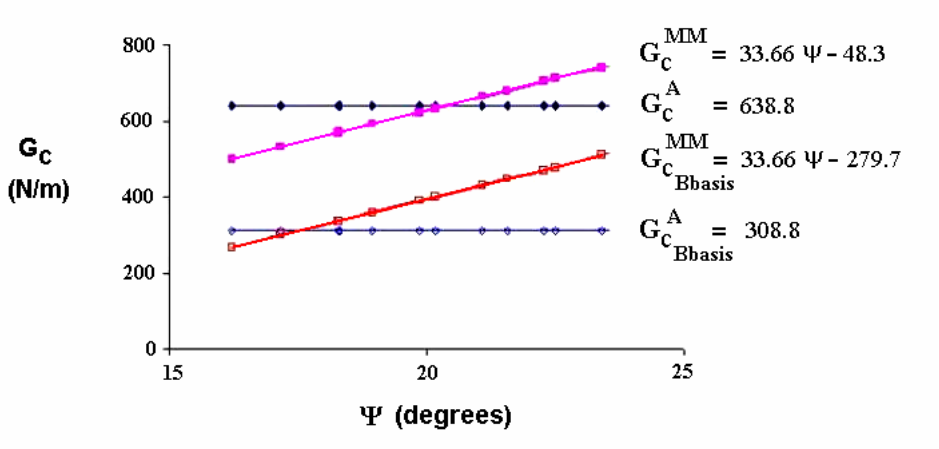

Figure 5-5. Fitted least square lines for fracture toughness, and derived B-basis allowables

While calculating the B-basis values for fracture toughness given in Table 5-2, we use N=16, which increases k_B to 2.035. Recall that the standard deviations (σ) of designs are obtained in the previous section. For example, for the first design the mean value is 638.8. The corresponding B-basis value is calculated as 638.8–2.035×162.2 = 308.8.

After obtaining the B-basis values in Table 5-2, we compute the allowable flight load p_{allow} by deterministic design philosophy. As noted earlier, besides the use of B-basis material properties, a safety factor of 1.4 is also used for loads. Hence, Eq. (5.3) is modified to calculate the allowable flight loads for thirteen different designs as

$$p_{allow} = \frac{1}{1.4}\sqrt{\frac{(G_c)_{Bbasis}}{G_0}} \tag{5.7}$$

The calculated p_{allow} values corresponding to the use of G_c^A and G_c^{MM} are given in Table 5-3. The last column of Table 5-3 shows the percent change in the allowable flight load by using G_c^{MM} instead of G_c^A. We see that allowable flight load is increased by 13.1% on average by using the mode-mixity based B-basis properties. This is the improvement in allowable flight load using a deterministic approach. As shown in the next section, this increase in allowable flight load is accompanied by a reduction in probability of failure, so that the additional gains may be realized by using probabilistic approach.

Table 5-3. Allowable flight load of failure of the sandwich panels designed using deterministic approach. The superscript 'A' denotes the use of average fracture toughness of experiments and 'MM' indicates the use of mode-mixity dependent fracture toughness

Design number	p_{allow}^A (kPa)	p_{allow}^{MM} (kPa)	% Δp
1	51.2	47.6	-7.0
2	267.0	262.0	-1.9
3	158.6	170.8	7.7
4	77.1	90.9	18.0
5	45.2	55.8	22.3
6	247.2	258.2	4.4
7	154.1	175.3	13.7
8	73.1	90.2	23.4
9	42.8	54.8	28.3
10	247.2	257.7	4.2
11	146.2	164.1	12.2
12	70.1	84.3	20.2
13	40.8	50.7	24.3
		Average	13.1

Assessment of Probability of Failure

The probability of failure of a structural component can be expressed in terms of its structural response R and its capacity C corresponding to that response by

$$P_f = \Pr\left(C \le R\right) \tag{5.8}$$

For the sandwich structure analyzed here the response R=G is the energy release rate (Eq. 5.2), and the capacity C=G_c is the interfacial fracture toughness. G depends on structural dimensions through G_0 (see Eq. (5.2)). Both response G and the capacity G_c have variability that needs to be included in the calculation of the probability of failure. We assume that the variability in G is mainly due to the variability in load p rather than G_0. Besides variability, there exist errors in assessing G and G_c (e.g., errors in load, G_0, and material property calculations).

The general equation for probability of failure given in Eq. (5.8) can be expressed in this problem as

$$P_f = \Pr\left(G_c \le G_0 p^2\right) \tag{5.9}$$

Then, the probability of failure can be written in a functional form as

$$P_f = P_f\left(\overline{G}_c, e_{G_c}, VAR_{G_c}, p_{allow},\ VAR_P, G_0\right) \tag{5.10}$$

where $\overline{G}_c$ is the mean value of G_c, e_{G_c} is the error in G_c predictions (that we reduce by using mode-mixity dependent G_c instead of average G_c), VAR_{G_c} is the variability in G_c, p_{allow} is the allowable flight load (or mean value of the loading p), VAR_P is the variability in p and G_0 is the strain energy release rate corresponding to unit pressure that we assume to be deterministic. Since the limit-state function for this problem, $g = G_c - G_0 P^2$, is a simple function with only two random variables, we easily calculate the probability of failure by analytical means as follows

The probability distribution function (PDF) of a function Z of two random variables X and Y, Z=h(X, Y) can be calculated as (Ang and Tang (1975), p.170)

$$f_Z(z) = \int_{-\infty}^{\infty} f_{X,Y}(x,y)\left|\frac{\partial x}{\partial z}\right| dy \tag{5.11}$$

where $f_{X,Y}$(x,y) is the joint probability distribution function of X and Y. We can write the limit-state function for the sandwich panel problem as

$$g = G_c - G_0 p^2 \tag{5.12}$$

Therefore, to calculate the PDF of g from Eq. (5.11), we replace Z with g, X with G_c, Y with p, and also we have $G_c = g + G_0 p^2$, so $\left|\frac{\partial x}{\partial z}\right| = \left|\frac{\partial G_c}{\partial g}\right| = 1$. After these substitutions and noting that p only takes positive values, we get from Eq. (5.11) that

$$f_G(g) = \int_0^{\infty} f_{G_c,p}(G_c, p)\, dp \tag{5.13}$$

Here we assume that G_c and p are statistically independent, hence the joint distribution in Eq. (5.13) is calculated as

$$f_{G_c,p}(G_c, p) = f_{G_c}\left(g + G_0 p^2\right) f_p(p) \tag{5.14}$$

Then, the cumulative distribution function (CDF) of g is calculated as

$$F_G(g) = \int_{-\infty}^{g} f_G(g')\, dg' \tag{5.15}$$

which allows us to compute the probability of failure simply as $P_f = F_G(0)$.

Table 5-4 shows the probabilities of failure corresponding to deterministic allowable flight loads. We observe that in addition to the 13.1% average increase in allowable flight load, the average probability of failure was reduced by about a factor of five.

Table 5-4. Corresponding probabilities of failure of the sandwich panels designed using deterministic approach. The superscript 'A' denotes the use of average fracture toughness of experiments and 'MM' indicates the use of mode-mixity dependent fracture toughness. The B-basis values are calculated considering that the improvements in accuracy affect the B-basis values (adjusted B-basis values).

Design number	P_f^A (10^{-3})	P_f^{MM} (10^{-3})
1	1.869	1.064
2	1.869	0.762
3	1.869	0.407
4	1.869	0.211
5	1.869	0.153
6	1.869	0.504
7	1.869	0.275
8	1.869	0.153
9	1.869	0.117
10	1.869	0.511
11	1.869	0.304
12	1.869	0.184
13	1.869	0.145
Average	1.869	0.369

Notice that the probabilities of failure given in Table 5-4 are high. These probabilities of failure correspond to component failure probabilities. The probability of the actual structure will be much smaller due to the redundancy in the structure. For example, if we define the failure of the structure as simultaneous failures of two components having a correlation coefficient (of probability of failure) of 0.5, then component probabilities of failure 1.869×10^{-3} and 0.369×10^{-3} given in the last row of Table 5-4 correspond to system probabilities of failure 1.28×10^{-4} and 1.39×10^{-5}, respectively.

Analyzing the Effects of Improved Model on Allowable Flight Loads via Probabilistic Design

As seen from Eq. (5.10), there are four distinct ways to increase the allowable flight load of a structure: (a) Use a different material to increase $\overline{G}_c$; (b) Develop more accurate solutions that reduce e_{G_c} (such as the use of mode-mixity dependent G_c instead of

average G_c); (c) Improve quality control and manufacturing processes to reduce variability VAR_{G_c} or employ measures to reduce VAR_P ; (d) Use a heavier design to reduce G_0. For a structure that is already built, only option (b) is available.

The previous section showed how reductions in variability can increase allowable flight load using deterministic design. For probabilistic design, the mode-mixity approach is treated as accuracy improvement and we calculate its effect on the safe allowable flight load.

For a target probability of failure, $\left(P_f\right)_{\text{target}}$, the allowable flight load can be calculated from

$$P_f = P_f\left(\overline{G}_c, e_{G_c}, VAR_{G_c}, p_{allow}, VAR_P, G_0\right) = \left(P_f\right)_{\text{target}} \tag{5.16}$$

Thus, given the target probability of failure, the allowable flight loads corresponding to different error factors on fracture toughness, e_{G_c}, can be calculated from Eq. (5.17).

$$P_f\left(e_{G_{c1}}, p_{allow1}\right) = P_f\left(e_{G_{c2}}, p_{allow2}\right) = \left(P_f\right)_{\text{target}} \tag{5.17}$$

For the present calculation, the target probability of failure is taken 1.869×10^{-3}, which is the probability of failure with the deterministic allowable flight load using the average G_c (see Table 5-4). Table 5-5 shows the comparison of allowable flight load for the average G_c and mode-mixity dependent G_c approaches in case of probabilistic design. We see in Table 5-5 that by fixing the probability of failure rather than adjusting the B-basis properties, the average allowable flight load can be increased by 26.5%. It must be noted, however, that for some structures the improved analysis may indicate a small reduction in allowable flight loads. With the deterministic approach, this applied to

Designs 1 and 2 (Table 5-3), while with the probabilistic approach, only Design 1 suffers (a small) load reduction.

Table 5-5. Allowable flight loads of the sandwich panels calculated via probabilistic approach. The superscript 'A' denotes the use of average fracture toughness of experiments and 'MM' indicates the use of mode-mixity dependent fracture toughness. The probabilities of failure of the all designs are 1.869×10^{-3}.

Design number	p_{allow}^{A} (kPa)	p_{allow}^{MM} (kPa)	% Δp
1	51.2	50.5	-1.3
2	266.9	283.9	6.4
3	158.6	190.1	19.9
4	77.1	102.6	33.1
5	45.2	63.2	39.8
6	247.3	285.2	15.3
7	154.2	196.9	27.7
8	73.1	102.3	39.9
9	42.8	62.4	45.8
10	247.3	284.4	15.0
11	146.2	184.0	25.8
12	70.1	95.4	36.1
13	40.8	57.6	41.1
		Average	26.5

Summary

The effect of improved model for fracture toughness on allowable flight load was investigated using both deterministic and probabilistic design methodologies. For deterministic allowable flight load calculation, the improved model reduces scatter and allows increase in the fracture toughness allowable calculated by B-basis properties, while for probabilistic allowable flight load calculation, the reduced error is incorporated into the calculation of probability of failure. We find that the deterministic approach leads to 13.1% increase on average in the allowable flight load and reduction of the probability of failure by a factor of five. The use of B-basis properties in the deterministic de-sign does not permit translating the full potential of improved modeling to increase allowable

flight loads. In contrast, the probabilistic approach allows 26.5% increase on average in the allowable flight load, while still maintaining the original probability of failure.

CHAPTER 6
TRADEOFF OF UNCERTAINTY REDUCTION MECHANISMS FOR REDUCING STRUCTURAL WEIGHT

Inspired by work on allocating risk between the different components of a system for a minimal cost, we explore the optimal allocation of uncertainty in a single component. The tradeoffs of uncertainty reduction measures on the weight of structures designed for reliability are explored. The uncertainties in the problem are broadly classified as error and variability. Probabilistic design is carried out to analyze the effect of reducing error and variability on the weight. As a demonstration problem, the design of composite laminates at cryogenic temperatures is chosen because the design is sensitive to uncertainties. For illustration, variability reduction takes the form of quality control, while error is reduced by including the effect of chemical shrinkage in the analysis. Tradeoff plots of uncertainty reduction measures, probability of failure and weight are generated that could allow choice of optimal uncertainty reduction measure combination to reach a target probability of failure with minimum cost. In addition, we also compare response surface approximations to direct approximation of a probability distribution for efficient estimation of reliability.

The research presented in this chapter will also be published in Acar et al. (2006c). Dr. Theodore F. Johnson of NASA Langley Research Center is acknowledged for his contribution to this work.

Introduction

For systems composed of multiple components, system failure probability depends on the failure probabilities of the components, and the cost of changing the failure probability may vary from one component to another. The risk or reliability allocation problem can be defined (Mohamed *et al*. 1991, Knoll 1983, Hurd 1980) as determining the optimal component reliabilities such that the system objective function (e.g., cost) is optimized and all design constraints (e.g., system reliability level) are met. Several researchers applied risk and reliability allocation methods to optimize the total cost of nuclear power plants by allocating the risk and reliability of individual subsystems such that a specified reliability goal is met (Gokcek *et al*. 1978, Cho *et al*. 1986, Yang *et al*. 1989 and Yang *et al*. 1999). Ivanovic (2000) applied reliability allocation to design of a motor vehicle. The vehicle reliability is allocated to its elements for minimum vehicle cost while keeping the reliability of the vehicle at a specified level. Acar and Haftka (2005) investigated reliability allocation between the wing and tail of a transport aircraft. The concept of risk allocation is also used in finance applications, where risk allocation is defined as the process of apportioning individual risks relating to projects and service delivery to the party best placed to manage each risk. Risks are allocated across the supply chain – that is, between the department, its customers, its suppliers and their subcontractors. Vogler (1997), Bing *et al*. (2005) and Niehaus (2003) are some examples of numerous publications on risk allocation in finance applications.

Instead of considering a system of multiple components, we may also consider multiple sources of uncertainty for a single component. Again, the probability of failure can be reduced by reducing the uncertainty from each source, with different cost associated with each. That is, the probability constraints can be satisfied by reducing

different types of uncertainties. The objective of this chapter is to demonstrate this approach for reliability based design optimization (RBDO) of structures.

As in earlier chapters, uncertainty is divided into error and variability, to distinguish between uncertainties that apply equally to an entire fleet of a structural model (error) and the uncertainties that vary for an individual structure (variability).

In aircraft structural design there are different players engaged in uncertainty reduction. Researchers reduce errors by developing better models of failure prediction and this leads to safer structures (see Chapter 5). Aircraft companies constantly improve finite element models, thus reducing errors in structural response. The Federal Aviation Administration (FAA) leads to further reduction in error through the process of certification testing. Aircraft makers also constantly improve manufacturing techniques and quality control procedure to reduce variability between airplanes. Airlines reduce variability in structural failure due to operating conditions by conducting inspections, and the FAA contributes to reduced variability by licensing pilots, thereby reducing the risk that incompetent pilots may subject airplanes to excessively high loads.

These uncertainty reduction mechanisms are costly, and their cost can be traded against the cost of making the structure safer by increasing its weight. Kale *et al*. 2005 investigated the tradeoff of inspection cost against the cost of structural weight, and found that inspections are quite cost effective. Qu *et al*. (2003) analyzed the effect of variability reduction on the weight savings from composite laminates under cryogenic conditions. They found that employing quality control to -2sigma for the transverse failure strain may reduce the weight of composite laminates operating at cryogenic

temperatures by 25% marking such laminates as a structure where weight is sensitive to the magnitude of uncertainties.

Here, we use the example of this composite laminate to explore tradeoffs between the variability reduction, considered by Qu *et al*. (2003), and error reduction in the form of improved accuracy of structural analysis.

The chapter is organized as follows. The design of composite laminates for cryogenic temperatures is discussed in the next section. Then, probability of failure estimation of the laminates is described, followed by the formulation of the probabilistic design optimization for our problem. Next, weight savings using error and variability reduction mechanisms are given. Finally, the optimum use of uncertainty reduction mechanisms is discussed, followed by the summary of the chapter.

Design of Composite Laminates for Cryogenic Temperatures

We consider the design of a composite panel at cryogenic temperatures as demonstration for trading off uncertainty reduction mechanisms. The definition of the problem is taken directly from Qu *et al*. (2003). The laminate (Fig. 6-1) is subject to mechanical loading (N_x is 4,800 lb/inch and N_y is 2,400 lb/inch) and thermal loading due to the operating temperature -423°F, where the stress-free temperature is 300°F.

The objective is to optimize the weight of laminates with two ply angles $\left[\pm\theta_1/\pm\theta_2\right]_s$. The design variables are the ply angles θ_1, θ_2 and ply thicknesses t_1, t_2. The material used in the laminates is IM600/133 graphite-epoxy of ply thickness 0.005 inch. The minimum thickness necessary to prevent hydrogen leakage is assumed to be 0.04 inch. The geometry and loading conditions are shown in Fig. 6-1. Temperature-dependent material properties are given in Appendix G.

The deterministic design optimization of the problem was solved by Qu *et al*. (2003). They used continuous design variables and rounded the thicknesses to integer multiples of the basic ply thickness 0.005 inches. In the deterministic optimization, they multiplied the strains by a safety factor of S_F=1.4.

The deterministic optimization problem is formulated as

$$\begin{aligned} &\min_{\theta_1,\theta_2,t_1,t_2} \quad h = 4\left(t_1 + t_2\right) \\ &\text{such that} \quad \varepsilon_1^L \le S_F\varepsilon_1 \le \varepsilon_1^U, \varepsilon_2^L \le S_F\varepsilon_2 \le \varepsilon_2^U, S_F\left|\gamma_{12}\right| \le \gamma_{12}^U \\ &\qquad\qquad t_1, t_2 \ge 0.005\,in \end{aligned} \tag{6.1}$$

where the allowable strains are given in Table 6-1.

Table 6-1. Allowable strains for IM600/133

ε_1^L	ε_1^U	ε_2^L	ε_2^U	γ_{12}^U
-0.0109	0.0103	-0.013	0.0154	0.0138

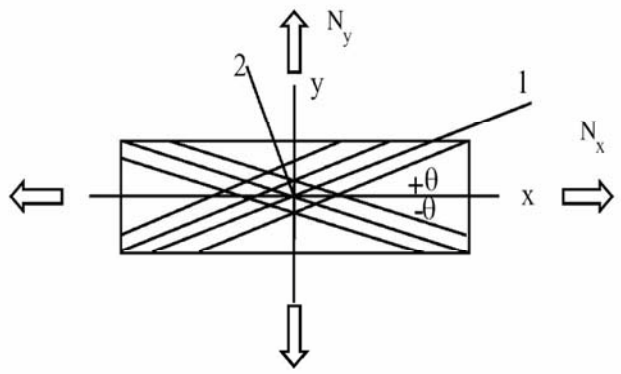

Figure 6-1. Geometry and loading of the laminate with two ply angles. Note that x-is the hoop direction and y is the axial direction.

Since designs must be feasible for the entire range of temperatures, strain constraints were applied at twenty-one different temperatures, which were uniformly distributed from 77°F to –423°F. Qu *et al*. (2003) found the optimum design given in Table 6-2.

Table 6-2. Deterministic optimum design*. The number in parentheses denotes the unrounded design thicknesses.

θ_1 (deg)	θ_2 (deg)	t_1 (in)	t_2 (in)	h (in)
27.04	27.04	0.010	0.015	0.100 (0.095)

* taken from Qu *et al*. (2003)

Calculation of Probability of Failure

The failure of the laminates is assessed based on the first ply failure according to the maximum strain failure criterion. The strain allowables listed in Table 6-1 are the mean values of the failure strains according to Qu *et al*. (2003).

The first step in the calculation of the probability of failure is to quantify uncertainties included in the problem. As in earlier chapters, we use a simple classification for uncertainty to distinguish between the uncertainties that apply equally to the entire fleet of a structural model (errors) and the uncertainties that vary for an individual structure (variability).

Since errors are epistemic, they are often modeled using fuzzy numbers or possibility analysis (Antonsson and Otto 1995, Nikolaidis *et al*. 2004 and Vanegas and Labib 2005). We model the errors probabilistically by using uniform distributions to maximize the entropy. Variability refers to the departure of a quantity in individual laminates that have the same design. Here, the elastic properties (E_1, E_2, G_{12}, and ν_{12}), coefficients of thermal expansion (α_1 and α_2), failure strains (ε_1^L, ε_1^U, ε_2^L, ε_2^U, and γ_{12}^U) and the stress-free temperature (T_{zero}) have variability. These random variables are all assumed to follow uncorrelated normal distributions, with coefficients of variations listed in Table 6-3.

Table 6-3. Coefficients of variation of the random variables (assumed uncorrelated normal distributions)

E_1, E_2, G_{12}, and ν_{12}	α_1 and α_2	T_{zero}	ε_1^L and ε_1^U	ε_2^L, ε_2^U, and γ_{12}^U
0.035	0.035	0.03	0.06	0.09

We also use a simple error model, assuming that calculated values of failure strains differ from actual values due to experimental or measurement errors. Using standard classical lamination theory (CLT) for ply strain calculation leads to errors in part, because standard CLT does not take chemical shrinkage into account. We relate the actual values of the strains to their calculated values via Eq. (6.2)

$$\varepsilon_{calc} = (1+e)\varepsilon_{true} \tag{6.2}$$

where *e* is the representative error factor that includes the effect of all error sources on the values of strains and failure strains. For example, if the estimated failure strain is 10% too high, this is approximately equivalent to the strain being calculated 10% too low. For the error factor e, we use a uniform distribution with bounds of ±be. This error bound can be reduced by using more accurate failure models. For example, the cure reference method (Ifju *et al*. 2000) may be used to account for the shrinkage due to a chemical process. In Sections 6-4 and 6-5, we will investigate the effect of reducing be on the probability of failure and the weight.

To calculate the probability of failure, we use Monte Carlo Simulation (MCS). For acceptable accuracy, sufficient strain analyses (simulations) must be obtained through standard CLT analysis. However, this is computationally expensive and needs to be repeated many times during the optimization. In order to reduce the computational cost, Qu *et al*. [19] used response surface approximations for strains (ε_1 in θ_1, ε_1 in θ_2, ε_2 in θ_1, ε_2 in θ_2, γ_{12} in θ_1, and γ_{12} in θ_2). They fitted quadratic response surface approximations to strains in terms of four design variables (t_1, t_2, θ_1, and θ_2), material parameters (E_1, E_2, G_{12}, ν_{12}, α_1, and α_2) and service temperature T_{serv}. These response surfaces were called the analysis response surfaces (ARS), because they replace the CLT analysis. A quadratic

response surface approximation in terms of 12 variables includes 91 coefficients, so they used 182 realizations from Latin hypercube sampling (LHS) design. As seen from Table 6-4 the root mean square error predictions are less than 2% of the mean responses, so the accuracies of the ARS is good.

Table 6-4. Evaluation of the accuracy of the analysis response surface[(a)]. Note that the strains are in millistrains.

	ε_1 in θ_1	ε_1 in θ_2	ε_2 in θ_1	ε_2 in θ_2	γ_{12} in θ_1	γ_{12} in θ_2
R^2_{adj}[(b)]	0.9977	0.9978	0.9956	0.9961	0.9991	0.9990
RMSE Predictor[(c)]	0.017	0.017	0.060	0.055	0.055	0.060
Mean of response	1.114	1.108	8.322	8.328	-3.13	-3.14

(a) taken from Qu *et al*. (2003)
(b) adjusted coefficient of multiple determination
(c) root mean square error predictor

We found, however, that even small errors in strain values may lead to large errors in probability of failure calculations, so we considered approximate cumulative distribution functions (CDF) of strains instead of ARS. We assume normal distributions for strains and estimate the mean and the standard deviation of strains conservatively by MCS. That is, the mean and standard deviation of the assumed distribution are found so that the CDF of the approximated distribution is smaller than or equal to (i.e., more conservative) the CDF calculated via MCS, except for strain values very near the tail of the distribution. Detailed information on conservative CDF fitting is given in Appendix H. We use 1,000 MCS simulations, which are accurate to a few percent of the standard deviation for estimating the mean and standard deviation. Cumulative distribution function obtained through 1,000 MCS, the approximate normal distribution and the conservative approximate normal distributions for ε_2 corresponding to one of the deterministic optimum are compared in Figs. 6-2(a) and 6-2(b).

Next, we compare the accuracy of the analysis response surface and approximate CDF approaches by using 1,000,000 MCS in Table 6-5. We can see that the use of approximate CDFs for strains leads to more accurate probability of failure estimations than the use of ARS. Furthermore, the case of conservative fit to CDF leads to overestimation of the probability of failure. However, the approximate CDFs were obtained by performing 1,000 MCS, while the ARS were constrained by using only 182 MCS. In addition, the approximate CDF needs to be repeatedly calculated for each design. It is possible that some combination of ARS with approximate CDF may be more efficient and accurate than either using ARS or approximate CDF alone, and this might be explored in future work.

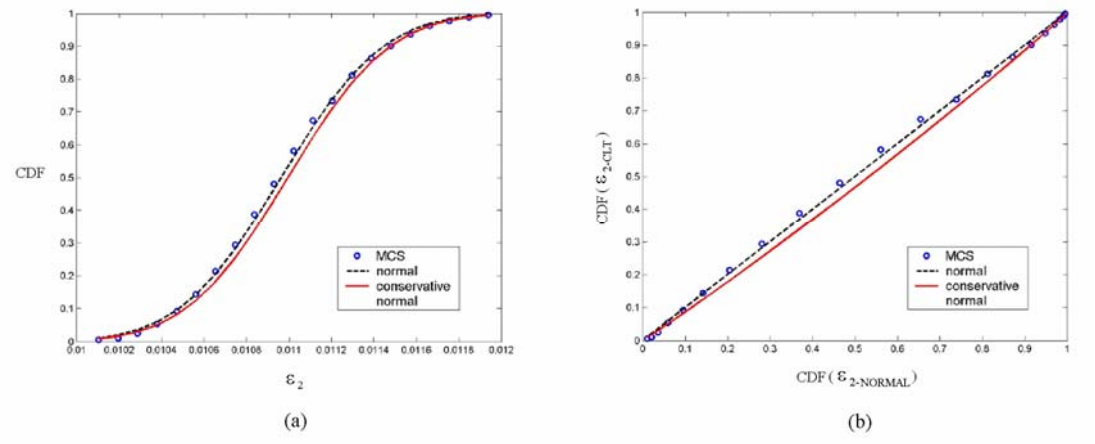

Figure 6-2. Comparison of CDF obtained via 1,000 MCS, the approximate normal distribution and conservative approximate normal distributions for ε_2 on θ_1 corresponding to the deterministic optimum.

Table 6-5. Comparison of probability of failure estimations for the deterministic optimum[(a)]. Samples size of MCS is 1,000,000.

Approach followed	Probability of Failure, P_f ($\times 10^{-4}$)	Standard error in P_f due to limited sampling ($\times 10^{-4}$)
MCS with CLT (exact analysis)	10.21	0.320
MCS with ARS* of strains	16.83	0.410
MCS with approximation to CDF of strains	11.55	0.340

[(a)] Taken from Qu *et al*. (2003)
[(b)] ARS: Analysis response surface approximation

Probabilistic Design Optimization

The laminates are designed for a target failure probability of 10^{-4}. The optimization problem can be formulated as given in Eq. (6.3). The design variables are the ply thicknesses and angles.

$$\begin{aligned} &\min_{\theta_1,\theta_2,t_1,t_2} \quad h = 4\left(t_1 + t_2\right) \\ &\text{such that} \quad P_f \le \left(P_f\right)_{target} \\ &\qquad\qquad t_1, t_2 \ge 0.005\,in \end{aligned} \tag{6.3}$$

For this optimization, we need to fit a design response surface (DRS) to the probability of failure in terms of the design variables. The accuracy of the DRS may be improved by using an inverse safety measure. We use the probabilistic sufficiency factor (PSF) developed by Qu and Haftka (2004).

Probabilistic Sufficiency Factor (PSF)

The safety factor S is defined as the ratio of the capacity G_C of the structure to the structural response G_R. The PSF is the probabilistic interpretation of the safety factor S with its CDF defined as

$$F_S\left(s\right) = \text{Prob}\left(\frac{G_C}{G_R} \le s\right) \tag{6.4}$$

Given a target probability of failure, $\left(P_f\right)_{target}$, PSF is defined as the solution to

$$F_S\left(s\right) = \text{Prob}\left(\frac{G_C}{G_R} \le PSF\right) = \text{Prob}\left(S \le PSF\right) = \left(P_f\right)_{target} \tag{6.5}$$

That is, the PSF is the safety factor obtained by equating the CDF of the safety factor to the target failure probability. The PSF takes values such that

$$PSF = \begin{cases} <1 \;\; if \;\; P_f > \left(P_f\right)_{target} \\ =1 \;\; if \;\; P_f = \left(P_f\right)_{target} \\ >1 \;\; if \;\; P_f < \left(P_f\right)_{target} \end{cases} \tag{6.6}$$

When MCS are used, the PSF can be estimated as the nth smallest safety factor over all MCS, where n = N×$\left(P_f\right)_{target}$. Using the PSF, the optimization problem can be formulated as

$$\begin{aligned} \min_{\theta_1,\theta_2,t_1,t_2} \quad & h = 4\left(t_1 + t_2\right) \\ \text{such that} \quad & PSF \le 1 \\ & t_1, t_2 \ge 0.005\,in \end{aligned} \tag{6.7}$$

The optimization problem given in Eq. (6.7) is solved by using Sequential Quadratic Programming (SQP) in MATLAB.

Design Response Surface (DRS)

We have three components of strain for each angle: ε_1, ε_2 and $\gamma 12$. The strain ε_2 and γ_{12} are more critical than ε_1. The mean and standard deviation of four strains (ε_2 in θ_1, ε_2 in θ_2, γ_{12} in θ_1 and γ_{12} in θ_2) are computed by using MCS of sample size 1,000 and fitted with conservative normal distributions as shown in Fig. 6-2. These distributions are used in MCS using 1,000,000 simulations at each design point to compute PSF. In order to perform the optimization, we need to approximate the PSF in terms of the design variables by a design response surface (DRS). We fit three DRS of the PSF as function of the four design variables (t_1, t_2, θ_1, and θ_2) for three different error bound (b_e) values of 0, 10%, and 20%. As shown in Appendix I, the use of the PSF leads to much more accurate estimate of the safety margin than fitting a DRS to the probability of failure.

Weight Savings by Reducing Error and Employing Manufacturing Quality Control

As noted earlier, the probabilistic design optimizations of the composite laminates were performed for three different values of the error bound, be, namely 0, 10%, and 20%. Schultz *et al*. (2005) have shown that neglecting chemical shrinkage leads to substantial errors in strain calculations. Based on Schultz *et al*. (2005), we assume that using the standard CLT without chemical shrinkage leads to 20% errors in strain calculations, while using the modified CLT (i.e., CLT that takes chemical shrinkage into account) leads to the reduction of error bounds from 20% to 10%. As noted earlier, the errors are assumed to have uniform distribution, which corresponds to maximum entropy.

For the error bounds discussed, we solve the optimization problem given in Eq. (6.7). The results of the optimization are presented in Table 6-6 and the weight (proportional to thickness) savings due to error reduction are shown in Fig. 6-3. We see that reducing the error bounds from 20% to 10% leads to 12.4% weight saving. In addition, reducing error from 20% to 0 (clearly only a hypothetical case) leads to weight saving of 23.1%.

Table 6-6. Probabilistic optimum designs for different error bounds when only error reduction is applied. The PSF and P_f given in the last two columns are calculated via Monte Carlo simulations (sample size of 10,000,000) where the strains are directly computed via standard CLT analysis. The numbers in parentheses under PSF and P_f show the standard errors due to limited Monte Carlo sampling.

Error bound	θ_1 θ_2 (deg)	t_1 t_2 (in)	h (in) [Δh* (%)]	*PSF*	P_f (1×10^{-4})
0	25.47 26.06	0.0156 0.0137	0.1169 [23.1]	0.9986 (0.0030)	1.017 (0.032)
10%	25.59 25.53	0.0167 0.0167	0.1332 [12.4]	1.018 (0.0035)	0.598 (0.024)
20%	23.71 23.36	0.0189 0.0191	0.1520 [0.0]	0.9962 (0.0035)	1.111 (0.105)

* The optimum laminate thickness for 20% error bound is taken as the basis for Δh computations

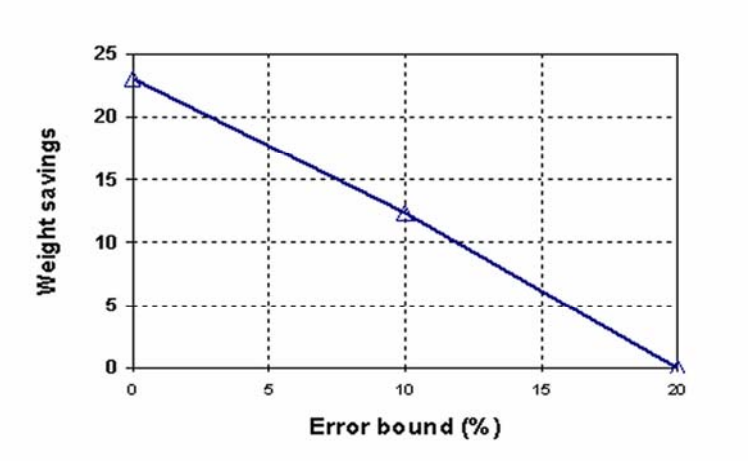

Figure 6-3. Reducing laminate thickness (hence weight) by error reduction (no variability reduction)

We have shown that it is possible to reduce the laminate thickness by 12.4% through reducing the error from 20% to 10%. Now, we combine error reduction with variability reduction and analyze the overall benefit of both uncertainty reduction mechanisms. An example of variability reduction is testing a set of composite laminates and rejecting the laminates having lower failure strains as a form of quality control. The test can involve a destructive evaluation of a small coupon cut out from laminate used to build the structure. Alternatively, it can involve a non-destructive scan of laminates to detect flaws known to be associated with lowered strength. We study the case where specimens that have transverse failure strains lower than two standard deviations below the mean are rejected (2.3% rejection rate). We construct three new DRS for PSF corresponding to error bounds of 0, 10% and 20%.

The probabilistic design optimizations of composite laminates for three different values of error bound (b_e) are performed and the results are presented in Table 6-7 and in Fig. 6-4. We note that when this form of variability reduction is applied, the laminate

thickness can be reduced by 19.5%. If the error bound is reduced from 20% to 10% together with the variability reduction, the laminate thickness can be reduced by 36.2%.

Table 6-7. Probabilistic optimum designs for different error bounds when both error and variability reduction are applied. PSF and P_f given in the last two columns are calculated via MCS (sample size of 10,000,000) where the strains are directly computed via the standard CLT analysis. The numbers in parentheses under PSF and P_f show the standard errors due to limited sample size of MCS.

Error bound	θ_1 θ_2 (deg)	t_1 t_2 (in)	h (in) [Δh^* (%)]	PSF	P_f ($\times 10^{-4}$)
0	28.52 28.71	0.0089 0.0114	0.0813 [-46.6]	0.9965 (0.0014)	1.255 (0.035)
10%	27.34 27.37	0.0129 0.0114	0.0970 [-36.2]	1.0016 (0.0015)	0.906 (0.030)
20%	25.57 25.66	0.0168 0.0138	0.1224 [-19.5]	0.9968 (0.0015)	1.190 (0.109)

* The optimum laminate thickness for the 20% error bound given in Table 6-6 (i.e. h=0.1520 in) is taken as the basis for Δh computations

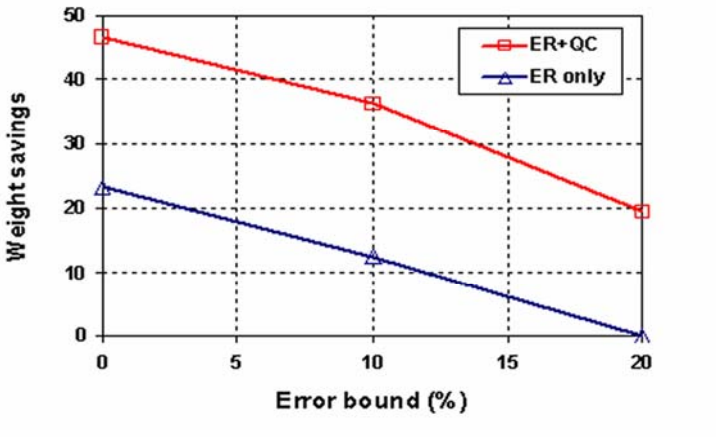

Figure 6-4. Reducing laminate thickness by error reduction (ER) and quality control (QC).

The numbers in the last two columns of Table 6-7 show the PSF and P_f calculated by using the 10,000,000 MCS where strains are directly calculated through the standard CLT analysis. The design values for PSF and P_f of the optimum designs are expected to be 1.0 and 10^{-4}. Discrepancies can be the result of the following.

- Error due to the use of normal distributions for strains which may not exactly follow normal distributions.
- Error due to limited sample size of MCS while calculating the mean and standard distribution of strains.
- Error due to limited sample size of MCS while computing the probabilistic sufficiency factor PSF.
- Error associated with the use of response surface approximations for PSF.

Next, a plot for the probability of failure (calculated via 1,000,000 MCS), weight and error reduction measures is shown in Fig. 6-5. The optimum ply angles for the case with 20% error bound and no variability reduction are 25.59º and 25.53º. Here we take both ply angles at 25º. We note from Fig. 6-5 that for our problem, the error reduction is a more effective way of reducing weight compared to the specified variability reduction when the target probability of failure of the laminates is higher than 2×10^{-4} and quality control is more effective for lower probabilities.

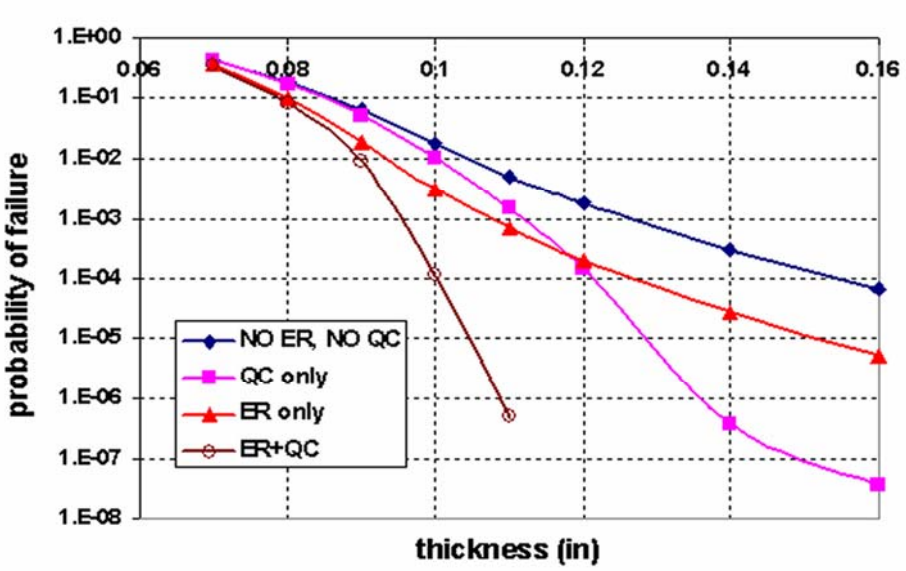

Figure 6-5. Trade-off plot for the probability of failure, design thickness and uncertainty reduction measures. ER: error reduction (reducing from 20% to 10%), QC: quality control to -2 sigma.

Choosing Optimal Uncertainty Reduction Combination

Obviously, when it comes to a decision of what uncertainty reduction mechanisms to use, the choice depends on the cost of the uncertainty reduction measures. For a company, the costs of small error reduction may be moderate, since they may involve only a search of the literature for the best models available. Substantial error reduction may entail the high cost of doing additional research. Similarly, small improvements in variability, such as improved quality control may entail using readily available non-destructive testing methods, while large improvements may entail developing new methods, or acquiring expensive new equipment. To illustrate this, we assume a hypothetical cost function in quadratic form

$$Cost = A\left(ER\right)^2 + B\left(QC + 3\right)^2 \tag{6.8}$$

where A and B are cost parameters, ER represents the error reduction and QC stands for the number of standard deviations that are the threshold achieved by quality control. We generated hypothetical cost contours by using Eq. (6.8) as shown in Fig. 6-6. The nominal value of error is taken as 20% and we assume that the quality control to -3 sigma is associated with no cost. For example, if error is reduced from 20% to 15%, ER=0.20-0.15=0.05. Similarly, if quality control to -2.5sigma is employed, then QC+3 takes the value of 0.5. As an example we take A=$20 million and B=$100,000.

Next, we generated trade-off plot for probability of failure and uncertainty reduction measures for laminates of thickness t_1=0.010 in and t_2=0.015 in as shown in Fig. 6-6. The optimum ply angles are calculated such that they minimize the probability of failure. The probabilities of failure are calculated via MCS (sample size of 10^6). The hypothetical cost contours for the uncertainty reduction measures given in Fig. 6-6 enable

a designer to identify the optimal uncertainty reduction selection. We see in Fig. 6-6 that for high probabilities quality control is not cost effective, while for low failure probabilities quality control becomes more effective and a proper combination of error reduction and quality control leads to a minimum cost.

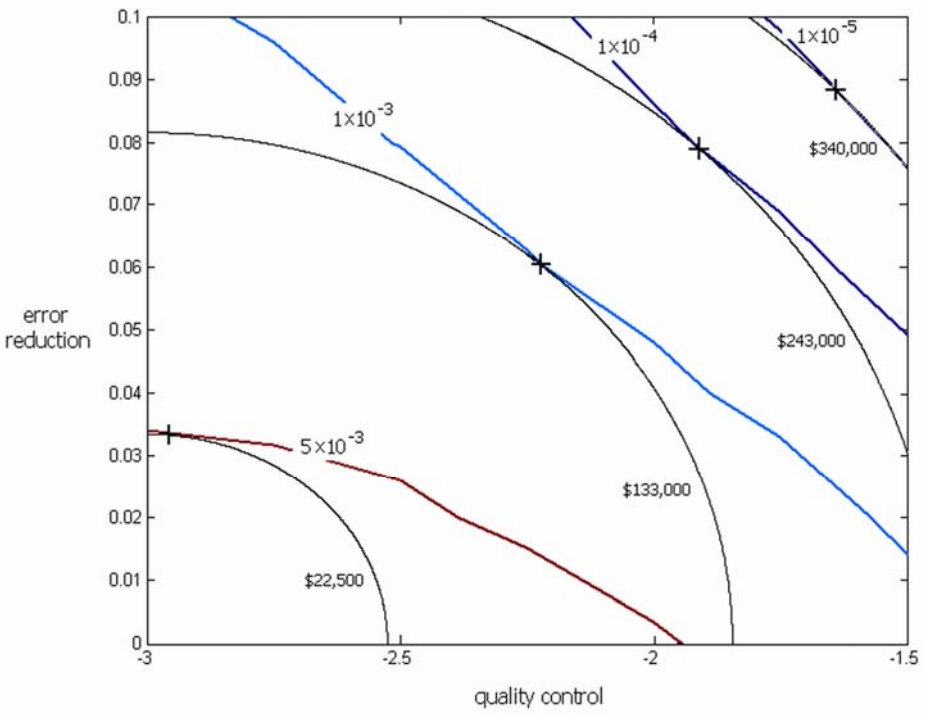

Figure 6-6. Tradeoff of probability of failure and uncertainty reduction. Probabilities of failure are calculated via MCS (sample size of 1,000,000). The crosses in the figure indicate the optimal uncertainty reduction combination that minimizes the cost of uncertainty reduction for a specified probability of failure.

Summary

The tradeoffs of uncertainty reduction measures for minimizing structural weight were investigated. Inspired by the allocation of the risk between the components of a system for minimal cost, the optimal allocation of uncertainty as error and variability was analyzed. As a demonstration problem, the design of composite laminates at cryogenic temperatures is chosen because the design is very sensitive to uncertainties. Quality control was used as a way to reduce variability, and its effect was compared to the effect

of reducing error in the analysis. Tradeoff plots of uncertainty reduction measures, probability of failure and weight were generated that would enable a designer to choose the optimal uncertainty reduction measure combination to reach a target probability of failure with minimum cost.

For this specific example problem we observed the following

- Reducing errors from 20% to 10% led to 12% weight reduction
- Quality control to -2 sigma led to 20% weight reduction
- The use combined of error reduction and quality control mechanisms reduced the weight by 36%.
- Quality control was more effective at low required failure probabilities, while the opposite applied for higher required probabilities of failure.

In addition, a computational procedure for estimating the probability of failure based on approximating the cumulative distribution functions for strains in a conservative manner was developed. We found that this approach led to more accurate probability of failure estimates than response surface approximations of the response.

CHAPTER 7
OPTIMAL CHOICE OF KNOCKDOWN FACTORS THROUGH PROBABILISTIC DESIGN

Structural design of aircraft components still relies on deterministic (or code-based) approach governed by the Federal Aviation Administration (FAA) regulations. The use of a load safety factor of 1.5 and conservative material properties in design accompanied with certification testing of aircraft are required to follow the FAA requirements. On top of the FAA requirements aircraft companies add their own knockdown factors, for example while updating the allowable stresses based on the results of structural element tests. These knockdown factors are mostly based on worst-case scenarios, so they are implicit rather than explicit and because of material variability they depend on chance. This paper aims to show, however, that these knockdown factors can be selected explicitly by taking advantage of probabilistic analysis based on structural element test results. The knockdown factors can be chosen so as to minimize the chance of failure in certification or proof tests. We find that selection to minimize certification or proof test failure rate provides a choice that is also close to the optimum choice that minimizes structural failure in flight. We show that explicit knockdown factors can reduce weight for the same level of safety and they are also less variable than worst-case knockdown factors. In addition, the effects of coupon tests, structural element tests and uncertainty reduction mechanisms (such as error reduction by improved structural modeling or improved failure prediction, variability reduction by tighter quality control) on structural weight are investigated. In particular, since structural tests are expensive, the effect of

number of tests on the structural weight is translated to life-time cost by considering manufacturing cost and fuel cost.

Prof. Peter J. Ifju of University of Florida and Dr. Theodore F. Johnson of NASA Langley Research Center are acknowledged for their contributions for the research presented in this chapter.

Introduction

In Chapters 3 and 4, we analyzed the effects of measures that improve aircraft structural safety and compared the relative effectiveness of safety measures taken during aircraft structural design. The safety measures that we included were the load safety factors of 1.5, conservative material properties, redundancy, certification test, and error and variability reduction. The most common form of error reduction is conducting structural element tests, which is the focus of the present work. Similarly, one possible form of variability reduction is employing tighter quality control. Structural element tests are usually used conservatively, by taking the worst result of a batch of nominally identical tests. This constitutes an implicit knockdown factor because of material and test-condition variability. Here we aim to show, however, that it is better to use average test results and add explicit safety factors selected by using probabilistic optimization to reduce certification or proof test failure rates.

This chapter is organized as follows. The next section briefly discusses the building block approach followed in testing of aircraft structures. Then, the quantification and simulation of uncertainties, the allowable stress updating using the results of structural element tests through explicit knockdown factors and formulation of total safety factor is discussed. Next, a brief discussion on simulation of certification testing and probability of failure calculation are given. Then, the results of the optimal choice of knockdown

factors based on minimum certification failure rate and minimum probability of failure along with the analysis of effects of safety measures on the optimal choice of knockdown factors are presented. Finally, the chapter culminates with the concluding remarks are given in the Summary section.

Testing of Aircraft Structures

Testing of aircraft structures is performed following a building-block approach similar to that of composite structures as shown in Fig. 7-1. First, generic specimens are tested where coupon tests are followed by element tests. Then, non-generic specimens are tested where details, subcomponents and components are tested. The last level of testing is the full scale certification testing of the structural system.

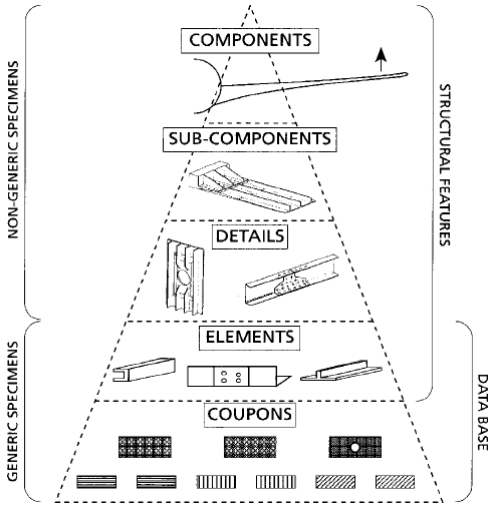

Figure 7-1. Building-block approach for aircraft structural testing (Reprinted, with permission, from MIL 17- The Composite Materials Handbook, Vol. 1, Chapter 2, copyright ASTM International, 100 Barr Harbor Drive, West Conshohocken, PA 19428)

Here we simplify the pyramid of tests depicted in Fig. 7-1 to three levels as shown in Fig. 7-2. The first level is the coupon testing level, where coupons (i.e., material samples) are tested. The FAA regulation FAR 25-651 requires aircraft companies to perform “enough” tests to establish design values of material strength properties (A-basis

or B-basis value). As the number of coupon tests increases, the errors in the assessment the material properties are reduced. However, since testing is costly, the number of coupon tests is limited to about 100 to 300 for A-basis calculation and 30+ (i.e., more than 30) for B-basis value calculation. In our analysis, the nominal value of the number of coupon tests is taken 40, and in the Results section of the chapter we analyze the effect of number of coupon tests on the optimal choice of the explicit knockdown factors.

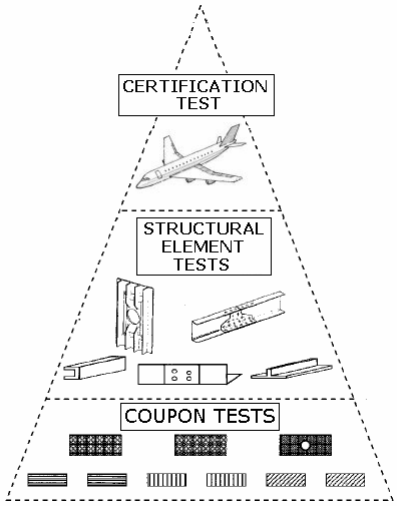

Figure 7-2. Simplified three level of tests

At the second level of testing, structural elements and details are tested. In this chapter, we refer to tests at this at this level as structural element tests. The main target of structural element tests is to reduce errors related to failure theories (e.g., Tresca, von Mises) used in assessing the failure load of the structural details/elements. In this chapter, the nominal value of the number of structural element tests is taken as 3.

At the uppermost level, certification testing of the overall structure is conducted. This final certification testing is intended to reduce errors in the structural analysis of the overall structure (e.g., errors in finite element analysis, errors in failure mode prediction).

Quantification of Errors and Variability

This section first discusses the errors in estimating the material strength properties due to limited number of coupon tests. Then, errors due to inaccuracies of the failure theories used to predict the failure load in the structural element tests are introduced. Next, the explicit knockdown factors employed on the allowable stresses using the results of structural element tests are discussed. Then, the errors in certification tests are presented. All the errors are combined to form a total error factor, and a total safety factor is defined. Finally, the variabilities in loading, geometry parameters and failure stress are discussed.

Errors in Estimating Material Strength Properties from Coupon Tests

As noted earlier, the first level in testing sequence is coupon testing to assess the statistical characterization of material strength properties, such as failure stress, and their corresponding design values (A-basis or B-basis). Since a finite number of coupon tests are performed, statistical characterization of the material properties involves errors. For example, the error e_{fc} in assessing the mean value of the failure stress at the coupon level, σ_{fc}, relates the average value of the failure stress calculated from n_c coupon tests, $\left(\bar{\sigma}_{fc}\right)_{calc}$, to the true mean value of the failure stress (mean of the infinite size population), $\left(\bar{\sigma}_{fc}\right)_{true}$

$$\left(\bar{\sigma}_{fc}\right)_{calc} = \left(1 - e_{fc}\right)\left(\bar{\sigma}_{fc}\right)_{true} \tag{7.1}$$

where the subscript '*c*' stands for coupon level tests. The population average $\left(\bar{\sigma}_{fc}\right)_{calc}$ is estimated as the sample average $\left(\sigma_{fc}\right)^{ave}$ obtained from n_c coupon tests

$$\left(\bar{\sigma}_{fc}\right)_{calc} \cong \left(\sigma_{fc}\right)^{ave} = \frac{1}{n_c}\sum_{i=1}^{n_c}\sigma_{fc_i} \tag{7.2}$$

where σ_{fc_i} is the failure stress calculated from each coupon test. The error e_{fc} is due to variability of the failure stress, hence the standard deviation of $\left(\bar{\sigma}_{fc}\right)_{calc}$ (and of e_{fc}) is $\sqrt{n_c}$ times smaller than the standard deviation of σ_{fc}. Details of assessment of the error e_{fc} is given in Appendix J. Notice that in Eq. (7.1) the sign in front of the error e_{fc} is negative, because we consistently formulate the expressions such that a positive error implies a conservative decision.

The error e_{fc} may have several components since the failure of many materials is characterized by several parameters and related tests, such as tensile limit, compressive limit, shear limit, etc. However, we make here a simplifying assumption that all components of σ_{fc} have the same coefficients of variation (c.o.v.) and are based on the same number of coupon tests, so they have the same error e_{fc}, since e_{fc} depends only on the c.o.v. and number of coupon tests (see Appendix J).

The allowable stress at the coupon level, σ_{ac}, can be computed from the failure stress calculated at the coupon level, $\left(\bar{\sigma}_{fc}\right)_{calc}$, by using a knockdown factor, k_{dc}, as

$$\sigma_{ac} = k_{dc}\left(\bar{\sigma}_{fc}\right)_{calc} \tag{7.3}$$

The knockdown factor k_{dc} is specified by the FAA regulations (FAR). For instance, for a redundant structure, FAR-25.613 states that the allowable stress must be the B-basis value of the failure stress, that is, 90% of the failure stresses (measured in coupon tests) must exceed the allowable stress with 95% confidence. The requirement of

90% probability and 95% confidence is responsible for the knockdown factor k_{dc} in Eq. (7.3). For normal distribution, the knockdown factor depends on the number coupon tests and the c.o.v. of the failure stress as

$$k_{dc} = 1 - k_B \left(c_{fc} \right)_{calc} \tag{7.4}$$

where $\left(c_{fc} \right)_{calc}$ is the c.o.v. of failure stress calculated from coupon tests. For lognormal distribution the formulation is more complicated, but can be derived utilizing a logarithmic transformation. The tolerance coefficient k_B is a function of the number of coupon tests n_c as given in the Composite Material Handbook (2000, Volume 1, Chapter 8, page 84) as

$$k_B \approx 1.282 + \exp\left(0.958 - 0.520 \ln(n_c) + \frac{3.19}{n_c} \right) \tag{7.5}$$

Similar to the error e_{fc}, the knockdown factor k_{dc} also has several components since σ_{fc} has several components. With the assumption of the same c.o.v. and same number of coupon tests for different components of σ_{fc}, a single k_{dc} can be used.

Errors in Structural Element Tests

The second level in the testing sequence is the structural element testing level, where structural elements/details are tested to validate the accuracy of the failure criterion used (e.g., von Mises, Tsai-Wu). Here, we assume that structural element tests are conducted for a specified combination of loads corresponding to critical loading. For this load combination, the failure surface can be boiled down to a single failure stress σ_{fe} (see Fig. 7-3), where the subscript '*e*' stands for structural element tests.

If the failure theory used to predict the failure was perfect, and we performed thousands of coupon tests (that essentially reduces the error e_{fc} to zero), then we could obtain the true element failure stress at the structural element test from

$$\left(\sigma_{fe}\right)_{true} = \sigma_{fe}\left[\left(\sigma_{fc}\right)_{true}\right] \tag{7.6}$$

where $\sigma_{fe}[\cdot]$ refers to the failure criterion functional used (e.g., von Mises, Tsai-Wu). So, the calculated value of failure stress, $\left(\sigma_{fe}\right)_{calc}$, is

$$\left(\sigma_{fe}\right)_{calc} = \sigma_{fe}\left[\left(\sigma_{fc}\right)_{calc}\right] \tag{7.7}$$

To relate $\left(\sigma_{fe}\right)_{calc}$ to $\left(\sigma_{fe}\right)_{true}$ we make a simplifying assumption that the failure criterion $\sigma_{fe}[\cdot]$ is a homogenous functional of order one, such as von Mises or Tsai-Hill. Then,

$$\sigma_{fe}\left[\left(\sigma_{fc}\right)_{calc}\right] = \left(1-e_{fc}\right)\sigma_{fe}\left[\left(\sigma_{fc}\right)_{true}\right] \tag{7.8}$$

Since there are errors in failure prediction in structural element testing level due to limitations of the failure theory used, we write

$$\sigma_{fe}\left[\left(\sigma_{fc}\right)_{true}\right] = \left(1-e_{fe}\right)\left(\sigma_{fe}\right)_{true} \tag{7.9}$$

Combining Eqs. (7.7), (7.8) and (7.9), the calculated failure stress at the structural element level can be related to its true value as

$$\left(\sigma_{fe}\right)_{calc} = \left(1-e_{fc}\right)\left(1-e_{fe}\right)\left(\sigma_{fe}\right)_{true} \tag{7.10}$$

The structural element test is repeated n_e times yielding a sample average failure stress $\left(\sigma_{fe}\right)_{test}^{ave}$, which is used to estimate the population average $\left(\bar{\sigma}_{fe}\right)_{test}$. The

population average is now used to update the allowable stresses for the element design. We assume that similarly to the knockdown factor k_{dc} mandated by the FAA, the designer may add additional knockdown factor k_{fe} to compensate for the uncertainty in the element test. The value of k_{fe} is likely depend on whether the failure stress at the element test exceeds or falls below the predicted failure stress $\left(\bar{\sigma}_{fe}\right)_{calc}$. That is, the allowable stress based on the element test is calculated from

$$\sigma_{ae} = k_{fe}\left(\bar{\sigma}_{fe}\right)_{test} \tag{7.11}$$

Allowable stress updating and the use of explicit knockdown factors

This section describes updating of the allowable stress based on the results of structural element tests. First, we discuss updating using worst-case approach, which amounts to implicit knockdown factors. Next, allowable stress updating through using explicit knockdown factors is explained. Then, updating of error in failure prediction in structural element tests is discussed

Current industrial practice on updating allowable stresses using worst-case conditions (implicit knockdown factors)

Current practice followed in industry is using the *smallest* of the failure stresses measured in structural element tests, $\left(\sigma_{fe}\right)_{test}^{worst}$, is used to update the allowable stresses. We define the ratio of failure stress measured in the tests and calculated (or predicted) failure stress, $\left(\bar{\sigma}_{fe}\right)_{calc}$, as

$$\left(r_{et}\right)^{worst} = \frac{\left(\sigma_{fe}\right)_{test}^{worst}}{\left(\bar{\sigma}_{fe}\right)_{calc}} \tag{7.12}$$

Then, according to this practice the allowable stress is updated as

$$\left(\sigma_{ae}\right)_{upd}^{worst} = k_c\left[\sigma_{ae}\left(r_{et}\right)^{worst}\right] \tag{7.13}$$

where k_c is an additional knockdown factor corresponding to worst-case operational conditions (e.g., high temperature, humidity). Note here that k_c does not depend on the results of element tests, that is, $k_c \neq k_c\left(r_{et}\right)$. Figure 7-3 shows three aircraft companies A, B and C performing three structural element tests. Since we are interested in the implicit knockdown factor associated with worst-case conditions, we assume that all three companies use the same failure theory. That is, the difference in test results is *entirely due to material variability*. Under these conditions, $\left(r_{et}\right)^{worst}$ constitutes an implicit knockdown factor. For the examples in this paper, we assume 8% variability in failure stress (lognormal distribution). This translates to an average knockdown factor of 0.932 with a standard deviation of 0.0598. The red knockdown factors in Fig. 7-3 corresponds to $\left(r_{et}\right)^{worst}$ in Eq. (7.13), blue knockdown factor represents additional knockdown factor k_c (notice in Figure 7-3 that k_c does not depend on element test results).

Proposal for a better way to update allowable stresses: Using the average failure stress measured in the tests and using optimal explicit knockdown factors

Instead of using the smallest failure stresses measured in tests, we propose to use average value of the failure stresses measured in the tests accompanied by an explicit knockdown factor selected based on probabilistic analysis. Now, we define the failure stress ratio in the structural elements, $\left(r_{et}\right)^{ave}$, as the ratio of the *average* failure stress measured in the element test and the calculated failure stress, $\left(\bar{\sigma}_{fe}\right)_{calc}$, as

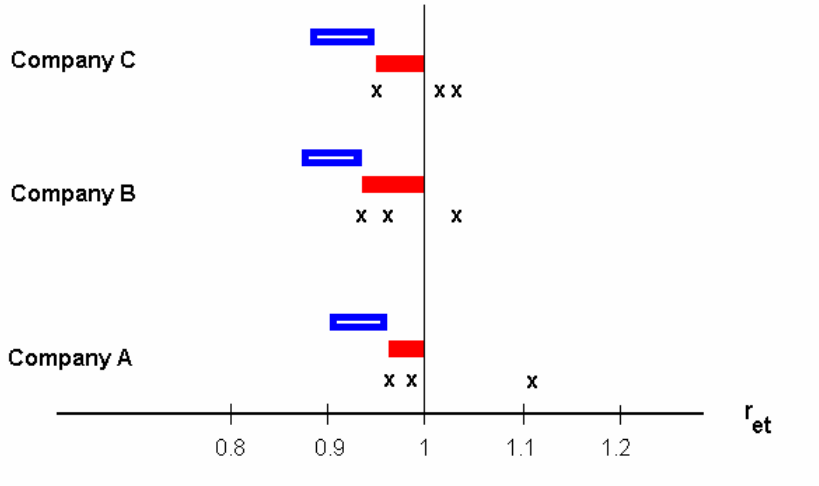

Figure 7-3. Current use of knockdown factors based on worst-case scenarios. The red knockdown factors are due to updating the allowable stress using the worst failure stress measured in the test, and the blue knockdown factors are test independent and due to testing structural elements at worst-case conditions (e.g., high temperature, high humidity). For a lognormal distribution and 8% coefficient of variation, the implicit knockdown factor is 0.932 with a standard deviation of 0.0598.

$$\left(r_{et}\right)^{ave} = \frac{\left(\bar{\sigma}_{fe}\right)_{test}}{\left(\bar{\sigma}_{fe}\right)_{calc}} \tag{7.14}$$

The use of an explicit knockdown factor is required because a limited number of structural element tests are performed, so the value of failure stress ratio ret can have substantial variability. In addition, these knockdown factors may be used to reduce the likelihood of failing certification or proof test. The updated failure surfaces with and without additional knockdown factors are depicted Fig. 7-4.

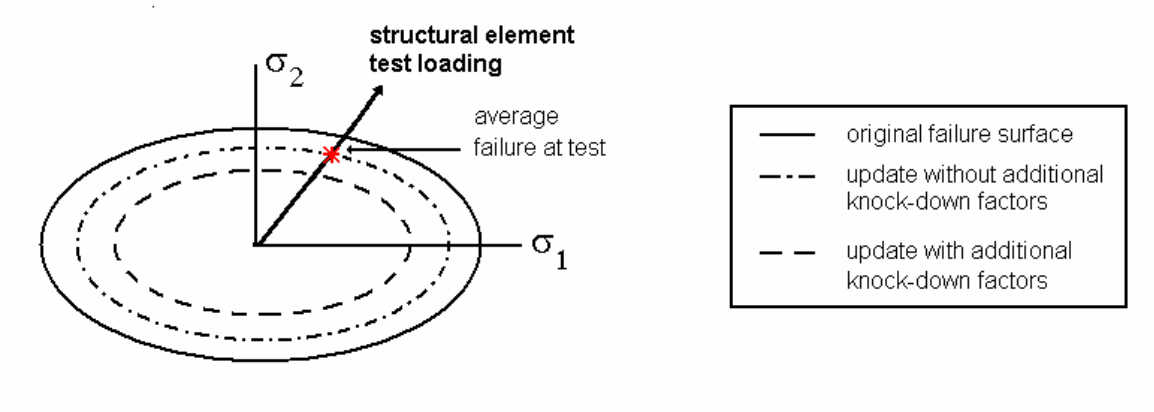

Figure 7-4. Shrinkage of the failure surface. Original failure surface, updated failure surface without explicit knockdown factor and the failure surface updated with an explicit knock factor k_{cl}. Asterisk shows the failure at the structural element test.

In general, we may expect that an optimal explicit knockdown factor will be a function of r_{et}. Since we assume that the failure prediction error e_{fe} has zero mean, when $(r_{et})^{ave}$ is smaller or larger than one, it is likely that this is caused by variability. Since we increase the allowable stress when $(r_{et})^{ave} > 1$, we run a chance that this increase is dangerous. So as we will see later, the optimal k_c is smaller for $(r_{et})^{ave} > 1$ than for $(r_{et})^{ave} < 1$.

We require that the explicit knockdown factor does not increase so fast that the allowable stress may decrease with increasing r_{et}. So for the allowable stress to be monotonic with respect to failure stress ratio ret we require

$$\frac{d(\sigma_{ae})_{upd}}{dr_{et}} = \frac{d}{dr_{et}}(k_c\,\sigma_{ae}\,r_{et}) > 0 \tag{7.15}$$

which leads to

$$\frac{k_c}{r_{et}} + \frac{dk_c}{dr_{et}} > 0 \tag{7.16}$$

Here we assume that $k_c(r_{et})$ has the simple form of two constants connected by a ramp, with the angle θ selected to satisfy Eq. (7.16) as depicted in Fig. 7-5. That is,

$$k_c = \begin{cases} k_{cl} & \text{if } r_{et} \le 1.0 \\ k_{cl} + \dfrac{r_{et} - 1}{r_h - 1}\left(k_{ch} - k_{cl}\right) & \text{if } 1.0 \le r_{et} \le r_h \\ k_{ch} & \text{if } r_{et} \ge r_h \end{cases} \tag{7.17}$$

The parameter defining the transition interval, r_h, is also taken constant in our analysis for the sake of simplicity. Our numerical studies showed that the use of $r_h = 1.10$ is an acceptable value.

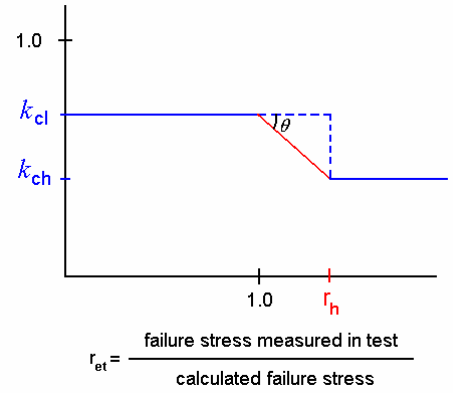

Figure 7-5. The variation of the explicit knockdown factors with ratio of the failure stress measured in the test and calculated failure stress with and without transition interval

Figure 7-6 illustrates this approach for the three aircraft companies A, B and C performing three structural element tests shown earlier in Fig. 7-3. The red knockdown factors in Fig. 7-6 correspond to updating the allowable stress using the average failure stress measured in tests (Eq. (7.14)), while blue knockdown factor represents an explicit knockdown factor k_c (notice in Fig. 7-6 that k_c depends on element test results as depicted in Fig. 7-5).

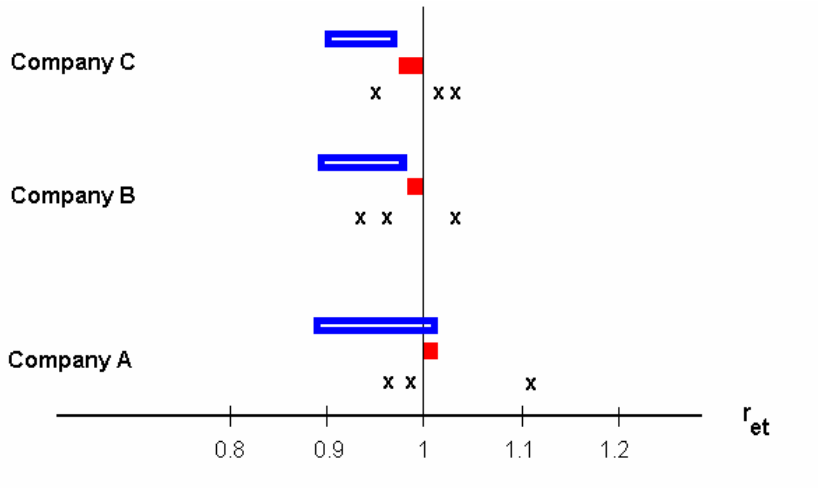

Figure 7-6. Proposed use of explicit knockdown factors dependent on test results. The red knockdown factors are due to updating the allowable stress using the average failure stress measured in the test, and the blue knockdown factors are test dependent explicit safety factor.

Error updating via element tests

The main effect of structural element tests is to reduce the error in failure prediction at the element level, e_{fe}. The error e_{fe} after element tests are updated as follows.

After the element tests, the calculated failure stress is updated using tests results as

$$\left(\sigma_{fe}\right)_{calc}^{upd} = r_{et}\left(\sigma_{fe}\right)_{calc} \tag{7.18}$$

Hence, the updated error e_{fe} can be calculated from

$$e_{fe}^{\,upd} = \frac{\left(\sigma_{fe}\right)_{calc}^{upd}}{\left(\sigma_{fe}\right)_{true}} - 1 = \frac{r_{et}\left(\sigma_{fe}\right)_{calc}}{\left(\sigma_{fe}\right)_{true}} - 1 = r_{et}\left(1 + e_{fe}^{\,ini}\right) - 1 \tag{7.19}$$

and the updated allowable stress can be written as

$$\left(\sigma_{ae}\right)^{upd} = k_{fe}\left(\bar{\sigma}_{fe}\right)_{calc}^{upd} \tag{7.20}$$

where the total knockdown factor used in setting the allowable stress, k_{fe}, is defined as

$$k_{fe} = k_c\, k_{dc} \tag{7.21}$$

Errors in Design

For structural design, first the loads acting on the structure are calculated. For an aircraft structure, the design load P_d is computed by following the FAA design specifications (e.g., gust-strength specifications). However, the calculated design load value, P_{calc}, differs from the true design loading P_d. Since each aircraft company has different design practices, the error in load calculation, e_p, is different from one company to another. The calculated design load P_{calc} is expressed in terms of true value P_d as

$$P_{calc} = (1 + e_P) P_d \tag{7.22}$$

Here, we examine a small part of the overall structure, which can be characterized by its width, w, and thickness, t. If stress calculations are performed without errors, the true value of the stress in the structure is

$$\sigma_{true} = \frac{P_{calc}}{wt} \tag{7.23}$$

However, an aircraft company may also commit errors in stress calculation. The calculated value of stress, σ_{calc}, can be expressed by introducing the error in the stress analysis, e_σ, as

$$\sigma_{calc} = (1 + e_\sigma) \frac{P_{calc}}{wt} \tag{7.24}$$

If there were no errors in failure prediction of the overall structure, failure prediction at the structural element testing level, and failure stresses calculated at the coupon level, then the true failure stress at the structural design level, $\left(\sigma_{fs}\right)_{true}$, could be related to true failure stress at element testing level, $\left(\sigma_{fe}\right)_{true}$ via Eq. (7.25) (as in the

case of relating the true failure stress at the element testing level to the failure stress at the coupon level, Eq. (7.6)).

$$\left(\sigma_{fs}\right)_{true} = \sigma_{fs}\left[\left(\sigma_{fe}\right)_{true}\right] \tag{7.25}$$

where $\sigma_{fs}[\cdot]$ is the failure functional used to predict the overall structural failure in terms of the failure stress results of structural element test. Since the above mentioned errors do all exist, the failure stress calculated at structural design level, $\left(\sigma_{fs}\right)_{calc}$, differs from its true value, $\left(\sigma_{fs}\right)_{true}$. So, we have

$$\left(\sigma_{fs}\right)_{calc} = \sigma_{fs}\left[\left(\sigma_{fe}\right)_{calc}\right] = \left(1-e_{fc}\right)\left(1-e_{fe}^{\,upd}\right)\left(1-e_{fs}\right)\left(\sigma_{fs}\right)_{true} = \left(1-e_{fT}\right)\left(\sigma_{fs}\right)_{true} \tag{7.26}$$

where e_{fs} includes the errors in predicting the structural failure of the overall structure (e.g., errors in predicting the failure mode). As before, Eq. (7.26) assumes that the overall structural failure is a homogenous functional of order one in terms of the element failure stress.

The allowable stress at the structural design level, σ_{as}, can be computed from the failure stress calculated at the element level, $\left(\bar{\sigma}_{fs}\right)_{calc}$, by using the knockdown factor k_{fe} as

$$\sigma_{as} = k_{fe}\left(\bar{\sigma}_{fs}\right)_{calc} \tag{7.27}$$

Combining Eqs. (7.26) and (7.27), the allowable stress at the structural design level, σ_{as}, can be related to the true mean failure stress at the structural design level as

$$\sigma_{as} = k_{fe}\left(1-e_{fT}\right)\left(\bar{\sigma}_{fs}\right)_{true} \tag{7.28}$$

A structural designer uses Eq. (7.29) to calculate the design thickness t_{design} required to carry the calculated design load, P_{calc}, times the safety factor, S_{FL}. That is,

$$t_{design} = \left(1+e_\sigma\right)\frac{S_{FL}\,P_{calc}}{w_{design}\,\sigma_{as}} = \frac{\left(1+e_\sigma\right)\left(1+e_P\right)}{\left(1-e_{fT}\right)}\frac{S_{FL}\,P_d}{w_{design}\;k_{fe}\left(\bar{\sigma}_{fs}\right)_{true}} \tag{7.29}$$

where w_{design} is the design width of the part. Then, the design value of the load carrying area can be expressed as

$$A_{design} = t_{design}\,w_{design} = \frac{\left(1+e_\sigma\right)\left(1+e_P\right)}{\left(1-e_{fT}\right)}\frac{S_{FL}\,P_d}{k_{fe}\left(\bar{\sigma}_{fs}\right)_{true}} \tag{7.30}$$

Errors in Construction

In addition to the above errors, there will also be construction errors in the geometric parameters. These construction errors represent the difference between the values of these parameters in an average airplane (fleet-average) built by an aircraft company and the design values of these parameters. For the structural part, errors in width, e_w, represent the deviation of the values of structural part width designed by an individual aircraft company, w_{design}, from the average value of the width built by the company, w_{built}. Thus, we have

$$w_{built} = \left(1+e_w\right)w_{design} \tag{7.31}$$

Similarly, the built thickness value will differ from its design value such that

$$t_{built} = \left(1+e_t\right)t_{design} \tag{7.32}$$

Then, the built load carrying area A_{built} can be expressed as

$$A_{built} = \left(1+e_t\right)\left(1+e_w\right)A_{design} \tag{7.33}$$

Table 7-1 presents nominal values for the error factors. In the Results section of the chapter we will vary these error bounds and investigate the effects of reducing these errors on the built area, probability of failure, etc.

Table 7-1. Distribution of error factors and their bounds

Error factors	Distribution Type	Mean	Scatter
Error at the coupon level, e_{fc}	Normal	0	Std $\cong \frac{c_f}{\sqrt{n_c}}$
Error in failure prediction in structural element test, e_{fe}	Uniform	0	± 10%
Error in failure prediction of the overall structure, e_{fs}	Uniform	0	± 10%
Error in stress calculation, e_σ	Uniform	0	± 5%
Error in load calculation, e_P	Uniform	0	± 10%
Error in width, e_w	Uniform	0	± 1%
Error in thickness, e_t	Uniform	0	± 2%

Total Error Factor

The expression for the built area, A_{built}, of a structural part can be reformulated to Eq. (7.34) by combining Eqs. (7.30) and (7.33) as

$$A_{built} = \left(1 + e_{total}\right) \frac{S_{FL} P_d}{k_{fe} \left(\bar{\sigma}_{fs}\right)_{true}} \tag{7.34}$$

where

$$e_{total} = \frac{\left(1+e_\sigma\right)\left(1+e_P\right)\left(1+e_t\right)\left(1+e_w\right)}{\left(1-e_{fT}\right)} - 1 \tag{7.35}$$

Here e_{total} represents the cumulative effect of the individual errors (e_σ, e_P, …) on the load carrying area of the built structural part.

Total Safety Factor

The total safety factor, S_F, of a structural part represents the effects of all errors and the safety measures on the built structural part. Without errors and safety measures, we would calculate the load carrying area by simply dividing the design load by the mean

value of the true failure stress at the structural design level, $\left(\bar{\sigma}_{fs}\right)_{true}$. That is, the load carrying area without safety measures, A_0, is calculated from

$$A_0 = \frac{P_d}{\left(\bar{\sigma}_{fs}\right)_{true}} \tag{7.36}$$

Then, the total safety factor can be defined as the ratio of A_{built}/A_0. Using Eqs. (7.34) and (7.36), we can write the total safety factor as

$$S_F = \frac{A_{built}}{A_0} = \left(1 + e_{total}\right)\frac{S_{FL}}{k_{fe}} \tag{7.37}$$

Variability

In the previous sections we analyzed the different types of errors committed during design and construction stages, representing the differences between the true and calculated values of the fleet average of the material properties, the geometry parameters and the loading. These parameters (the material properties, the geometry parameters and the loading), however, vary from one aircraft to another in the fleet due to variabilities in tooling, construction, flying environment, etc. For instance, the actual value of the thickness of a structural part, t_{act}, is defined in terms of its fleet average value, t_{built}, by

$$t_{act} = U\left(t_{built}, b_{t_{act}}\right) \tag{7.38}$$

Here '*U*' indicates that the distribution is uniform, 't_{built}' is the average value of thickness (fleet average) and '$b_{t_{act}}$' defines the bounds for the variability in thickness. Table 7-2 shows that the scatter in t_{act} is taken here to be 3%, that is $b_{t_{act}}$=0.03. Hence, the lower bound for thickness value is the average value minus 3% of the average and the upper bound for thickness value is the average value plus 3% of the average. Then, the actual thickness can be calculated from Eq. (7.39)

$$t_{act} = (1 + v_t) t_{built} \tag{7.39}$$

where $v_t = b_{t_{act}} (2r - 1)$ represents effect of the variability on built thickness and r is a uniformly distributed random number between 0 and 1.

Then, the actual load carrying area, A_{act}, can be defined as

$$A_{act} = t_{act} w_{act} = (1 + v_t)(1 + v_w) A_{built} = (1 + v_t)(1 + v_w)(1 + e_{total}) \frac{S_{FL}}{k_{fe}} \frac{P_d}{(\bar{\sigma}_{fs})_{true}} \tag{7.40}$$

where v_w represents effect of the variability on built width, $b_{w_{act}}$ = 0.01, and the second equality is obtained by using Eq. (7.34).

Note that the thickness error in Table 7-1 is uniformly distributed with bounds of ±2%. Thus the difference between all thicknesses over the fleets of all companies is up to ±5%. However, the combination of error and variability which is the sum of two uniformly distributed components is not uniformly distributed. Table 7-2 presents the assumed distributions for variabilities. The actual service loading P_{act} is assumed to follow extreme value distribution type I, since we consider the maximum (over a lifetime) loading. The failure stress is assumed to follow lognormal distribution.

Table 7-2. Distribution of random variables having variability

Variables	Distribution type	Mean	Scatter
Actual service load, P_{act}	Extreme type I	P_d = 100	10% c.o.v.
Actual width, w_{act}	Uniform	w_{built}	±1% bounds
Actual thickness, t_{act}	Uniform	t_{built}	±3% bounds
Variability in built width, v_w	Uniform	0	±1% bounds
Variability in built thickness, v_t	Uniform	0	±3% bounds
Actual failure stress, σ_{fs}	Lognormal	$\bar{\sigma}_{fs}$ =150	c_f = 0.08 (i.e., 8% c.o.v.)

Simulation of Certification Test and Probability of Failure Calculation

Simulation of Certification Test

After a structural part is built with all the errors, variabilities and safety factors, we simulate certification testing for the structural part. That is, the structural part with cross-sectional area of A_{act}, Eq. (7.40), is loaded with the design axial force of S_F times P_{calc}, and if the stress exceeds the failure stress σ_{fs}, then the structure fails and the design is rejected; otherwise it is certified for use. That is, the structural part is certified if the following inequality is satisfied

$$\sigma - \sigma_{fs} = \frac{S_{FL} P_{calc}}{A_{act}} - \sigma_{fs} \le 0 \tag{7.41}$$

Figure 7-7(a) shows the distributions of the built and certified total safety factors. Notice that the structural parts designed with low total safety factors are likely to be rejected in the certification testing. The mean and standard deviations of built and certified total safety factor are listed in Table 7-3, which shows that the mean is increased and the standard deviation is reduced due to certification testing. Notice that the effect of certification test is very small. If there were no structural element tests, on the other hand, the effect would be more significant (Fig. 7-7(b)).

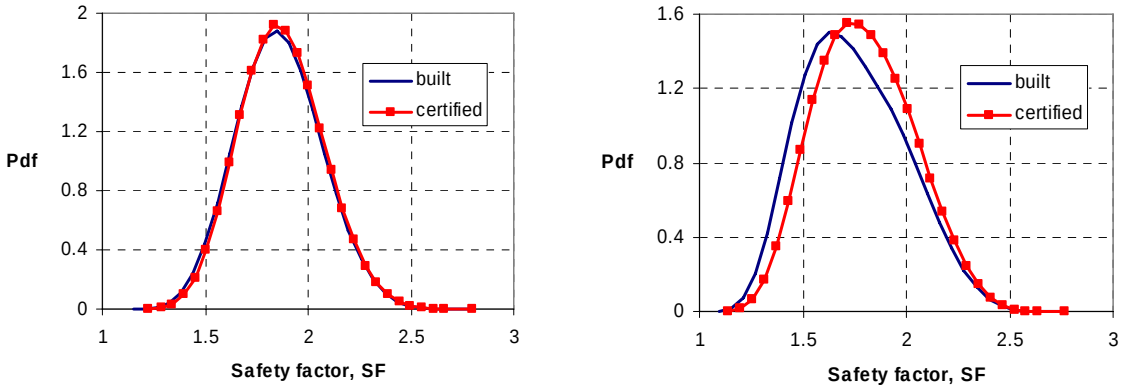

(a) with structural element tests (b) without structural elements tests

Figure 7-7. Initial and updated distribution of the total safety factor S_F. (a) with structural element tests, (b) without structural element test. The distributions are obtained via Monte Carlo Simulations with 1,000,000 structural part models. Note that in (a) three structural element tests, forty coupon tests, and company safety factors k_{cl}=0.9, k_{ch}=0.83 and r_h=1.1 are used. See Tables 7-1 and 7-2 for error and variability data.

Table 7-3. Mean and standard deviations of the built and certified distribution of the total safety factor S_F. The calculations are performed with 1,000,000 MCS.

	Mean	Std. dev.
Built safety factor	1.861	0.193
Certified safety factor	1.871	0.188

Calculation of Probability of Failure

To calculate the probability of failure, first we incorporate the statistical distributions of errors and variability in a Monte Carlo simulation. Errors are uncertain at the time of design, but do not change for individual realizations (in actual service) of a particular design. On the other hand, all individual realizations of a particular design are different from each other due to variability.

Errors and variability could be simulated through a double-loop Monte Carlo simulation (as in Chapter 3), in the upper loop we could simulate different aircraft companies assigning random errors to each, and in the lower loop we could simulate variability in dimensions, material properties, loads related to manufacturing variability

and variability in service conditions. However, this process would require trillions of simulations for good accuracy. In order to address the computational burden we turned to the separable Monte Carlo procedure (e.g., Smarslok *et al*. 2006), which consists of a single loop that comprises two stages. The first stage is for simulation of variabilities only, and the second stage is for simulating errors and tests (coupon, structural element and certification). The discussion on separable MCS is given in Appendix K. To achieve separable form, the failure condition is written as

$$\text{Failure without certification tests:} \quad (S_F)_{req} - (S_F)_{built} > 0 \tag{7.42}$$

$$\text{Failure with certification tests:} \quad (S_F)_{req} - (S_F)_{cert} > 0 \tag{7.43}$$

where $(S_F)_{built}$ and $(S_F)_{cert}$ are the built and certified total safety factors, and $(S_F)_{req}$ is the required safety factor necessary to account for the variabilities. For a given $(S_F)_{built}$ we can calculate the probability of failure, Eq. (7.42), by simulating all the variabilities with an MCS.

Figure 7-8 shows the dependence of the probability of failure on the total safety factor using MCS with 1,000,000 variability samples. Note that the probability of failure, P_f, presented here is the probability of failure of a structural part built by *a single aircraft company* with a total safety factor of $(S_F)_{built}$. This probability of failure is different from the average probability of failure over all companies. We see from Fig. 7-8 that the nominal load safety factor of 1.5 is associated with a probability of failure of about 10^{-3}, while the probabilities of failure observed in practice (about 10^{-7}) correspond to a total safety factor of about 2.4. The average probability of failure over all companies, P_F, is

calculated by performing Monte Carlo simulations with first stage sample size of M=1,000,000 and second stage sample size of N=1,000,000.

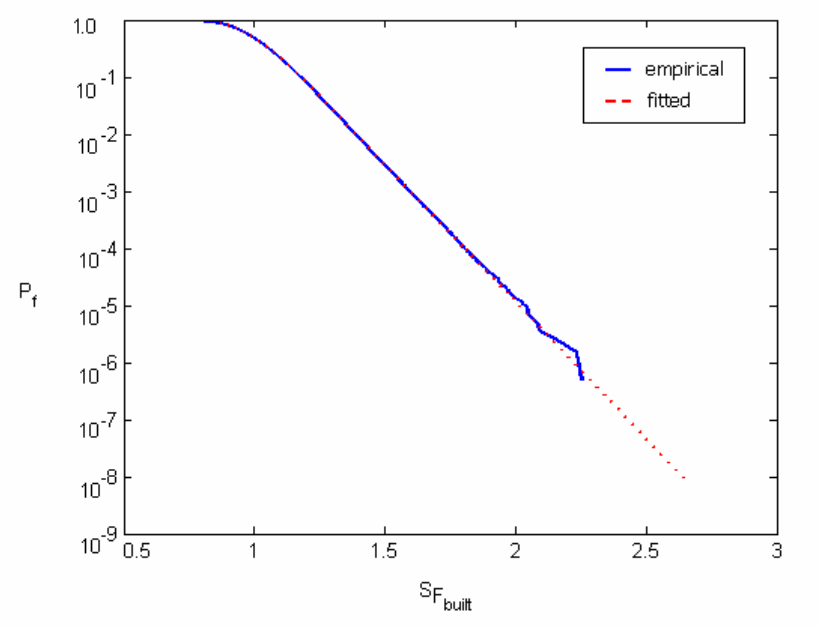

Figure 7-8. The variation of probability of failure of a structural part built by a single aircraft company. Note that P_f is one minus the cumulative distribution function of $(S_F)_{req}$. See Tables 7-1 and 7-2 for error and variability data used for this case.

Results

In this section we first analyze the optimal choice of explicit knockdown factors for minimum weight, minimum likelihood of failure in certification (or proof) test, and minimum probability of failure under actual flight loads. Next, the effects of coupon tests and element tests on reducing the errors in failure prediction are explored. Then, the effect of using different approaches and different formulation for knockdown factors are analyzed. Finally, the effects of uncertainty reduction mechanisms (error and variability reduction), number of coupon tests and number of structural element tests on the optimal choice of knockdown factors and on the probability of failure are investigated.

Optimal Choice of Explicit Knockdown Factors for Minimum Weight and Minimum Certification Failure Rate

Even though using smaller knockdown factors reduces the likelihood of failure of the structure in the certification test (certification failure rate, *CFR*), the weight of the structure increases accordingly. The cost of weight increase of aircraft structure is discussed in Appendix L. Since a company aims to have both minimal *CFR* and minimum weight, the optimal choice of k_{cl} and k_{ch} is formulated here as a multi-objective optimization problem with two objective functions: the first being the built area A_{built} (or the built safety factor $(S_F)_{built}$) and the second is the certification failure rate *CFR*. We seek to find the Pareto front, the curve of optimal trade-off between the two objectives.

There are two popular ways to obtain the Pareto front. One is to optimize a weighted sum of the objectives for different combinations of weights. Another approach is to add one of the objective functions as the constraint and change the constraint margin to generate the front. Here we follow the second approach. We minimize the built safety factor, $(S_F)_{built}$, for a series of specified certification failure rates. So the optimization problem can be stated as

$$\begin{aligned} \min_{k_{cl},k_{ch}} \quad & A/A_0 = (S_F)_{built} \\ \text{such that} \quad & CFR \le CFR_{spec} \\ & k_{cl}, k_{ch} \le 1 \end{aligned} \tag{7.44}$$

Solving Eq. (7.44) requires calculation of *CFR* many times, which is computationally very expensive. To alleviate the computational cost, we estimate *CFR* and $(S_F)_{built}$ by using response surface approximations (RSA) for the reliability index of *CFR*, β_{CFR}, which is defined as

$$\beta_{CFR} = -\Phi(CFR) \tag{7.45}$$

where Φ is the cumulative distribution function of the standard normal distribution. We use fifth-order polynomial RSAs for the built safety factor, $(S_F)_{built}$, and reliability index of *CFR*, β_{CFR}. The average (over all aircraft companies) probability of failure of a structural part P_F is also approximated with RSA for its reliability index β_{P_F}

$$\beta_{P_F} = -\Phi(P_F) \tag{7.46}$$

The accuracy of RSAs is discussed in Appendix M. Figure 7-8 depicts the tradeoff of safety (*CFR* and corresponding P_F) against weight (built safety factor) when 40 coupons tests and 3 structural element tests are employed. Each point in the trade-off plot is associated with a different k_{cl} and k_{ch} combination as given in Table 7-4. We see from Fig. 7-9 that as lower *CFR* are specified, larger built safety factors are needed. We also see that as expected larger safety factors leads to lower failure probabilities.

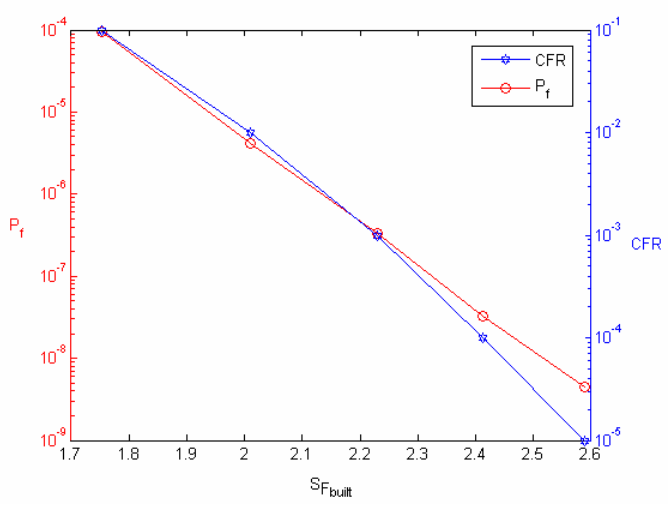

Figure 7-9. Optimal choice of explicit knockdown factors k_{cl} and k_{ch} for minimum built safety factor for specified certification failure rate. The number of coupons tests is 40, and the number of structural element tests is 3. See Tables 7-1 and 7-2 for error and variability data.

The optimal values of k_{cl} and k_{ch} for minimum built safety factor for specified *CFR* are given in Table 7-4. When *CFR* is reduced, smaller knockdown factors k_{cl} and k_{ch} are used. We also notice that as expected k_{ch} is smaller than k_{cl}. This may appeal to a designer when the tests allow weight reduction trading some of the weight for some extra margin as insurance against variability in the results of structural element tests. The monotonicity constraint, Eq. (7.16), is active for $CFR=10^{-3}$ and 10^{-4}, indicating that the parameter defining the transition interval, r_h, is important. Investigation of the effect of this parameter is left for a future work.

The comparison of the certification failure rates and probabilities of failure obtained from RSAs and calculated using MCS of 1,000,000 sample size is also given in Table 7-4. We see that the values obtained from RSAs are very close to MCS values and the differences are within the limits of MCS error due to finite sample size. For example, while predicting a probability of failure 8.14×10^{-5}, two-stage separable MCS with 10^6 samples (for each stages) is equivalent to about 10^8 crude MCS, so the error for predicting P_F of 8.14×10^{-5} within two standard deviation is about 2.2%, which larger than the actual error 1.6% that we see in the first row of Table 7-4. We also see in Table 7-4 that as *CFR* (or P_F) reduce the error grows. There are two contributions to the error: (i) error due to limited MCS sample size (which grows as *CFR* reduces), (ii) error in RSA (that can be high if *RSA* is performed near design boundaries). However, even for $CFR=10^{-4}$, the error in *CFR* is only 6%.

Table 7-4. Comparing explicit knockdown factors for minimum built safety factor for a specified certification failure rate. Note that CFR and P_F are calculated using MCS of 1,000,000 sample size, while CFR-RS and P_F-RS are obtained from the RSAs.

CFR-RS	CFR	A/A_0*	k_{cl}	k_{ch}	P_F-RS	P_F
10^{-1}	9.95×10^{-2}	1.750	1.000	0.963	8.01×10^{-5}	8.14×10^{-5}
10^{-2}	1.04×10^{-2}	1.987	0.892	0.820	4.09×10^{-6}	4.25×10^{-6}
10^{-3}	1.03×10^{-3}	2.193	0.809	0.742	3.46×10^{-7}	3.58×10^{-7}
10^{-4}	9.40×10^{-4}	2.372	0.747	0.687	3.99×10^{-8}	4.29×10^{-8}

* A/A_0 is the ratio of the built cross sectional area, A, and the area without safety measures, A_0. Note that the area ratio is equal to the total safety factor $(S_F)_{built}$

Optimal Choice of Explicit Knockdown Factors for Minimum Weight and Minimum Probability of Failure

Instead of designing the structure for minimum certification failure rate, the structure can be designed for minimum probability of failure (i.e., performing probabilistic optimization). In that case the optimization problem can be stated as

$$\begin{aligned} \min_{k_{cl},k_{ch}} \quad & A/A_0 = (S_F)_{built} \\ \text{such that} \quad & P_F \le (P_F)_{spec} \\ & k_{cl}, k_{ch} \le 1 \end{aligned} \tag{7.47}$$

where $(P_F)_{spec}$ is the specified probability of failure. The Pareto front can be obtained by varying the specified probability of failure, $(P_F)_{spec}$. Surprisingly Fig. 7-10(a) shows that the *CFR* of the structures designed for minimum *CFR* and *CFR* of the structures designed for minimum P_F are very close to each other. The same observation is also true for the P_F of the structures designed either for minimum *CFR* or for minimum P_F (Fig. 7-10(b)). So choosing the explicit knockdown factors to minimize the failure in certification test offers a rational way of choosing the explicit knockdown factor.

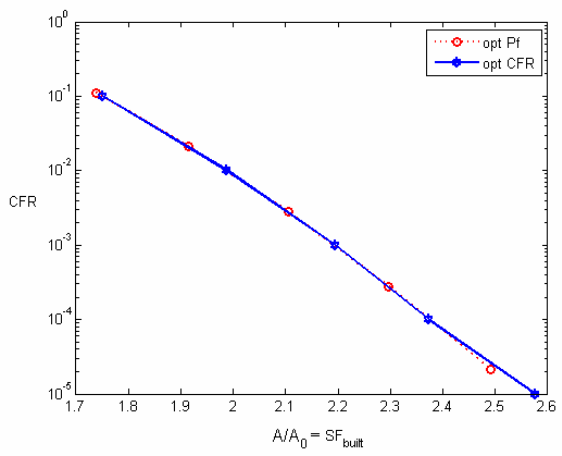

(a) *CFR* comparison

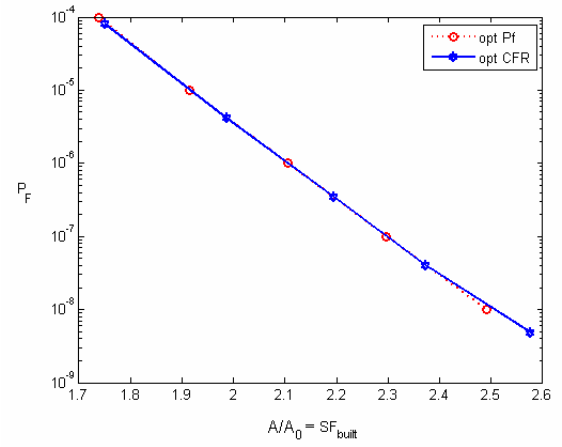

(b) P_F comparison

Figure 7-10. Comparing *CFR* and P_F of the structures designed for minimum *CFR* and minimum P_F (a) Comparison of *CFR* of the structures designed for minimum *CFR* and minimum P_F, (b) Comparison of P_F of the structures designed for minimum *CFR* and minimum P_F

The optimal values of k_{cl} and k_{ch} for minimum built safety factor for specified P_F are given in Table 7-5. We see the trend in the explicit knockdown factor is similar to that given in Table 7-4 in that k_{cl} is larger than k_{ch}. We see that *CFR*s and P_Fs obtained from RSAs and MCS of 1,000,000 sample size are very close to each other. So from this point on we only present the *CFR* and P_F values obtained from RSAs.

Table 7-5. Comparing explicit knockdown factors for minimum built safety factor for a specified probability of failure

P_F-RS	P_F	A/A_0*	k_{cl}	k_{ch}	CFR-RS	CFR
10^{-4}	1.00×10^{-5}	1.739	1.000	0.984	1.12×10^{-1}	1.11×10^{-1}
10^{-5}	1.04×10^{-5}	1.914	0.926	0.853	2.13×10^{-2}	2.21×10^{-2}
10^{-6}	1.03×10^{-6}	2.105	0.843	0.773	2.80×10^{-3}	2.89×10^{-3}
10^{-7}	1.06×10^{-7}	2.295	0.773	0.709	2.75×10^{-4}	2.73×10^{-4}

* A/A_0 is the ratio of the built cross sectional area, A, and the area without safety measures, A_0. Note that the area ratio is equal to the total safety factor $(S_F)_{built}$

Effect of Coupon Tests and Structural Element Tests on Error in Failure Prediction

As noted earlier, coupon tests and structural element tests contribute to structural safety mainly by reducing the error in failure prediction. Here we analyze the effect of number of these tests on reducing the error in failure prediction. First, we analyze the effect of number of coupon tests alone for a fixed number of element tests (here we take the fixed number of element tests as three). Then, the effect of structural element tests are explored for a fixed number of coupon tests (here we take fixed number of coupon tests as forty).

Effect of number of coupon tests alone (for a fixed number of element tests, n_e=3)

The effect of number of coupon tests, n_c, on error in failure prediction at the coupon level, e_{fc}, and total error in failure prediction, e_{fT}, is depicted in Fig. 7-11(a) and 7-11(b), respectively. Here we consider increasing n_c from 10 to 40 and from 40 to 100. Note that n_c=10 is not realistic, but included here for the sake of illustration. We see in Fig. 7-11(a) that as n_c is increased from 10 to 40, and then from 40 to 100, standard deviation of e_{fc} is reduced significantly. The effect of n_c on e_{fT}, on the other hand, shows a different trend (Fig. 7-11(b)). Even though we see a significant reduction of standard deviation of e_{fT} when n_c is increased from 10 to 40, the change of standard deviation of e_{fT} is barely noticeable when n_c is further increased to 100.

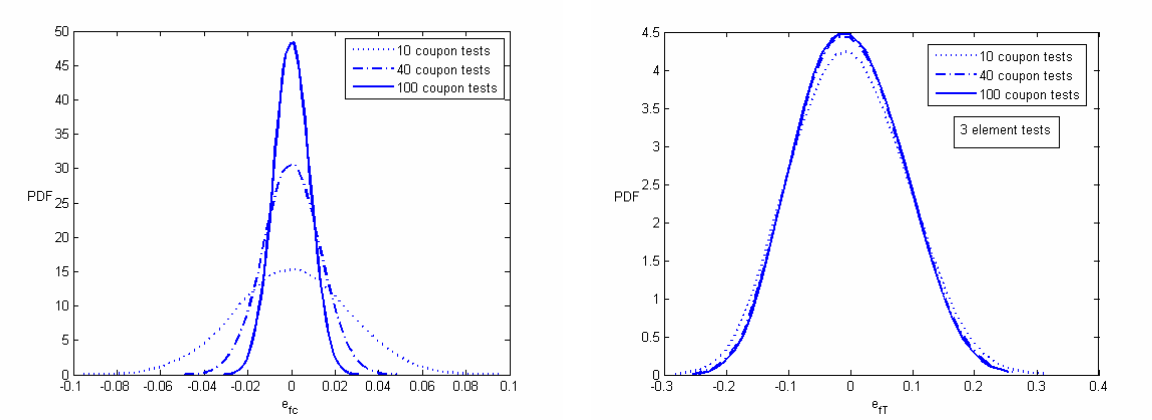

(a) error in failure prediction at the coupon level, e_{fc}

(b) total error in failure prediction, e_{fT}

Figure 7-11. Effect of number of coupon tests on the error in failure prediction for a fixed number of element tests (3 element tests). The probability densities are obtained through MCS of 10,000 sample size.

Effect of number of element tests alone (for a fixed number of coupon tests, n_c=40)

The effect of number of element tests, n_e, on error in failure prediction at the element level, e_{fe}, and total error in failure prediction, e_{fT}, is depicted in Fig. 7-12(a) and 7-12(b), respectively. Here we consider no element tests, a single element test, three element tests and five element tests. Note that the scatter in error e_{fe} is smaller when no element test is performed compared to performing a single element tests. That is, performing only a single element test is not effective due to variability in the failure stress. We see that as n_e is increased from 1 to 3, and then from 3 to 5, standard deviation of e_{fe} is reduced significantly (Fig. 7-12(a)) and the mean error is increased. The increase of the mean error makes sense since it indicates the tendency towards conservative error. The effect of n_c on e_{fT}, on the other hand, shows a different trend (Fig. 7-12(b)) in view of standard deviation. Even though we see a significant reduction of standard deviation of e_{fT} when n_e is increased from one to three, the reduction of standard deviation of e_{fT} diminishes when n_e is further increased from three to five.

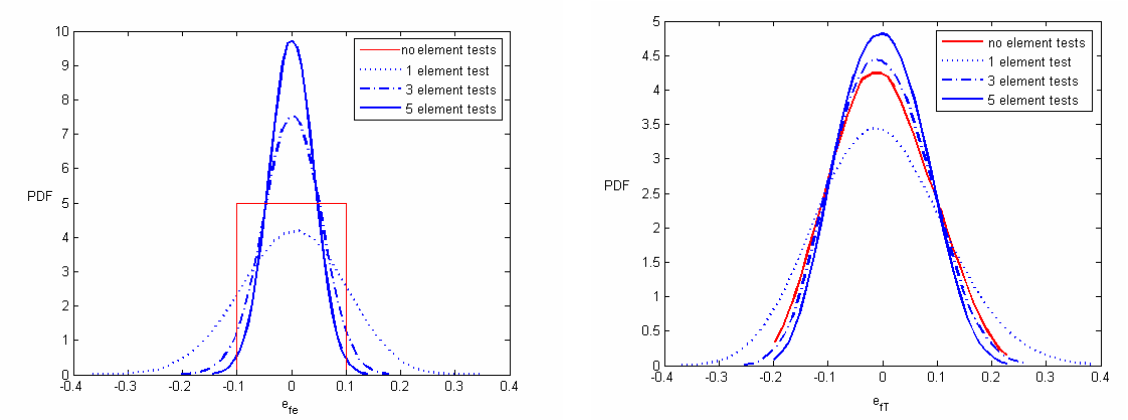

(a) error in failure prediction at the element level, e_{fe}

(b) total error in failure prediction, e_{fT}

Figure 7-12. Effect of number of element tests on the error in failure prediction for a fixed number of coupon tests (40 coupon tests). The probability densities are obtained through MCS of 10,000 sample size.

Figure 7-12 showed us that performing a single structural element test is not enough to reduce the error in failure prediction due to variability in failure stress. One way to solve this deficiency is to use Bayesian updating that can be successfully used to update the error distribution. Figure 7-13(a) shows the evolution of mean failure stress using the test results. Initial mean stress distribution is taken uniform with ±10% bounds around mean value, which is 150. When a single test is performed, due to the variability in failure stress, the updated distribution has a wider range compared to the initial one. The evolution of the mean stress requires more element tests to be performed as seen in Fig. 7-13(a). On the other hand, Bayesian updating allows a more effective updating process. We see in Fig. 7-13(b) that even a single test is effective now. Discussion of Bayesian updating is not analyzed in this chapter, but more information on error updating using Bayesian updating can be found in Chapter 3.

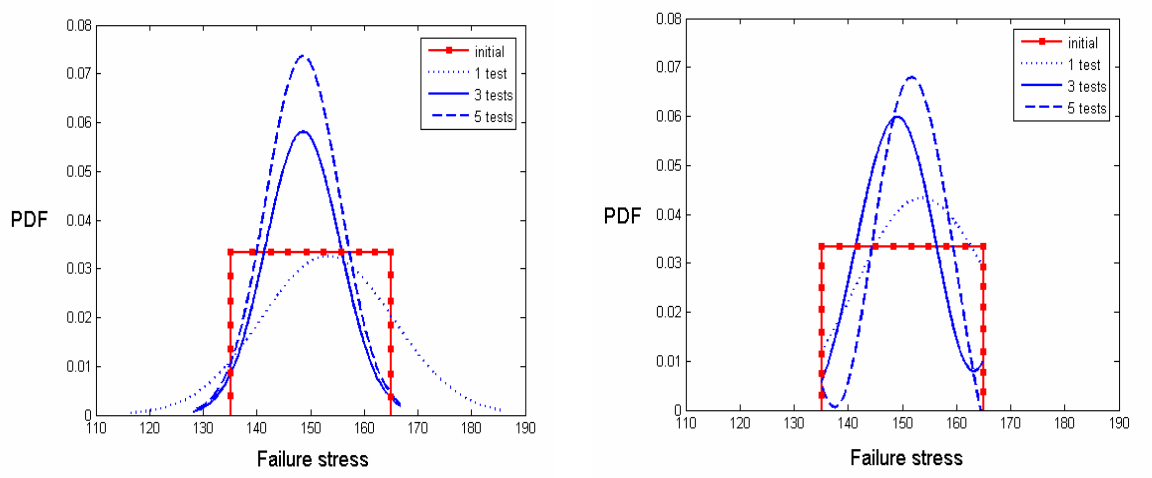

(a) without Bayesian updating (b) with Bayesian updating

Figure 7-13. Evolution of the mean failure stress distribution with and without Bayesian updating

Advantage of Variable Explicit Knockdown Factors

To see the advantage of using a variable explicit knockdown factor that depends on the test results, we compare its Pareto front with that of a constant explicit knockdown factor. Figure 7-14 shows comparison of Pareto fronts for certification failure rate and normalized area (Fig. 7-14(a)) and Pareto fronts for probability of failure (Fig. 7-14(b)). Table 7-6 presents the knockdown factors and the normalized areas. We see that for a specified *CFR* or P_F, lower weight (area) is required if a variable explicit knockdown factor is used. For instance, for *CFR* of 10^{-3}, using variable explicit knockdown factor leads to 0.77% lighter structure, which corresponds to about $520,000 life-time cost saving for a typical large transport aircraft such as Boeing 777 (see Appendix L for the cost model used).

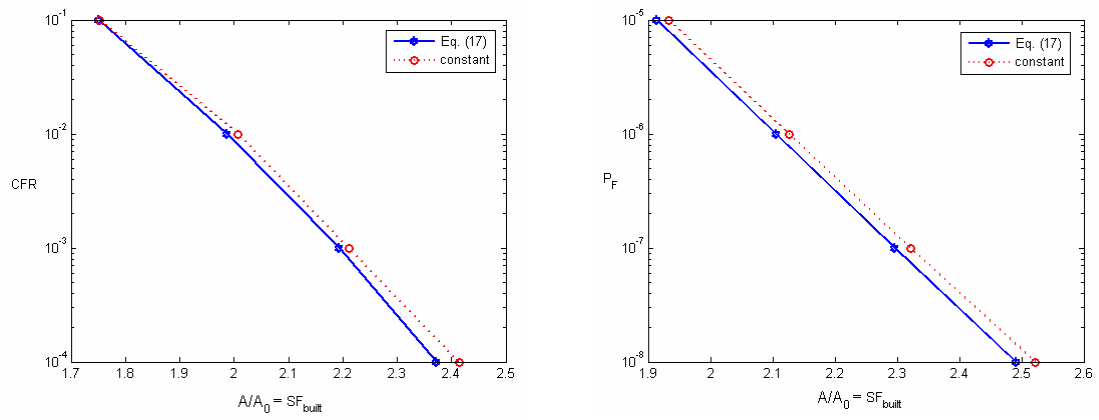

(a) *CFR* comparison (b) P_F comparison

Figure 7-14. Comparison of variable and constant explicit knockdown factor

Table 7-6. Comparison of constant and variable explicit knockdown factors case and corresponding area ratios, A/A_0.

	Constant—average		Variable (Eq. (7.17))		
CFR	A/A_0*	$k_{cl}=k_{ch}$	A/A_0*	k_{cl}	k_{ch}
10^{-1}	1.752	0.988	1.750	1.000	0.963
10^{-2}	2.008	0.862	1.987	0.892	0.820
10^{-3}	2.211	0.783	2.193	0.809	0.742
10^{-4}	2.413	0.717	2.372	0.747	0.687

* A/A_0 is the ratio of the built cross sectional area, A, and the area without safety measures, A_0. Note that the area ratio is equal to the total safety factor $(S_F)_{built}$

We next examine the effect of using the implicit knockdown factor associated with worst (i.e., smallest) failure stress measured in structural element tests instead of using the average. The comparison of Pareto fronts of certification failure rate and total safety factor is shown in Fig. 7-15. The knockdown factors and total failure stress corresponding to these two approaches are shown in Table 7-7. We find that the use of the implicit safety factor carries a weight penalty. For example, for a certification failure rate of one in a thousand, the use of the smallest of the failure stress measured in element tests leads to 0.95% heavier structure compared to the use of the average failure stress measured in element test. The cost function in Appendix L indicates that the cost of structure is increased by about $640,000. The ratio of the knockdown factors

corresponding to use of average and worst case failure stress results are also listed in Table 7-7 (the last column). We see that instead of using a worst-case failure stresses, a company might use average failure stresses measured in element tests and by adding a knockdown factor on top of it more efficient design decisions can be made.

The combined effect of using a variable explicit knockdown factor, Eq. (7.17), along is seen by comparing results given in Tables 7-6 and 7-7. For $CFR=10^{-3}$ for instance, we see that 1.75% of structural weight can be corresponding to lifetime cost reduction of about $ 1.2 million.

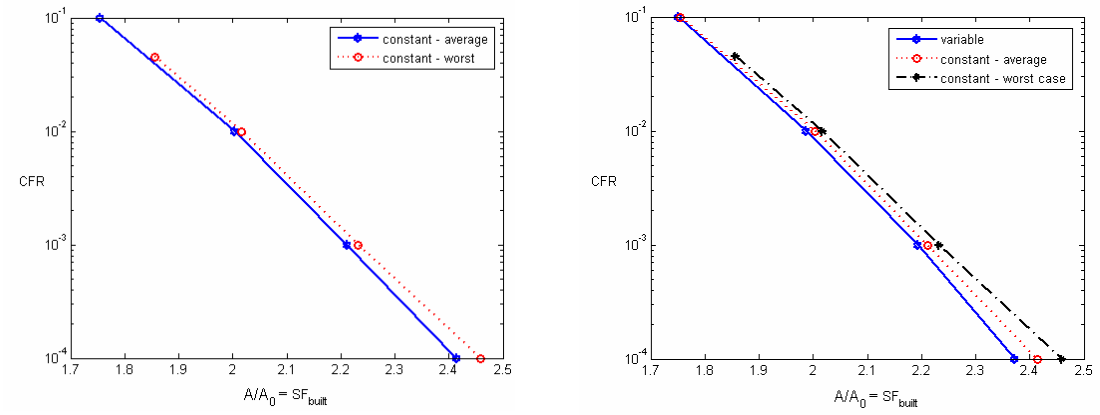

(a) comparing constant explicit and constant implicit knockdown factors

(b) comparing variable explicit, constant explicit and constant implicit knockdown factors

Figure 7-15. Comparison of Pareto fronts of certification failure rate and built safety factor for two different approaches while updating the allowable stress based on failure stresses measured in element tests. One approach uses the smallest of the failure stresses measured in tests while the other used the average failure stress while updating the allowable stresses.

Table 7-7. Comparison of constant (i.e., test independent) implicit and explicit knockdown factors and corresponding area ratios A/A_0. One approach uses the smallest of the failure stresses measured in the tests while the other used the average failure stress while updating the allowable stresses.

	Constant explicit knockdown factor		Constant implicit knockdown factor		Ratio of knockdown factors
CFR	A/A_0*	$k_c=k_{cl}=k_{ch}$	A/A_0*	$k_c=k_{cl}=k_{ch}$	$(k_c)_{exp}/(k_c)_{imp}$
10^{-1}	1.752	0.988	1.856	1.000**	0.989**
10^{-2}	2.008	0.862	2.017	0.921	0.939
10^{-3}	2.211	0.783	2.232	0.832	0.942
10^{-4}	2.413	0.717	2.460	0.755	0.951

* A/A_0 is the ratio of the built cross sectional area, A, and the area without safety measures, A_0. Note that the area ratio is equal to the total safety factor $(S_F)_{built}$

** Note that using k_c=1.0 leads to CFR=0.049 so the ratio is different compared to other CFR.

The main reason that the variable explicit safety factor is more efficient is that it reduces the element of chance introduced by material variability on the total knockdown factor. For lognormal failure stress with 8% coefficient of variation used here, the average implicit knockdown factor has a mean value of 0.932, and a coefficient of variation of 0.0642. The average failure stress, on the other hand, is 1.0 (as expected) and its coefficient of variation is 0.0467. That is, the average is 27% less variable than the worst value. In addition, the variable knockdown factor reduces the scatter further since it is higher for high test results than for low test results. This is demonstrated by calculating the mean and coefficient of variation of the actual knockdown factor obtained from a Monte Carlo simulation of one million companies. Table 7-8 shows that using test dependent (i.e., variable, Eq. (7.17)) knockdown factor further indeed reduces the coefficient of variation of the knockdown factor. For *CFR*=10-3, for instance, the total reduction in the coefficient variation is 36%.

Table 7-8. Comparison of mean and coefficient of variation of total knockdown reduction at the element test level for the cases of implicit constant knockdown factor and explicit variable knockdown factors

	A) Total knockdown factor for use of worst failure stress and constant additional knockdown		B) Total knockdown factor for use of average failure stress and variable (i.e., test dependent, Eq. (7.17)) additional knockdown		Ratios (A / B)	Ratios (A / B)
CFR	mean	c.o.v.	mean	c.o.v.	mean	c.o.v.
10^{-2}	0.859	0.0639	0.871	0.0409	1.02	0.64
10^{-3}	0.776	0.0642	0.790	0.0409	1.02	0.64
10^{-4}	0.704	0.0642	0.730	0.0394	1.04	0.61

Effect of Other Uncertainty Reduction Mechanisms

This section provides the effects of other uncertainty reduction mechanisms on and the optimum values of the explicit knockdown factors k_{cl} and k_{ch}, the probabilities of failure and the certification failure rates.

Effect of variability reduction

Recall in Chapter 4, we found that the reduction variability in the failure stresses is a very efficient way of reducing probability of failure, but it leads to increased certification failure rates. In that chapter, we argued that when companies reduce the variability in failure stresses, they also must employ additional knockdown factors to reduce the increased certification failure rates. In a view to analyze that argument, we explore the effect of reduced variability on the optimal choice of k_{cl} and k_{ch}. We reduce the coefficient of variation of the failure stress by half of its nominal value, that is, we reduce it from 8% to 4%. We kept the number coupon tests and the number of structural element tests at their nominal values 40 and 3, respectively.

Figure 7-14 shows that as the coefficient of variation is reduced to 4%, the Pareto fronts move to the left, allowing the use of smaller built safety factor for specified *CFR*

and P_F, or alternatively allowing smaller *CFR* and P_F for a given built safety factor. We see that the variability reduction is most effective at low probability of failure (and certification failure rate). Figure 7-16 also shows that *CFR* is more sensitive to variability reduction than P_F. The optimal values of the explicit knockdown factors for minimum *CFR* are given in Table 7-9. We see that the reduced variability allows using larger (i.e., less conservative) knockdown factors k_{cl} and k_{ch} for the same *CFR*. In Chapter 4, we found the opposite trend when element tests were not performed. That is, without the element tests variability reduction needed to be accompanied by using more conservative knockdown factors for acceptable certification failure rates. Thus the reduced uncertainty due to structural element tests allows us to take fuller advantage of variability reduction.

Table 7-9 shows that, for a certification failure rate of one in a thousand, the variability reduction allows 11.9% lower total built safety factor. That is, the same certification failure rate can be attained with 11.9% lighter structure if the variability in failure stress can be reduced by half. The cost model in Appendix L indicates us that variability reduction leads to saving about 8 million dollars. Hence, the company might compare the cost of variability reduction (reducing the coefficient of variation of the failure stress by half) with the cost saving due to reduced structural weight and decide whether paying more for more uniform material is worth it.

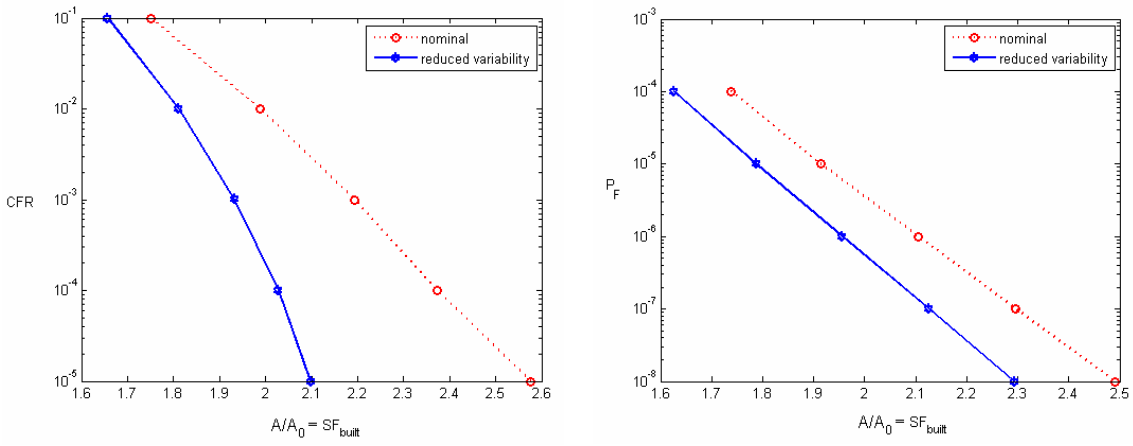

(a) minimum *CFR* (b) minimum P_F

Figure 7-16. Reducing (a) certification failure rate and (b) probability of failure using variability reduction. The number of coupons tests is 40, and the number of structural element tests is 3.

Table 7-9. Optimal explicit knockdown factors for minimum *CFR* when variability in failure stress is reduced by half

	c.o.v.=8%*			c.o.v.=4%		
CFR	A/A_0**	k_{cl}	k_{ch}	A/A_0**	k_{cl}	k_{ch}
10^{-1}	1.750	1.000	0.963	1.657	0.964	1.000
10^{-2}	1.987	0.892	0.820	1.811	0.905	0.850
10^{-3}	2.193	0.809	0.742	1.932	0.845	0.805
10^{-4}	2.372	0.747	0.687	2.028	0.809	0.757

* From Table 7-4

** A/A_0 is the ratio of the built cross sectional area, A, and the area without safety measures, A_0. Note that the area ratio is equal to the total safety factor $(S_F)_{built}$

Effect of error reduction

Similar to variability reduction, error reduction is another powerful way of reducing certification failure rate and probability of failure. We consider a hypothetical error control mechanism that would reduce all the errors by half. So we scale all error components with a single multiplier, *k*, replacing Eq. (7.35) by

$$e_{total} = \frac{(1+k\,e_\sigma)(1+k\,e_P)(1+k\,e_t)(1+k\,e_w)}{(1-k\,e_{fc})(1-k\,e_{fe})(1-k\,e_{fs})} - 1 \tag{7.48}$$

and explore the effect of reducing it from its nominal value 1.0 to 0.5. Figure 7-17 shows that indeed error reduction is also effective in reducing *CFR* and P_F. We also see that variability reduction is more effective than error reduction, especially when *CFR* (and P_F) are low. Note also that *CFR* is more sensitive to error reduction than P_F. The company safety factors for error reduction are listed in Table 7-10, which shows that as error is reduced a specified certification failure rate can be attained by using lower built safety factors. For instance, for certification failure rate of one in a thousand, we see that the error reduction leads to 4.9% lower total safety factor. That is, the same certification failure rate can be attained with 4.9% lighter weight if the errors are reduced by half. The cost model in Appendix L indicates us that error reduction leads to about 3.3 million dollars cost saving. Hence, the company might compare the cost of error reduction with the cost saving due to reduced structural weight and decide whether investing resources on error reduction mechanisms is profitable. The superior effect of variability reduction over error reduction is all the more remarkable, since only one component of the variqabilities was reduced, compared to all errors.

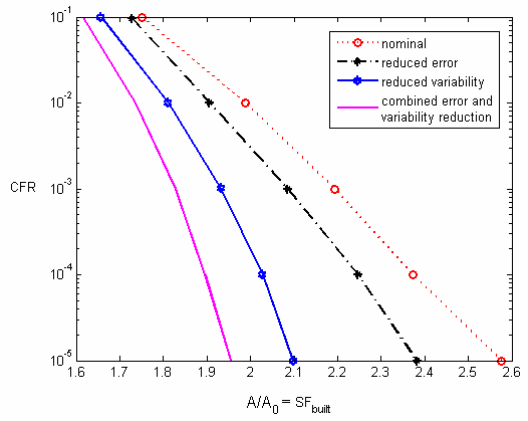

Figure 7-17. Reducing certification failure rate using error reduction, variability reduction and combination of error and variability reduction. The number of coupons tests is 40, and the number of structural element tests is 3.

Table 7-10. Optimal explicit knockdown factors for minimum *CFR* when all errors reduced by half.

	k=1.0			*k=0.5*		
CFR	A/A_0^*	k_{cl}	k_{ch}	A/A_0^*	k_{cl}	k_{ch}
10^{-1}	1.750	1.000	0.963	1.728	1.000	1.000
10^{-2}	1.987	0.892	0.820	1.906	0.923	0.846
10^{-3}	2.193	0.809	0.742	2.084	0.844	0.774
10^{-4}	2.372	0.747	0.687	2.241	0.785	0.720

* A/A_0 is the ratio of the built cross sectional area, A, and the area without safety measures, A_0. Note that the area ratio is equal to the total safety factor $(S_F)_{built}$

Effect of Number of Coupon Tests

Next, we analyze the effect of number of coupon tests on the optimal choice of knockdown factors. Figure 7-18 shows the Pareto fronts corresponds to three different numbers of coupon tests: 10 tests, 40 tests and 100 tests. Note here that performing only 10 coupon tests is not realistic, but it is included here for illustrative purposes. We see that increasing number of tests from 10 to 40 leads Pareto front to shift to left substantially, whereas the Pareto fronts for 40 coupon tests and 100 coupon tests are quite close. Table 7-11 shows that the company safety factors (and hence the total safety factor) corresponding to 40 coupon tests and 100 coupon tests are very close. The optimal k_{cl} and k_h values are more conservative (that is, smaller) when 100 coupon tests are used for small *CFR*s. This is because as the number of coupon tests increases the B-basis value grows, so the total safety factor reduces. Then the company needs to compensate for that by introducing explicit knockdown factors to reach a desired level of certification failure rate. When *CFR* is large (e.g., *CFR*=0.1), on the other hand, the error reduction due to large number of coupon tests overcomes the change in B-basis.

Table 7-11 shows that, for certification failure rate of 10^{-3}, the total built safety factor can be reduced by 1.3% if 100 coupon tests are performed rather than 40. The cost model given in Appendix L indicates that these additional coupon tests leads to about

$890,000 cost saving. Hence, the company might compare the cost of extra coupon tests with the cost saving due to reduced structural weight and decide whether performing these additional coupon tests is profitable.

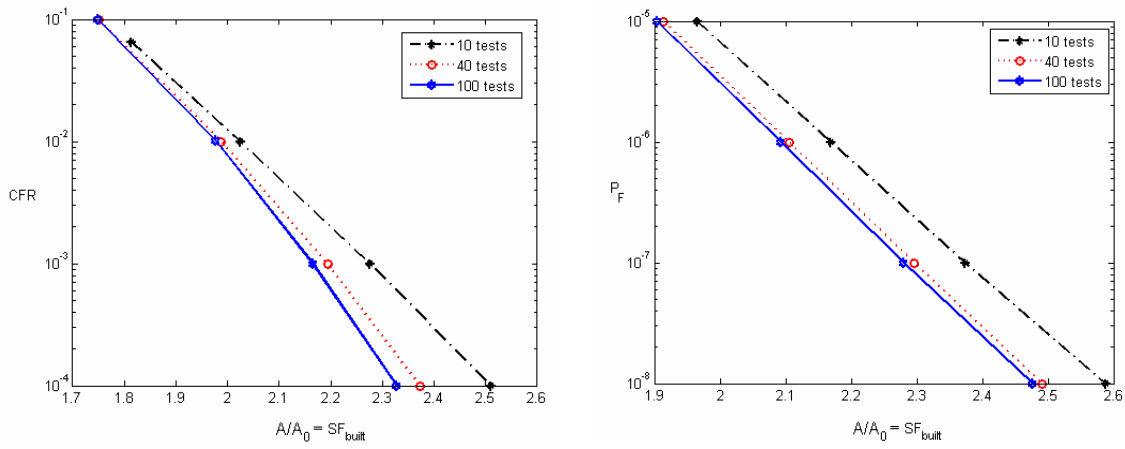

(a) minimum *CFR* (b) minimum P_F

Figure 7-18. Optimal explicit knockdown factors for different number of coupon tests for minimum *CFR* and P_F. The number of structural element tests is 3. Number of coupon tests is indicated as 'n_c' in the figure.

Table 7-11. Optimal explicit knockdown factors for minimum *CFR* different number of coupon tests, n_c.

	n_c=40			n_c=100		
CFR	A/A_0*	k_{cl}	k_{ch}	A/A_0*	k_{cl}	k_{ch}
10^{-1}	1.750	1.000	0.963	1.748	0.996	0.934
10^{-2}	1.987	0.892	0.820	1.978	0.885	0.814
10^{-3}	2.193	0.809	0.742	2.165	0.809	0.742
10^{-4}	2.372	0.747	0.687	2.328	0.752	0.691

* A/A_0 is the ratio of the built cross sectional area, A, and the area without safety measures, A_0. Note that the area ratio is equal to the total safety factor $(S_F)_{built}$

Effect of Number of Structural Element Tests

Finally, we explore the effect of structural element tests. Figure 7-19 shows that as the number of tests increases from one to three, the probability of failure and certification failure rates are reduced by about one order of magnitude. However, as the number of tests further increased to five, for instance, the effectiveness of tests reduces. Table 7-12 shows that as the number of element tests increases, the knockdown factors k_{cl} and k_{ch}

increase and hence the total safety factor reduce. That is, the additional element tests possess a hidden safety factor by reducing the error in failure prediction. For example, for certification failure rate of 10^{-3}, the total built safety factor must be increased by 3.0% if only one structural element test is performed rather than three structural element tests. According to the cost model given in Appendix L, performing three structural tests leads to about 2 million dollars cost saving. Hence, the company might compare the cost of two extra structural elements with the cost saving due to reduced structural weight and decide whether these additional element tests are preferable.

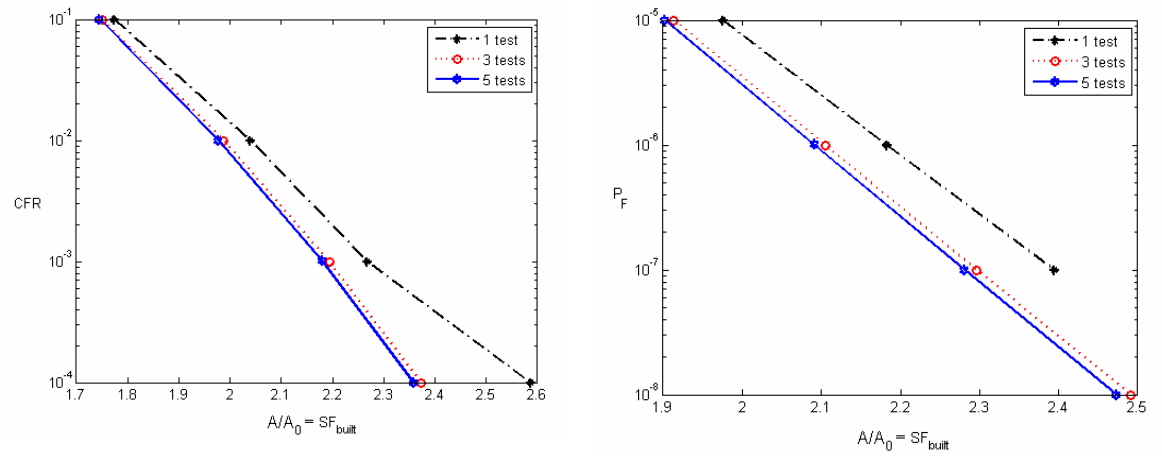

(a) minimum *CFR* (b) minimum P_F

Figure 7-19. Effect of number of structural element tests, n_e

Table 7-12. Optimal explicit knockdown factors for different number of structural element tests, n_e.

	$n_e = 1$			$n_b = 3$		
CFR	A/A_0*	k_{cl}	k_{ch}	A/A_0*	k_{cl}	k_{ch}
10^{-1}	1.774	1.000	0.936	1.750	1.000	0.963
10^{-2}	2.038	0.876	0.803	1.987	0.892	0.820
10^{-3}	2.259	0.790	0.724	2.193	0.809	0.742
10^{-4}	2.586	0.675	0.667	2.372	0.747	0.687

* A/A_0 is the ratio of the built cross sectional area, A, and the area without safety measures, A_0. Note that the area ratio is equal to the total safety factor $(S_F)_{built}$

Summary

The effects of optimal choice of explicit knockdown factors, structural tests, and uncertainty reduction mechanisms were analyzed. From the results obtained in this study, we drew the following conclusions

- Companies can minimize the probabilities of the failure of the aircraft structures by rationally choosing explicit knockdown factors that are based on test results. Currently these knockdown factors are implicit and based on worst-case scenarios (e.g., testing the structural elements at worst-case operational conditions, using the smallest measured failure stress in design). We found that optimally chosen explicit knockdown factors may lead to 1 or 2% weight savings, which can be translated into cost savings in the order of a million dollars over the lifetime of a typical airliner.

- Surprisingly, we found that a lower (i.e., more conservative) knockdown factor should be used if the failure stresses measured in tests exceeds predicted failure stresses, because good test results can simply be due to luck. The use of variable explicit safety factor based on average test results was found to reduce the variability in knockdown factor generated by variability in material properties by about 36%. It is this reduction in variability that is responsible for the weight savings.

- Selecting explicit knockdown factor to minimize certification failure rate, *CFR*, leads to designs very near to probabilistic optimum (minimum probability of failure, P_F).

- Uncertainty reduction mechanisms are powerful ways of increasing aircraft structural safety. They reduce *CFR* and P_F by one or more orders of magnitudes for a given safety factor. When the effectiveness of error reduction and variability reduction is compared, we found that reducing variability in failure stress to half of its nominal value is more effective than reducing all errors by half.

- We found that the efficiency of tests depends on the number of tests conducted. As the number of tests increases, the cost effectiveness of tests diminishes.

- Given a cost function for coupon tests, structural element tests, error and variability reduction mechanisms, the optimum choice of explicit knockdown factors can be carried out in a rational way to minimize the lifetime cost of aircraft without changing the aircraft structure's probability of failure in the certification tests and under the actual flight loads.

CHAPTER 8
RELIABILITY BASED AIRCRAFT STRUCTURAL DESIGN PAYS EVEN WITH LIMITED STATISTICAL DATA

Probabilistic structural design tends to apply higher safety factors to inexpensive or light-weight components, because it is a more efficient way to achieve a desired level of safety. In this chapter we show that even with limited knowledge about stress probability distributions we can increase the safety of an airplane by following this paradigm. The structural optimization for safety of a representative system composed of a wing, a horizontal tail and a vertical tail is used to demonstrate the paradigm. In addition, to alleviate the problem of computational expense we propose an approximate probabilistic design optimization method, where the probability of failure calculation was confined only to failure stresses to dispense with most of the expensive structural response calculations (typically done via finite element analysis). The proposed optimization methodology is illustrated with the design of the wing and tail system.

The work presented in this chapter is also submitted for publication (Acar et *al*. 2006e). Prof. Efstratios Nikolaidis is acknowledged for his valuable suggestions for this work.

Introduction

The FAA design code is based on uniform safety factors (that is, the same safety factor is used for all components). Probabilistic design derives an important part of its advantage over deterministic design by allowing the use of substantially non-uniform safety factors and hence there is growing interest in replacing safety factors by

probabilistic design (e.g., Lincoln 1980, Wirsching 1992, Aerospace Information Report of SAE 1997, Long and Narciso 1999). However, with only partial information on statistical distributions of variabilities, and guesswork on reasonable distributions for errors, engineers are reluctant to pursue probabilistic design. Also, it has been shown that insufficient information may lead to large errors in probability calculations (e.g., Ben-Haim and Elishakoff 1990, Neal, et al. 1992). The main objective of this chapter is to show that we can increase the safety of an airplane without increasing its weight even with the limited data available today following the design paradigm mentioned (higher safety factors for light-weight components). Our approach utilizes two statistical data that are well understood. The first is the statistical distribution of failure stress, which is required by the FAA for choosing A-basis or B-basis allowables. The second is a special property of the normal distribution: when large number of uncertainties contributes to a distribution, it tends to become similar to a normal distribution. This applies to the stress estimation because it is influenced by large number of error and variability sources. Finally, we show that even though the limited statistical data may substantially affect the probabilities of failure of both the probabilistic design and the code-based deterministic design, the ratio of probabilities of failure of the probabilistic design and the deterministic design is insensitive to even large errors due to limited data.

The chapter is structured as follows. First, reliability-based design optimization of a representative wing and tail system with perfect and limited statistical data is given. Next, we discuss the effects of errors in statistical information for the deterministic design. Then, we propose an approximate method that allows probabilistic design based only on

probability distribution of failure stresses, followed by the application of the method to the wing and tail system. Finally, the concluding remarks are listed in Summary section.

Demonstration of Gains from Reliability-Based Structural Design Optimization of a Representative Wing and Tail System

Problem Formulation and Simplifying Assumptions

Calculating the probability of stress failure in a structure can be done by generating the probability distribution functions (PDF) $s(\sigma)$ of the stress σ, and the PDF $f(\sigma_f)$ of the failure stress σ_f (see solid lines in Fig. 8-1). Once these distributions are available, calculating the probability of failure can be accomplished by simple integration, as discussed later. The distribution of failure stress is typically available from experiments, and so it does not require much computation. For materials used in aircraft design, the FAA regulations mean that statistical information on failure stresses is often available quite accurately. On the other hand, the PDF for the stress requires data such as analysis error distributions that are difficult to estimate, and it also requires expensive finite element computations. Fortunately, though, the PDF of the stress contains contributions from large number of parameters such as variabilities and errors in material properties, geometry and loading, and so it is likely to be well represented by a normal distribution. However, estimating well the mean and standard deviation of that normal distribution is difficult due to limited data. First, we momentarily disregard this difficulty in order to demonstrate the advantage of probabilistic design deriving from the use of higher safety factors for lighter structural components. Then, the effects of limited statistical data will be addressed.

We consider a representative wing and tail system. In general, in order to perform reliability-based design, we need to re-calculate the stress PDF as we change the design.

For the sake of simplicity, we assume that structural redesign changes the entire stress distribution as shown in Fig. 8-1 by a simple scaling of σ to $\sigma(1+\Delta)$. This assumption will be accurate when the uncertainties are in the loading, and the relative errors in stress calculation are not sensitive to the redesign.

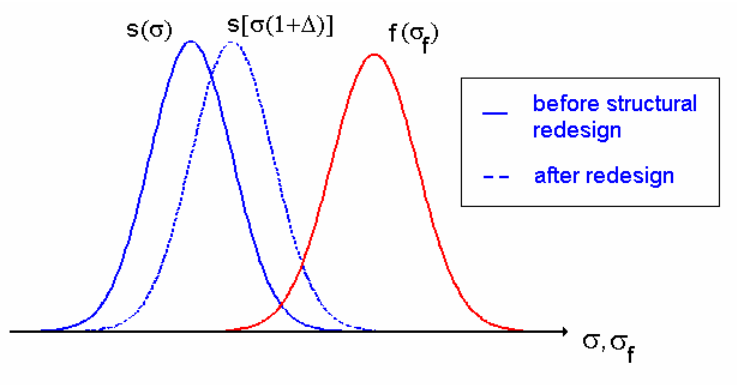

Figure 8-1. Stress distribution $s(\sigma)$ before and after redesign in relation to failure-stress distribution $f(\sigma_f)$. We assume that re-designs scales the entire stress distribution.

We denote the failure probabilities of wing and tail obtained from deterministic design by $(P_{fW})_d$ and $(P_{fT})_d$, respectively. If failure of the two components is uncorrelated, the probability that at least one of them will fail is

$$P_{f0} = 1-[1-(P_{fW})_d][1-(P_{fT})_d] \tag{8.1}$$

If the two failure probabilities are correlated, the calculation is still simple for a given correlation coefficient. For the purpose of demonstration, we make simplifying assumptions that the structure is approximately fully stressed, and that the stresses are inversely proportional to weight. This allows us to treat the wing and the tail as a system with a single stress level and perform the demonstration without resorting to finite element modeling and analysis of these two components. That is, denoting the stresses in the wing and the tail by σ_W and σ_T, respectively, we use

$$\sigma_W = \frac{W_{dW}}{W_W}\sigma_{dW}, \quad \sigma_T = \frac{W_{dT}}{W_T}\sigma_{dT} \tag{8.2}$$

where W_W and W_T are the wing and the tail structural weights, respectively, and the subscript '*d*' denotes the values of stresses and structural weights for the deterministic design. Using Eq. (8.2) we can now formulate the following probabilistic design problem to minimize the probability of failure for constant weight

$$\begin{aligned} &\min_{W_W, W_T} \quad P_f\left(W_W, W_T\right) = 1 - \left[1 - P_{fW}\left(W_W\right)\right]\left[1 - P_{fT}\left(W_T\right)\right] \\ &\text{such that} \quad W_W + W_T = W_{dW} + W_{dT} \end{aligned} \tag{8.3}$$

In the following subsection, we first perform probabilistic optimization for safety of the wing and tail system. Next, the effect of adding a vertical tail to the wing and horizontal tail system on the overall safety enhancement will be explored.

Probabilistic Optimization with Correct Statistical Data

For a typical transport aircraft, the structural weight of the horizontal tail is about 20% of that of the wing. So the weights of the wing and the tail before probabilistic optimization are taken as 100 and 20 units, respectively. We assume that wing and the tail are built from the same material and the failure stress of the material follows lognormal distribution with a mean value , μ_f, of 100 and coefficient of variation (c.o.v), c_f, of 10%. The c.o.v. of the stresses in the wing and the tail, c_σ, is assumed to be 20%. This may appear large in that stress calculation is quite accurate. However, there is substantial uncertainty in loading and geometry changes due to damage. For illustrative purpose, we assume that the historical record showed that the wing had lifetime probability of failure of 1×10^{-7}. Since the deterministic design uses uniform safety factors (that is, the same safety factor is used for all components), and we assume that the wing

and tail are made from the same material and have the same failure mode (point stress failure here), it is reasonable to assume that the probability of failure for the deterministic design of the tail is also 1×10^{-7}. As indicated earlier, we assume that the stresses follow normal distribution, which is characterized by only two parameters, mean and standard deviation. Therefore, given full information on the failure-stress distribution (lognormal with μ_f =100 and c_f =10%), the probability of failure (P_f=10^{-7}) and the c.o.v. of the stress (c_σ =20%), the mean stresses in the wing and the tail are calculated as 39.77. The reader is referred to Appendix N for details of calculation of the unknown mean stresses in the wing and the tail for given probability of failure and c.o.v. of the stresses.

With the simple relation of stress to weight, Eq. (8.2), and the assumptions on the distributions of stresses and failure stresses, the probability of failure can be easily calculated by a variety of methods. One of these methods will be discussed later. Then the probabilistic design optimization is solved assuming a zero correlation coefficient between the probabilities of failure of wing and tail. We see from Table 8-1 that the probabilistic design and deterministic design are very close in that probabilistic design is achieved by a small perturbation of deterministic design (moving 0.75% of wing weight to tail, see columns 2 and 3). Table 8-1 shows that by moving 0.75% of the wing material to the tail, the probability of failure of the wing is increased by 31% of its original value. On the other hand, the weight of the tail is increased by 3.77% and thereby its probability of failure is reduced by 74%. The overall probability of failure of the wing and tail system is reduced by 22%.

Table 8-1. Probabilistic structural design optimization for safety of a representative wing and tail system. In the optimization only the mean stresses are changed, the c.o.v. of the stresses are fixed at c.o.v.=0.20. Probability of failure of the wing and the tail for deterministic design are both 1×10^{-7}.

	W_0	W	P_f ratio [(a)]	Mean stress before optim.	Mean stress after optim.
Wing	100	99.25	1.309	39.77	40.07
Hor. Tail	20	20.75	0.257	39.77	38.32
System	120	120	0.783		

[(a)] P_f ratio is the ratio of the probabilities of failure of the probabilistic design and deterministic design

The mean stresses and the c.o.v. of the stresses in the wing and the tail before and after probabilistic optimization are also listed in Table 8-1. We note that the mean stress in the wing is increased (by 0.76%) while the mean stress in the tail is reduced (by 3.6%). That is, a higher safety factor is used for the tail than the wing, but the difference is not large. For example, if the safety factor for the both structures was 1.5 for the deterministic design, it would be 1.49 for the wing and 1.55 for the tail. *Since aircraft companies often use additional knockdown factors on top of those required by the FAA code, they can slightly increase the knockdown factor for the wing to achieve the probabilistic design that satisfies all the FAA requirements for a deterministic design!*

A striking result in Table 8-1 is that the ratio of probabilities of failure of the tail and the wing is about 1/5. Recall that the ratio of the tail weight and the wing weight is also 1/5. That is, at optimum the ratio of the probabilities of failure of the components is almost equal to the ratio of their weights. This optimum probability ratio depends on the following parameters: the target probability of failure, mean and c.o.v. of the stress and c.o.v. of the failure stress. We checked and found that the ratio of probabilities falls between 4.5 and 6.5 for a wide range of these parameters. Appendix O provides analytical proof that the ratios of the weights and probabilities are indeed approximately the same.

Recall that for deterministic design we assumed that the probabilities of failure of the wing and tail are the same because the components are designed with the same safety factor. So, it is worthwhile checking the historical record. Cowan *et al*. (2006) reports that according to the historical result, 18 out of 717 aircraft accidents between 1973 and 2003 were due to wing structural failure, while 9 of the accidents were due to tail structural failure (see also Appendix P). Even though wing and tail are designed with the same nominal safety factors, the large weight differential may lead to different actual safety factors. Designers may intuitively attempt to reduce the structural weight of the heavier wing by squeezing out the weight down to the limit, while they may be laxer with the tail. This, for example, may happen if more approximate methods, with higher safety margins of safety are used for the tail. The probabilistic design supports this incentive and indicates that the design paradigm of using higher safety factors for inexpensive components can further be exploited to increase the structural safety of aircraft.

Adding a Vertical Tail to the System

Next, we added a vertical tail to the wing and horizontal tail system. For a typical transport aircraft, the structural weight of the vertical tail is about 10% of that of wing. The weights of the wing, the horizontal tail and the vertical tail of our representative system before probabilistic optimization are taken as 100, 20 and 10 units, respectively. The probability of failure of the deterministic designs of the wing, and the tails are taken 1×10^{-7} each. The results of structural optimization for safety are listed in Table 8-2. By moving material from the wing to the tails the probability of failure of the wing is increased by 53%, but the probabilities of failure of the horizontal tail and the vertical tail are reduced by 70% and 85%, respectively. Table 8-2 demonstrates that by including the

vertical tail in the system, the system probability of failure is reduced by 34% compared to 22% with two-component (Table 8-1). An increase in number of components may thus increase the safety improvement of the system.

Table 8-2 shows a similar finding of Table 8-1, in that at optimum the ratio of the probabilities of failure of the components are nearly 10:2:1, which is the same ratio of the weights of the components. This optimum probability ratio is obtained by using different safety factors for the different components. The mean stresses and the c.o.v. of the stresses in the wing, the horizontal tail and the vertical tail before and after probabilistic optimization are also listed in Table 8-2. The mean stress in the wing is increased by 1.2%, while the mean stress in the horizontal tail and the mean stress in the vertical tail are reduced by 3.2% and 5.0%, respectively. Again, the substantial reduction in probability of failure is accomplished with a small perturbation of the safety factor. So a company that employs an additional knockdown factor of just a few percent would be able to reduce it for the wing, and fully comply with the FAA regulations while achieving superior safety.

Table 8-2. Probabilistic structural optimization of wing, horizontal tail and vertical tail system. In optimization only the mean stresses are changed, the c.o.v. of the stresses are fixed at c.o.v.=0.20. Probability of failure of the wing and the tails for deterministic design are all 1×10^{-7}.

	W_0	W	P_f Ratio [(a)]	Mean stress before optim.	Mean stress after optim.
Wing	100	98.80	1.531	39.77	40.25
Hor. Tail	20	20.67	0.300	39.77	38.48
Ver. Tail	10	10.53	0.149	39.77	37.78
System	130	130	0.660		

[(a)] P_f ratio is the ratio of the probabilities of failure of the probabilistic design and deterministic design

Effect of Errors in Information about Deterministic Design

The demonstration of the pay-off from probability-based design in the previous section was based on assumptions on the stress distribution and probability of failure. It is known that the calculation of probability of failure can be very sensitive to errors in distribution (Ben-Haim and Elishakoff 1990, Neal *et al*. 1992). So here we seek to demonstrate that because we merely seek to obtain a design with the same weight as the deterministic design, and because the probabilistic design is close to the deterministic design, the effect of errors on the ratio of the probabilities of failure of the probabilistic design and the deterministic design is minimal. In measuring the effects of error in the statistical data, we distinguish between loss of accuracy and loss of opportunity. That is, we report on the accuracy of our estimate of the improvement in the probability of failure compared to the deterministic design. We also report on the missed opportunity to make the design even safer if we had the correct statistical data.

Errors in Coefficient of Variation of Stresses

We first assume that we under-estimated the c.o.v. of stresses in the wing and the tail by 50% and performed the optimization using the wrong c.o.v. of stresses. That is, even though the true values of c.o.v. of stresses for the wing and the tail are both 40%, we performed the optimization based on 20% c.o.v. and obtained the design shown in Table 8-1. With the overall probability of failure of the deterministic design being fixed, an under-estimate of the c.o.v must go with an over-estimate of the mean. Following the procedure in Appendix N, we find that the mean is over estimated by about 45% (actual mean is 31% lower than value used in Table 8-1). Table 8-3 shows both the error in the estimation of the probability gain and the loss of opportunity to make the design safer. For the wing, we over-estimate the P_f ratio (ratio of P_{fW} of the probabilistic and the

deterministic designs) by 4.2% and under-estimate the P_f ratio for the tail by 19%. However, that the system probability of failure is under-estimated by only -0.5%, because the two errors canceled each other out (see Fig. 8-2). We also see from the table that the probability of failure of the true optimum is very close to our estimate of the probability of failure for the optimum obtained based on the erroneous data. This is a well known result for the effect of a parameter on the optimum of an unconstrained problem (e.g., Haftka and Gürdal 1992, Section 5.4). *That is the loss of accuracy is approximately equal to the opportunity loss for small changes in the design.*

Table 8-3. Errors in the ratios of failure probabilities of the wing and tail system when the c.o.v. of the stresses under-estimated by 50%. The estimated values of c.o.v. of stresses for wing and tail are both 20%, while their actual values are both 40%. Note that the under-estimate of the c.o.v corresponds to an overestimate of the mean stress, so that its actual value is 31% percent lower than the value given in Table 8-1.

	Optimization based on erroneous data						True optimum		
	Optimized weight [(a)]	Estimated [(a)] P_f ratio	Actual [(b)] P_f ratio	% Error in P_f estim.	Mean stress before optim.	Mean stress after optim. (assumed)	True optimal weight	True optimal P_f ratio	Mean stress after optim. (true)
Wing	99.25	1.309	1.256	4.2	27.42	27.62	99.11	1.309	27.66
H. Tail	20.75	0.257	0.317	-19.0	27.42	26.42	20.89	0.257	26.24
System	120	0.783	0.786	**-0.5**				0.783	

(a) From Table 8-1.

(b) Note that the P_f given here is the actual P_f of the assumed optimum (obtained via erroneous c.o.v. of the stress), which is different than the true optimum corresponding to the use of true c.o.v. of the stress

The variation of the component and system probability-of-failure ratios with the error in c.o.v. of stresses in the wing and the tail are shown in Fig. 8-2. We see that for negative errors (under-estimated c.o.v. of stress) the P_f ratio of the wing is over-estimated while the P_f ratio of the tail is under-estimated. The two errors mostly cancel each other out and error in the system P_f ratio (and hence the opportunity loss) is very small. Similarly, for positive errors (over-estimated c.o.v. of stress) even though the P_f ratio of

the wing is under-estimated and the P_f ratio of the tail is over-estimated, the estimate of system P_f ratio is quite accurate over a wide range of error magnitude. As important is that we lose very little in terms of the potential improvement in the probability of failure due to the error. The smallness of the opportunity loss is a manifestation of the fact that the optimum ratio of the probabilities of failure is insensitive to the coefficient of variation of the stress.

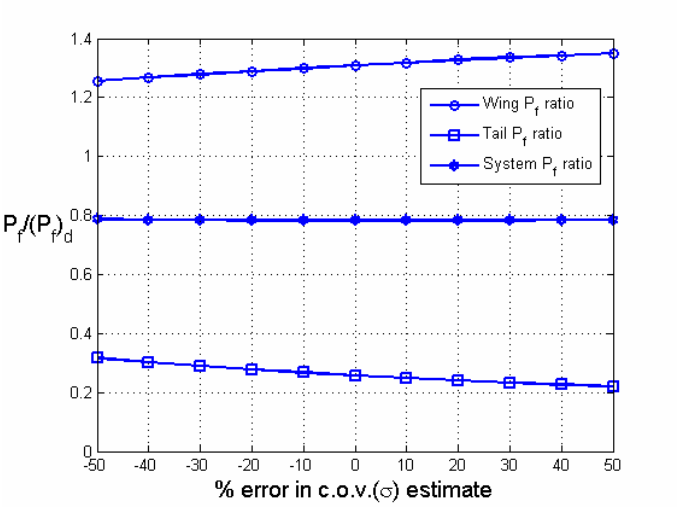

Figure 8-2. The change of the ratios of probabilities of failure of the probabilistic design of Table 8-1 versus the error in c.o.v.(σ). Negative errors indicate under-estimate, while positive errors indicate over-estimate.

We have this remarkable insensitivity of ratio of probabilities of failure to errors because the probabilistic design is close to the deterministic design. For a given probability of failure of the deterministic design, errors in the mean lead to compensating errors in the standard deviation as shown in Fig. 8-3, which shows two different possible distributions of the stresses in the wing (one with c.o.v.=0.20% and the other with c.o.v.=0.40%) leading to the same probability of failure, 1×10^{-7}. We observe in Fig. 8-3 that when c.o.v. is 20%, the mean stress is 39.77, while the mean stress is lower, 27.42, for a higher c.o.v.=40% so that they both lead to the same probability of failure. Of

course, these errors can greatly affect the probability of failure. Had we performed a probabilistic design for a given probability of failure, these errors could have caused us to get a design which was much less safe than the deterministic design. To complete the investigation, we also discuss the effect of erroneous estimates of probability of failure of deterministic design.

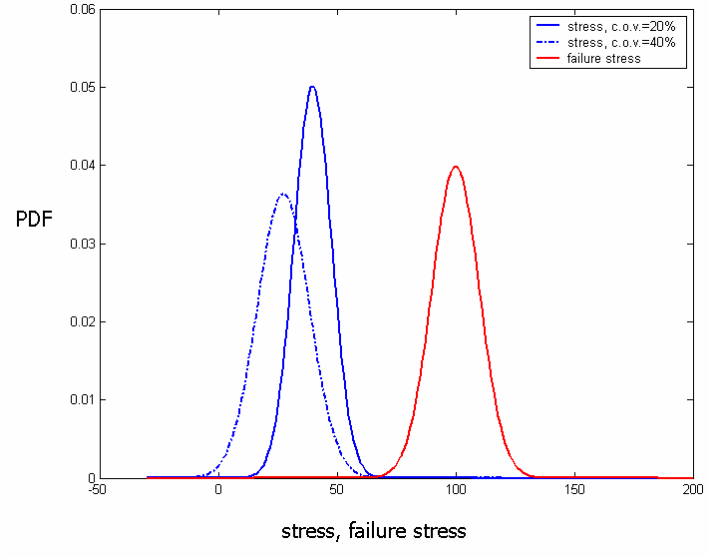

Figure 8-3. Two different stress distributions at the wing leading to the same probability of failure of 1×10^{-7}.

Erroneous Mean Stresses

Instead of erroneous estimates for c.o.v. of stresses, we now check the effect of errors in estimates of the mean stresses in the wing and the tail. We first assume that we under-estimated the mean stresses in the wing and the tail by 20% for the wing and the tail system of Table 8-1. That is, even though the true values of mean stresses in the wing and the tail are both 49.71, we under-estimated them as 39.77 to obtain the design of Table 8-1. Since the overall probability of failure of the deterministic design is fixed, an under-estimate of the mean stress must go with an over-estimate of the coefficient of variation. Following the procedure in Appendix N, we find that the c.o.v is over

estimated by about 193% (actual c.o.v. is 48% lower than value used in Table 8-1). Table 8-4 shows that under-estimation of mean stresses leads to under-estimating the wing P_f ratio by 4.9%, and over-estimating the tail P_f ratio by 27.6%. On the other hand, the system probability of failure ratio is estimated with a very small error, because the two errors mostly cancel each other out. Comparing Table 8-1 and Table 8-4 we see that under-estimate of the mean stresses led to an over-estimate of c.o.v. of the stresses and thus compensated for the errors in probability of failure estimations.

Table 8-4. Errors in the ratios of failure probabilities of the wing and tail system when the mean stresses are under-estimated by 20%. The estimated values of mean and c.o.v. of stresses for wing and tail are both (39.77, 20%). Note that the under-estimate of the mean stress corresponds to an overestimate of the coefficient of variation, so that its actual value is 48% percent lower than the value given in Table 8-1 (c.o.v.=0.1038).

	Optimization based on erroneous data						True optimum		
	Optimized weight (a)	Estimated (a) P_f ratio	Actual (b) P_f ratio	% Error in P_f estim.	Mean stress before optim.	Mean stress after optim. (assumed)	True optimal weight	True optimal P_f ratio	Mean stress after optim. (true)
Wing	99.25	1.309	1.377	-4.9	49.71	50.09	99.36	1.309	50.03
H. Tail	20.75	0.257	0.198	29.4	49.71	47.91	20.64	0.257	48.18
System	120	0.783	0.788	**-0.6**				0.783	

(a) From Table 8-1

(b) Note that the P_f given here is the actual P_f of the assumed optimum (obtained via erroneous c.o.v. of the stress), which is different than the true optimum corresponding to the use of true c.o.v. of the stress

Figure 8-4 shows that negative errors (under-estimated mean stress) lead to over-estimated probability of failure ratio of the wing, under-estimated probability of failure ratio of the tail. However, the two errors are mostly cancelled and the error in the system failure probability ratio estimation is very small. Positive errors have the opposite effect.

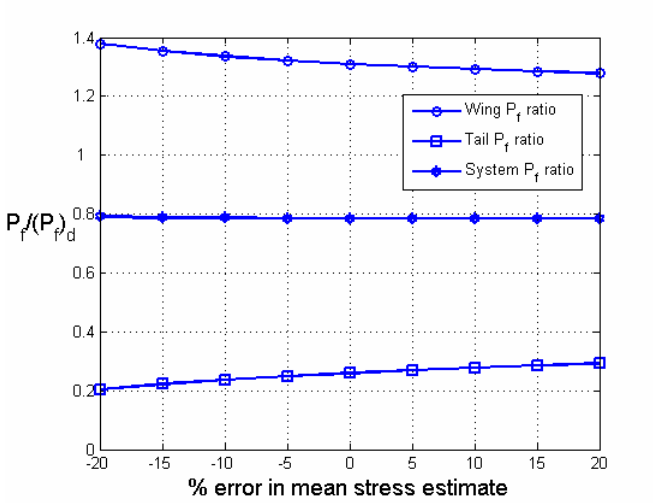

Figure 8-4. The change of the ratios of probabilities of failure with respect to the error in mean stress. The negative errors indicate under-estimate, while the positive errors indicate over-estimate.

Errors in Probability of Failure Estimates of Deterministic Design

Mansour (1989) showed that there can be a significant variation in the failure probabilities of designs constructed using the same deterministic code. Supposedly, this reflects the effect of errors in predicting structural failure that may be different between designers, companies, or materials. This means that the probability of failure estimate of the deterministic design which we used in previous calculations may be inaccurate. To address this issue, we explore the sensitivity of the ratio of the probabilities of failure of the probabilistic design and the deterministic design to erroneous estimates of probability of failure of the deterministic design. Note, however, that we still assume that the several structural components are made from the same material and are designed for the same failure mode, so that they have approximately the same probability of failure in the deterministic design.

We consider an under-estimate of the probability of failure of deterministic design by two orders of magnitudes. That is, we assume that we performed probabilistic design

by taking the probability of failure of deterministic design as 10^{-7} instead of using true value 10^{-5}. Table 8-5 shows that under-estimated P_f of deterministic design leads to transferring lower amount of material (0.75% column 6) than optimum (0.95%; column 5) from the wing to the tail. However, even though the wing is designed to be 5.4% safer than the true optimum and the tail is designed to be 32.9% less safe, the actual system probability of failure ratio is only 0.8% larger than its estimated value (columns 2-4).

Table 8-5. Errors in the ratios of failure probabilities of the wing and tail system when the probability of failure of the deterministic design is under-predicted. The actual P_f is 10^{-5}, while it is predicted as 10^{-7}. Note that the c.o.v. of the stress is 20%.

	Optimum weight	Estimated= Actual (a) P_f ratio	Mean stress before optim.	Mean stress after optim. (assumed)	True optimal weight	True optimal Pf ratio	% safety loss	Mean stress after optim. (true)
Wing	99.25	1.240	45.91	46.26	99.05	1.310	-5.4	46.35
H. Tail	20.75	0.336	45.91	44.24	20.95	0.253	32.9	43.83
System	120	0.788				0.782	0.8	

(a) Estimated an actual probabilities of failure of the assumed optimum are the same, since the mean and c.o.v. of the stress do not involve any error

Similarly, we checked what happens when we over-estimate the probability of failure of the deterministic design by two orders of magnitudes. Table 8-6 shows similar results as Table 8-5, but this time a larger amount of material is transferred from the wing to the tail compared to the true optimum (columns 5 and 6). This time, the wing is designed to be 5.1% less safe and the tail is designed to be 22% safer than their optimum values, the probability of failure ratio is only 0.6% greater than its estimated value (columns 2-4).

Table 8-6. Errors in the ratios of failure probabilities of wing and tail system when the probability of failure of the deterministic design is over-predicted. The actual P_f is 10^{-9}, while it is predicted as 10^{-7}.

	Optimum weight	Estimated =Actual (a) P_f ratio	Mean stress before optim.	Mean stress after optim. (assumed)	True optimal weights	True optimal Pf ratio	% safety loss	Mean stress after optim. (true)
Wing	99.25	1.374	35.33	35.60	99.36	1.306	5.1	35.56
Hor. Tail	20.75	0.202	35.33	34.05	20.64	0.261	-22.4	34.24
System	120	0.788				0.783	0.6	

(a) Estimated an actual probabilities of failure of the assumed optimum are the same, since the mean and c.o.v. of the stress do not involve any error

Effect of Using Wrong Probability Distribution Type for the Stress

Apart from the parameters we investigated (c.o.v. of the stresses, the mean stresses, and the probability of failure deterministic design), the distribution type of the stress also affects the results of probabilistic design. Here we explore the sensitivity of the probabilistic design to using wrong distribution type for the stress. We assume that even though the stress follows the lognormal distribution, the optimization is performed using a normal probability distribution to obtain the results in Table 8-1.

Table 8-7 shows that if the true stress probability distribution is lognormal, the P_f ratio of the wing is over-estimated and the P_f ratio of the tail is under-estimated, so smaller amount of material is moved from the wing to the tail compared to the true optimum design. The error in the total system P_f ratio estimate is only 2.3%. Also, as in Tables 8-3 to 8-6 the loss of accuracy is approximately equal to the opportunity loss since the changes in the design are small. The loss of optimality reflects the fact that with lognormal distribution of the stress it is advantageous to transfer more material from the wing to the tail than with the normal distribution. Of course, the true distribution may be different from lognormal, however, the insensitivity is still encouraging. It is also interesting to note that even with the lognormal distribution the optimal probabilities of

failure are still proportional to the weight of the two components. Analytically, we have obtained a proof of this phenomenon only for the normal distribution (see Appendix O).

Table 8-7. Errors in the ratios of failure probabilities of the wing and tail system if the optimization is performed using wrong probability distribution type for the stress. The probability of failure of the deterministic design is 10^{-7}. The c.o.v. of the stress is 20%.

	Optimization assuming stress is normal						Optimization using the correct distribution type: lognormal		
	Optimized weight [(a)]	Estimated [(a)] P_f ratio	Actual [(b)] P_f ratio	% Error in P_f estim.	Mean stress before optim.	Mean stress after optim. (assumed)	True optimal weight	True optimal P_f ratio	Mean stress after optim. (true)
Wing	99.25	1.309	1.201	9.0	32.04	32.28	98.90	1.307	32.39
H. Tail	20.75	0.257	0.402	-36.1	32.04	30.87	21.10	0.265	30.36
System	120	0.783	0.801	**-2.3**				0.786	

(a) From Table 8-1.

(b) The actual P_f of the optimum obtained via erroneous stress distribution type

Approximate Probabilistic Design Based on Failure Stress Distributions

One of the main barriers to the application of probabilistic structural optimization is computational expense. Probabilistic structural optimization is expensive because repeated stress calculations (typically FEA) are required for updating probability calculation as the structure is being changed. That is, the simplified approach that we used in Eq. (8.2) is replaced by costly FEAs.

Traditionally, reliability based design optimization (RBDO) is performed based on a double-loop optimization scheme, where the outer loop is used for design optimization while the inner loop performs a sub-optimization for reliability analysis using methods such as First Order Reliability Method (FORM). Since this traditional approach is computationally expensive, even prohibitive for problems that require complex finite element analysis (FEA), alternative methods have been proposed by many researchers (e.g., Lee and Kwak 1987, Kiureghian *et al*. 1994, Tu *et al*. 1999, Lee *et al*. 2002, Qu and

Haftka 2004 and Du and Chen 2004). These methods replace the probabilistic optimization with sequential deterministic optimization using inverse reliability measures to reduce the computational expense. The down side of these approaches is that they do not necessarily converge to the optimum design. We note, however, that most of the computational expense is associated with repeated stress calculation and we have just demonstrated insensitivity to the details of the stress distribution. This allows us to propose an approximate probabilistic design approach that might lead to a design nearer the optimum (depending, of course, on the accuracy of the approximation).

Structural failure, using most failure criteria, occurs when a stress σ at a point exceeds a failure stress σ_f. For a given deterministic stress σ, the probability of failure is

$$P_f = \text{Prob}\left(\sigma \geq \sigma_f\right) = F\left(\sigma\right) \tag{8.4}$$

where F is the cumulative distribution function of the failure stress σ_f. For random stress, the probability of failure is calculated by integrating Eq. (8.4) for all possible values of the stress σ

$$P_f = \int F\left(\sigma\right) s\left(\sigma\right) d\sigma \tag{8.5}$$

where s is the probability density function of the stress. For the calculations of the probability of failure in the preceding section, numerical integration of Eq. (8.5) was performed. It is clear from Eq. (8.5) that accurate estimation of probability of failure requires accurate assessments of the probability distributions of the stress σ and the failure stress σ_f. For the failure stress σ_f, the FAA requires aircraft builders to perform characterization tests, use them to construct a statistical model, and then select failure allowables (A-basis or B-basis values) based on this model. Hence, the statistical characterization of the failure stress is solid. On the other hand, the probability density

function of the stress, $s(\sigma)$, is poorly known, because it depends on the accuracy of structural and aerodynamic calculations, the knowledge of the state of the structure, damage progression and pilot actions. As we discussed earlier, it is reasonable to assume that stress is normally distributed, because a large number of sources contribute to the uncertainty in stress, such as errors in load and stress calculations, variabilities in geometry, loads and material properties. Recall that more detailed discussion on the sources of uncertainty in stress is discussed in Chapter 4.

By using the mean value theorem, Eq. (8.5) can be re-written as

$$P_f = F\left(\sigma^*\right)\int s\left(\sigma\right)d\sigma = F\left(\sigma^*\right) \tag{8.6}$$

where the second equality is obtained by using the fact that the integral of $s(\sigma)$ is one. Equation (8.6) basically states that the effect of the poorly characterized probability of the stress can be boiled down to a single characteristic stress value σ^*. This value can be obtained by estimating $s(\sigma)$ and integrating as specified in Eq. (8.6). However, it is equally possible to use historical data on probabilities of failure of aircraft structural components to do the reverse. That is, given an estimate of the probability of failure, we can obtain the characteristic stress σ^* that corresponds to this historical aircraft accident data when airplanes are designed using the deterministic FAA process (see Fig. 8.5).

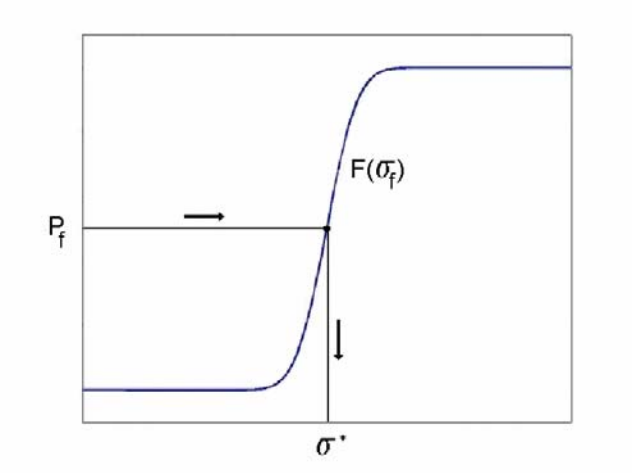

Figure 8-5. Calculation of characteristic stress σ^* from probability of failure

Recall that in probabilistic design of the wing and tail system we deviate from the deterministic process by reducing the structural margin on the wing and increase the margin on the tail, assuming that the structural redesign changes the stress distribution by simple scaling of σ to $\sigma(1+\Delta)$. Under this simple stress scaling, the characteristic stress will change from σ^* to $\sigma^*(1+\Delta^*)$ to allow probabilistic design with a minimum number of stress analyses. We assume here that the relative change in the characteristic stress, Δ^*, is proportional to the relative change in the stress, Δ. That is,

$$\Delta^* = k\,\Delta \tag{8.7}$$

The value of k depends on the mean and c.o.v. of the stress and the failure stress. For lognormally distributed failure stress with mean = 100 and c.o.v.=10%, and normally distributed stress with mean = 39.77 and c.o.v.=20% (the values from our representative example), Figure 8-6(a) shows the relation of Δ and Δ^*. Notice that the variation is almost linear. Figure 8-6(b) shows the effect of the Δ^* approximation on the probability of failure. We see that the linearity assumption is quite accurate over the range $-10\% \le \Delta \le 10\%$.

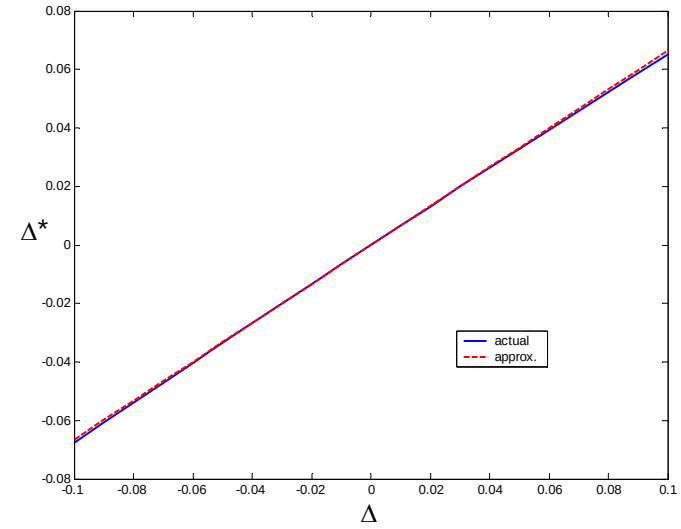

(a)

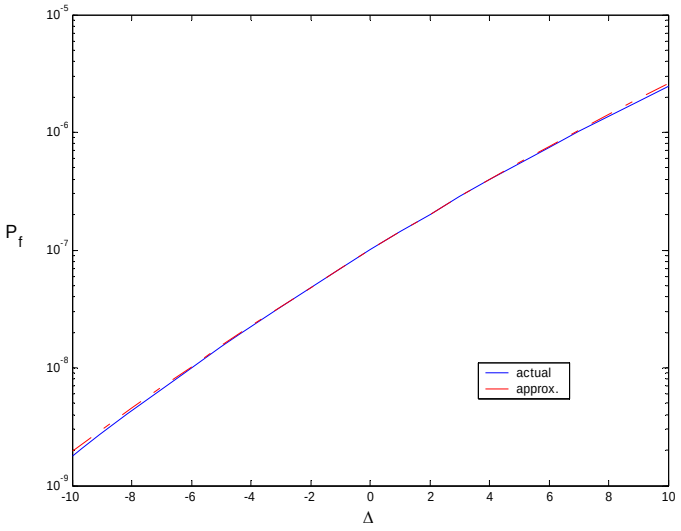

(b)

Figure 8-6. (a) Comparison of approximate and exact Δ and Δ* and (b) the resulting probabilities of failure for lognormal failure stress (with mean=100 and c.o.v.=10%) and normal stress (with mean=39.77 and c.o.v.=20%)

Application of Characteristic Stress Method to Wing and Tail Problem

In this section, we apply the probability of failure estimation to the wing and tail problem. The weights of the wing and the tail before probabilistic optimization are taken as 100 and 20 units, respectively. The probability of failure of the wing and the tail are both taken as 1×10^{-7}. The failure stress of the wing and tail materials is assumed to follow lognormal distribution with a mean value of 100 and 10% c.o.v. The coefficients of

variations of the stresses in the wing and the tail are assumed 20%. The correlation coefficient for probabilities of failure of wing and tail is assumed zero.

As we discussed earlier, some material is taken from the wing and added to the tail so that stresses in the wing and the tail are scaled by $(1+\Delta_W)$ and $(1+\Delta_T)$, respectively. Similarly, the characteristic stresses in the wing and the tail, σ_W^* and σ_T^*, are scaled by $(1+\Delta_W^*)$ and $(1+\Delta_T^*)$, respectively. Then, the probabilistic design optimization problem stated earlier in Eq. (8.3) can now be re-formulated as

$$\begin{aligned} &\min_{W_W, W_T} \quad P_f^*(W_W, W_T) = \left[1 - P_{fW}^*(W_W)\right]\left[1 - P_{fT}^*(W_T)\right] \\ &\text{such that} \quad W_W + W_T = W_{dW} + W_{dT} \end{aligned} \tag{8.8}$$

The weights of the components and characteristic stresses are related via

$$\sigma_W^* = (1 + k_W \Delta_W)\sigma_{dW}^*, \quad \sigma_T^* = (1 + k_T \Delta_T)\sigma_{dT}^* \tag{8.9}$$

where the relative changes in the stresses are calculated from

$$\Delta_W = \frac{W_{dW}}{W_W} - 1, \quad \Delta_T = \frac{W_{dT}}{W_T} - 1 \tag{8.10}$$

The probabilistic optimization problem stated in Eq. (8.8) is solved, and the probabilities of failure are computed. Table 8-8 shows that the P_f ratios of the wing and the tail are estimated as 1.307 and 0.263, instead of their actual values 1.305 and 0.261. So, the characteristic-stress method estimates the system P_f ratio as 0.785, while the actual P_f ratio corresponding to the redesign is 0.783, which is the same system P_f ratio in Table 8-1.

Table 8-8. Probabilistic design optimization for safety of the representative wing and tail system using the characteristic-stress method. The c.o.v. of the stresses in the wing and tail are both 20%.

	Table 8-1		Proposed method		
	ΔW	P_f ratio	ΔW [(a)]	P_f^* ratio	*Actual* P_f ratio
Wing	-0.75	1.309	-0.75	1.307	1.305
Hor. Tail	3.77	0.257	3.73	0.263	0.261
System	0.0	0.783	0.0	0.785	0.783

(a) $\%\Delta W$ is percent changes in weight

Table 8-8 shows that the error associated with the approximation of the characteristic stress in Eq. (8.7) is small. This is expected based on Fig. 8-6 that shows that the approximation of Δ^* is very good. However, the main issue here is to show what happens if we commit errors in evaluating the k value in Eq. (8.7) due errors in the distribution parameters in the stresses and the failure stress. We investigated the effects of over-estimating and under-estimating k with 20% error. Table 8-9 shows that 20% under-estimate of k leads to designing the wing for a higher P_f ratio (1.392 instead of 1.306) and designing the tail for a lower P_f ratio (0.187 instead of 0.269). The overall system P_f ratio, however, is increased by only 0.4%. The variation of P_f ratio of the wing, the tail and the system with the error in k is depicted in Fig. 8-7. It is seen that the effect is small for a wide range of errors.

Table 8-9. Effect of 20% under-estimate of k on the ratios of probability of failure estimate

	k		Table 8-1		Characteristic-stress method with erroneous k		
	correct	With 20% under-estimate	ΔW	P_f Ratio	ΔW [(a)]	P_f^* ratio	*Actual* P_f ratio
Wing	0.664	0.532	-0.75	1.309	-0.93	1.306	1.392
Hor. Tail	0.664	0.532	3.77	0.257	4.64	0.269	0.187
System			0.0	0.783	0.0	0.787	0.790

[(a)] $\%\Delta W$ is percent changes in weight

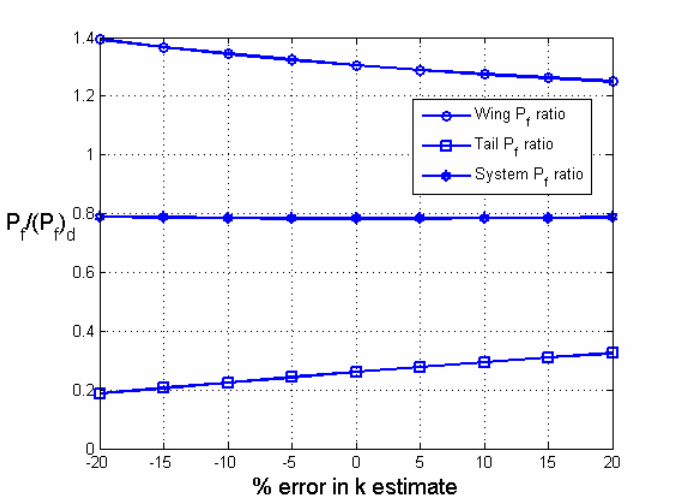

Figure 8-7. The variation of the ratios of probabilities of failure with respect to the error in *k*. The negative errors indicate under-estimate, while the positive errors indicate over-estimate.

For a more complicated problem, when the stresses are calculated via FEA, the application the proposed method is as follows. After calculating the stresses from FEA, the relative changes in the stresses (that is, the Δ values) are calculated. Then, the characteristic stresses are updated by using Eqs. (8.7) and (8.9). Finally, the probabilities of failure of the components are updated using Eq. (8.6). The computational expense regarding with probability calculations are reduced greatly, and the probabilistic optimization problem is reduced to a semi-deterministic optimization problem.

Summary

Probabilistic structural design achieves better performance than deterministic design by applying higher safety factors to lower -weight components. This was demonstrated on a design problem of distributing structural material between the wing, horizontal tail and vertical tail of a typical airliner. While deterministic design leads to similar probabilities of failure for the three components, the probabilistic design led to probabilities of failure that were approximately proportional to structural weight. This

result has shown to be a property of the normal distribution. Remarkably, even though the ratios of weights and probability of failure ratios of the three components were 10:2:1, this was accomplished by reducing the safety factor on the wing by only about one percent and using the material to increase the safety factor on the horizontal and vertical tails by 3 and 5 percent, respectively. This led to a reduction of 34% in the probability of failure for the same total weight. The small perturbation of the safety factor can be accommodated by the additional knockdown factors that aircraft companies often use on top of those required by the FAA code. So the aircraft companies can slightly increase these additional knockdown factors for the wing to achieve the probabilistic design that satisfies all the FAA requirements for a deterministic design!

We used estimates of the probability of failure of the deterministic design (obtained from historical record) as starting point of the probabilistic optimization. Because the exact values of the probability of failure of the deterministic design and the parameters of the probability distribution of structural response are rarely known, we checked the sensitivity of the ratio of probabilities of the probabilistic design and the deterministic design to large inaccuracies in the parameters of the stress distribution, the type of distribution, and probability of failure estimate of the deterministic design. In particular, 50% errors in the standard deviation of the stress, or 20% error in the mean stress led to less than 1% difference in the probability of failure ratios (i.e., ratio of P_fs of the probabilistic and the deterministic designs). We also found that two orders of magnitude of errors in the probability of failure estimate of the deterministic design led to less than 1% difference in the system probability of failure ratio.

Finally, these results inspired us to offer an approximate characteristic-stress method that dispenses with most of the expensive structural response calculations (typically done via finite element analysis). We showed that this approximation still leads to similar re-distribution of material between structural components and similar system probability of failure.

CHAPTER 9
CONCLUDING REMARKS

The two primary objectives of this dissertation were the following: (i) Analyze and compare the effectiveness of safety measures that improve structural safety such as safety factors (can be explicit or implicit), structural tests, redundancy and uncertainty reduction mechanisms (e.g., improved structural analysis and failure prediction, manufacturing quality control). (ii) Explore the advantage of uncertainty reduction mechanisms (e.g., improved structural analysis and failure prediction, tighter manufacturing quality control) versus safety factors. That is, we considered the possibility of allocating the resources for reducing uncertainties, instead of living with the uncertainties and allocating the resources for heavier aircraft structures designed for the given uncertainties.

We started with a point stress design analysis of an aircraft structure by incorporating the uncertainties and safety measures that protect against these uncertainties. The uncertainties are classified as error and variability. Errors reflect inaccurate modeling of physical phenomena, errors in structural analysis, errors in load calculations, or deliberate use of materials and tooling in construction that are different from those specified by the designer. Variability, on the other hand, reflects the departure of material properties, geometry parameters or loading of an individual component from the fleet-average values. The safety measures included in this dissertation were the load safety factor of 1.5, conservative material properties, structural redundancy, coupon tests, structural element tests, certification tests and error and variability reduction mechanisms (e.g., improving the accuracy of structural analysis and failure prediction to reduce error,

employing tighter manufacturing quality controls to reduce variability in material properties).

First a simple analysis was performed in Chapter 3 to understand the basics. A simple error model was used, and coupon tests and element tests are excluded at first. We found that

(1) The load safety factor of 1.5 accompanied with conservative material properties, redundancy, and certification testing raised the actual safety factor to about 2.

Next, the analysis was refined in Chapter 4 by using a more detailed error model and modeling the structural redundancy. We found in this analysis that

(2) While certification testing was more effective than increased safety factors for improving safety, it cannot compete with even a small reduction in errors.

(3) Variability reduction was even more effective than error reduction, but it needed to be accompanied by increased knockdown factors to compensate for the increase in the B-basis value.

Discovering the power of error and variability reduction in increasing the structural safety, we were motivated to analyze the tradeoffs of uncertainty reduction mechanisms, structural weight and structural safety. The effect of error reduction (due to improved failure prediction model) on increasing the allowable flight loads of existing aircraft structures was investigated in Chapter 5. We found that

(4) The allowable flight load of existing aircraft structures can be substantially increased on average by improved failure prediction modeling.

Next, the improved structural analysis through taking the chemical shrinkage of composite laminates was considered in Chapter 6 as the error reduction mechanism to

investigate the tradeoffs of error and variability reduction mechanisms for reducing the weight of the composite laminates at cryogenic temperatures. Tradeoff plots of uncertainty reduction mechanisms, probability of failure and weight were generated that enable a designer to choose the optimal uncertainty control mechanism combination to reach a target probability of failure with minimum cost.

Investigation of the interaction and effectiveness of safety factors was culminated with our final analysis in Chapter 7, which included coupon tests and element tests that we disregarded in our first analysis. In particular, emphasis was placed on analyzing the optimal choice of additional knockdown factors. These knockdown factors refer to conservative decisions of aircraft companies while updating the allowable stresses based on the results of structural element tests. Currently these knockdown factors are implicit and based on worst-case scenarios (e.g., testing the structural elements at worst-case operational conditions, using the smallest measured failure stress in design). Here, we proposed use of explicit knockdown factors, which depend on structural element test results. The effects of coupon tests, structural element tests and uncertainty control mechanisms on the choice of company safety factors were investigated. The Pareto fronts of structural weight and likelihood of structure's failure in certification testing are generated. The following observations were drawn.

(5) Instead of using implicit knockdown factors based on worst-case scenarios, the use of test-dependent explicit knockdown factors may lead to 1 or 2% weight savings. Surprisingly, we found that a lower (i.e., more conservative) knockdown factor should be used if the failure stresses measured in tests exceeds predicted failure stresses in order to reduce the variability in knockdown factor generated by

variability in material properties. A thirty-six percent reduction in variability was observed, and it is likely to be responsible for the weight savings.

(6) Selecting additional knockdown factors to minimize certification failure rate provides a choice that is also very close to the optimum choice that minimizes structural failure in flight.

(7) Using a simple cost function in terms of structural weight, we have shown that decisions can be made whether to invest resources on coupon tests, structural element tests, uncertainty reduction mechanisms or extra structural weight.

The analyses mentioned earlier showed how probabilistic design could be exploited to improve aircraft structural safety. A first step was taken towards the two main barriers in front of the probabilistic design in Chapter 8. These barriers are the sensitivity of the probabilistic design to limited statistical data and the computational expense associated to the probabilistic design. Probabilistic design optimization of a representative wing and tail system was performed with limited statistical data. We showed that

(8) Errors in statistical data affect the probability of failure of both probabilistic and deterministic designs, but the ratio of these probabilities is quite insensitive to even very large errors.

(9) The probabilistic design was found to be a small perturbation of deterministic design. This small perturbation could be achieved by a small redistribution of additional knockdown factors.

To alleviate the problem of computational expense an approximate probabilistic design optimization method was proposed, where the probability of failure calculation was confined only to failure stresses to dispense with most of the expensive structural

response calculations (typically done via finite element analysis). The proposed optimization methodology is illustrated with the design of the wing and tail system. We showed that this approximation still leads to similar re-distribution of material between structural components and similar system probability of failure.

More detailed conclusions corresponding to each stage of the dissertation can be found in the Summary sections of individual chapters.

APPENDIX A
A-BASIS AND B-BASIS VALUE CALCULATION

A-basis value is the value exceeded by 99% of the population with 95% confidence. Similarly, B-basis value is the value exceeded by 90% of the population with 95% confidence. The basis values are calculated by

$$Basis = \bar{X} - k\,s \tag{A1}$$

where $\bar{X}$ is the sample mean, s is the sample standard deviation and k is the tolerance coefficient for normal distribution given by Eq.(A2)

$$k = \frac{z_{1-p} + \sqrt{z_{1-p}^2 - ab}}{a},\ a = 1 - \frac{z_{1-\gamma}^2}{2(N-1)},\quad b = z_{1-p}^2 - \frac{z_{1-\gamma}^2}{N} \tag{A2}$$

where N is the sample size and z_{1-p} is the critical value of normal distribution that is exceeded with a probability of $1-p$ (for A-basis value p=0.99 while for B-basis value p=0.90). Similarly, $z_{1-\gamma}$ is the critical value of normal distribution that is exceeded with a probability of $1-\gamma$ (γ=0.95 for both A-basis and B-basis values). The tolerance coefficient k for a lognormal distribution is obtained by first transforming the lognormally distributed variable to a normally distributed variable. Equations (A1) and (A2) can be used to obtain an intermediate value. This value is then converted back to the lognormally distributed variable using inverse transformation.

In order to obtain the A-basis or B-basis values, we assume that 40 panels are randomly selected from a batch. Here the uncertainty in material property is due to allowable stress. The mean and standard deviation of 40 random values of allowable

stress is calculated and used in determining the A-basis value of allowable stress. For instance, when the failure stress is lognormal with 8% coefficient of variation and 40 tests are performed, the coefficient of variation of A-basis value is about 3 percent.

APPENDIX B
PROBABILITY CALCULATIONS FOR CHAPTER 3

Calculation of Pr(CT|e), the Probability of Passing Certification Test

The probability that the structure will pass the certification testing is calculated from

$$\begin{aligned}\Pr(CT \mid e) &= \Pr(\sigma_f \geq \sigma) = \Pr\left(\sigma_f \geq \frac{S_F P_d}{wt}\right) = \Pr\left(\sigma_f wt \geq S_F P_d\right) \\ &= \Pr(C \geq R)\end{aligned} \tag{B.1}$$

where $C = \sigma_f\, t\, w$ is the load carrying capacity of structure and $R = S_F P_d$ is the applied load in the certification testing.

Since the coefficients of variations of the geometry parameters *t* and *w* are small compared to the coefficient of variation of σ_f, we assume *t* and *w* can be assumed lognormal, so the capacity *C* can be treated as lognormal with distribution parameters λ_C and ζ_C given as

$$\lambda_C(e) = \lambda_{\sigma_f} + \lambda_t(e) + \lambda_w \quad \text{and} \quad \zeta_C^2 = \zeta_{\sigma_f}^2 + \zeta_t^2 + \zeta_w^2 \tag{B.2}$$

where

$$\lambda_t(e) = \ln(t_{design}(e)) - 0.5\,\zeta_t^2 \tag{B.3}$$

Recall that the design thickness t_{design} is defined earlier in Eq. (3-4, Chapter 3) as

$$t_{design} = (1+e)\frac{S_F P_d}{w_{design}\sigma_a} \tag{B.4}$$

Since the response R_c is a deterministic value, the probability Pr(CT|e) can be calculated as

$$\Pr(CT \mid e) = \Pr(C \geq R) = \Phi\left(\frac{\lambda_C(e) - S_F P_d}{\sqrt{\zeta_C^2}}\right) = \Phi\left[\beta(e)\right] \tag{B.5}$$

where Φ is the cumulative distribution function of the standard normal distribution.

Calculations of Mean and Standard Deviation of Probability of Failure

Failure is predicted to occur when the load carrying capacity of the structure C is less than the applied load P. So the probability of failure is given as

$$P_f = \Pr\left(C \leq P\right) \tag{B.6}$$

The load P is lognormally distributed, and as explained in above in this appendix, the distribution of capacity C can also be approximated by a lognormal distribution, which allows us to immediately obtain the probability of failure of a single aircraft model.

To calculate the probability of failure over all aircraft models, we take into account the fact that that t_{design} is a random variable. Then, the expected value of probability of failure is given as

$$\overline{P}_f = \int P_f(t_{design})\, f(t_{design})\, dt_{design} \tag{B.7}$$

where t_{design} is the non-deterministic distribution parameter, and $f(t_{design})$ is the probability density function (PDF)of t_{design}.

The standard deviation of failure probability can be calculated from

$$\sigma_{P_f} = \left[\int \left(P_f - \overline{P}_f\right)^2 f(P_f)\, dP_f\right]^{1/2} \tag{B.8}$$

where

$$P_f = P_f(t_{design})$$

$$f(P_f) = f(t_{design}) \left| \frac{dt_{design}}{dP_f} \right| \tag{B.9}$$

$$dP_f = \frac{1}{dt_{design} / dP_f} dt_{design}$$

Hence, Eq. (B.8) can be re-written as

$$\sigma_{P_f} = \left\{ \int \left[P_f(t_{design}) - \overline{P}_f \right]^2 f(t_{design})\, dt_{design} \right\}^{1/2} \tag{B.10}$$

As seen from Eqs. (B.8) and (B.10), the mean and standard deviation of the probability of failure can be expressed in terms of the $f(t_{design})$. Therefore, we can perform the failure probability estimations to after calculating the $f(t_{design})$. The random variables contributing to t_{design} are *e*, *w* and σ_a (see Eq. (B.4)). Since the variations of *w* and σ_a are small compared to error *e*, we neglect the contribution of w and and σ_a, and calculate the $f(t_{design})$ from

$$f(t_{design}) = f_e(e) \frac{de}{dt_{design}} \tag{B.11}$$

where $f_e(e)$ is the PDF of *e*.

APPENDIX C
CONFLICTING EFFECTS OF ERROR AND VARIABILITY ON PROBABILITY OF FAILURE IN CHAPTER 3

As explained in the discussion of Table 3-5 and Figure 3-3, large errors coupled with certification tests can improve the average (over all companies) safety of an aircraft model. This was most apparent when mean material properties are used for design (Table 3-5) because for this case airplanes would be tested at their average failure load, so that fifty percent will fail certification. A large error bound means a wide variation in design thicknesses. Certification testing fails most of the airplane models with unconservative designs and passes a group of airplane models with high average thickness (that is, over-designed planes).

When the additional safety factor of conservative material properties is used, as in Table 3-6, the picture is more complex. Certification is still done at the same loads, but the test airplane is designed for higher loads because of the conservative material properties. For high errors, many airplanes will still fail certification, but small errors will be masked by the conservative properties. Thus in Table 3-6, the certification failure rate varies from 29.4% for the largest errors to 1.3% for the smallest errors. At the highest error bound (50%), the certification process increases the average thickness from 0.847 to 0.969, and this drops to 0.866 for 30% error bound. This substantial drop in average certified model thicknesses increases the probability of failure. Below an error bound of 30%, the change in thickness is small, and then reducing errors reduces the probability of

failure. This is because small negative errors are not caught by certification, but they still reduce the effective safety factor.

A similar phenomenon is observed when the variability is changed in Tables 3-8 to 3-10. When the coefficient of variation in failure stress is increased from 0% to 16%, the average design thickness before certification increases by about 60% and so the probability of failure without certification is reduced by factors of 16-70. Note, however, that for the smallest error bound (Table 3-10), the drop occurs from zero to 8% coefficient of variation. At the higher coefficients of variation the probability of failure before certification increases again as the increased design thickness does not suffice to compensate for the large variation between airplanes .Once certification is included in the process, variability is mostly detrimental. Certification does not amount to much for large variability, because the certified airplane can be very different from the production aircraft. For large error bounds (Table 3-8) there are large errors that can be masked during certification by the high material safety factor. Thus in Table 3-8, while the probability of failure without certification is reduced by a factor of 16, the probability of failure with certification is increased by a factor of 1320 as the coefficient of variation in the failure stressed is increased from 0 to 16%. For small errors (Table 3-10) the picture is more mixed as the non-monotonic behavior without certification is mirrored with certification.

APPENDIX D
COMPARISON OF RESULTS OF SINGLE ERROR FACTOR AND MULTIPLE ERROR FACTOR CASES

In Chapter 3, we used a single error factor model (SEF model), where the overall error is represented with a single error factor *e*, and uniform distribution is used for the initial distribution of this error. On the other hand, Chapter 4 utilizes a multiple error factor model (MEF model), which uses a more complex representation of error with individual error factors and where initial distributions of each individual error factor are represented with uniform distribution. In this case, the distribution of the total error is no longer uniform. We find that the SEF model exaggerates the effectiveness of certification testing (see Figure 4-1). This is due to the fact that the SEF model does not consider the fact that errors in load calculation affect the load used in certification testing. In the SEF model (Chapter 3), the certification testing is assumed to be performed with the average value of the actual load (P_d), while in the MEF model certification testing is performed with the calculated load (P_{calc}). Therefore, one component of the error cannot lead to failure in certification testing and this reduces the effectiveness of certification testing.

Note that the single error of the SEF model is symmetric. On the other hand, even though the individual errors of MEF model are symmetric, the total error has a bell-shaped distribution with a positive, hence conservative, mean. One of the interesting differences between the SEF and MEF models is that we have a built-in safety factor due to asymmetric error distribution. This asymmetry is due mostly to the term $1/\left(1-e_f\right)$ in

Eq. (4.12). While e_f is symmetrically distributed (-0.2, 0.2), $1/(1-e_f)$ varies in (0.833, 1.25). The conservative tilt of the total error may be serendipitous because it will partially account for designer bias response to the building block tests used to reduce e_f. Tests that show that the failure model is slightly conservative typically do not lead to updating of the model. In contrast, tests showing even small unconservative bias typically lead to correction of the failure model.

In order to compare the effect of the two models on the probability of failure calculations, we match the mean and standard deviation values of the total error distribution (MEF model) and those of a uniform distribution (SEF model). Then, the upper and lower bounds (*lb* and *ub*) for the uniformly distributed error factor can be calculated via Eq. (D.1), where μ_e and σ_e are the mean and standard deviation of the total error, respectively.

$$lb = \mu_e - \sqrt{3}\sigma_e, \quad ub = \mu_e + \sqrt{3}\sigma_e \tag{D.1}$$

Using the equivalent error bounds of the SEF model given in the right-hand side of Table D-1 we calculate the probabilities of failure before and after certification testing for the SEF model and we compare them in Table D-2 with corresponding failure probabilities of the MEF model from Table 4-8.

Table D-1. Equivalent error bounds for the SEF model corresponding to the same standard deviation in the MEF model. The average and standard deviation is calculated via 1,000,000 MCS.

k	Average e_{total}^{ini}	Standard deviation of e_{total}^{ini}	From MEF model → to SEF model	Lower bound for e_{total}^{ini}	Upper bound for e_{total}^{ini}
0.25	0.0009	0.033		-0.057	0.059
0.50	0.0034	0.067		-0.113	0.119
0.75	0.0076	0.101		-0.168	0.183
1.0	0.0137	0.137		-0.223	0.250
1.5	0.0317	0.212		-0.336	0.400

The comparison of the probability of failures after certification for the two models is presented in Fig. D-1.

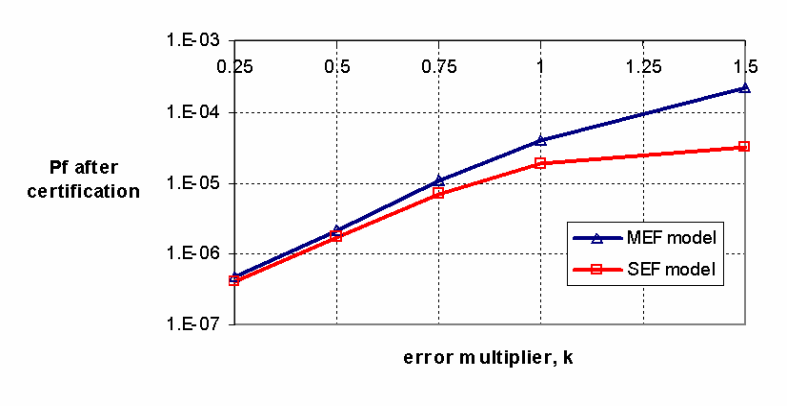

Figure D-1. System failure probabilities for the SEF and MEF models after certification

The total safety factor for the SEF model is defined as

$$(S_F)_{design} = \frac{A_{design}}{A_0} = (1+e) S_{FL} \frac{\bar{\sigma}_f}{\sigma_a} \tag{D.2}$$

Similarly, the design area for the SEF model is expressed as

$$A_{design} = (1+e) \frac{S_{FL} P_d}{\sigma_a} \tag{D.3}$$

Using the SEF model, we repeat the calculation of the probabilities of failures. The comparison of the SEF and MEF models probability of failure calculations are given in Table D-2.

Table D-2. Comparison of system failure probabilities for the SEF and MEF models. The coefficient correlation between failures of structural parts is taken 0.5.

k	$\bar{P}_{nc}^{MEF}$ /10^{-4}	$\bar{P}_{c}^{MEF}$ /10^{-4}	P_f Ratio*	$\bar{P}_{nc}^{SEF}$ /10^{-4}	$\bar{P}_{c}^{SEF}$ /10^{-4}	P_f Ratio[(a)]
0.25	0.0	0.0	0.	0.	0.	0.
0.50	0.029	0.022	0.749	0.026	0.018	0.689
0.75	0.195	0.106	0.543	0.165	0.069	0.419
1	1.11	0.390	0.350	1.03	0.186	0.181
1.5	17.2	2.21	0.129	27.7	0.311	0.112

[(a)] P_f is the ratio of the average failure probabilities before and after certification testing; $\bar{P}_c / \bar{P}_{nc}$

When we compare the probability of failure before certification, the mean values of the failure probabilities are higher for the SEF model than those for the MEF model at high errors (see columns 2 and 5, Table D-2) due to the use of uniform distribution for the total error factor. Comparing the failure probabilities after certification, we notice that the MEF model leads to higher probability of failure values, and higher $\bar{P}_c / \bar{P}_{nc}$ ratios (less effective certification testing). Recall that this is due to the fact that in the MEF model error in load calculation is also included in the certification testing. This effect is also apparent when we compare the total safety factor values for these two models in Table D-3 and in Fig. D-2.

The single error factor after certification of failure probabilities in Table D-2 also indicates that the effect of the error bound on the probability of failure after certification is not monotonic. One possible explanation for this behavior are the competing effects of error and the total safety factor. For the highest error bound, the total safety factor is increased to 2.108 (see Table D-3), which overcomes the effect of high error on the probability of failure.

Table D-3. Comparison of the total safety factor S_F used in the design of structural parts for the SEF and MEF models

k	$(S_F)^{MEF}_{built}$	$(S_F)^{MEF}_{cert}$	S_F Ratio[(a)]	$(S_F)^{SEF}_{built}$	$(S_F)^{SEF}_{cert}$	S_F Ratio[(a)]
0.25	1.725	1.728	1.002	1.725	1.729	1.002
0.5	1.730	1.741	1.007	1.730	1.745	1.009
0.75	1.737	1.764	1.016	1.737	1.776	1.023
1	1.747	1.799	1.030	1.747	1.825	1.044
1.5	1.779	1.901	1.069	1.779	1.954	1.099

[(a)] S_F is the ratio of total safety factors before and after certification

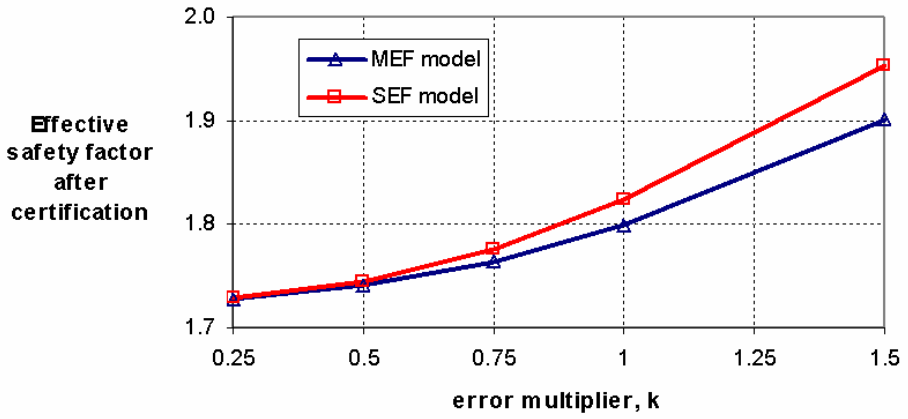

Figure D-2. Total safety factors for the SEF and MEF model after certification

Comparing the total safety factors, S_F, after certification corresponding to the MEF and SEF models (columns 3 and 6, Table D-3), we see that the total safety factor corresponding to the SEF model is larger, which will in turn lead to a smaller probability of failure (see Table D-2). Columns 4 and 7 of Table D-3 exhibit the expected trend of an increase in the total safety factor ratio with increasing error bounds, reflecting more effective certification testing.

In short, the effect of using a more detailed error model can be summarized as follows:

- The uniformly distributed individual error components add up to a bell-shaped representative total error. This total error has an asymmetric distribution and this asymmetry results in a built-in safety factor.
- The single error model exaggerates the effectiveness of certification testing, because it does not include the fact that error in load calculation is also present in the certification process. The single error model inflates the design area after certification, thereby leading to under-estimation of probabilities of failures.

APPENDIX E
DETAILS OF SEPARABLE MONTE CARLO SIMULATIONS FOR PROBABILITY OF FAILURE CALCULATIONS IN CHAPTER 4

The separable MCS procedure applies when the failure condition can be expressed as $g_1(x_1)>g_2(x_2)$, where x_1 and x_2 are two disjoint sets of random variables. For that case, the probability of failure can be written as

$$P_f = \int f_2(t)\left[1 - F_1(t)\right]dt \tag{E.1}$$

where f_2 is the probability density function of g_2 and F_1 is the cumulative distribution function of g_1. Since the two sets of random variables are disjoint, we can perform one Monte Carlo simulation with x_1 to calculate F_1 and then perform a second Monte Carlo simulation on x_2 to calculate P_f from Eq. (E.1). Note that 1-F_1 in Eq. (E.1) is the probability of failure if g_2 takes the value t, and the second Monte Carlo simulation calculates the average of this probability over all possible values of g_2.

For our problem, f_2 is the probability density function of the built safety factor, A_{built} / A_0, and F_1 is the cumulative distribution function of the required safety factor, A'_{req} / A_0. Since $f_1(\ )$ and $F_2(\ )$ depend on different sets of random variables, we separate the MCS into two stages.

In the first stage, the cumulative distribution function of the required safety factor, A'_{req} / A_0, is assessed. We use 1,000,000 MCS for this purpose. It is possible to assess CDF numerically by dividing the range of A'_{req} / A_0 into a number of bins (for instance,

1,000 bins) and calculating the CDF for each bin. Then, in the second stage, the CDF value can be obtained by interpolation.

On the other hand, we notice for our problem that the dominant terms in A'_{req} / A_0 are P_{act} and σ_f, since they have much larger variabilities than v_t and v_w (see Table 4-2, Chapter 4). Since P_{act} and σ_f follow the lognormal distribution, it is possible to represent A'_{req} / A_0 with lognormal distribution. We indeed found that numerical CDF is in good agreement with the assumed lognormal as shown in Fig. E-1.

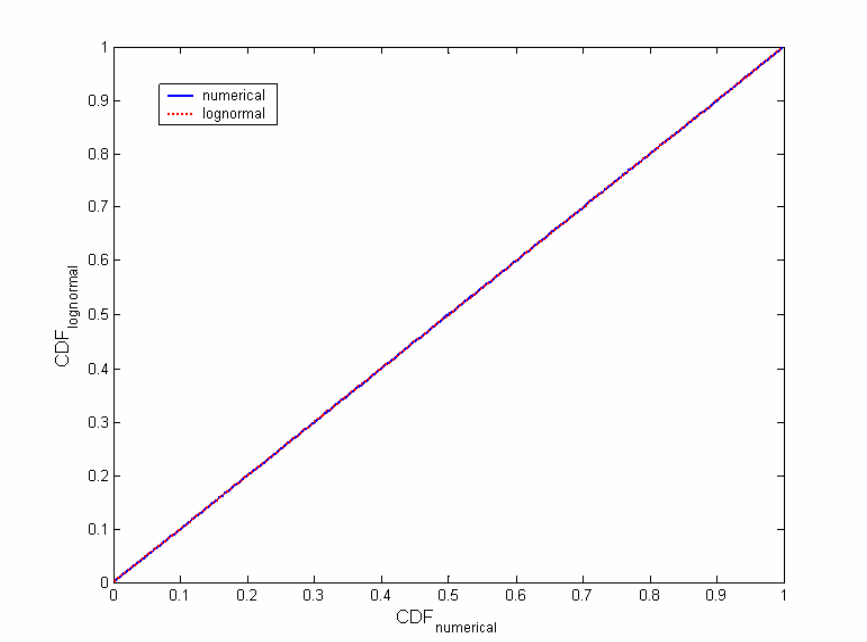

Figure E-1. Comparison of numerical CDF with the assumed lognormal CDF for the distribution of the required safety factor

To ensure that the assumed lognormal distribution leads to an accurate probability of failure estimations, we performed the following study. Five different sets of A'_{req} / A_0 values are obtained from five different MCS with 1,000,000 sample size. Then, the probabilities of failure are calculated using the same second-stage random numbers for both numerical CDF and assumed lognormal CDF. Table E-1 shows that the probability

of failure estimation using assumed lognormal CDF is accurate to the third digit and also has a smaller standard deviation indicating that the numerical noise is reduced.

Table E-1. Comparison of the probability of failure estimations

	P_f estimation using numerical CDF ($\times 10^{-4}$)	P_f estimation using assumed lognormal CDF ($\times 10^{-4}$)
MCS 1	8.961	8.855
MCS 2	8.902	8.807
MCS 3	8.901	8.825
MCS 4	8.734	8.856
MCS 5	8.859	8.816
Average	8.871	8.832
Std. dev.	0.085	0.023

APPENDIX F
CALCULATION OF THE SYSTEM FAILURE PROBABILITY USING BIVARIATE NORMAL DISTRIBUTION

Bivariate normal distribution describes the joint behavior of two random variables X1 and X2, for which the marginal distributions are normally distributed and correlated through the correlation coefficient ρ. The probability density function is defined as (Melchers, 1999)

$$f_{X_1X_2}\left(x_1,x_2,\rho\right)=\frac{1}{2\pi\,\sigma_{X_1}\sigma_{X_2}}\exp\left(-\frac{1}{2}\frac{h^2+k^2-2\rho hk}{1-\rho^2}\right) \tag{F.1}$$

where $h=\dfrac{x_1-\mu_1}{\sigma_1}$ and $k=\dfrac{x_2-\mu_2}{\sigma_2}$, μ_1 and σ_1 are the mean and standard deviation of variable X_1, and μ_2 and σ_2 are the mean and standard deviation of variable X_2.

The joint cumulative distribution is defined as

$$F_{X_1X_2}\left(x_1,x_2,\rho\right)\equiv\Pr\left[\bigcap_{i=1}^{2}\left(X_i\le x_i\right)\right]=\int_{-\infty}^{x_1}\int_{-\infty}^{x_2}f_{X_1X_2}\left(u,v,\rho\right)du\,dv=\Phi_2\left(x_1,x_2,\rho\right) \tag{F.2}$$

In addition, $\Phi_2(\ )$ can be reduced to a single integral (Owen, 1956)

$$\Phi_2\left(h,k,\rho\right)=\frac{1}{2\pi}\int_0^{\rho}\frac{1}{\sqrt{1-z^2}}\exp\left(-\frac{1}{2}\frac{h^2+k^2-2\rho hk}{1-z^2}\right)dz+\Phi\left(h\right)\Phi\left(k\right) \tag{F.3}$$

where Φ is the standard normal cumulative distribution function.

The two local failure events requirement of our problem is modeled as a parallel system. Thus we aim at computing the probability of failure of a parallel system composed of two elements having equal failure probabilities. We assume that the limit-

state functions for these two elements follow normal distribution. Thus we can use the bivariate normal distribution to calculate the system probability of failure. Since the failure probabilities are identical, the reliability indices are also identical (i.e., $h=k=\beta$). Then Eq. (F.3) can further be simplified into Eq. (F.4). Thus, given the probability of failure of a single element and the correlation coefficient ρ, Eq. (F.4) can be used to calculate system failure probability P_{FS}.

$$P_{FS} = \Phi_2\left(-\beta, -\beta, \rho\right) = P_f^2 + \frac{1}{2\pi}\int_0^{\rho} \frac{1}{\sqrt{1-z^2}} \exp\left(-\frac{\beta^2}{1+z}\right) dz \tag{F.4}$$

where P_f and β are the probability of failure and the reliability index for a single element, respectively, which are related to each other through Eq. (F.5).

$$P_f = \Phi\left(-\beta\right) \tag{F.5}$$

APPENDIX G
TEMPERATURE DEPENDENT MATERIAL PROPERTIES FOR THE CRYOGENIC LAMINATES IN CHAPTER 6

Since we analyze the problem that was addressed by Qu *et al*. (2003), the geometry, material parameters and the loading conditions are taken from that paper. Qu *et al*. (2003) obtained the temperature dependent properties by using the material properties of IM600/133 given in Aoki *et al*. (2000) and fitted with smooth polynomials in order to be used in calculations. The reader is referred to Appendix 1 of Qu *et al*. (2003) for the details. The temperature dependent material properties are shown in Figures G-1 and G-2.

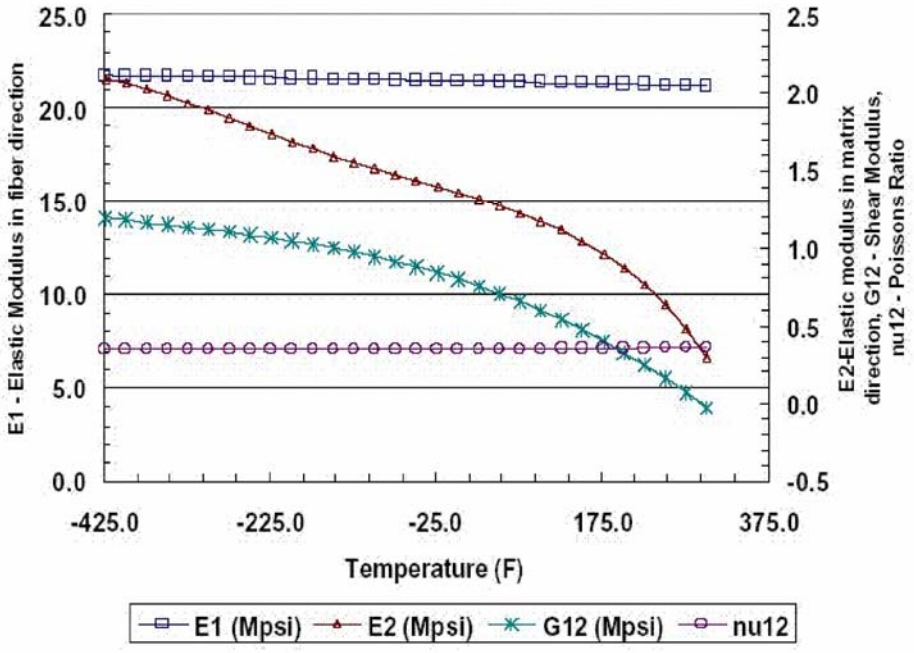

Figure G-1. Material properties E_1, E_2, G_{12} and ν_{12} as a function of temperature

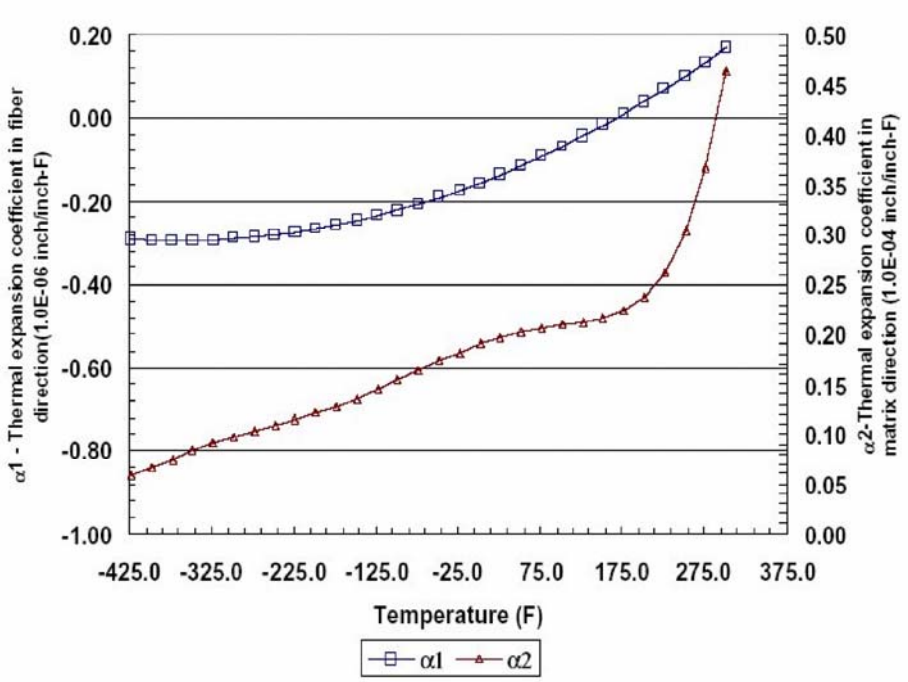

Figure G-2. Material properties α_1 and α_2 as a function of temperature

APPENDIX H
DETAILS OF CONSERVATIVE CUMULATIVE DISTRIBUTION FUNCTION (CDF) FITTING

In Chapter 6, we assume normal distributions for strains in the cryogenic laminates and estimate the mean and the standard deviation of the assumed distributions conservatively. Conservative fitting is assessed as follows. We first perform Monte Carlo simulations with sample size of 1,000 and calculate the mean and the standard deviation of the strains. Then we assume that the strains follow normal distribution with the calculated mean and standard deviation. We see in Fig. 6-2 (of Chapter 6) that the normal CDF is smaller than the empirical CDF for some strain values, and larger for other strain values. That is, the normal CDF leads to conservative estimates for some strain values, while it leads to unconservative estimates for other strain values. It is desirable to have conservative estimates for all strain values, that is, to have a conservative CDF fit which is smaller than the empirical CDF for all strain values. However, the tails of the distribution are volatile, and fitting conservative CDF including these values can lead to over conservative results. Accordingly, we do not apply constraints to the first 5 points (out of 1,000 points) of the left tail and last 5 points of the right tail. Out of the remaining 990points, we choose uniformly spaced 100 points and calculate the maximum deviation of the normal CDF fit from the empirical CDF fit at these 100 points. The maximum deviation of the fitted CDF for the empirical CDF is called the Kolmogorov-Smirnov distance. We shift the mean value of the fitted CDF to close the Kolmogorov-Smirnov distance between the normal fit and empirical fit. The normal distribution with this

shifted mean and original standard deviation is our conservative normal fit. As we see in Fig. 6-2 (of Chapter 6) that the conservative normal CDF lies below the empirical CDF for all strains except near the tails.

A better conservative fit can possibly be obtained by varying the mean and standard deviation at the same time. Detailed investigation on conservative estimation of CDF for probability of failure calculations is provided in Picheny *et al*. (2006).

APPENDIX I
DETAILS OF DESIGN RESPONSE SURFACE FITTING FOR THE PROBABILITY SUFFICIENCY FACTOR FOR THE CRYOGENIC LAMINATES IN CHAPTER 6

Qu *et al*. (2003) showed that using the combination of face centered central composite design (FCCCD) and Latin hypercube sampling (LHS) designs gives accurate results, so we follow the same procedure.

The ranges for design variables for design response surface (DRS) are decided as follows. The initial estimates of the ranges for design variables were taken from Qu *et al*. (2003). When we used these ranges, we found that the prediction variances at the optimum designs were unacceptably large. The ranges for DRS were then reduced by zooming around the optimum designs obtained from the wider ranges. After zooming, the prediction variances at the optimum designs were found to be smaller than the RMSE predictors. The final ranges for response surfaces are given in Table I-1.

Table I-1. The ranges of variables for the three DRS constructed for *PSF* calculation

	t_1 and t_2 (in)	θ_1 and θ_2 (deg)
b_e=0	0.012-0.017	24-27
b_e=10%	0.013-0.018	24-26
b_e=20%	0.015-0.022	22-25

Qu et al. (2003) used a fifth-order DRS for the probability of failure, and found it to be quite accurate. We also use a fifth-order DRS. A fifth-order response surface in terms of four variables has 126 coefficients. Following Qu *et al*. (2003), we used 277 design points, 25 correspond to FCCCD and 252 are generated by LHS. In addition to response surfaces for probability sufficiency factor, three more DRS were also fitted to the probability of failure for comparison purpose. The comparison of the accuracies of DRS

for *PSF* and DRS for P_f are shown in Table I-2. For instance, for error bound of 20%, the root mean square error predictions of DRS for *PSF* and DRS for P_f are 3.610×10^{-3} and 7.664×10^{-4}, respectively. Since *PSF* and P_f are not of the same order of magnitude, we cannot compare these errors directly. One possibility is to compare the ratios of RMSE and mean of the response. When we compare the ratios for error bound of 20%, we see that the ratio of RMSE and mean of the response DRS for P_f is 0.1868, while the same ratio of DRS for PSF is 0.0042. It is an indication that DRS for *PSF* is more accurate than DRS for P_f.

Table I-2. Accuracies of DRS fitted to *PSF* and P_f in terms of four design variables (t_1, t_2, θ_1 and θ_2) for error bounds, b_e, of 0, 10%, and 20%

		Mean of response	RMSE predictor*	Ratio of RMSE to the mean of response	Equivalent error in P_f	Equivalent error in *PSF*
b_e=0%	*PSF*	1.077	4.655×10^{-3}	4.332×10^{-3}	5.397×10^{-7} (< 9.447×10^{-4})	---
	P_f	8.081×10^{-4}	9.447×10^{-4}	1.196	---	4.205×10^{-2} (> 4.655×10^{-3})
b_e=10%	*PSF*	0.9694	4.645×10^{-3}	4.792×10^{-3}	4.615×10^{-6} (< 8.281×10^{-4})	---
	P_f	1.340×10^{-3}	8.281×10^{-4}	0.6180	---	1.862×10^{-2} (> 4.645×10^{-3})
b_e=20%	*PSF*	0.8621	3.610×10^{-3}	4.187×10^{-3}	6.308×10^{-5} (< 7.664×10^{-4})	---
	P_f	4.103×10^{-3}	7.664×10^{-4}	0.1868	---	1.013×10^{-2} (> 3.610×10^{-3})

Another way of comparing the accuracies is to calculate equivalent errors of DRS for PSF to those of DRS for Pf. That is, the equivalent error in Pf due to error in DRS for PSF can be compared to the equivalent error in PSF due to error in DRS for Pf.

The standard errors in calculation of *PSF* and P_f due to limited MCS sample size are given in the last two columns of Table I-2. The standard error for P_f is calculated from

$$\sigma_{P_f} = \sqrt{\frac{P_f\left(1-P_f\right)}{N}} \tag{I.1}$$

The standard error in *PSF* is calculated as illustrated in the following example. Assume that for calculating a probability of failure of 1×10^{-4}, we use sample size of 106 in MCS. Then, the number of simulations failed is 100 and the standard error for P_f calculation from Eq. (I.1) is 1×10^{-5}. Thus, 10 simulations out of 100 represent the standard error. The standard error in *PSF* can be approximated as the difference between the 105th smallest safety factor and 95th smallest safety factor. A better estimation for *PSF* can be obtained by utilizing the CDF of the safety factor *S*.

The equivalent error in Pf due to the error in DRS for *PSF*, for error bound of 20% for instance, can be approximated as follows. The mean of response and RMSE prediction of DRS for *PSF* are $\mu=0.8621$ and $\sigma=3.610\times10^{-3}$, respectively. We calculate the P_f values corresponding to *PSF* values of $\mu-\sigma/2$ and $\mu-\sigma/2$ as 4.605×10^{-4} and 3.974×10^{-4}, respectively. The difference between these two P_f values, 6.31×10^{-5}, gives an approximation for the equivalent error in P_f. We see that this equivalent error in P_f is smaller than the error in DRS for P_f, 7.664×10^{-4}, indicating that the DRS for *PSF* has better accuracy than DRS for Pf. The equivalent error in *PSF* due to errors in DRS for P_f can be computed in a similar manner. The equivalent error in *PSF* (1.013×10^{-2}) due to error in DRS for P_f is larger than the error in DRS for *PSF* (3.610×10^{-3}) indicating that the DRS for P_f does not have good accuracy. The errors in DRS for P_f are clearly unacceptable in view that the required probability of failure is 1×10^{-4}.

DRS for error and quality control case

Table I-1 showed the ranges of design variables for DRS when only error reduction was of interest. When quality control is also considered, we changed the ranges of the design variables. All properties such as the design of experiments and the degree of polynomial were kept the same for the new response surfaces; the only change made was the ranges of design variables. The new ranges of design variables used while constructing the new response surfaces are given in Table I-3. Notice that the ranges for laminates thicknesses are reduced and ranges for ply angles are increased, the safety of the laminates are further improved by addition of quality control.

Table I-3. Ranges of design variables for the three DRS constructed for probability of failure estimation for the error and variability reduction case

	t_1 *and* t_2 (in)	θ_1 and θ_2 (deg)
b_e=0	0.008-0.012	27-30
b_e=10%	0.009-0.014	26-29
b_e=20%	0.013-0.018	24-27

APPENDIX J
ASSESSMENT OF THE ERROR DUE TO LIMITED NUMBER OF COUPON TESTS

Since the (mean) failure stress of a material is estimated based on a finite number of coupon tests, the estimate involves error. Recall that the true mean of the failure stress (i.e., the population mean) $\left(\bar{\sigma}_{fc}\right)_{true}$ and the estimated mean failure stress $\left(\bar{\sigma}_{fc}\right)_{calc}$ are related to each other via

$$\left(\bar{\sigma}_{fc}\right)_{calc} = \left(1 - e_{fc}\right)\left(\bar{\sigma}_{fc}\right)_{true} \tag{J.1}$$

Now, the error term can be written as

$$e_{fc} = 1 - \frac{\left(\bar{\sigma}_{fc}\right)_{calc}}{\left(\bar{\sigma}_{fc}\right)_{true}} \tag{J.2}$$

Even though the true mean failure stress is a deterministic value, the calculated mean failure stress is random due to limited number of coupon tests. The mean and standard deviation of the calculated mean failure stress are given by

$$E\left(\left(\bar{\sigma}_{fs}\right)_{calc}\right) = \left(\bar{\sigma}_{fs}\right)_{true} \tag{J.3}$$

$$Std\left(\left(\bar{\sigma}_{fs}\right)_{calc}\right) = \frac{Std\left(\left(\sigma_{fs}\right)_{true}\right)}{\sqrt{n}} \tag{J.4}$$

where E and Std denote the expected value and the standard deviation, respectively. Then, the mean and standard deviation of e_{fc} can be estimated as follows.

The mean value of e_{fc} can be estimated by using first order Taylor series expansion as

$$E\left(e_{fc}\right) \cong 1 - \frac{E\left(\left(\bar{\sigma}_{fc}\right)_{calc}\right)}{\left(\bar{\sigma}_{fc}\right)_{true}} \tag{J.5}$$

Since the mean value of the calculated mean and true mean are the same, Eq. (J.3), we have

$$E\left(e_{fc}\right) \cong 0 \tag{J.6}$$

Similarly, the standard deviation of e_{fc} can be calculated by using uncertainty propagation equation as

$$Std\left(e_{fc}\right) \cong \left|\frac{\partial e_{fc}}{\partial\left(\bar{\sigma}_{fc}\right)_{calc}}\right| Std\left(\left(\bar{\sigma}_{fc}\right)_{calc}\right) \tag{J.7}$$

where $\frac{\partial e_m}{\partial\left(\bar{\sigma}_{fc}\right)_{calc}} = -\frac{1}{\left(\bar{\sigma}_{fc}\right)_{true}} = -\frac{1}{E\left(\bar{\sigma}_{fc}\right)_{calc}}$. Hence, combining Eqs. (J.4) and (J.7) we can obtain the standard deviation of e_{fc} as

$$Std\left(e_{fc}\right) \cong \frac{\text{c.o.v.}\left(\left(\bar{\sigma}_{fc}\right)_{calc}\right)}{\sqrt{n}} \tag{J.8}$$

where c.o.v. denotes the coefficient of variation.

APPENDIX K
PROBABILITY OF FAILURE CALCULATIONS FOR CHAPTER 7 USING SEPARABLE MCS

As noted earlier, the separable Monte Carlo procedure applies when the failure condition can be expressed as $g_1(x_1)>g_2(x_2)$, where x_1 and x_2 are two disjoint sets of random variables. To take advantage of this formulation, we need to formulate the failure condition in a separable form, so that g_1 will depend only on variabilities and g_2 only on errors.

The separable MCS procedure applies when the failure condition can be expressed as $g_1(x_1)>g_2(x_2)$, where x_1 and x_2 are two disjoint sets of random variables. For that case, the probability of failure can be written as

$$P_F = \int f_2(t)\left[1 - F_1(t)\right]dt \tag{K.1}$$

where f_2 is the probability density function of g_2 and F_1 is the cumulative distribution function of g_1. Since the two sets of random variables are disjoint, we can perform one Monte Carlo simulation with x_1 to calculate F_1 and then perform a second Monte Carlo simulation on x_2 to calculate P_F from Eq. (K.1). Note that 1-F_1 in Eq. (K.1) is the probability of failure if g_2 takes the value t, and the second Monte Carlo simulation calculates the average of this probability over all possible values of g_2.

The common formulation of structural failure condition is in the form of a stress exceeding the material limit. This form, however, does not satisfy the separability requirement. For example, the stress depends on variability in material properties as well as design area which reflects errors in the analysis process. To bring the failure condition

to the right form, we formulate it instead as the required cross section area A'_{req} being larger than the built area A_{built} as given in Eq. (K.2)

$$A_{built} < \frac{A_{req}}{(1+v_t)(1+v_w)} \equiv A'_{req} \tag{K.2}$$

where A_{req} is the cross-sectional area required to calculate the actual service load, which is defined as

$$A_{req} = P/\sigma_f \tag{K.3}$$

The required area depends only on variability, while the built area only on errors. When certification testing is taken into account, the built area, A_{built}, is replaced by the certified area, A_{cert}, which is the same as the built area for companies that pass certification, but companies that fail are not included. That is, the failure condition is written as

$$\text{Failure without certification tests:} \quad A'_{req} - A_{built} > 0 \tag{K.4a}$$

$$\text{Failure with certification tests:} \quad A'_{req} - A_{cert} > 0 \tag{K.4b}$$

Equations (K.4a) and (K4.b) can be normalized by diving the terms with A_0 (load carrying area without safety measures). Since A_{built}/A_0 or A_{cert}/A_0 are the total safety factors, Eq. (K.5) states that failure occurs when the required safety factor is larger than the built one.

$$\text{Failure without certification tests:} \quad (S_F)_{req} - (S_F)_{built} > 0 \tag{K.5a}$$

$$\text{Failure with certification tests:} \quad (S_F)_{req} - (S_F)_{cert} > 0 \tag{K.5b}$$

So for our problem, f_2 is the probability density function of the built safety factor, $(S_F)_{built}$, and F_1 is the cumulative distribution function of the required safety factor, $(S_F)_{req}$. So we can re-write the probability of failure as

$$P_f = \int f_{S_{F_{built}}}\left(S_{F_{built}}\right)\left[1 - F_{S_{F_{req}}}\left(S_{F_{built}}\right)\right] dS_{F_{built}} \tag{K.6}$$

Here the probability of failure for a single company is $P_f = 1 - F_{S_{F_{req}}}$, and integration of P_f over all aircraft companies gives the average probability of failure P_F. For a given $(S_F)_{built}$ we can calculate the probability of failure, Eq. (K.5a), by simulating all the variabilities with an MCS. Figure K-1 shows the dependence of the probability of failure on the total safety factor obtained using MCS with 1,000,000 variability samples. The zigzagging in Figure K-1 at high safety factor values is due to limited sample of MCS.

The dependence on $\log_{10}(P_f)$ on $(S_F)_{built}$ can be represented with response surface approximations (RSA), which also eliminates the noise at high failure probabilities. The fitted RSA for $\log_{10}(P_f)$ in terms of the required safety factor $(S_F)_{built}$ is given in Eq. (K.7).

$$\log_{10}\left(P_f\right) = \begin{cases} 1 \quad for\ 0 \le (S_F)_{built} \le 0.8 \\ 5.783(S_F)_{built}^4 - 18.06(S_F)_{built}^3 + 13.29(S_F)_{built}^2 + 1.55(S_F)_{built} - 2.886 \quad for\ 0.8 \le (S_F)_{built} \le 1.3 \\ -4.801(S_F)_{built} + 4.657 \quad for\ (S_F)_{built} \ge 1.3 \end{cases}$$

(K.7)

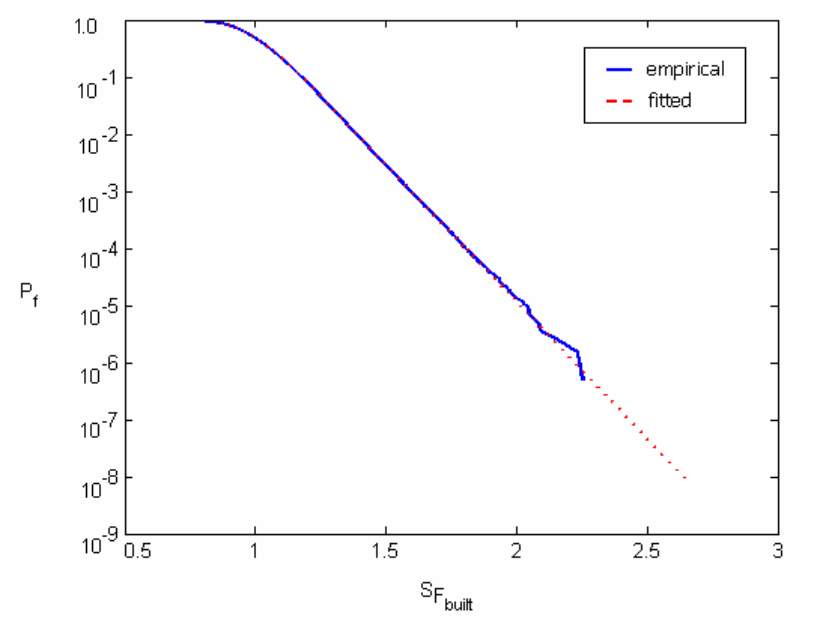

Figure K-1. The variation of probability of failure with built total safety factor. Note that P_f is one minus the cumulative distribution function of $(S_F)_{req}$.

Figure K-2 represents flowchart of separable MCS procedure. In Stage-1 of separable MCS, we first assess the cumulative distribution function $F_{S_{F_{req}}}$ numerically, that is we calculate the empirical CDF. Then, we compute $1-F_{S_{F_{req}}}\left(S_{F_{built}}\right)$, which is equal to the probability of failure for a single company. As noted earlier we find that the dependence on $\log_{10}(P_f)$ on $(S_F)_{built}$ can be represented accurately with response surface approximations. We use 1,000,000 MCS for generating the RSA. Using Fig. K-1 (that is, Eq. (K.7), we calculate probability of failure for a given $(S_F)_{built}$ for an individual aircraft company. The integration of P_f over all companies to estimate the average probability of failure over all companies, P_F, is performed in Stage-2.

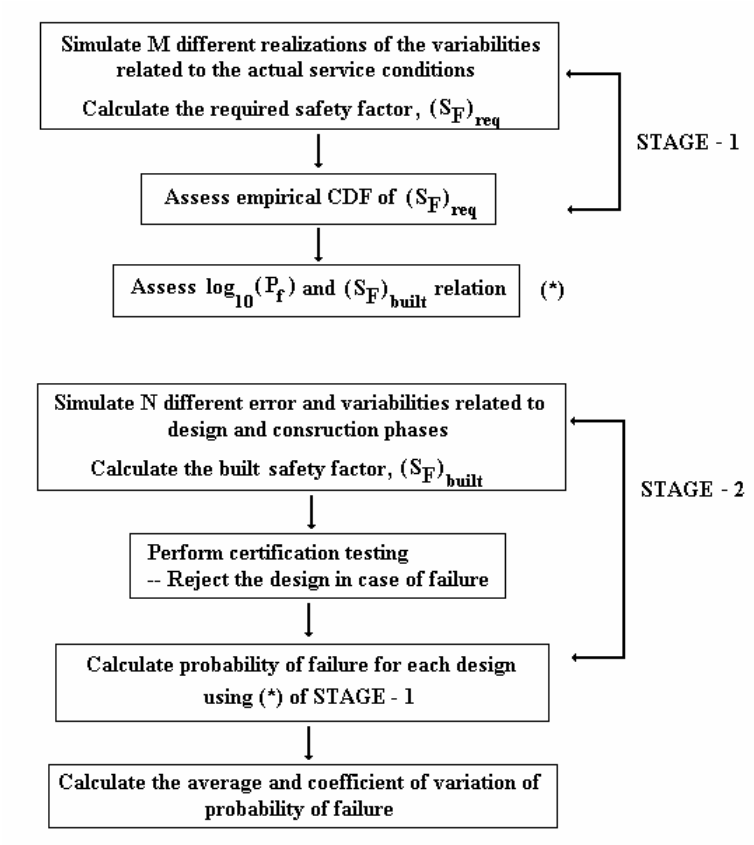

Figure K-2. Flowchart for MCS of component design and failure

In Stage-2, *N* designs are generated for *N* different aircraft companies. For each new design, different random errors are picked from their corresponding distributions. The testing of designs is performed in a building-block type of approach. In this sequence, first simulate coupon tests (i.e., unidirectional laminate tests) that reduce errors in the material constants and failure limits. The nominal value of the number of tests is taken as 40, but the number of tests is varied to see their effect on the results. Then, we simulate structural element tests and material allowable stress is updated based on these tests. Finally, certification testing is simulated in this stage.

The separable Monte Carlo procedure reduces the computational burden greatly. For instance, if the probability of failure is 2.5×10^{-5}, a million MCS estimates this probability with 20% error. We found for our problem that the use of separable Monte

Carlo procedure requires only 20,000 simulations (10,000 simulations for Stage-1 and 10,000 for Stage-2) for the same level of accuracy.

Once the probability of failure of a single structural part is calculated, the probability of failure of the system can be calculated from

$$P_{FS} = P_f^2 + \frac{1}{2\pi}\int_0^{\rho} \frac{1}{\sqrt{1-z^2}} \exp\left(-\frac{\beta^2}{1+z}\right) dz \tag{K.8}$$

Calculation of system probability of failure utilizing bivariate normal distribution is discussed in detail in Appendix E.

APPENDIX L
CHANGE IN COST DUE TO INCREASE OF THE STRUCTURAL WEIGHT

The cost associated with a change in the structural weight and the fuel cost is taken from PhD thesis of Kale (2005). Kale refers to Venter (1999) who assumed a jet fuel cost of \$0.89 per gallon and calculated that a pound of structural weight costs 0.1 pound of fuel per flight. Using this information Kale (2005) calculated a pound of structural weight costs \$0.015 per flight for fuel. Here, in this paper, we update the fuel cost by simply doubling it to take the recent fuel price increase into account. That is, we assume that fuel cost is \$1.78 per gallon. So, a pound of structural weight costs \$0.03 per flight. The material and manufacturing cost per pound of structural weight is taken as \$150 as in Kale (2005). Following the cost function formulation of Kale (2005), we write the cost function as

$$Cost = \left(M_c + F_c \, N_f \right) W_{struc} \tag{L.1}$$

where M_c is material and manufacturing cost per pound of structural weight, F_c is fuel cost per flight per pound of structural weight, N_f is the number of flights (taken as 40,000 following Kale (2005)) and W_{struc} is the structural weight. Using M_c=\$150/lb, F_c=\$0.03 / (lb-flight) and N_f=40,000, the cost function in Eq. (L.1) becomes

$$Cost = \left(150 + 1200 \right) W_{struc} = 1350 \, W_{struc} \tag{L.2}$$

where *Cost* is in dollars when W_{struc} is in pounds. Notice from Eq. (L.2) that fuel cost dominates over material and manufacturing cost (fuel cost is eight times larger than material and manufacturing cost). The structural weight of a typical large transport

aircraft is about 100,000 pounds. We assume that half of the structure is designed for point stress failure. So, half of the structural weight will be affected from the simple analysis presented herein. For example, when our analysis results in 1% weight reduction, it translates into $675,000 cost saving. Note that we use a simple cost function with representative cost parameters, but still it helps to translate the weight saving due to of structural element tests and uncertainty reduction mechanisms to lifetime cost saving.

APPENDIX M
RESPONSE SURFACE APPROXIMATIONS FOR RELIABILITY INDEX OF CERTIFICATION FAILURE RATE, RELIABILITY INDEX OF PROBABILITY OF FAILURE AND BUILT SAFETY FACTOR IN CHAPTER 7

In order to alleviate the computational cost of the optimization problems stated in Eqs. (7.44) and (7.47) we use response surface approximations, RSA. The reliability index of CFR, β_{CFR}, reliability index of P_F, β_{P_F}, and built safety factor, $(S_F)_{built}$, are approximated with fifth-order polynomial RSAs. For design of experiments, we use combination of face centered composite central design (FCCCD) and Latin hypercube sampling (LHS). A fifth-order polynomial in two variables (here S_{cl} and S_{ch}) have 21 coefficients. FCCCD provides 9 designs for two variables, and we generate 33 designs via LHS so that the number of designs is twice the number of coefficients. Table M-1 presents evaluation of the accuracies of RSAs for the nominal case (i.e., number of coupon tests is 40, number of element tests is 3, error bounds are at their nominal values and coefficient of variation of the failure stress is 8% as given in Tables 7-1 and 7-2 of Chapter 7). We see that accuracies of RSAs are at acceptable level.

Table M-1. Accuracy of response surfaces

	RSA for β_{CFR}	RSA for β_{P_f}	RSA for $(S_F)_{built}$
R^2_{adj}	0.9991	0.9988	1.000
RMSE predictor/mean of the response	0.95%	0.54%	0.01%
e_{rms} in 10 tests points/mean of the response*	2.62%	0.39%	0.01%

* Test points are generated via Latin hypercube sampling

APPENDIX N
CALCULATION OF THE MEAN AND THE C.O.V. OF THE STRESS DISTRIBUTION USING PROBABILITY OF FAILURE INFORMATION

The probability of failure is defined in terms of the probability distribution functions of the stress and the failure stress in Chapter 8, Eq. (8.5)

$$P_f = \int F(\sigma) s(\sigma) d\sigma$$

We assume that the stress follows normal distribution. The parameters of the normally distributed stress are the mean, μ_σ, and standard deviation (or coefficient of variation, c_σ, can also be used instead of standard deviation). We assume that material characterization tests provide us an accurate failure stress distribution. If the failure stress also follows normal distribution with mean value of μ_f and coefficient of variation of c_f then Eq. (8.5) can be reduced to

$$P_f = 1 - \Phi(\beta) \tag{N.1}$$

where Φ is the cumulative distribution function of the standard normal distribution and β is the reliability index, which is calculated as

$$\beta(\mu_\sigma, c_\sigma) = \frac{\mu_f - \mu_\sigma}{\sqrt{\mu_f^2 c_f^2 + \mu_\sigma^2 c_\sigma^2}} \tag{N.2}$$

Now consider the reverse situation. Given the estimate of the probability of failure, $P_{f\,\text{given}}$, and the coefficient of variation of the stress c_σ, we can compute the mean value of the stress μ_σ from

$$\mu_\sigma = \frac{-B \pm \sqrt{B^2 - 4AC}}{2A} \tag{N.3}$$

where $A = \beta_{given}^2 c_\sigma^2 - 1$, $B = 2\mu_f$, $C = \mu_f^2 \left(\beta_{given}^2 c_f^2 - 1\right)$, and $\beta_{given} = \Phi^{-1}\left(1 - P_{f\,given}\right)$.

Similarly, if the mean value of the stress is known, then the coefficient of variation of the stress can be calculated from Eq. (N.1).

When the failure stress follows lognormal distribution, then the probability of failure is calculated via the integral given in Eq. (8.5). Hence, given the distribution parameters of lognormally distributed failure stress λ_f and ζ_f, probability of failure is a function of the mean and coefficient of variation of the stress as given in Eq. (N.4)

$$P_f\left(\mu_\sigma, c_\sigma\right) = \int F\left(\lambda_f, \zeta_f, \sigma\right) s\left(\mu_\sigma, c_\sigma, \sigma\right) d\sigma \tag{N.4}$$

So given the estimate of the probability of failure, $P_{f\,given}$, the mean and coefficient of variation of the stress distribution can be calculated from

$$P_f\left(\mu_\sigma, c_\sigma\right) - P_{f\,given} = 0 \tag{N.5}$$

Equation (N.5) is nonlinear in terms of μ_σ and c_σ. When c_σ is known, then μ_σ can be calculated using Bisection method or Newton's method. Alternatively, if the mean value of the stress is known, then the coefficient of variation of the stress can be calculated.

The computations are performed using MATLAB which has the following built-in functions for numerical computations. Equation (N.5) can be solved for the mean or coefficient of variation of the stress using the function `fzero`, which uses a combination of bisection, secant, and inverse quadratic interpolation methods. The integral given in Eq. (N.4) can be computed using the function `quadl`, which numerically evaluates the

integral using adaptive Lobatto quadrature technique. The integrand of Eq. (N.4) can be easily calculated using MATLAB. For normally distributed stress, the function `normpdf` can be used to compute the probability density function s(σ) and for lognormally distributed failure stress the function `logncdf` can be used to compute the cumulative distribution function $F(\sigma)$.

APPENDIX O
RELATION OF COMPONENT WEIGHTS AND OPTIMUM COMPONENT FAILURE PROBABILITIES IN CHAPTER 8

In Chapter 8, we found that the ratio of probabilities of failure of the wing and the tail are very close to the ratio of their weights. Here we aim to provide an analytical proof by utilizing some approximations.

The probability of failure of the wing and tail system is defined as

$$P_f = 1-\left(1-P_{fW}\right)\left(1-P_{fT}\right) \tag{O.1}$$

Let w be the weight transferred from the wing to the tail as a result of probabilistic optimization. The optimality condition of optimization for safety is

$$\frac{\partial P_f}{\partial w} = \left(1-P_{fW}\right)\frac{\partial P_{fT}}{\partial w} + \left(1-P_{fT}\right)\frac{\partial P_{fW}}{\partial w} \cong \frac{\partial P_{fT}}{\partial w} + \frac{\partial P_{fW}}{\partial w} = 0 \tag{O.2}$$

Noting that $P_{fT} = F\left(\sigma_T{}^*\right)$ and $P_{fW} = F\left(\sigma_W{}^*\right)$, where F is the cumulative distribution function of the failure stress, and using the chain rule the partial derivatives in Eq. (O.2) can be written as

$$\frac{\partial P_{fT}}{\partial w} = \frac{\partial P_{fT}}{\partial \sigma_T{}^*}\frac{\partial \sigma_T{}^*}{\partial w} = f_T\frac{\partial \sigma_T{}^*}{\partial w}, \quad \frac{\partial P_{fW}}{\partial w} = \frac{\partial P_{fW}}{\partial \sigma_W{}^*}\frac{\partial \sigma_W{}^*}{\partial w} = f_W\frac{\partial \sigma_W{}^*}{\partial w} \tag{O.3}$$

where and f_T and f_W are the values of probability density function (PDF) of the failure stress evaluated at $\sigma_T{}^*$ and $\sigma_W{}^*$, respectively. That is, $f_T = f\left(\sigma_T{}^*\right)$ and $f_W = f\left(\sigma_W{}^*\right)$, where f is the PDF of the failure stress. Now, combining (O.2) and (O.3) we get

$$f_T \frac{\partial \sigma_T^*}{\partial w} + f_W \frac{\partial \sigma_W^*}{\partial w} = 0, \quad \text{or} \quad \frac{f_T}{f_W} = -\frac{\partial \sigma_W^* / \partial w}{\partial \sigma_T^* / \partial w} \tag{O.4}$$

Recall that we assumed the stresses and weights are inversely proportional. That is,

$$\sigma_W^* = \frac{W_{dW}}{W_W}\sigma_{dW}^* = \frac{W_{dW}}{W_{dW} - w}\sigma_{dW}^*, \quad \sigma_T^* = \frac{W_{dT}}{W_T}\sigma_{dT}^* = \frac{W_{dT}}{W_{dT} + w}\sigma_{dT}^* \tag{O.5}$$

Then, the ratio of partial derivatives $\partial \sigma_W^* / \partial w$ and $\partial \sigma_T^* / \partial w$ can be approximated as

$$\frac{\partial \sigma_W^* / \partial w}{\partial \sigma_T^* / \partial w} = \frac{\dfrac{W_{dW}}{\left(W_{dW} - w\right)^2}\sigma_{dW}^*}{-\dfrac{W_{dT}}{\left(W_{dT} + w\right)^2}\sigma_{dT}^*} \cong -\frac{W_{dT}}{W_{dW}} \tag{O.6}$$

where we the second equality holds true since the moved material *w* is much smaller than both component weights W_{dT} and W_{dW}, and the deterministic characteristic stresses are equal (since they are made of the same material and designed for the same probability of failure). Then, Eqs. (O.4) and (O.6) can be combined to yield

$$\frac{f_T}{f_W} \cong \frac{W_{dT}}{W_{dW}} \tag{O.7}$$

Now, we need to relate the ratio of PDFs to the ratio of probabilities of failure. The probability of failure is defined in terms of the PDF of the failure stress as

$$P_f = \int_{-\infty}^{\sigma^*} f\left(x\right) dx \tag{O.8}$$

If we assume that the failure stress is normally distributed, then the probability of failure can be written as

$$P_f = \int_{-\infty}^{s^*} c\, e^{-x^2/2}\, dx \tag{O.9}$$

where c is a constant and s^* is the characteristic stress scaled with the mean and standard deviation of the failure stress as given in Eq. (O.10)

$$c = \frac{1}{\sqrt{2\pi}}, \quad s^* = \frac{\sigma^* - \mu_f}{std_f} \tag{O.10}$$

Here μ_f and std_f are the mean and standard deviation of the failure stress. Since the normal distribution is symmetric, the probability of failure, Eq. (O.9), can be re-written as

$$P_f = \int_{-\infty}^{s^*} c\, e^{-x^2/2}\, dx = \int_{-s^*}^{\infty} c\, e^{-x^2/2}\, dx \tag{O.11}$$

The probability of failure can be re-formulated by using the equality, Eq. (O.12), given in Abramovitz and Stegun (p. 298, eq. 7.1.14)

$$2\, e^{z^2} \int_z^{\infty} e^{-x^2}\, dx = \frac{1}{z+}\,\frac{1/2}{z+}\,\frac{1}{z+}\,\frac{3/2}{z+}\,\frac{2}{z+}\cdots \left(\Re z > 0\right) \tag{O.12}$$

where $\frac{1}{z+}\,\frac{1/2}{z+}\,\frac{1}{z+}\,\frac{3/2}{z+}\,\frac{2}{z+}\cdots$ is a continued fraction (let's denote as CF(z)) which can also be written as

$$CF\left(z\right) = \frac{1}{z+}\,\frac{1/2}{z+}\,\frac{1}{z+}\,\frac{3/2}{z+}\,\frac{2}{z+}\cdots = \cfrac{1}{z+\cfrac{1/2}{z+\cfrac{1}{z+\cfrac{3/2}{z+\cfrac{2}{z+\cdots}}}}} \tag{O.13}$$

Then, Eq. (O.12) is re-written as

$$\int_z^{\infty} e^{-x^2}\, dx = \frac{CF\left(z\right)}{2} e^{-z^2} \tag{O.14}$$

or

$$\int_{z}^{\infty} e^{-x^2/2}dx = \frac{1}{\sqrt{2}} CF\left(\frac{z}{\sqrt{2}}\right) e^{-z^2/2} \tag{O.15}$$

Then, the probability of failure, Eq. (O.11), is reduced to

$$P_f = \frac{c}{\sqrt{2}} CF\left(\frac{-s^*}{\sqrt{2}}\right) e^{-\left(-s^*\right)^2/2} \tag{O.16}$$

Since the probabilities of failure of aircraft structures are on the orders of 10^{-7}, the scaled characteristic stress is negative and its absolute value is much smaller than one. That is,

$$\left|s^*\right| >> 1, \quad s^* < 0 \tag{O.17}$$

Based on Eq. (O.17), the continued fraction in Eq. (O.13) can be approximated as $CF\left(z\right) \cong \frac{1}{z}$. Then, the probability of failure, Eq. (O.16), becomes

$$P_f \cong -\frac{c}{s^*} e^{-\left(s^*\right)^2/2} = -\frac{f\left(s^*\right)}{s^*} \tag{O.18}$$

Thus, from Eq. (O.18) the probabilities of failure of the wing and the tail are

$$P_{fT} \cong -\frac{f\left(s^*\right)}{s^*} = -\frac{f_T}{\left(\frac{\sigma_T{}^* - \mu_f}{std_f}\right)}, \quad P_{fW} \cong -\frac{f\left(s_W{}^*\right)}{s_W{}^*} = -\frac{f_W}{\left(\frac{\sigma_W{}^* - \mu_f}{std_f}\right)} \tag{O.19}$$

which leads to

$$\frac{P_{fT}}{P_{fW}} \cong \frac{f_T}{f_W}\left(\frac{\sigma_W{}^* - \mu_f}{\sigma_T{}^* - \mu_f}\right) \tag{O.20}$$

Note that the stresses at the deterministic design are close to stresses at probabilistic design, so $\frac{\sigma_W{}^*}{\sigma_T{}^*} \cong 1$. Then, Eq. (O.20) can be simplified to

$$\frac{P_{fT}}{P_{fW}} \cong \frac{f_T}{f_W} \tag{O.21}$$

Finally, combining Eqs. (O.7) and (O.21) we find that the ratio of failure probabilities is approximately equal to the ratio of weights. That is,

$$\frac{P_{fT}}{P_{fW}} \cong \frac{f_T}{f_W} \cong \frac{W_{dT}}{W_{dW}} \tag{O.22}$$

APPENDIX P
HISTORICAL RECORD FOR AIRCRAFT PROBABILITY OF FAILURE

Since aircraft structural design still relies on deterministic optimization, we first look at the historical record on the probability of failure of traditionally (i.e., via deterministic design) designed aircraft structures. Tong (2001) performed a thorough literature review on aircraft structural risk and reliability analysis. Tong (2001) refers to the paper by Lincoln (1996) that reports the overall failure rate for all systems due to structural faults is one aircraft lost in more than ten million flight hours, i.e. $P_f = 10^{-7}$ per flight hours. The Boeing Company publishes the Statistical Summary of Commercial Jet Aviation Accidents each year, and provides data back to 1959 to indicate trends. The number of accidents that occurred between 1959 and 2001 due to structural failure, the total number of accidents and the accident rate corresponding to different aircraft generations are listed in Table P-1. Table P-1 shows that failure probability per departure of second generation airplanes is 4.31×10^{-8}, whereas the failure probability of early widebody airplanes and current generation airplanes are 2.0×10^{-7} and 1.86×10^{-8}, respectively.

Cowan *et al*. (2006) presented data on commercial jet plane accidents involving aircraft operated by U.S. Air Carriers between 1983 and 2003, and listed the number of accidents that caused failure of structural components. The number of accidents resulted in wing failure is given as 18, while the number of accidents due to tail failure is 9. This indicates that the probability of failure of the tail is about half of that of the wing.

Table P-1. Aircraft accidents and probability of failure of aircraft structures. Examples of first generation airplanes are Comet 4, 707, 720, DC-8. Boeing 727, Trident, VC-10, 737-100/-200 are examples of second generation airplanes. Early widebody airplanes are 747-100/-200/-300/SP, DC-10, L-1011 and A300. Examples of current generation airplanes are MD-80/-90, 767, 757, A310, A300-600, 737-300/-400/-500, F-70, F-100, A320/319/321.

Aircraft Generation*	Accident Rate per million departures* (A)	Total Number of accidents* (B)	Accidents due to structural failure* (C)	Structural failure rate per departure (A×C / B)
First	27.2	49	0	0
Second	2.8	130	2	4.31×10^{-8}
Early widebody	5.3	53	2	2.00×10^{-7}
Current	1.5	161	2	1.86×10^{-8}
Total	---	393	6	---

* These columns are taken from the Boeing accident report (2001)

LIST OF REFERENCES

Abramovitz, M., and Stegun, I. (1970), *Handbook of Mathematical Functions*. Dover, New York.

Acar, E., Kale, A., and Akgün, M.A. (2004a), Reliability-Based Design and Inspection Schedule Optimization of an Aircraft Structure Containing Multiple Site Damage. *Proceedings of New Trends in Fatigue and Fracture IV*, Paper no. 19, Aleppo, Syria, 10-12 May 2004.

Acar, E., Kale, A., and Haftka, R.T. (2004b), Effects of Error, Variability, Testing and Safety Factors on Aircraft Safety. *Proceedings of the NSF workshop on Reliable Engineering Computing*, Savannah, Georgia, September 2004, pp. 103-118.

Acar, E., Kale, A., Haftka, R.T., and Stroud, W.J. (2006a), Structural Safety Measures for Airplanes. *Journal of Aircraft*, Vol. 43, No. 1, pp. 30-38.

Acar, E., Haftka, R.T., Sankar, B.V., and Qui, X. (2006b), Increasing Allowable Flight Loads by Improved Structural Modeling. *AIAA Journal*, Vol. 44, No. 2, pp. 376-381.

Acar, E., Haftka, R.T., and Johnson, T.F. (2006c), Tradeoff of Uncertainty Reduction Mechanisms for Reducing Structural Weight. *ASME Journal of Mechanical Design*, in press.

Acar, E., Kale, A., and Haftka, R.T. (2006d), Comparing Effectiveness of Measures that Improve Aircraft Structural Safety. *ASCE Journal of Aerospace Engineering*, submitted.

Acar, E., and Haftka, R.T. (2006e), Reliability Based Aircraft Structural Design Pays Even with Limited Statistical Data, *Journal of Aircraft*, submitted.

Aerospace Information Report, (1997), Integration of Probabilistic Methods into the Design Process. *Society of Automotive Engineers*, Report No: AIR-5080.

Ang, A.H-S., and Tang, W.H. (1975), *Probability Concepts in Engineering Planning and Design, Volume I: Basic Principles*. John Wiley & Sons, New York.

Antonsson, E.K., and Otto, K.N. (1995), Imprecision in Engineering Design. *ASME Journal of Mechanical Design*, Vol. 117 B, pp. 25-32.

Aoki, T. Ishikawa, T., Kumazawa, H., and Morino, Y. (2000), Mechanical Performance of CF/Polymer Composite Laminates under Cryogenic Conditions. *41st AIAA/ASME/ASCE/AHS/ASC Structures, Structural Dynamics, and Materials Conference*, Atlanta, GA, AIAA Paper 2000-1605.

Arbocz, J., Starnes, J. H. Jr., and Nemeth, M. P. (2000), A Comparison of Probabilistic and Lower Bound Methods for Predicting the Response of Buckling Sensitive Structures. *41st AIAA/ASME/ASCE/AHS/ASC Structures, Structural Dynamics, and Materials Conference*, Atlanta, GA, AIAA Paper-2000-1382.

Arbocz, J., and Starnes, J. H. (2005), Hierarchical High-Fidelity Analysis Methodology for Buckling Critical Structures. *ASCE Journal of Aerospace Engineering*, Vol. 18, No. 3, 2005, pp. 168–178.

Avery, J.L., and Sankar, B.V. (2000), Compressive Failure of Sandwich Beams with Debonded Face-sheets. *Journal of Composite Materials*, Vol. 34, No. 14, pp. 1176-1199.

Ayyub, B.M., and Haldar, A. (1984), Practical Structural Reliability Techniques. *Journal of Structural Safety*, Vol. 11, No. 2, pp. 131-146.

Ayyub, B.M., and Lai, K.L. (1989), Structural Reliability Assessment Using Latin Hypercube Sampling. *Proceedings of the 5th International Conference on Structural Safety and Reliability, Vol. 2.* Ang, A.H.S., Shinozuka, M. and Schueller, G.I., Eds. New York, American Society for Civil Engineers, pp. 1193-1200.

Ayyub, B.M., and McCuen, R.H. (1995), Simulation-Based Reliability Methods. *In: Probabilistic Structural Mechanics Handbook, Theory and Industrial Applications*, Sundararajan, C., Editor. New York: Chapman & Hall, pp. 53-69.

Barnett, R.L., and Hermann, P.C. (1965), Proof Testing in Design with Brittle Materials. *Journal of Spacecraft and Rockets*, Vol. 2, pp. 956-961.

Ben Haim, Y., and Elishakoff, I. (1990), *Convex Models of Uncertainty in Applied Mechanics*. Elsevier, Amsterdam.

Bing, L., Akintoye, A., Edwards, P. J., and Hardcastle, C. (2005), The allocation of risk in PPP/PFI construction projects in the UK. *International Journal of Project Management*, Vol. 23, No. 1, pp. 25-35.

Breitung, K. (1984), Asymptotic Approximations for Multi-Normal Integral. *Journal of Engineering Mechanics*, Vol. 110, pp 357-366.

Bucher, C.G. (1988), Adaptive Sampling-An Iterative Fast Monte Carlo Procedure. *Structural Safety*, Vol. 5, pp. 119-126.

Bucher, C.G., and Bourgund, U. (1987), Efficient Use of Response Surface Methods., Institute of Engineering Mechanics, Report 9-87, University of Innsburg. Innsbruck, Austria.

Chamis, C.C., and Murthy, P.L.N. (1991), Probabilistic Composite Analysis. *First NASA Advanced Composites Technology Conference, Part 2,* NASA CP-3104-PT-2, pp. 891–900.

Chamis, C.C. (1997), Probabilistic Composite Design. *Composite Materials: Testing and Design*, Vol. 13, ASTM STP 1242, ed. by S. J. Hooper, pp. 23-42.

Chen, X., and Hasselman, T.K., and Neill, D.J. (1997), Reliability Based Structural Design Optimization for Practical Applications. *38th AIAA/ASME/ASCE/AHS/ASC Structures, Structural Dynamics and Materials Conference*, Kissimmee, FL, AIAA Paper 1997-1403.

Cho, N.Z., Papazoglou, I.A., and Bari, R.A. (1986), A Methodology for Allocating Reliability and Risk. Brookhaven National Laboratory, NUREG/CR-4048.

Composite Materials Handbook MIL-HDBK-17 (2002), "Guidelines for Property Testing of Composites," *ASTM Publications*, Vol. I., Chapter 2.

Composite Materials Handbook MIL-HDBK-17 (2002), "Statistical Methods," *ASTM Publications*, Vol. I., Chapter 8.

Cornell, C.A. (1967), Bounds on the Reliability of Structural Systems. *ASCE Journal of the Structural Division,* Vol. 93, No. ST1, pp. 171-200.

Cowan, T., Acar, E., and Francolin, C. (2006). Analysis of Causes and Statistics of Commercial Jet Plane Accidents between 1983 and 2003. Unpublished, available online at http://plaza.ufl.edu/eacar/paper/accident_report.pdf.

Das, P.K., and Zheng, Y. (2000a), Cumulative Formulation of Response Surface and Its Use in Reliability Analysis. *Probabilistic Engineering Mechanics*, Vol. 15, pp.309-315.

Das, P.K., and Zheng, Y. (2000b), Improved Response Surface Method and Its Application to the Stiffened Plate Reliability Analysis. *Engineering Structures*, Vol. 22, pp. 544-551.

Der Kiureghian, A., Lin, H.Z., and Hwang, S.J. (1987), Second-Order Reliability Approximations. *Journal of Engineering Mechanics*, Vol. 113, pp. 1208-1225.

Der Kiureghian, A., and De Stefano, M. (1991). Efficient Algorithm for Second-Order Reliability Analysis. *Journal of Engineering Mechanics*, Vol. 117, pp. 2904-2923.

Du, X., and Chen, W. (2000), Towards a Better Understanding of Modeling Feasibility Robustness in Engineering. *ASME Journal of Mechanical Design*, Vol. 122, No. 4, pp. 357–383.

Du, X., and Chen, W. (2004), Sequential Optimization and Reliability Assessment Method for Efficient Probabilistic Design. *Journal of Mechanical Design*, Vol. 126, No. 2, pp. 225-233.

Elishakoff, I. (2001), Interrelation between Safety Factors and Reliability, *NASA Report* CR-2001-211309.

Enevoldsen, I., and Sorensen, J.D. (1993), Reliability-Based Optimization of Series Systems of Parallel Systems. *Journal of Structural Engineering*, Vol.119, pp.1069-1084.

Fadale, T., and Sues, R. H. (1999), Reliability-Based Analysis and Optimal Design of an Integral Airframe Structure Lap Joint. *40th AIAA/ASME/ASCE/AHS/ASC Structures, Structural Dynamics, and Materials Conference*, St. Louis, MO, AIAA Paper 1999-1604.

Federal Aviation Regulations, Part 25, Airworthiness Standards: Transport Category Airplanes, Sec. 25.303, Factor of Safety.

Federal Aviation Regulations, Part 25, Airworthiness Standards: Transport Category Airplanes, Sec. 25.307, Proof of Structure.

Federal Aviation Regulations, Part 25, Airworthiness Standards: Transport Category Airplanes, Sec. 25.613, Material Strength Properties and Material Design Values.

Fissler, B., Neumann H.J., and Rackwitz R. (1979), Quadratic Limit States in Structural Relaibility. *ASCE Journal of the Engineering Mechanics Division*, Vol.105, 1979, pp. 661- 676.

Fox, E. P. (1994), The Pratt & Whitney Probabilistic Design System. *Proceedings of 35th AIAA/ASME/ASCE/AHS/ASC Structures, Structural Dynamics, and Materials Conference*, Hilton Head, SC, AIAA Paper 1994-1442.

Fox, E. P. (1996), Issues in Utilizing Response Surface Methodologies for Accurate Probabilistic Design. *Proceedings of 37th AIAA/ASME/ASCE/AHS/ASC Structures, Structural Dynamics, and Materials Conference*, Salt Lake City, UT, AIAA Paper1996-1496.

Freudenthal, A.M. (1947), Safety of Structures. *Transactions of ASCE*, Vol. 112, pp. 125-180.

Fujimoto, Y., Kim, S.C., Hamada, K. and Huang, F. (1998), Inspection Planning Using Genetic Algorithm for Fatigue Deteriorating Structures. *Proceedings of the International Offshore and Polar Engineering Conference*, ISOPE, Golden, CO, pp. 461-468.

Fujino, Y., and Lind, N.C. (1977), Proof-Load Factors and Reliability. *ASCE Journal of Structural Division*, Vol. 103, No. ST4, pp. 853-870.

Gayton, N., Bourinet, J.M., and Lemaire, M. (2003), CQ2RS: A new Statistical Approach to the Response Surface Method for Reliability Analysis. *Structural Safety*, Vol. 23, pp.99-121.

Gokcek, O., Temme, M.I., and Derby, S.L. (1978), Risk Allocation Approach to Reactor Safety Design and Evaluation. *Proceedings of Topical Meeting on Probabilistic Analysis of Nuclear Reactor Safety*.

Gollwitzer, S., and Rackwitz, R. (1983), Equivalent Components in First-Order System Reliability. *Reliability Engineering*, Vol. 5, pp 99-115.

Grandhi, R. V., and Wang, L. P. (1998), Reliability-Based Structural Optimization Using Improved Two-Point Adaptive Nonlinear Approximations. *Finite Element Analysis and Design*, Vol. 29, No.1, pp. 35–48.

Grau, D. (2003), Relating Interfacial Fracture Toughness to Core Thickness in Honeycomb Core Sandwich Composites. M.S. Thesis, Dept. of Mechanical and Aerospace Engineering, University of Florida, Gainesville, FL.

Grau, D.L., Qiu, S., and Sankar, B.V. (2006), Relation between Interfacial Fracture Toughness and Mode-mixity in Honeycomb Core Sandwich Composites, *Journal of Sandwich Structures & Materials*, Vol. 8, No. 3, pp. 187-203.

Gupta, S.S. (1963), Probability Integrals of Multivariate Normal and Multivariate t^1, *The Annals of Mathematical Statistics*, Vol. 34, No.3, pp.792-828.

Haftka, R.T. (2005). Reflections on Jim Starnes' Technical Contributions. *45th AIAA/ASME/ASCE/AHS/ASC Structures, Structural Dynamics, and Materials Conference*, Austin, TX, AIAA Paper 2005-1872.

Haftka, R.T., and Gurdal, Z. (1992), *Elements of Structural Optimization*. Kluwer Academic Publishers, 3rd edition.

Haimes, Y.Y., Barry, T., and Lambert, J.H. (1994), When and How Can You Specify a Probability Distribution When You Don't Know Much? *Risk Analysis*, Vol. 14, No. 5, pp. 661-706.

Hall, W.B., and Lind, N.C. (1979), Safety Verification by Load Tests: A Literature Review. Department of Civil Engineering, University of Waterloo, Canada.

Hall, W.B., and Tsai, M. (1989), Load Testing, Structural Reliability and Test Evaluation. *Structural Safety*, Vol. 6, pp. 285-302.

Harbitz, A., and Veritas, D.N. (1983), Efficient and Accurate Probability of Failure Calculation by Use of the Importance Sampling. *Proceedings of the Fourth International Conference on Applications of Statistics and Probability in Soil and Structural Engineering*, pp. 825-836.

Harkness, H.A., Fleming, M., Moran, M., and Belytschko, T. (1994), Fatigue Reliability Method with In-Service Inspections. *FAA/NASA International Symposium on Advanced Structural Integrity Methods for Airframe Durability and Damage Tolerance*, pp. 307-325.

Hasofer, A.M., and Lind, N. (1974), An Exact and Invariant First-Order Reliability Format. *Journal of Engineering Mechanics*, Vol. 100, pp.111-121.

Herbert, J.J., and Trilling, L.H. (2006), Development of Factors of Safety for Structural Analysis and Verification of Cryogenic Structures Using Probabilistic Methods, *47th AIAA/ASME/ASCE/AHS/ASC Structures, Structural Dynamics, and Materials Conference*, Newport, RI, AIAA Paper 2006-1992.

Hoffman, F.O., and Hammonds, J.S. (1994), Propagation of Uncertainty in Risk Assessments: The Need to Distinguish Between Uncertainty Due to Lack of Knowledge and Uncertainty Due to Variability. *Risk Analysis*, Vol. 14, No. 5, 1994, pp. 707-712.

Hohenbichler, M., and Rackwitz, R. (1983), First-order Concepts in System Reliability. *Structural Safety*, Vol.1, pp 177-188.

Hohenbichler, M., Gollwitzer, S., Kruse, W., and Rackwitz, R. (1987), New Light on First and Second-Order Reliability Methods. *Structural Safety*, Vol. 4, No. 4, pp. 267-284.

Hurd, D.E. (1980), *Risk Analysis Methods Development*. General Electric, GEFR-14023-13, April-June 1980.

Ifju, P.G., Niu, X., Kilday, B.C., Liu, S.C., and Ettinger, S.M. (2000), Residual Strain Measurement in Composites Using the Cure-Referencing Method. *Journal of Experimental Mechanics*, Vol. 40, No. 1, pp. 22-30.

Iman, R.L., and Canover, W.J. (1980), Small Sample Sensitivity Analysis Techniques for Computer Models with an Application to Risk Assessment. *Communications in Statistics, Theory and Methods*, Vol. A9, No. 17, pp. 1749-1842.

Ivanovic, G. (2000), The Reliability Allocation Application in Vehicle Design. *International Journal of Vehicle Design*, Vol. 24, No.2-3, pp. 274-286.

Jiao, G., and Moan, T. (1990), Methods of Reliability Model Updating through Additional Events. *Structural Safety*, Vol. 9, pp. 139-153.

Kale, A., Haftka, R.T., Papila, M., and Sankar, B.V. (2002), Tradeoffs of Weight and Inspection Cost in Safe-Life Design. *44th Structures, Structural Dynamics, and Materials Conference*, Denver, CO, AIAA Paper 2002-1402.

Kale, A.A. (2005), Interaction of Conservative Design Practices, Tests and Inspections in Safety of Structural Components. Ph.D. Dissertation, Dept. of Mechanical and Aerospace Engineering, Univ. of Florida, Gainesville, FL.

Kale, A.A., Haftka, R.T., and Sankar, B.V. (2005), Reliability Based Design and Inspection of Stiffened Panels Against Fatigue. *46th AIAA/ASME/ASCE/AHS/ASC Structures, Structural Dynamics & Materials Conference*, AIAA Paper 2005-2145, April, 2005.

Kale, A.A., and Haftka, R.T. (2005), Effect of Safety Measures on Reliability of Aircraft Structures Subjected to Damage Growth. *31st ASME Design and Automation Conference, Simulation Based Design under Uncertainty*, Long Beach, CA.

Karamchandani, A., Bjerager, P., and Cornell, C.A. (1989), Adaptive Importance Sampling. *In: Proceedings of the 5th International Conference on Structural Safety and Reliability*. Ang, A.H-S, Shinozuka, M. and Scheuller, G.I., Eds. New York, American Society of Civil Engineers, pp. 855-862.

Ke, H.Y. (1999), Sampling Plans for Vehicle Component Reliability Verification. *Quality and Reliability Engineering International*, Vol. 15, pp. 363-368.

Kelton, W.D., Sadowski, R.P., and Sadowski, D.A. (1998), *Simulations with Arena*. WCB McGraw Hill, Boston, Massachusetts.

Kiureghian, A.D., Zhang, Y., and Li, C.C. (1994), Inverse Reliability Problem. *Journal of Engineering Mechanics*, Vol. 120, No. 5, pp. 1154-1159.

Kjerengtroen, L. (1985), Reliability Analysis of Series Structural Systems. PhD Dissertation, University of Arizona.

Knoll. A. (1983), Component cost and reliability importance for complex system optimization. *Proceedings of International ANS/ENS Topical Meeting on Probabilistic Risk Assessment*, Vol. 11, Port Chester, NY.

Koch, P.N., and Kodiyalam, S. (1999), Variable Complexity Structural Reliability Analysis for Efficient Reliability-Based Design Optimization. *40th AIAA/ASME/ASCE/AHS/ASC Structures, Structural Dynamics, and Materials Conference*, St. Louis, MI, AIAA Paper 99-1210.

Koyluoglu, H.U., and Nielsen, S.R.K. (1994), New Approximations for SORM Integrals, *Structural Safety*, Vol. 13, No. 4, pp. 235-246.

Kuschel, N., and Rackwitz, R. (2000), A New Approach for Structural Optimization of Series Systems, In: Melchers, R.E. and Stewart, M.G., (eds). *Applications of Statistics and Probability*, Balkema, Rotterdam, pp. 987-994.

Kwon, Y.W., and Berner, J.M. (1997), Matrix Damage of Fibrous Composites: Effect of Thermal Residual Stresses and Layer Sequences. *Computes and Structures*, Vol. 64, No. 1-4, pp. 375-382.

Law, A.M., and Kelton, W.D. (1982), *Simulation Modeling and Analysis*,:McGraw-Hill, New York, NY.

Lee, T.W., and Kwak, B.M. (1987), A Reliability-based Optimal Design Using Advanced First Order Second Moment Method. *Mechanics of Structures and Machines*, Vol. 15, No. 4, pp. 523 – 542.

Lee, J.O., Yang, Y.S., and Ruy, W.S. (2002), A Comparative Study on Reliability-index and Target Performance-based Probabilistic Structural Design Optimization. *Computers and Structures*, Vol. 80, No. 3-4, pp. 257-269.

Li, Y.W., Elishakoff, I., Starnes, J.H., Jr., and Bushnell, D. (1997), Effect of the Thickness Variation and Initial Imperfection on Buckling of Composite Cylindrical Shells: Asymptotic Analysis and Numerical Results by BOSOR4 and PANDA2. *International Journal of Solids and Structures*, Vol. 34, No. 28, pp. 3755-3767.

Li, H., and Foschi, O. (1998), An Inverse Reliability Measure and Its Application," *Structural Safety*, Vol. 20, No. 3, pp. 257-270.

Liang, J., Mourelatos, Z.P., and Tu, J. (2004), A Single Loop for Reliability Based Design Optimization. *Proceedings of the 30th ASME Design Automation Conference*, Salt Lake City, UT, Paper No. DETC2004/DAC-57255.

Lincoln, J.W. (1980), Method for Computation of Structural Failure Probability for an Aircraft. ASD-TR-80-5035.

Lincoln, J.W. (1996), Aging Aircraft Issues in the United States Air Force. *41st International SAMPE Symposium and Exhibition*, Anaheim, California.

Lind, N.C., Krenk, S., and Madsen, H.O. (1985), *Safety of Structures*, Prentice-Hall, Englewood Cliffs.

Long, M.W., and Narciso. J.D. (1999), Probabilistic Design Methodology for Composite Aircraft Structures. DOD/FAA/AR-99/2, Final Report, June 1999.

Madsen, H.O., Krenk, S., and Lind, N.C. (1986), *Methods of Structural Safety*. Englewood Cliffs, New-Jersey, Prentice-Hall.

Mansour, A. (1989), *An Introduction to Structural Reliability Theory*. Ship Structure Committee Report, SSC-351, January 1989, p. 145.

Martz, H.F., and Walker, R.A. (1982). *Bayesian Reliability Analysis*. Wiley, New York.

Melchers, R.E. (1989), Improved Importance Sampling for Structural System Reliability Calculation, In: *Proceedings of the 5th International Conference on Structural Safety and Reliability*. Ang, A.H-S, Shinozuka, M. and Scheuller, G.I., Eds. New York, American Society of Civil Engineers, pp. 1185-1192.

Melchers, R.E. (1999), *Structural Reliability Analysis and Prediction*. John Wiley&Sons, New York, NY.

Mohamed, A., Lawrence, L.M., and Ravindran, A. (1991), Optimization Techniques for System Reliability: A Review. *Reliability Engineering and System Safety*, Vol. 35, No. 2, pp. 137-146.

Morgan, B.W. (1968), *An Introduction to Bayesian Statistical Decision Processes*. Prentice Hall, New-Jersey.

Muller, G.E., and Schmid, C.J. (1978), Factor of Safety-USAF Design Practice, AFFDL-TR-78-8, U.S. Air Force.

Murthy, P.N., and Chamis, C.C. (1995), Probabilistic Analysis of Composite Material Structure. *NASA Tech Briefs*, November 1995, pp. 60-61.

Neal, D.M., Matthews, W. T., and Vangel, M.G. (1992), Uncertainties in Obtaining High Reliability from Stress-Strength Models. *Proceedings of the 9th DOD-/NASA/FAA Conference on Fibrous Composites in Structural Design*, Lake Tahoe, NV, 1991, DOT/FAA/CT 92-95, Vol. I, pp. 503-521.

Nikolaidis E., Chen, S., Cudney, H., Haftka, R.T., and Rosca, R. (2004), Comparison of Probability and Possibility for Design Against Catastrophic Failure Under Uncertainty. *ASME Journal of Mechanical Design*, Vol. 126, pp. 386-394.

Niehaus, G. (2002), The Allocation of Catastrophe Risk. *Journal of Banking & Finance*, Vol. 26, No. 2-3, Pages 585-596.

Niu, M.C.Y. (1988), *Airframe Structural Design*. Conmilit Press Ltd, Hong Kong.

Oberkampf, W.L., Deland, S.M., Rutherford, B.M., Diegert, K.V., and Alvin, K.F. (2000), Estimation of Total Uncertainty in Modeling and Simulation. *Sandia Report*, SAND2000-0824, Albuquerque, NM.

Oberkampf, W.L., Deland, S.M., Rutherford, B.M., Diegert, K.V., and Alvin, K.F. (2002), Error and Uncertainty in Modeling and Simulation. *Reliability Engineering and System Safety*, Vol. 75, pp. 333-357.

Owen, D.B. (1956), Tables for Computing Bivariate Normal Probabilities. *Annals of Mathematical Statistics*, Vol. 27, pp. 1075-1090.

Pai, S.S. (1990), Probabilistic Structural Analysis of a Truss Typical for Space Station. NASA Technical Memorandum 103277.

Pai, S.S., and Chamis, C.C. (1991), Probabilistic Progressive Buckling of Trusses. NASA Technical Memorandum 105162.

Pai, S.S., and Chamis, C.C. (1992), Probabilistic Assessment of Space Trusses Subjected to Combined Mechanical and Thermal Loads. NASA Technical Memorandum 105429.

Park, C.H., and McManus, H.L. (1996), Thermally Induced Damage in Composite Laminates: Predictive Methodology and Experimental Investigation. *Composites Science and Technology*, Vol. 56, pp.1209-1219.

Picheny, V., Kim, N.H, and Haftka, R.T. (2006), Conservative Estimation of CDF for Probability of Failure Calculation. *11th AIAA/ISSMO Multidisciplinary Analysis and Optimization Conference*, Portsmouth, Virginia.

Provan, J.W., and Farhangdoost, K. (1994), A new Stochastic Systems Approach to Structural Integrity. *FAA/NASA International Symposium on Advanced Structural Integrity Methods for Airframe Durability and Damage Tolerance*, September 1994. Part I, p 603-619.

Pugsley, A.G. (1944), The History of Structural Testing. *International Journal of Structural Engineering*, December 1944.

Qu, X., Haftka, R.T., Venkataraman, S., and Johnson, T.F. (2003). Deterministic and Reliability-Based Optimization of Composite Laminates for Propellant Tanks. *AIAA Journal*, Vol. 41, No. 10, pp. 2029-2036.

Qu, X., and Haftka, R.T. (2004), Reliability-based Design Optimization Using Probabilistic Sufficiency Factor. *Journal of Structural and Multidisciplinary Optimization*, Vol. 27, No.5, pp. 314-325.

Qu, X., Singer, T., and Haftka, R.T. (2004), Reliability-based Global Optimization of Stiffened Panels Using Probabilistic Sufficiency Factor. *45th AIAA/ASME/ASCE/AHS/ASC Structures, Structural Dynamics, and Material Conference*, Palm Springs, CA, 2004, AIAA Paper 2004-1898.

Rackwitz, R., and Fiessler, B. (1978), Structural Reliability under Combined Random Load Sequences. *Computers and Structures*, Vol. 9, No.5, pp. 489-494.

Rackwitz, R., and Schrupp, K. (1985), Quality Control, Proof Testing and Structural Reliability. *Structural Safety*, Vol. 2, pp. 239-244.

Rajashekhar, M.R., and Ellingwood, B. (1993), A New Look at the Response Surface Approach for Reliability Analysis. *Structural Safety*, Vol. 12, No. 3, pp. 205-220.

Ramu, P., Qu, X., Youn, D.B., Haftka, R.T., and Choi, K.K. (2004), *45st AIAA/ASME/ ASCE/AHS/ASC Structures, Structural Dynamics, and Materials Conference*, 19-22 April 2004, Palm Springs, CA, AIAA Paper 2004-1670.

Romero, V.J., and Bankston, S.D. (1998), Efficient Monte Carlo Probability Estimation with Finite Element Response Surfaces Built from Progressive Lattice Sampling. *Proceedings of 39th AIAA/ASME/ASCE/AHS/ASC Structures, Structural Dynamics, and Materials Conference*, Long Beach, CA, pp.1103-1119.

Royset, J.O., Der Kiureghian, A., and Polak, E. (2001), Reliability-based Optimal Structural Design by the Decoupling Approach. *Reliability Engineering and System Safety*, Vol. 73, pp. 213-221.

Sankar, B.V., and M. Narayanan (2001), Finite Element Analysis of Debonded Sandwich Beams under Axial Compression. *Journal of Sandwich Structures & Materials*, Vol. 3, No. 3, pp. 197-219.

Schuller, G.I., Bucher, C.G., Bourgund, U., and Ouypornprasert, W. (1989), An Efficient Computational Scheme to Calculate Structural Failure Probabilities. Probabilistic *Engineering Mechanics*, Vol. 4, No. 1, pp. 10-18.

Schultz, W., Smarslok, B., Speriatu, L., Ifju, P.G., and Haftka, R.T. (2005), Residual Stress Determination Using Temperature Dependent Material Properties and Uncertainty Analysis. *SEM Annual Conference and Exposition*, Portland, OR.

Shinozuka, M. (1969), Structural Safety and Optimum Proof Load. *Proc. Symp. Concepts of Safety of Structures and Methods of Design*, Int. Assoc. Bridge and Struc. Eng., London.

Smarslok, B., Haftka, R.T., and Kim, N.H. (2006), Comparison and Efficiency Analysis of Crude and Separable Monte Carlo Simulation Methods. *47th AIAA/ASME/ASCE/AHS/ASC Structures, Structural Dynamics and Materials Conference*, Newport, RI, AIAA Paper 2006-1632.

Soundappan, P., Nikolaidis, E., and Dheenadayalan, P. (2004), Targeted Testing for Reliability Validation. *SAE 2004 World Congress & Exhibition*, Paper no. 2004-01-0239.

Suo, Z. (1999), Singularities, Interfaces and Cracks in Dissimilar Anisotropic Media. *Proceedings of the Royal Society of London*, A427, 331-358.

Thoft-Cristensen, P., and Baker, M.J. (1982). *Structural Reliability Theory and Its Applications*. Springer-Verlag, NewYork, NY.

Tong, Y.C. (2001), Literature Review on Aircraft Structural Risk and Reliability Analysis. *DSTO Aeronautical and Maritime Research and Laboratory Technical Report*, DSTO-TR-1110.

Tu, J., Choi, K.K., and Park, Y.H. (1999), A New Study on Reliability Based Design Optimization. *ASME Journal of Mechanical Design*, Vol. 121, No. 4, 1999, pp. 557-564.

Turkstra, C.J. (1970), Theory of Structural Safety. SM No. 2, Solid Mechanics Division, University Waterloo, Onteria, Canada.

Vanegas, L.V., and Labib, A.W. (2005), Fuzzy Approaches to Evaluation in Engineering Design. *ASME Journal of Mechanical Design*, Vol. 127, pp. 24-33.

Venter, G. (1998), Non-Dimensional Response Surfaces for Structural Optimization with Uncertainty, Ph.D. Dissertation, Dept. of Mechanical and Aerospace Engineering, Univ. of Florida, Gainesville, FL.

Venter, G., and Sobieszczanski-Sobieski, J. (2002).Multidisciplinary Optimization of a Transport Aircraft Wing using Particle Swarm Optimization. *9th AIAA/ISSMO Symposium on Multidisciplinary Analysis and Optimization,* Atlanta, GA, AIAA Paper 2002–5644.

Vogler, K.H. (1997), Risk Allocation and Inter-dealer Trading. *European Economic Review*, Vol. 41, No. 8, pp. 1615-1634.

Whittemore, H.L. (1954), Why Test Building Constructions? *Symposium on Methods of Testing Building Constructions*, Annals of Society of Testing Materials, Special Technical Publication, No. 166.

Wirsching, P.H. (1992), Literature Review on Mechanical Reliability and Probabilistic Design. Probabilistic Structural Analysis Methods for Select Space Propulsion System Components (PSAM), *NASA Contractor Report* 189159, Vol. III, 1992.

Wu, Y.T. (1994), Computational Methods for Efficient Structural Reliability and Reliability Sensitivity Analysis. *AIAA Journal*, Vol. 32, No.8, pp. 1717–1723.

Wu, Y.T., Shin, Y., Sues, R., and Cesare, M. (2001), Safety-Factor Based Approach for Probabilistic-based Design Optimization. *42nd AIAA/ASME/ASCE/AHS/ASC Structures, Structural Dynamics and Materials Conference*, Seattle, WA, AIAA Paper 2001-1522.

Yang, J., Hwang, M., Sung, T., and Jin, Y. (1999), Application of Genetic Algorithm for Reliability Allocation in Nuclear Power Plants. *Reliability Engineering and System Safety*, Vol. 65, pp. 229–238.

Yang, J.N. (1976), Reliability Analysis of Structures under Periodic Proof Test in Service. *AIAA Journal*, Vol. 14, No. 9, pp.1225-1234.

Yang, J-S. (1989), System Reliability Optimization of Aircraft Wings. PhD Dissertation, Virginia Polytechnic Institute.

Yang, X.P., Kastenberg, W.E., and Okrent, D. (1989), Optimal Safety Goal Allocation for Nuclear Power Plants. *Reliability Engineering and System Safety*, Vol. 25, No. 3, pp. 257-278.

Youn, B.D., and Choi, K.K. (2004), A New Response Surface Methodology for Reliability-Based Design Optimization. Computers and Structures, Vol. 82, pp.241-256.

Zang, T.A., Hemsch, M.J., Hilburger, M.W., Kenny, S.P., Luckring, J.M., Maghami, P., Padula, S.L., and Stroud, W.J. (2002), Needs and Opportunities for Uncertainty-Based Multidisciplinary Design Methods for Aerospace Vehicles. NASA/TM-2002-211462.

Zhang, R., and Mahadevan, S. (2001), Integration of Computation and Testing for Reliability Estimation. *Reliability Engineering and System Safety*, Vol. 74, pp. 13-21.

Zhao, Y.G., and Ono, T. (1999), New Approximations for SORM: Part 1 and 2. *Journal of Engineering Mechanics*, Vol. 125, pp 79-93.

BIOGRAPHICAL SKETCH

Erdem Acar was born in Ankara, Republic of Türkiye, in 1977. He received his Bachelor of Science in aeronautical engineering from Middle East Technical University in June 1999. Mr. Acar started his graduate studies as a graduate research assistant in the same institution. He did his master's on the subject of thermo-mechanical fatigue life assessment of jet engine components. His interest in conducting research motivated him to join the Structural and Multidisciplinary Optimization Group of Professor Haftka at the University of Florida, in July 2003, to pursue his PhD degree in aerospace engineering. During his PhD study, he did internship in EMBRAER aircraft company in Brazil, where he worked on multidisciplinary design optimization of tail boom of an aircraft.